United States
Consumer Product Safety Commission

November 2022

CPSC Staff[1] Statement on SEA, Ltd. Report "Development of Proof-of-Concept (POC) Electronic Stability Control (ESC) System for ATV Stability"

The report titled, "Development of Proof-of-Concept (POC) Electronic Stability Control (ESC) System for ATV Stability," presents the results of laboratory and dynamic testing of two all-terrain vehicles (ATVs) equipped with rudimentary ESC systems that were developed by SEA. This work was conducted for CPSC under Task Order 61320621F1012 of CPSC contract 61320618D0003.

SEA conducted a series of static and autonomously controlled dynamic tests (on paved surfaces and groomed dirt) on a model year 2021 ATV equipped with an anti-lock brake system (ABS) and a model year 2014 ATV without ABS. Both ATVs had rudimentary ESC systems installed. This exploratory work examined how an ESC system's intervention can monitor real-time vehicle states and then react in an appropriate manner to limit lateral rollover. Other physical parameters were measured utilizing the SEA Vehicle Inertia Measurement Facility (VIMF), Tilt Table, and other laboratory equipment.

This report will assist CPSC staff as they continue to work to improve standards associated with ATV stability, including working with the Specialty Vehicle Association of America (SVIA) and other interested parties.

[1] This statement was prepared by the CPSC staff, and the attached report was produced by SEA for CPSC staff. The statement and report have not been reviewed or approved by, and do not necessarily represent the views of, the Commission.

U.S. Consumer Product Safety Commission
4330 East-West Highway
Bethesda, MD 20814

National Product Testing & Evaluation Center
5 Research Place
Rockville, MD 20850

Development of Proof-of-Concept (POC) Electronic Stability Control (ESC) System for ATV Stability

for:
Consumer Product Safety Commission

October 2022

Vehicle Dynamics Division
7001 Buffalo Parkway
Columbus, Ohio 43229

Development of Proof-of-Concept (POC) Electronic Stability Control (ESC) System for ATV Stability

for:
Consumer Product Safety Commission

"These comments are those of SEA, Ltd. staff, and they have not been reviewed or approved by, and may not necessarily reflect the views of, the Commission."

Report prepared by Gary J. Heydinger, Ph.D., P.E. and Scott Zagorski, Ph.D., P.E., with primary support from Austin Bower, Hank Jebode, Jon Coyle, and Dale Andreatta, Ph.D., P.E.

Vehicle Dynamics Division
7001 Buffalo Parkway
Columbus, Ohio 43229

TABLE OF CONTENTS

1. OVERVIEW

This report contains the description of work conducted and results from measurements made by SEA, Ltd. (SEA) for the Consumer Product Safety Commission (CPSC) under CPSC contract 61320618D0003, a contract that covers general testing and evaluation of All-Terrain Vehicles (ATVs). The work done for this study was conducted during FY2022 and was done under Task Order 61320621F1012.

The objective of this task order is to design, construct, and test a rudimentary Electronic Stability Control (ESC) system on an ATV equipped with Anti-lock Braking System (ABS) capabilities to evaluate its effectiveness in improving ATV stability and reduce the likelihood of rollover. Specifically, the objective is to perform the following:

- Design and construct an ESC / Instability Mitigation System (IMS) that can be fitted onto an ATV equipped with ABS capabilities: install the appropriate test instrumentation and sensors to measure yaw rate, velocity, acceleration, and steering angle; develop an algorithm to detect pending yaw or lateral instability; create a feedback loop system to actuate the appropriate amount of braking and/or drop throttle signal when instability conditions are met.
- Conduct static and autonomously controlled dynamic tests on the ESC / IMS equipped ATV on different terrains and vehicle turn scenarios.
- Conduct static and autonomously controlled dynamic tests on a similar ATV not equipped with ESC / IMS to produce baseline data.

Specific tasks for this task order include:

1. If necessary, purchase an ATV equipped with ABS or modify an ATV to have ABS capabilities, and then modify with a proof-of-concept ESC / IMS. ABS and ESC capabilities will include independent control of front and rear brakes. If necessary to achieve desired mitigation of vehicle instability, capabilities will include individual braking of each front wheel.
2. If necessary, measure static metrics and properties in four (4) loading conditions of test vehicle.
    A. Curb weight
    B. Curb weight plus 95th percentile male
    C. Curb weight plus 95th percentile male plus max cargo load
    D. Curb weight plus driver, instrumentation, and outriggers
3. Conduct dynamic tests with autonomous ATV Robotic Test Driver (RTD) to evaluate rollover resistance and vehicle handling. Tests shall be conducted on paved and groomed dirt surfaces. The load condition for the testing is operator plus instrumentation and outriggers. Test procedures will include J-turns, constant radius, and yaw rate ratio testing.

The POC ESC system developed was implemented on two different vehicles, both selected with CPSC approval. Both vehicles are property of CPSC and both have been used for previous CPSC studies conducted by SEA. They have straddle seating, and their intended use is for a single occupant, the driver. Both vehicles have handlebar (tiller) steering, thumb activated throttles, and hand and foot activated brakes.

One of the vehicles, Vehicle G, is a 2014 Model Year (MY) vehicle that was tested several times for CPSC studies conducted by SEA between 2016 and 2018. Details of the previous laboratory results for Vehicle G can be found in the CPSC report titled *Vehicle Characteristics Measurements of All-Terrain Vehicles – Results from Tests on Twelve 2014-2015 Model Year Vehicles*.[1] Details of the previous autonomously-controlled dynamic tests on asphalt can be found in the CPSC report titled *Effects on ATV Vehicle Characteristics of Rider Active Weight Shift – Results from Tests on Twelve 2014-2015 Model Year Vehicles*.[2] Details of the previous autonomously-controlled dynamic tests on groomed dirt can be found in the CPSC report titled *Vehicle Characteristics Measurements of ATVs Tested on Groomed Dirt – Results from Tests on Twelve 2014-2015 Model Year Vehicles*.[3]

The other vehicle, Vehicle N, is a 2021 MY vehicle that was tested for CPSC in a FY2021 study conducted to evaluate ABS on ATVs. Details of the previous laboratory tests and autonomously-controlled dynamic tests on asphalt and groomed dirt for Vehicle N can be found in the CPSC report titled *Evaluation of Anti-lock Brake System (ABS) Technology on ATV Stability – Results from Tests on Two 2021 Model Year Vehicles*.[4]

Results from the previous laboratory tests for Vehicle G and Vehicle N are reproduced in Appendix A of this report, and some results from the previous dynamic tests conducted on asphalt and groomed dirt are reproduced in Appendix D of this report. The results for the previous dynamic tests were used in this study to establish threshold levels for when ESC should be activated.

Vehicle N has Original Equipment Manufacturer (OEM) installed ABS, and Vehicle G does not have ABS. It is important to have ABS in some situations when ESC activates. ABS prevents braked wheels from locking up, which would limit the effectiveness of ESC intervention. Therefore, for Vehicle G, the hand brake actuator of the RTD was programmed to modulate braking inputs to emulate ABS for this vehicle. This emulation of ABS is not as sophisticated as a commercial ABS, but it is useful for helping demonstrate the proof-of-concept ESC system developed.

Table 1 contains a list of assorted vehicle information and tire specifications for the two vehicles tested during this study. Listed are the measured curb weight, measured maximum speed, transmission type, rear suspension type, and OEM driveline setting options. Both vehicles have open rear differentials, and they were tested in two-wheel drive mode. Table 1 also lists the front and rear tire make, tire size, and tire pressure for each vehicle.

---

[1] *Vehicle Characteristics Measurements of All-Terrain Vehicles – Results from Tests on Twelve 2014-2015 Model Year Vehicles*, HHS Contract HHSP233201400030I, SEA, Ltd. Report to CPSC, November 2016. https://www.cpsc.gov/s3fs-public/SEA_Report_to_CPSC_Vehicle_Characteristics_Measurements_of_All_Terrain_Vehicles.pdf

[2] *Effects on ATV Vehicle Characteristics of Rider Active Weight Shift – Results from Tests on Twelve 2014-2015 Model Year Vehicles*, HHS Contract HHSP233201400030I, SEA, Ltd. Report to CPSC, January 2018. https://cpsc-d8-media-prod.s3.amazonaws.com/s3fs-public/SEA-Report-to-CPSC-Rider-Active-ATV-Study-December-2017_0.pdf

[3] *Vehicle Characteristics Measurements of ATVs Tested on Groomed Dirt – Results from Tests on Twelve 2014-2015 Model Year Vehicles*, HHS Contract HHSP233201400030I, SEA, Ltd. Report to CPSC, February 2018. https://www.cpsc.gov/s3fs-public/SEA-Report-to-CPSC-Groomed-Dirt-ATV-Study.pdf?eK1E6h7IXBtznyCDatWHofAoHHmwD_nr

[4] *Evaluation of Anti-lock Brake System (ABS) Technology on ATV Stability – Results from Tests on Two 2021 Model Year Vehicles*, CPSC Contract 61320618D0003, SEA, Ltd. Report to CPSC, In Review.

The vehicles were evaluated using both laboratory measurements and dynamic tests. The laboratory measurements were made by SEA in Columbus, Ohio using their Vehicle Inertia Measurement Facility (VIMF), Tilt Table, and other laboratory equipment. The dynamic tests were performed by SEA on six dates between August 1, 2022 and August 19, 2022. Both vehicles were tested at SEA in Columbus, Ohio, on their asphalt and groomed dirt vehicle dynamics test pads.

This report contains five main sections: Overview, Design of POC ESC for ATV Stability, Laboratory Testing, Dynamic Testing, and Discussion of Test Results. There are also four appendices containing test results, photographs of test equipment, and background information.

Table 1: Test Vehicle Information and Tire Specifications

Vehicle G – No ABS **Curb Weight: 694.0 lb** **Maximum Speed: 69.0 mph** **Test Weight for ESC Study: 912.3 lb**	**Automatic Transmission** **Independent Rear Suspension** **2WD or 4WD**	
	Front Tires	Rear Tires
Tire Make	Duro DI-K911	Duro DI-K911
Tire Size	AT25X8-12 4 Ply	AT25X10-12 4 Ply
Tire Pressure (psi)	5	5
Vehicle N – ABS Equipped **Curb Weight: 951.0 lb** **Maximum Speed: 70.0 mph** **Test Weight for ESC Study: 1,164.2 lb**	**Automatic Transmission** **Independent Rear Suspension** **2WD or 4WD**	
	Front Tires	Rear Tires
Tire Make	ITP Terra Cross R/T	ITP Terra Cross R/T
Tire Size	205/75R14 M/C 48M 6 Ply	255/65R14 M/C 55M 6 Ply
Tire Pressure (psi) For Driver plus Cargo < 155 kg (341 lb)	7.0	7.0
Tire Pressure (psi) For Driver plus Cargo > 155 kg (341 lb)	9.0	10.0

2. DESIGN OF POC ESC FOR ATV STABILITY

Figure 1 is a typical diagram used to depict ESC to mitigate vehicle limit oversteer. For on-road passenger vehicles, limit oversteer is generally described as handling or yaw instability that leads to a spin out (as shown on Figure 1). For a typical on-road passenger vehicle with oversteer, as vehicle speed increases the yaw rate gain (amount of yaw rate per degree of steering) increases, promoting conditions that can lead to spins out. For a vehicle with oversteer, as vehicle speed increases the lateral acceleration gain (amount of lateral acceleration per degree of steering) also increases, and it increases more than the yaw rate gain. For on-road passenger vehicles, during steering induced maneuvers the limits of yaw instability (spin out) generally occur before the limits of lateral instability (rollover).

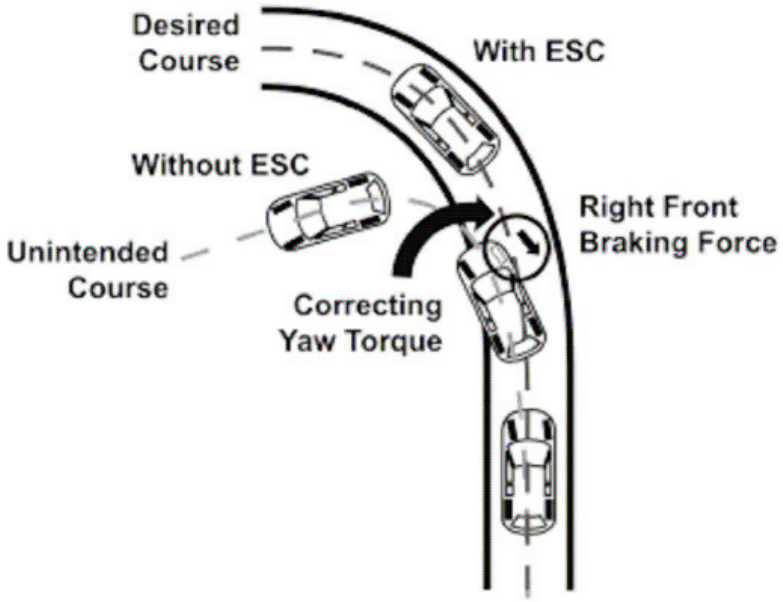

Figure 1: Diagram Depicting ESC to Mitigate Vehicle Oversteer

However, this is not the case for typical ATVs. For a typical ATV with oversteer, during steering induced maneuvers, as vehicle speed increases the lateral acceleration gain leads to lateral instability (rollover) before the yaw rate gain leads to yaw instability (spin out).

Previous testing conducted by SEA to evaluate ATV stability for CPSC has shown that even ATVs with neutral steer or understeer characteristics typically reach conditions of limit lateral instability before they reach a condition of limit understeer (plow out). Since the ESC system for ATVs developed in this study predominately mitigates lateral instabilities, it could be referred to more generally as a rollover Instability Mitigation System (IMS).

The point of this discussion is that any effort to mitigate yaw instability caused by high yaw rate gain will also limit lateral instability caused by high lateral acceleration gain. The POC ESC designed and implemented in this study does two things to prevent yaw and lateral instabilities, it drops vehicle speed, and it applies correcting yaw torque using the outside front brake as shown in Figure 1.

The vehicles were tested unmanned, using SEA's Robotic Test Driver (RTD). As such, there was

no human driver in-the-loop to maintain control of the vehicle during and after ESC intervention. Since this design is a proof-of-concept and not intended to serve as a final product ESC, the ESC intervention (dropping the throttle and braking the outside front wheel) was left on until the vehicle slowed to rest. In practice, commercial ESC systems cease intervention when pending instability conditions end.

2.1 Algorithm Development

A block diagram of the POC ESC strategy is shown in Figure 2. As mentioned, the POC ESC developed here is less sophisticated than typical commercial ESC systems. However, as shown in Figure 2, it does have the main features of a typical ESC system including a real time monitor of a suite of vehicle states, an algorithm to evaluate vehicle state conditions to detect pending instability, and a system to actuate ESC when intervention is needed.

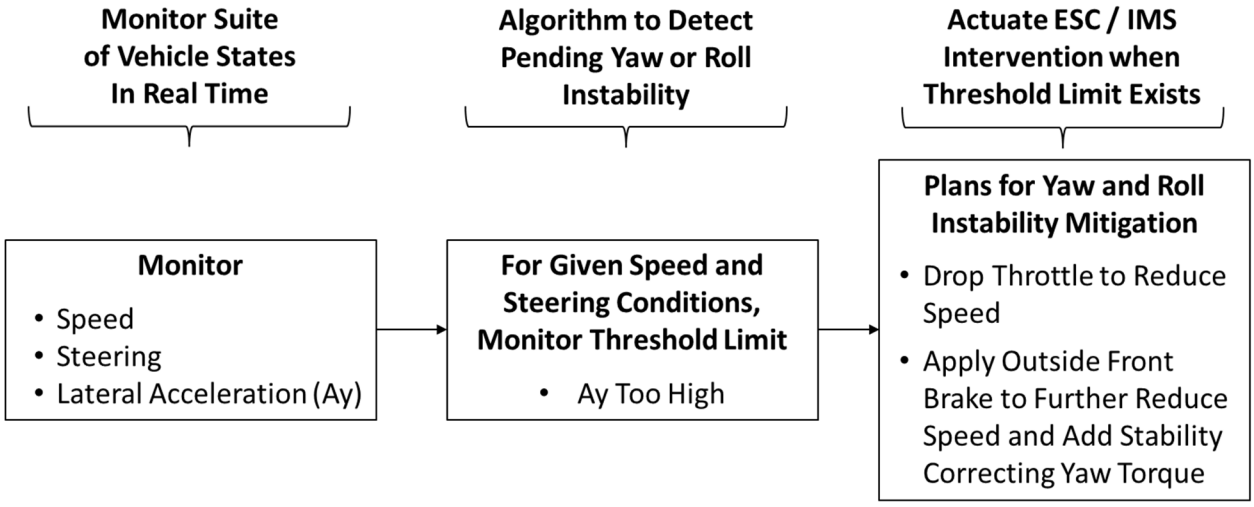

Figure 2: Block Diagram of POC ESC Strategy

For the POC ESC three vehicle states are monitored, forward speed, steering input, and ground plane lateral acceleration. The algorithm to detect pending instability compares the current filtered value of the measured lateral acceleration to a lateral acceleration threshold level based on previous stability measurements made on the vehicles. If the measured lateral acceleration signal exceeds the threshold level, and the vehicle speed and steering are high enough to suggest the vehicle is in a state of pending instability, the POC ESC system will intervene. The intervention will drop the throttle and apply braking to the outside front tire.

To determine ESC Threshold lateral acceleration (A_y) levels, previously collected data from dropped throttle J-turn tests, circle tests, and constant steer tests (yaw rate ratio tests) on asphalt and groomed dirt were analyzed (results from these previous dynamic tests conducted on Vehicles G and N are contained in Appendix D). Factors including the latency caused by real-time filtering the lateral acceleration signal, and the latency between actuating the hand brake and hydraulic brake actuation at the wheel were also considered in selecting the ESC Threshold A_y levels.

Table 2 lists the distinct ESC threshold levels for Vehicles G and N. The ESC Threshold A_y level is 85% of the two-wheel lift (2WL) Threshold A_y, the average minimum peak lateral acceleration that results in 2WL outcomes in 20 mph dropped-throttle J-turn tests conducted on asphalt and

groomed dirt. Page 1 of Appendix D contains additional details from the previous 2WL J-turn tests. Pages 2-7 of Appendix D contain plots of lateral acceleration, steer angle, and vehicle speed for all previous 2WL J-turn tests, circle tests, and yaw rate ratio tests for both vehicles on asphalt and on groomed dirt.

The lateral acceleration plots in Appendix D show that the lateral acceleration increases faster in the J-turn tests than in the circle or yaw rate ratio tests. The ESC Threshold A_y levels (which are 85% of the 2WL Threshold Ay values) are shown on the lateral acceleration plots. These ESC Threshold A_y levels were selected to allow enough time for the ESC system to intervene and prevent lateral instabilities that would result in rollovers. Time delays resulting from the real-time filter on the measured lateral acceleration, from the delay in vehicle speed reduction on thumb-throttle release, from the delay in response of the brake actuator, and from the delay of the hydraulic brake system all contribute to the overall latency in the ESC system. However, the total latency in the ESC system from the time the true lateral acceleration reaches the ESC Threshold level and the time the vehicle instability is mitigated is less than one second. As the lateral acceleration plots in Appendix D show, using the ESC Threshold A_y levels selected, and having an ESC system that can respond in one second, provides adequate time for the ESC system to intervene and mitigate instabilities even in highly dynamic maneuvers like the rapid steering J-turn tests. The plots also show that the ESC Threshold A_y levels will provide adequate time for intervention in the less dynamic (and quasi-static) maneuvers like the circle tests and yaw rate ratio tests.

The Steering Threshold levels and Speed Threshold levels given in Table 2 are shown on the steering and speed plots in Appendix D. As the plots show, these threshold levels are below the steering and speed values during the more severe portions of the maneuvers. Requiring the vehicle speed and steering input to be above some baseline level indicate that the vehicle is in a maneuver with an instability situation that could be mitigated by ESC intervention. Applying these steering and speed thresholds was done for the sake of including baseline levels of vehicle activity in the proof-of-concept ESC system, like what would likely be done in a commercial ESC system.

Table 2: Vehicle Specific ESC Threshold Levels

ESC Threshold	Vehicle G	Vehicle N
2WL Threshold A_y (g)	0.452	0.548
ESC Threshold A_y (g) (85% of 2WL Threshold A_y)	0.384	0.466
Steering Angle (deg)	9.0	8.0
Vehicle Speed (mph)	10.0	10.0

In this study there was no driver in-the-loop to maintain control of the vehicle during and after ESC intervention, so the RTD had to programmatically maintain steering control while the POC ESC intervened. During ESC intervention during the circle tests, the RTD continued to do path following steering to maintain the circular path. In the other maneuvers used in this study (J-Turn

tests, slowly increasing steer tests, and constant steer tests), the steering during ESC intervention was commanded to be the same as it would have been if the ESC had not intervened.

For Vehicle G the RTD hand brake applied both front services brakes and for Vehicle N the RTD hand brake applied both the front and rear service brakes. For this study, for both vehicles the left front brake was mechanically disconnected (disabled) and only left turning maneuvers were performed. This provided the ability to apply the outside front brake (and not the inside front brake), which is the best method for imparting a correcting yaw moment (see Figure 1). Page 5 of Appendix C shows the left front brake caliper removed from the brake rotor on Vehicle N, thus disabling left front braking.

2.2 Algorithm Implementation

The algorithm described above was implemented in the real-time controller of the RTD. For the real-time system, a National Instruments (NI) compact-RIO (cRIO) is programmed using LabVIEW. In general, the ESC algorithm is a subroutine that was incorporated such that it "interrupts" the signals which are determined by the main control loop. That is, depending on the state of the vehicle and whether ESC is enabled, and criteria are met, the desired signals for the brake, throttle, and steering may be interrupted in favor of the ESC intervention signals.

Further implementation required a state machine to handle some of the nuances that arise from real-time controllers. Three states were required:

- State 0 – ESC Off:
  - Wait for ESC to be Enabled and Criteria to be Met
  - Pass through Current Desired Throttle, Brake, and Steer Commands

- State 1 – ESC ON:
  - Drop Throttle
  - Apply ESC Brake Level
  - Path Following Steering for Circle Tests or Hold Steering for Other Tests

- State 2 – ESC ABORT
  - Drop Throttle
  - Apply Desired Brake Command (Brake Abort Level)
  - Hold Steering → Disable Drive

To go from State 0 to State 1, ESC criteria need to be met. From State 1 to State 2, vehicle speed needs to drop below 0.15 mph or RTD variable 'User Stop' (Stop or E-stop) needs to go TRUE. To go from State 2 to State 0, vehicle speed needs to drop below 0.1 mph or RTD variable 'RUN' goes from FALSE to TRUE. Figure 3 depicts the ESC state machine as implemented.

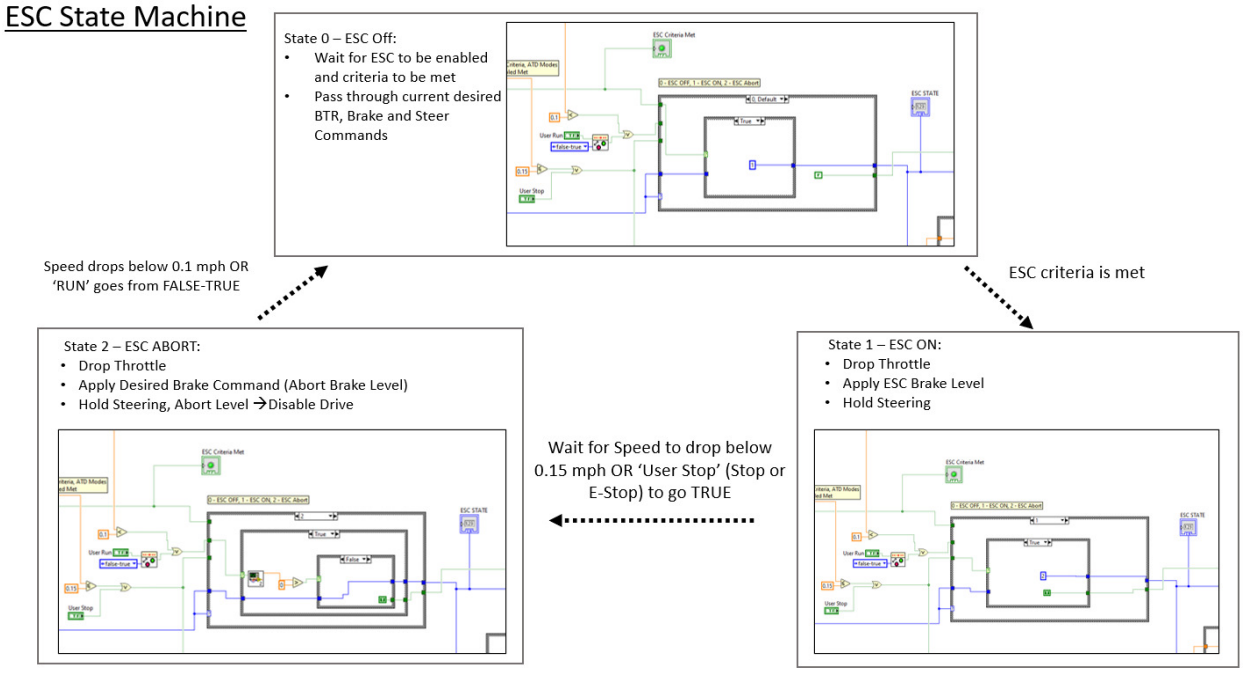

Figure 3: ESC State Machine

2.3 Real-Time Filtering

One of the challenges of this study was to determine a proper real-time filtering technique for filtering vehicle lateral acceleration. Acceleration measurements have inherently high noise levels. Moreover, ATVs have significantly higher vibration levels than typical passenger vehicles, which further confounds this problem. Real-time filters introduce delays that impact the ability of the controller to detect a particular acceleration level. Using MATLAB to analyze previously collected lateral acceleration data, several filtering techniques were explored including moving average filters and single pass low-pass filters. It was determined that an 8th order 6 Hz low-pass Butterworth filter would work best to filter out noise and minimize delay. Figure 3 shows lateral acceleration data from a J-turn maneuver, with MATLAB's *filter* function (a single pass filter representing a real-time filter) co-plotted with LabVIEW's Butterworth function (the actual real-time filter used in this study) for comparison. The plots from these two filters are on top of each other.

To illustrate the delay associated with single pass filters, data is also shown on Figure 4 from MATLAB's phaseless, two-pass, *filtfilt* routine. The delay in the real-time filters is approximately 150 milliseconds. This delay was accounted for in determining the ESC Threshold A_y levels. All the lateral acceleration plots shown in Appendix D are delayed, they have been filtered using a single pass 8th order 6 Hz low-pass Butterworth filter using MATLAB's *filter* function.

2.4 Emulating ABS on Vehicle G

For Vehicle G, the vehicle without ABS, the hand brake actuator of the RTD was programmed to modulate braking inputs to emulate ABS. Page 8 of Appendix D shows results from a braking and turning maneuver on wet grass that caused ABS activity on the right front wheel of Vehicle N, the vehicle with OEM ABS. The Speed graph on this page shows the timing of the cyclic ABS braking on the right front wheel. There are several cycles of on/off braking per second.

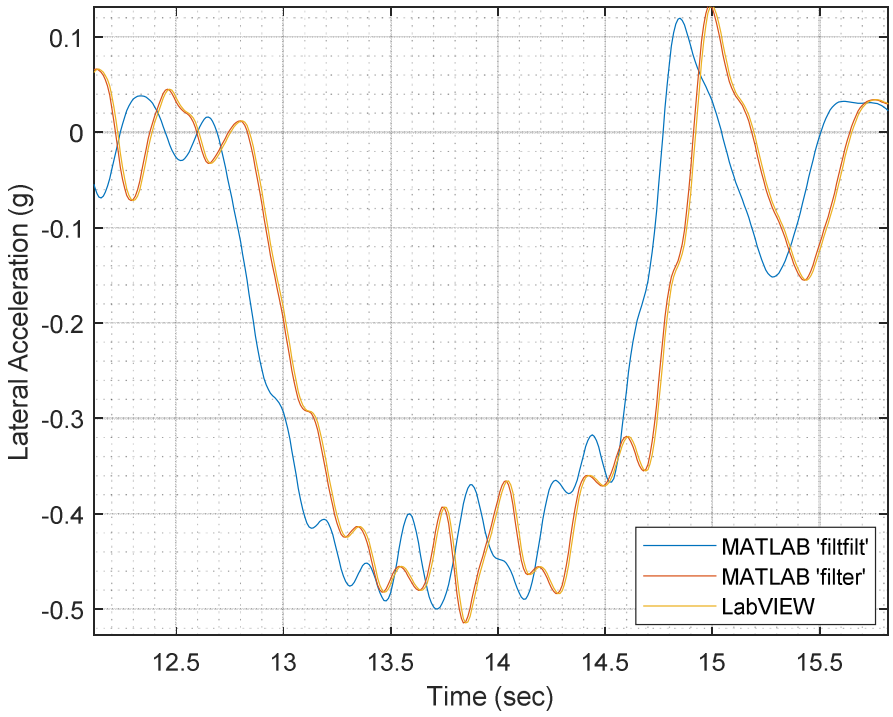

Figure 4: MATLAB and LabVIEW Filter Comparison

The electric motor used to actuate the hand brake of the ATV RTD is capable of following brake input commands under typical loading conditions at speeds above 40 mm/sec. As configurated on the ATV RTD, the actuator stroke needed for full brake actuation on most ATVs is about 20 mm. Based on this, for Vehicle G the ABS emulation used triangular braking pulses with amplitude up to 10 mm and a frequency of two cycles per second (2 Hz). The graph of Brake Position on Page 9 of Appendix D shows that the actual brake stroke position measured on Vehicle G does a good job of following the desired 10 mm amplitude, triangular brake pulses at 2 Hz. However, there is a delay between the requested (desired) position and actual position of approximately 60 milliseconds. As mentioned, this delay was accounted for when selecting the ESC Threshold A_y level for this vehicle.

The amount of braking applied during POC ESC intervention for both vehicles was test date adjustable. That is, the level of braking could be adjusted based on the vehicles' responses on the day of testing. Also, for Vehicle G, the ABS emulating cyclic braking was set up to have lower and upper bounds. For example, the ABS-like braking levels could be cycled between 40-80% full stroke, or between 60-100% full stroke, etc. Results in Appendix B from the tests conducted using POC ESC intervention include plots showing applied braking and wheels speeds. The wheel speed graphs show that there was no wheel lockup for either vehicle during any of the ESC runs (all of which used braking). Some of the wheel speed plots show ABS cycling the wheel speeds (on the runs with conditions where ABS prevented wheel lock up).

3. LABORATORY TESTING

Both vehicles used in this study were used in previous studies conducted for CPSC, and laboratory measurements of their static metrics and properties were made during the previous studies. Therefore, no new measurements were needed as part of this study. Initial publication of the laboratory results for Vehicle G can be found in the CPSC report titled *Vehicle Characteristics Measurements of All-Terrain Vehicles – Results from Tests on Twelve 2014-2015 Model Year Vehicles*[5] and for Vehicle N can be found in the CPSC report titled *Evaluation of Anti-lock Brake System (ABS) Technology on ATV Stability – Results from Tests on Two 2021 Model Year Vehicles*.[6]

This section describes the laboratory measurements made as well as computations of various rollover resistance metrics and other vehicle characteristics. This section is divided into three parts: one covering the Vehicle Inertia Measurement Facility (VIMF) tests, one covering the Tilt Table tests, and one covering the steering ratio tests. Tabular results from all the measurements and metrics discussed in this section are contained in Appendix A.

For both Vehicles G and N, there are results for three loading conditions: Curb (curb weight only), Driver (curb weight plus 95th percentile male driver), and Gross Vehicle Weight (curb weight plus 95th percentile male driver plus maximum cargo load). For Vehicle G, the fourth loading condition is Driver Plus Instrumentation (DPI), the loading condition used during the dynamic tests using Vehicle G conducted with a human driver, full instrumentation, and safety outriggers. For Vehicle N, the fourth loading condition is Autonomous Ballast to Driver Loading, the loading condition used during the unmanned dynamic tests using Vehicle N conducted using the Robotic Test Driver (RTD), full instrumentation, and safety outriggers. This unmanned loading condition is intended to closely match the DPI loading condition used for tests with a human driver.

3.1 Vehicle Inertia Measurement Facility (VIMF) Tests

Laboratory measurements of vehicle weight (including the four corner weights); vehicle center-of-gravity (CG) position (longitudinal, lateral, and vertical (CG height)); vehicle pitch, roll, and yaw moments of inertia; and roll/yaw product of inertia were made by SEA using their Vehicle Inertia Measurement Facility (VIMF).[7] Measurements of front track width, rear track width, and wheelbase were also made.

The vehicle CG longitudinal position is expressed as a distance from the front axle. The vehicle CG lateral position is expressed as a lateral distance from the vehicle centerline; CG positions to the right of the centerline are positive. The vehicle CG height is expressed as the distance of the vehicle center of gravity above the road plane.

The moments and product of inertia for a vehicle are computed relative to the vehicle's center of

---

[5] *Vehicle Characteristics Measurements of All-Terrain Vehicles – Results from Tests on Twelve 2014-2015 Model Year Vehicles*, HHS Contract HHSP233201400030I, SEA, Ltd. Report to CPSC, November 2016. https://www.cpsc.gov/s3fs-public/SEA_Report_to_CPSC_Vehicle_Characteristics_Measurements_of_All_Terrain_Vehicles.pdf

[6] *Evaluation of Anti-lock Brake System (ABS) Technology on ATV Stability – Results from Tests on Two 2021 Model Year Vehicles*, CPSC Contract 61320618D0003, SEA, Ltd. Report to CPSC, In Review.

[7] *The Design of a Vehicle Inertia Measurement Facility*, Heydinger, G.J., Durisek, N.J., Coovert, D.A., Guenther, D.A., and Novak, S.J., SAE Paper No. 950309, February 1995.

gravity, using an orthogonal coordinate system with its origin at the vehicle center of gravity. The X-axis of the coordinate system is directed forward and parallel to the road plane, the Y-axis is directed to the driver's right and is also parallel to the road plane, and the Z-axis is directed downward.

In addition to the direct measurements provided by the VIMF, two other metrics that are used to characterize vehicle rollover resistance were computed, namely, the Static Stability Factor (SSF) and the lateral stability coefficient (K_{ST}).

SSF is a fundamental rollover resistance metric which equals the lateral acceleration in units of g at which rollover begins in the most simplified rollover analysis of a vehicle represented by a rigid body without suspension movement or tire deflections. SSF is given by:

$$SSF = \frac{T_{AVE}}{2 \times H_{CG}}$$

where: T_{AVE} is the Average Track Width, and
H_{CG} is the Vehicle CG Height.

K_{ST} is similar to SSF in that it represents the acceleration in g's at which rollover begins in the most simplified rollover analysis of a vehicle with different front and rear track widths represented by a rigid body without suspension movement or tire deflections. For vehicles with equal front and rear track widths, K_{ST} and SSF are equal. K_{ST} is given by:

$$K_{ST} = \frac{L \times T_R + L_{CG} \times (T_F - T_R)}{2 \times L \times H_{CG}}$$

where: L is the Vehicle Wheelbase,
T_F is the Front Track Width,
T_R is the Rear Track Width, and
L_{CG} is the Longitudinal Distance from the Rear Axle to the CG, and
H_{CG} is the Vehicle CG Height.

Appendix A contains results from the VIMF tests conducted on both vehicles.

3.2 Tilt Table Tests

SEA built a tilt table consisting of a rigid steel platform mounted on top of a yaw bearing. The yaw bearing allows the platform to be rotated so that lateral tilts (left-side leading and right-side leading), forward tilts (front-end leading), and rearward tilts (rear-end leading) can be conducted without removing and reloading the vehicle. A hydraulic cylinder was used to tilt the yaw bearing and platform assembly, up to 60 degrees from horizontal. Tilt Table tests were conducted in all four loading conditions for both vehicles, and tilts were conducted in four directions: left-side leading, right-side leading, front-end leading, and rear-end leading.

For the lateral tilts, the vehicles were tilted such that the outsides of the low side tires were aligned to be parallel to the tilt axis prior to testing. This is approximately parallel to the longitudinal axis of the vehicle. The platform was gradually tilted to the point when both high side tires lifted off

the platform. The vehicles were prevented from tilting completely off the platform by straps that restrained further tilting once the high side tires lifted about two to three inches off the platform. A high friction surface, a steel plate with its top surface covered with marine grade safety walk paint, was secured to the platform in the areas beneath all four tires. This surface prevented the vehicles from sliding sideways during the lateral tilt table tests.

For the longitudinal tilts (the forward and rearward tilts), the vehicles were tilted in a direction nominally parallel to their pitch axis. To prevent the vehicles for rolling during these tests, the vehicle transmissions were locked (they were put in park or in gear), their hand brakes were applied using a hose clamp, and if necessary, straps were wrapped around the front and/or rear tires and secured to the vehicle chassis. The forward and rearward tilt angles needed to get two-wheel lift are greater than the tilt angles needed to get lateral tilt two-wheel lift. As was done during previous ATV longitudinal tilt table tests conducted by SEA for CPSC, to prevent the ATV tires from sliding off the tilt table platform at high tilt angles, a 2-inch-high trip rail (a 2x2 inch square aluminum tube) was used for all longitudinal tilt table tests. The tires were rolled up against the 2-inch-high trip rail prior to locking the transmissions, setting the brakes, and applying the roll-preventing tire straps.

For the longitudinal tilts, the low side tires were aligned to be parallel to the tilt axis. The platform was gradually tilted to the point when both high side tires lifted off the platform. The vehicles were prevented from pitching completely off the platform by straps that restrained further tilting once the high side tires lifted about two to three inches off the platform.

The important factors involved in accurate tilt table testing include having a rigid and flat platform; having the ability to produce slow, smooth, and consistent tilt rates; and having accurate and repeatable measures of tilt angle and point of wheel lift. The SEA tilt table platform is very rigid, and it was designed to have deflections of less than 0.1 inch for all ATV vehicles tested. It is also very flat, with a flatness tolerance of ±0.1 inch. The hydraulic cylinder used to tilt the platform is controlled to provide for smooth tilting at rates as slow as 0.1 deg/sec.

A high-accuracy, two-axis (one aligned with the right/left tilt axis and one aligned with the fore/aft tilt axis) angle sensor is mounted to the platform to record the tilt angles throughout the tilt table tests. The point of two-wheel lift is determined visually, and the observer generates a signal that is recorded by the data acquisition system by pushing a button on a handheld trigger. Typically, five or six tilts to two-wheel lift were conducted for each vehicle configuration tested. The tests with the closest three angles of two-wheel lift were selected and averaged together to determine the final angle of two-wheel lift. Based on repeatability evaluations conducted using a range of ATVs, SEA thinks that the repeatability of the measurements of two-wheel lift is within ±0.1 degrees.

For left side leading and right side leading tilts, the angle at which two-wheel lift occurs is referred to as the Tilt Table Angle (TTA). In addition to measuring TTA, the tilt table test results provide a measure of the rollover resistance metric Tilt Table Ratio (TTR). TTR is the tangent of the TTA. TTR is computed mathematically using:

$$\mathrm{TTR} = tan\left(\mathrm{TTA}\right)$$

For front end leading tilts, the angle at which two-wheel lift occurs is referred to here as Front Tilt Table Angle (FTTA); and for rear end leading tilts, the angle at which two-wheel lift occurs is

referred to here as Rear Tilt Table Angle (RTTA). In addition to measuring FTTA and RTTA, the tilt table test results provide measures of a vehicle's pitch-over resistance, metrics referred to here as Front Tilt Table Ratio (FTTR) and Rear Tilt Table Ratio (RTTR). FTTR and RTTR are computed using:

$$\text{FTTR} = tan\left(\text{FTTA}\right)$$

$$\text{RTTR} = tan\left(\text{RTTA}\right)$$

Appendix A contains results from the tilt table tests conducted on both vehicles.

3.3 Steering Ratio Tests

Steering ratio tests were conducted with the vehicles in their Autonomous Ballast to Driver Loading condition. The steering ratio tests consisted of placing the front tires on commercial low friction wheel alignment pads and placing the rear tires on blocks of the same thickness as the alignment pads. The steering column angle (the handlebar angle) was measured using the RTD's steer angle sensor, and the right and left roadwheel angles are measured using the angle gages on the alignment pads. To conduct the tests, the steering handlebar was moved incrementally from zero degrees, to its full lock position to the right, to its full lock position to the left, and returned back to zero degrees. The handlebar angle increments used were 0°, ±5°, ±10°, ±15°, ±20°, ±30°, ±40°, and full lock in both directions. Both the right side and left side roadwheel angles were recorded at all steering positions. Linear curve fits of the measured data in the range of ±10° of steering column (handlebar) angle were used to compute the overall steering ratios. The overall steering ratios and graphical results from the steering ratio tests for both vehicles are contained in Appendix A.

4. DYNAMIC TESTING

This section describes the dynamic tests conducted on six dates between August 1, 2022 and August 19, 2022. Both vehicles were tested at SEA in Columbus, Ohio, on their asphalt and groomed dirt vehicle dynamics test pads. Both vehicles tested have automatic transmissions and they were tested in two-wheel drive mode, and in their most-open driveline configuration.

This section describes the vehicle loading condition used during the dynamic field tests, the test instrumentation, and the four different dynamic test maneuvers that were conducted to evaluate the operation of the POC ESC. The maneuvers were selected to show that the POC ESC system developed could improve ATV stability and reduce the likelihood of rollovers. Graphical results from all the dynamic tests are contained in Appendix B.

4.1 Vehicle Loading Condition

The loading condition used for the dynamic testing was the Autonomous Ballast to Driver Loading condition, representing a 213 lb driver only loading condition. This loading condition is the vehicle curb weight plus the weight (nominally 213 lb) of the test instrumentation and equipment that included: measurement transducers, SEA's ATV RTD, SEA's ATV safety outrigger, wheel speed sensors, and a driver ballast weight frame. Pages 1-2 of Appendix C contain photographs of the fully loaded and instrumented test vehicles.

Page 2 of Appendix C identifies the safety outrigger mounted beneath the vehicle, the wheel speed sensors on the left side of the vehicle, and the driver ballast weight frame. The weight frame, constructed of 80/20 T-slot aluminum bars, is used to rigidly hold enough weight to bring the total test weight up to nominally 213 lb above the curb weight for each vehicle. The only weight added to the ballast frame for this study was a 12V battery (used to provide power to the RTD and test equipment) attached to the top of the frame.

The ATV RTD consists of a computer-controlled 24V electric motor (rotary actuator) that mounts to the front rack of an ATV for steering control. A four-bar linkage arrangement is used to connect the motor drive gear to an aluminum rod that is connected to the ATV steering column beneath the ATV handlebars. For throttle control, the ATV RTD includes a computer-controlled 24V electric motor (rotary actuator), with a pulley and wire attachment to the throttle lever, mounted to the aluminum rod. The RTD version used for this study also included a computer-controlled 24V electric motor (linear actuator) to actuate the right-side hand brake for Vehicle G (which operates the front service brakes on Vehicle G) and the left-side hand brake for Vehicle N (which operates the front and rear service brakes on Vehicle N). The brake lever was removed from its handlebar mount and replaced on the front base plate in line with the linear actuator. This configuration provided precise control of the braking inputs needed for the tests involving braking. Page 3 of Appendix C contains photographs of the RTD actuators used for this study. The ATV RTD also includes a GPS/IMU (OxTS RT3002), an electronics box (with a National Instruments (NI) cRIO, the on-vehicle computer with the motor controllers and data acquisition software), an auxiliary 24V battery, and antennas for wireless communication. These items are shown in the photograph on Page 4 of Appendix C. Page 5 of Appendix C shows the left front brake caliper removed from the brake rotor on Vehicle N, thus disabling left front braking.

Table 3 lists the nominal weights of the components that comprise the Autonomous Ballast to Driver Loading condition.

Table 3: Autonomous Ballast to Driver Loading	
Component	**Nominal Weight (lb)**
Components Mounted at Front of Each Vehicle Base Plate, Steer Actuator, Throttle Actuator, Brake Actuator, and Associated Mounts and Linkages	46.1
Components Mounted at Rear of Each Vehicle Base Plate, Electronics Box, GPS/IMU (RT3002), 24V Battery, and Antennas	62.3
Standard ATV Outrigger	30.8
Wheel Speed Sensors and Associated Electronics	19.8
Weight Frame and Miscellaneous Ballast	54.0
Total Nominal Driver Only Weight	**213.0**

4.2 Test Instrumentation

The on-vehicle instrumentation used during the dynamic testing is listed in Table 4. The GPS/IMU RT3002 was mounted on the rear base frame of each vehicle. For both vehicles tested, the longitudinal, lateral, and vertical offsets from the center of the RT3002 to the actual vehicle CG location were measured and entered into the RT3002 system software. This information was used to translate the measured quantities to those at the CG of the vehicle. The lateral accelerations measured and reported herein are accelerations parallel to the road plane, as opposed to vehicle body-fixed accelerations.

Table 4: Instrumentation Used During Dynamic Testing			
Transducer	**Measurement**	**Range**	**Accuracy**
Oxford Technical Solutions (OxTS) RT3002 Inertial and GPS Navigation System	Longitudinal, Lateral, and Vertical Accelerations	± 100 m/s^2 (± 10 g)	0.01 m/s^2 (0.001 g)
	Roll, Pitch, and Yaw Rates	± 100 deg/s	0.01 deg/s
	Speed	No Limit Specified	0.05 km/h (0.03 mph)
	Roll and Pitch Angles	-180 to +180 deg	0.03 deg
	Vehicle Heading	0 to 360 deg	0.1 deg
Wheel Speed Encoders WPT/E512	Wheel Speeds	2,000 rpm Maximum	± 0.25 deg (Angle Position Specification)

4.3 Dynamic Test Maneuvers

Four different dynamic test maneuvers were used during this study, J-Turn tests, Slowly Increasing Steer tests, Circle Tests, and Constant Steer tests. For both vehicles, all four test types were conducted on asphalt and groomed dirt surfaces. All test types on both surfaces were conducted without POC ESC to establish baseline test runs with lateral acceleration levels greater than the POC ESC Threshold A_y level. Then runs with POC ESC enabled were conducted, and the POC ESC intervened when the lateral acceleration levels reached the ESC Threshold A_y level. The runs conducted with the POC ESC enabled were used to demonstrate that the POC ESC system developed could improve ATV stability and reduce the likelihood of rollovers.

Descriptions of the four tests maneuvers is contained in the follow sections.

4.3.1 Dropped Throttle J-Turn Tests (Initial Speed of 20 mph)

J-Turn tests, often referred to as step steer tests, involve imparting a rapid steering input up to a fixed magnitude while the vehicle is initially traveling along a straight path. For the dropped throttle J-Turn tests, the RTD drove each vehicle along a straight-line path (defined by GPS coordinates) from low speed up to a speed of 21 mph. Once 21 mph was achieved, the RTD then dropped the throttle and triggered the steering input precisely when the vehicle speed reached 20 mph. The handlebar (motor) steering input rates used were 40 deg/sec, and the steering dwell or hold time used was 6.0 seconds, at which time the steering angle was programmed to return to 0 deg.

The J-Turn test procedure involved initially running tests with steering magnitudes less than the steering required to produce tip-up events, events that have visual two-wheel lift outcomes. The handlebar steering input magnitude was gradually increased in 1.0-degree increments to the point where a test run resulted in a two-wheel lift (2WL) event. A 2WL outcome is an event that is near the threshold of vehicle tip-up and rollover. The 2WL J-turns on asphalt and groomed dirt without ESC established baseline data. Then, for the ESC runs, when the vehicle lateral acceleration reached the ESC Threshold A_y level, the ESC algorithm dropped throttle (although for these runs the throttle was already at zero), applied ESC-level braking, and continued steering the desired steering input profile.

4.3.2 Slowly Increasing Steer Tests (Initial Speed of 15 mph)

For the Slowly Increasing Steer (SIS) tests, the RTD drove each vehicle along a straight path from low speed up to a speed of 15 mph. After a speed of 15 mph was achieved, a handlebar steering input at the rate of 5.0 deg/sec was applied. For the tests without ESC, the maneuver was ended programmatically by the RTD when the lateral acceleration reached a level approximately 0.05 g greater than the ESC Threshold A_y level. This level is referred to as the Limit A_y level, and it represents a lateral acceleration condition where the vehicle is, or is close to, tipping up onto the safety outriggers. For these non-ESC runs, when the Limit A_y level was reached, the RTD program dropped the throttle and continued steering the desired steering input profile. For the ESC runs, when the vehicle lateral acceleration reached the ESC Threshold A_y level, the ESC algorithm dropped throttle, applied ESC-level braking, and continued steering the desired steering input profile.

Like the J-Turn tests, the SIS tests are dynamic tests (not quasi-static like the Circle and Constant Steer Tests) and they were also used to drive the ATVs to a condition of near instability, with high lateral acceleration and near the point of 2WL. However, in the case of SIS maneuvers, the throttle was not dropped prior to steering, as the RTD applied the throttle necessary to try to maintain vehicle speed. While steering, the throttle was dropped during the non-ESC runs by the RTD end-of-run lateral acceleration threshold or during the ESC runs by the ESC algorithm's Threshold A_y.

4.3.3 Circle Tests (Constant 50 ft Radius)

Circle tests are quasi-steady-state maneuvers that involve driving a vehicle on a circular path of constant radius (50 ft in this case). The test vehicles were autonomously driven in counterclockwise direction using the RTD to steer the vehicles and control the vehicle throttle (speed) during these tests. A circular path of 50 ft radius was generated in GPS coordinates and the "path-following" feature of the RTD was used to control the steering input during these tests. The path-following algorithm has a collection of parameters used to model driver look-ahead distance, vehicle steering properties, and other steering-related control gains that were adjusted to provide path following for each vehicle tested.

For the Circle tests, the throttle input was increased in piecewise linear steps to generate speed profiles from a very low speed up to a speed where the lateral acceleration reached the Limit A_y level. For the non-ESC runs, when the Limit A_y level was reached, the RTD program dropped the throttle and continued using path-following steering. For the ESC runs, when the vehicle lateral acceleration reached the ESC Threshold A_y level, the ESC algorithm dropped throttle, applied ESC-level braking, and continued using path-following steering.

4.3.4 Constant Steer Tests (Yaw Rate Ratio Tests)

Constant Steer tests (tests used sometimes to determine Yaw Rate Ratios) are also quasi-steady-state maneuvers that involve driving a vehicle using a constant steering angle and with slowly increasing speed. The handlebar steer angles used were the same as those used during counterclockwise direction Constant Steer tests conducted in previous studies (-13° for Vehicle G on an initial 50 ft radius path and -21.75° for Vehicle N on an initial 25 ft radius path).

For the Constant Steer tests, the throttle input was increased in piecewise linear steps to generate speed profiles from a very low speed up to a speed where the lateral acceleration reached the Limit A_y level. For the non-ESC runs, the RTD program dropped the throttle and held the constant steering input. For the ESC runs, when the Limit A_y level was reached, the ESC algorithm dropped throttle, applied ESC-level braking, and held the constant steering input.

5. DISCUSSION OF TEST RESULTS

Appendix A (Laboratory Test Results) contains tables with results from the laboratory tests conducted on Vehicle G and Vehicle N. Graphical results from the dynamic tests are contained in Appendix C (Dynamic Test Results).

5.1 Discussion of Laboratory Test Results

Appendix A contains tabular results of laboratory measurements made by SEA. There are six pages of results, three pages for each vehicle. The first page for each vehicle contains a table of results from the VIMF and Steering Ratio tests, the second page for each vehicle contains a table of results from the Tilt Table tests, and the third page for each vehicle contains graphical results from its steering ratio test.

The first 19 rows of the first page for each vehicle contain measurements related to the mass (weight), track width, wheelbase, center-of-gravity location, and inertia properties, as well as static rollover propensity calculations, based on measurements made using the VIMF. These measurements are shown for all four laboratory loading conditions tested. The final row contains the value for steering ratio.

The second page of tabular results for each vehicle lists the tilt table angles and tilt table ratios for the lateral and longitudinal Tilt Table tests conducted. These tables also list which wheel lifted first for each Tilt Table test; either Front or Rear for the lateral tilts and either Right, Left, or Equal (indicating simultaneous right and left wheel lift) for the longitudinal tilts.

As mentioned, the results contained in Appendix A were originally published in reports from previous studies, and additional comments about these results are in the previous reports. While these laboratory results are not particularly germane to the current study, they do show that the POC ESC system developed can be used to improve ATV stability and reduce the likelihood of rollovers for mid-sized ATVs like Vehicle G and for large ATVs like Vehicle N.

5.2 Discussion of Dynamic Test Results

Appendix C contains graphical test results for both vehicles. All test results for each vehicle are presented together, with results for Vehicle G on Pages 1-24 and Vehicle N on Pages 25-48 of Appendix C. For both vehicles there are 12 pages of results from dynamic tests conducted on asphalt followed by 12 pages of results for tests conducted on groomed dirt.

The sections of graphical results for each vehicle and test surface are in the following order:

- Dropped Throttle J-Turn Tests (Initial Speed of 20 mph)
- Slowly Increasing Steer Tests (Initial Speed of 15 mph)
- Circle Tests (Constant 50 ft Radius)
- Constant Steer Tests (Yaw Rate Ratio Tests)

Some general comments regarding the graphs presented for all test types are:

- The lateral accelerations shown on the graphs are the lateral accelerations parallel to the road plane, not the vehicle body-fixed lateral accelerations. The plots show lateral acceleration filtered using a single pass 8th order 6 Hz low-pass Butterworth filter using MATLAB's *filter* function. This filter is the same as the real-time filter implanted in the POC ESC algorithm, so the plots show lateral acceleration with the same amount of filtering and latency as was used in the real-time monitoring of lateral acceleration.
- The steering angles shown on the graphs are roadwheel steer angles, which are the RTD steer actuator input angles (handlebar angles) divided by the measured steering ratio.

For every test, regardless of the test type or test surface type, there are three pages of graphical results. The first page contains time domain plots of Roadwheel Steer Angle, Speed, Lateral Acceleration, Pitch Angle, Roll Angle, and Yaw Rate, with results from the run with POC ESC plotted in red and results from the run without ESC plotted in blue (for example see Page 1 of Appendix B). The second page has two columns. The left column contains graphs from the run without ESC and the right column contains graphs from the run with POC ESC. Each column contains three graphs: a North versus East Path Plot, and time domain plots of Lateral Acceleration and Longitudinal Acceleration. The Lateral Acceleration graph in the right column, for tests with POC ESC, contains region(s) that are shaded when the ESC algorithm senses "active", when the criteria of ESC Threshold A_y, Threshold Steering, and Threshold Speed are all exceeded. Page 2 of Appendix A is one of the second pages. The third page also has two columns, one with graphs from the run without ESC and one with graphs from the run with POC ESC. Each column contains three graphs: time domain plots of Throttle Stroke, Brake Stroke, and Speed. The speed graphs contain plots of the left front (LF), right front (RF), left rear (LR), and right rear (RR) wheel speeds (with translational speed units of mph).

5.2.1 Dropped Throttle J-Turn Tests (Initial Speed of 20 mph)

Pages 1, 13, 25, and 37 of Appendix B contain the first pages of J-Turn test results for Vehicle G on Asphalt, Vehicle G on Dirt, Vehicle N on Asphalt, and Vehicle N on Dirt, respectively. As mentioned, the runs without ESC were stopped when the measured lateral acceleration exceeded the ESC Threshold A_y level. For runs with POC ESC, when the ESC Threshold Ay level was achieved the POC ESC system intervened by dropping the throttle and applying braking at the hand brake. However, for these dropped throttle J-Turn tests, the throttle was already at zero prior to ESC intervention. The first page graphs show that ESC intervention reduced vehicle speed and reduced the duration of high levels of lateral acceleration and yaw rate. The duration and magnitude of high roll angles were also reduced by ESC intervention. The pitch angles were generally greater for the runs with ESC, because braking generated higher levels of deceleration during the runs with ESC.

The path plots shown on the second pages illustrate that the POC ESC system developed could improve ATV stability and reduce the likelihood of rollovers, by slowing the vehicle speed and by not causing the vehicle to deviate much from its original path. That is, there were no spin-outs or plow outs caused by ESC intervention. The second page lateral acceleration graphs for the runs with ESC are the graphs that have shaded regions showing when the ESC algorithm senses "active", when the criteria of ESC Threshold A_y, Threshold Steering, and Threshold Speed are all exceeded. The shading ends when lateral acceleration, speed, or steering signals drop below their threshold levels. However, for this proof-of-concept study, ESC intervention did not go on and off when in and out of the shaded regions; rather when the ESC first sensed a state of "active", the

ESC intervention started and did not stop until the vehicle speed came close to zero. As mentioned previously, there was no human driver in-the-loop to maintain control of the vehicle during and after ESC intervention. In this proof-of-concept study, for the ESC runs steering was maintained like it was in the non-ESC runs, and this was sufficient for maintaining control of the ATVs. In practice, commercial ESC systems cease intervention when pending instability conditions end.

The throttle strokes, brake strokes, and wheels speeds are shown on the third page graphs. For all the dropped throttle J-Turn runs, the throttle strokes shown are all zero. For the non-ESC runs, the brake stroke is also zero, except for runs when the RTD applied hold-level braking of 10 mm at the end of the run. For runs with POC-ESC, the brake stroke goes to its ESC-specified braking level as soon as ESC becomes "active". For Vehicle G, the ESC-specified braking is the triangular pulse braking profile used to mimic ABS. Pages 3 and 15 of Appendix B show the Vehicle G ESC braking pulses for J-Turn runs on asphalt and groomed dirt. On both surfaces, plots on the Speed graph show that cyclic braking prevents the right front wheel from locking. This demonstrates that the POC ABS used on Vehicle G did prevent wheel lockup. For Vehicle N, the vehicle with OEM ABS, the ESC-specified braking is a constant brake stroke. There is also no wheel lockup on Vehicle N.

The wheel speed graphs for the non-ESC J-Turns show an interesting feature of these runs, that being that the left front (inside front) wheel speed drops relative to the other wheel speeds as the J-Turn progresses. Once the left front wheel (tire) lifts off the ground, its speed drops less than the other wheels to the point that it is rotating faster than the other wheels. This phenomenon can best be seen in the lower left graph on Page 27 of Appendix B. This is the non-ESC J-Turn run of Vehicle N on groomed dirt, which had in a major 2WL lift with an extended period of front left wheel lift. When the left front wheel (tire) drops back down to the ground, its speed returns to matching the other wheel speeds.

5.2.2 Slowly Increasing Steer Tests (Initial Speed of 15 mph)

The first page graphs of the SIS tests (Pages 4, 16, 28, and 40[8] of Appendix B) show that ESC intervention reduced vehicle speed and the peak magnitudes and durations of roll angle, lateral acceleration, and yaw rate. These results illustrate that the POC ESC system developed could improve ATV stability and reduce the likelihood of lateral instabilities and rollovers.

For the tests without ESC, the maneuver was ended programmatically by the RTD when the lateral acceleration reached the Limit A_y level. For these non-ESC runs, the RTD program dropped the throttle and continued steering the desired steering input profile. The desired steering input profile is maintained during ESC intervention runs, and the path plots on the second pages show that the POC ESC equipped vehicles do not deviate much from their original (non-ESC) paths. POC ESC activation reduces speed by dropping the throttle and applying right front braking, so the ESC paths are much shorter and turn in less at the end than the non-ESC paths.

The throttle stroke, brake stroke, and wheels speed graphs are shown on the third pages. For these SIS maneuvers, the throttle increases gradually as the RTD speed controller tries to maintain

[8] Note: The data file for the non-ESC SIS test of Vehicle N on groomed dirt did not capture the entire run (up to when vehicle speed was close to zero), but the lateral acceleration shown is greater than the ESC Threshold A_y (see Page 40 of Appendix B).

constant speed while speed is being scrubbed off because of turning. For the non-ESC runs, the brake stroke is zero. For runs with POC ESC, the brake stroke goes to its ESC-specified braking level as soon as ESC becomes "active". For Vehicle G, the ESC-specified braking is the triangular pulse braking profile used to mimic ABS. Pages 6 and 18 of Appendix B show the Vehicle G ESC braking pulses for SIS runs on asphalt and groomed dirt. On both surfaces, plots on the speed graph show that cyclic braking prevents the right front wheel from locking. This demonstrates that the POC ABS used on Vehicle G did prevent complete wheel lockup. The magnitudes of the braking pulses used for the Vehicle G runs could be tuned to prevent the occasions of brief wheel lockup exhibited during these runs. For Vehicle N, the vehicle with OEM ABS, the ESC-specified braking is a constant brake stroke. There is also no wheel lockup on Vehicle N. There is ABS activity present on the ESC run of Vehicle N on groomed dirt, as indicated by the cyclic front right wheel speed shown on the Page 42 of Appendix B.

The wheel speed graphs show that the left front (inside front) wheel speed drops significantly relative to the other wheel speeds as the SIS turns progress. The vehicles are rear wheel drive, so the rear wheel speeds become greater than the right front wheel speed as the maneuvers become more severe, particularly on groomed dirt. Also, there are periods of small vibrations in the left rear wheel speeds, the lightly loaded inside rear drive wheel, particularly on groomed dirt.

5.2.3 Circle Tests (Constant 50 ft Radius)

The J-Turn and SIS tests are dynamic tests that develop lateral accelerations much faster than the quasi-static Circle and Constant Steer tests. The first page graphs of the Circle tests (Pages 7, 19, 31, and 43[9] of Appendix B) show that ESC intervention reduced vehicle speed and the peak magnitudes and durations of roll angle, lateral acceleration, and yaw rate. These results illustrate that the POC ESC system developed could improve ATV stability and reduce the likelihood of lateral instabilities and rollovers.

For the tests without ESC, the maneuver was ended programmatically by the RTD when the lateral acceleration reached the Limit A_y level. For these non-ESC runs, at a high lateral acceleration level, the RTD program dropped the throttle and continued steering using circular path following steering. The path plots on the second pages show that the POC ESC equipped vehicles follow the circular path like the non-ESC vehicles do. The second page lateral acceleration graphs for the runs with ESC are the graphs that have shaded regions showing when the ESC algorithm senses "active", when the criteria of ESC Threshold A_y, Threshold Steering, and Threshold Speed are all exceeded. The shading ends when lateral acceleration, speed, or steering signals drop below their threshold levels. The shaded regions are similar in duration to the regions observed during the J-Turn and SIS runs, generally a few tenths of a second to one second long. Since the brakes were applied during ESC intervention, the longitudinal deceleration during the POC ESC runs is greater than the longitudinal deceleration during the non-ESC runs.

The throttle stroke, brake stroke, and wheels speed graphs are shown on the third pages. For these Circle tests, the throttle is increased in piecewise linear fashion. For the non-ESC runs, the brake stroke is zero. For runs with POC-ESC, the brake stroke goes to its ESC-specified braking level

[9] Note: The data file for the non-ESC Circle test of Vehicle N on groomed dirt did not capture the entire run (up to when vehicle speed was close to zero), but the lateral acceleration shown is greater than the ESC Threshold A_y (see Page 43 of Appendix B).

as soon as ESC becomes "active". For Vehicle G, the ESC-specified braking is the triangular pulse braking profile used to mimic ABS. For the ESC equipped vehicles on groomed dirt, right front wheel speed plots for both vehicles exhibit signs of ABS activity (Page 21 for Vehicle G and Page 45 for Vehicle N). Again, this demonstrates that the POC ABS used on Vehicle G did prevent complete wheel lockup. However, the magnitudes of the braking pulses used for Vehicle G could be tuned to prevent the occasions of brief wheel lockup exhibited during the ESC run.

The wheel speed graphs show that the left front (inside front) wheel speed drops relative to the other wheel speeds as the turns progress. Also, there are periods of small vibrations in the left rear wheel speeds, the lightly loaded inside rear drive wheel, particularly on groomed dirt.

5.2.4 Constant Steer Tests (Yaw Rate Ratio Tests)

Pages 10, 22, 34, and 46 of Appendix B contain the first pages of Constant Steer test results for Vehicle G on Asphalt, Vehicle G on Dirt, Vehicle N on Asphalt, and Vehicle N on Dirt, respectively. The results from the Constant Steer tests are much like the results from the Circle tests. The first page graphs show that ESC intervention reduced vehicle speed and the peak magnitudes and durations of roll angle, lateral acceleration, and yaw rate. Again, these results illustrate that the POC ESC system developed could improve ATV stability and reduce the likelihood of lateral instabilities and rollovers.

For the tests without ESC, the maneuver was ended programmatically by the RTD when the lateral acceleration reached the Limit A_y level. For the non-ESC runs, the maneuvers were ended by dropping the throttle and continuing to hold the constant steer input. The path plots on the second pages show that the POC ESC equipped vehicles follow a path like the non-ESC vehicle do, but the ESC paths are shorter because of ESC intervention. The second page lateral acceleration graphs for the runs with ESC are the graphs that have shaded regions showing when the ESC algorithm senses "active". The shaded regions are similar in duration to the regions observed during the other test types, generally a few tenths of a second to one second long. Since the brakes were applied during ESC activation, the longitudinal deceleration during the POC ESC runs is greater than the longitudinal deceleration during the non-ESC runs.

The throttle stroke, brake stroke, and wheels speed graphs are shown on the third pages. For these Constant Steer tests, the throttle is increased in piecewise linear fashion. For the non-ESC runs, the brake stroke is zero. For runs with POC-ESC, the brake stroke goes to its ESC-specified braking level as soon as ESC becomes "active". Like what happened during the ESC Circle tests on groomed dirt, for the ESC Constant Steer tests on groomed dirt the right front wheel speed plots for both vehicles exhibited signs of ABS activity (Page 24 for Vehicle G and Page 48 for Vehicle N).

Also like the results from the Circle tests, the wheel speed graphs show that the left front (inside front) wheel speed drops relative to the other wheel speeds as the turns progress. Likewise, there are periods of small vibrations in the left rear wheel speeds, the lightly loaded inside rear drive wheel, particularly on groomed dirt.

5.3 Summary

The objectives of this study were fulfilled. A proof-of-concept (POC) Electronic Stability Control (ESC) system was designed, built, and tested on two different ATVs. Results from tests with the POC ESC system turned on showed that it could improve ATV handling (yaw) stability and lateral (roll) stability, and that it could reduce the likelihood of rollover events.

An algorithm to monitor real-time vehicle states and to then react in appropriate fashion to limit potential lateral and rollover instabilities was developed and implemented. The ESC algorithm involved comparing measured vehicle states of speed, steering, and real-time filtered lateral acceleration to threshold level values. If the measured signals all exceeded threshold levels, and POC ESC system would intervene by dropping the throttle and braking the right front wheel, which during the left turn maneuvers used in this study helped reduce vehicle speed and also added a correcting (stabilizing) yaw moment to the vehicle.

One of the vehicles tested was equipped with an OEM Antilock Braking System (ABS) and the other vehicle was not. For the non-ABS equipped vehicle, Vehicle G, the electric motor of the Robotic Test Driver (RTD) was used to apply cyclical inputs to the hand brake to emulate ABS braking. Previous studies using Vehicle G indicated that it had oversteer characteristics, and this made it a good candidate ATV for this study.

Decisions on what levels to use for the ESC speed, steering, and lateral acceleration thresholds were based on results from previous tests conducted using the two test vehicles. These previous tests conducted on asphalt and groomed dirt provided baseline vehicle responses and stability characteristics needed to select the magnitude of lateral acceleration to use for the ESC Threshold A_y levels.

Four types of test maneuvers were used to evaluate the feasibility of the POC ESC system developed, J-Turn tests, Slowly Increasing Steer tests, Circle tests, and Constant Steer tests. For all four test types, runs were conducted on both asphalt and groomed dirt surfaces using both vehicles with and without the POC ESC turned on. In all cases, the runs without ESC were executed to severities with lateral accelerations above the ESC Threshold A_y levels to establish baselines representing near-instability conditions. Then the ESC runs were executed to show that, in all cases, the POC ESC system could improve handling and lateral stability. For all tests, no two-wheel lifts or tip-ups onto the outriggers resulted when the ESC system activated.

Since there was no human driver in-the-loop to maintain control of the vehicles during and after ESC intervention, for the ESC runs steering was maintained like it was in the non-ESC runs, and this was sufficient for maintaining control of the ATVs. Also, since there was no human driver used in this study, once the POC ESC dropped throttle and applied braking, the throttle was left off and braking left on until the vehicle came to a stop. In practice, commercial ESC systems would not steer the vehicle during ESC intervention or cease intervention when pending instability conditions ended.

For this proof-of-concept study, when ESC was activated, the throttle was dropped all the way to zero and there was no effort made to evaluate the efficacy of various degrees of non-zero throttle. Also, for this proof-of-concept study, the ESC braking inputs used were generally large, in some cases large enough to demonstrate ABS brake cycling. There were no efforts made to tune the

amount of ESC braking applied. The POC ESC system developed could be refined with further work by tuning the levels and timing of the dropped throttle and braking commands. The ESC threshold levels could also be refined and made dependent on the states of real-time measured or predicted vehicle responses.

Vehicle G

	Curb	Driver	Driver Plus Instrumentation (DPI)	Gross Vehicle Weight (GVW)
VIMF Test Number		5783	5784	5848
Total Vehicle Weight (lb)	694.0	909.4	928.6	1168.7
Left Front Weight (lb)	174.2	215.4	223.9	253.3
Right Front Weight (lb)	168.1	199.1	219.4	251.0
Left Rear Weight (lb)	175.9	246.6	242.5	332.9
Right Rear Weight (lb)	175.8	248.3	242.8	331.5
Front Track Width (in)	36.35	36.45	36.50	36.45
Rear Track Width (in)	35.60	36.10	36.06	36.60
Average Track Width (in)	35.98	36.28	36.28	36.53
Wheelbase (in)	50.55	50.65	50.60	50.60
CG Longitudinal (in)	25.62	27.56	26.44	28.77
CG Lateral (in)	-0.16	-0.29	-0.08	-0.06
CG Height (in)		24.07	23.34	26.13
Roll Inertia - I_{XX} (ft-lb-s^2)		79	75	109
Pitch Inertia - I_{YY} (ft-lb-s^2)		110	117	198
Yaw Inertia - I_{ZZ} (ft-lb-s^2)		88	96	163
Roll/Yaw - I_{XZ} (ft-lb-s^2)		5	5	17
SSF		0.753	0.777	0.699
KST		0.754	0.777	0.699
Steering Ratio (deg/deg)			1.41	

Vehicle G

		Driver	Driver Plus Instrumentation (DPI)	Gross Vehicle Weight (GVW)
Lateral Right Tilt	**Right Tilt First Wheel Lift**	Rear	Rear	Rear
	Right Tilt Angle (TTA) (deg)	28.2	28.4	24.1
	Right Tilt Ratio (TTR)	0.535	0.540	0.446
Lateral Left Tilt	**Left Tilt First Wheel Lift**	Rear	Rear	Rear
	Left Tilt Angle (TTA) (deg)	28.8	28.8	24.3
	Left Tilt Ratio (TTR)	0.550	0.551	0.452
	Average Lateral TTA (deg)	**28.5**	**28.6**	**24.2**
	Average Lateral TTR	**0.542**	**0.545**	**0.449**
Longitudinal Front Tilt	**Front Tilt First Wheel Lift**	Left	Left	Right
	Front Tilt TTA (FTTA) (deg)	49.3	48.1	45.3
	Front Tilt TTR (FTTR)	1.163	1.114	1.011
Longitudinal Rear Tilt	**Rear Tilt First Wheel Lift**	Left	Right	Left
	Rear Tilt TTA (RTTA) (deg)	43.1	44.1	38.7
	Rear Tilt TTR (RTTR)	0.935	0.969	0.802

Vehicle G

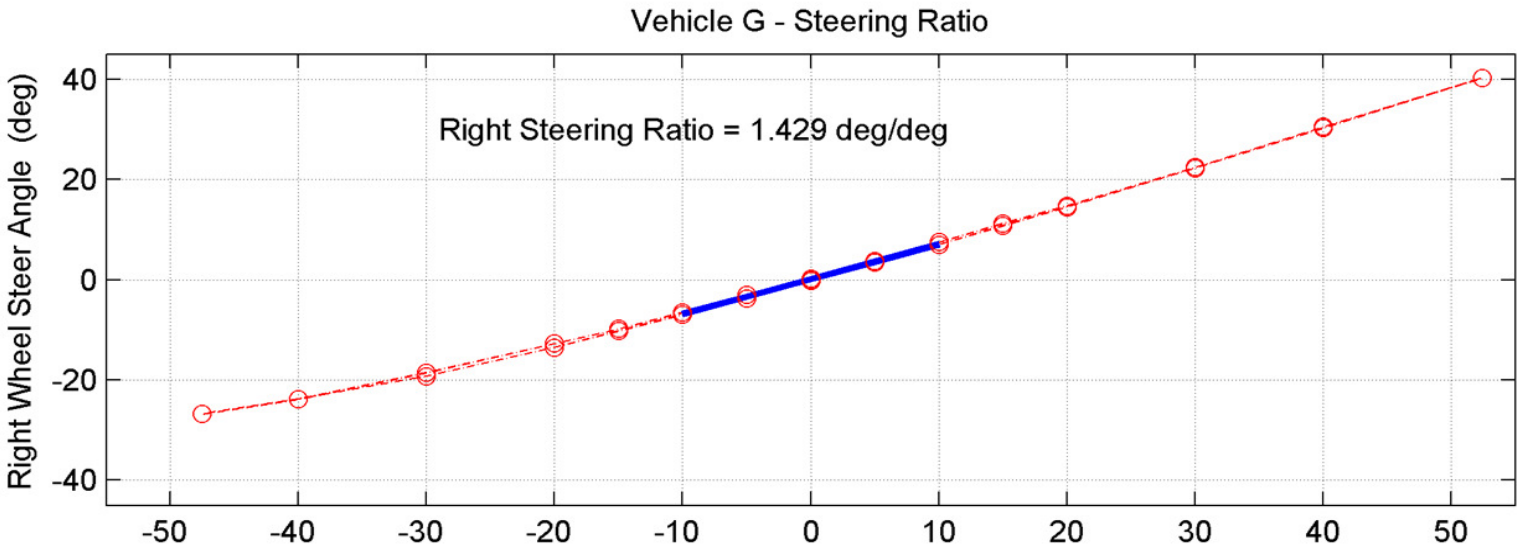

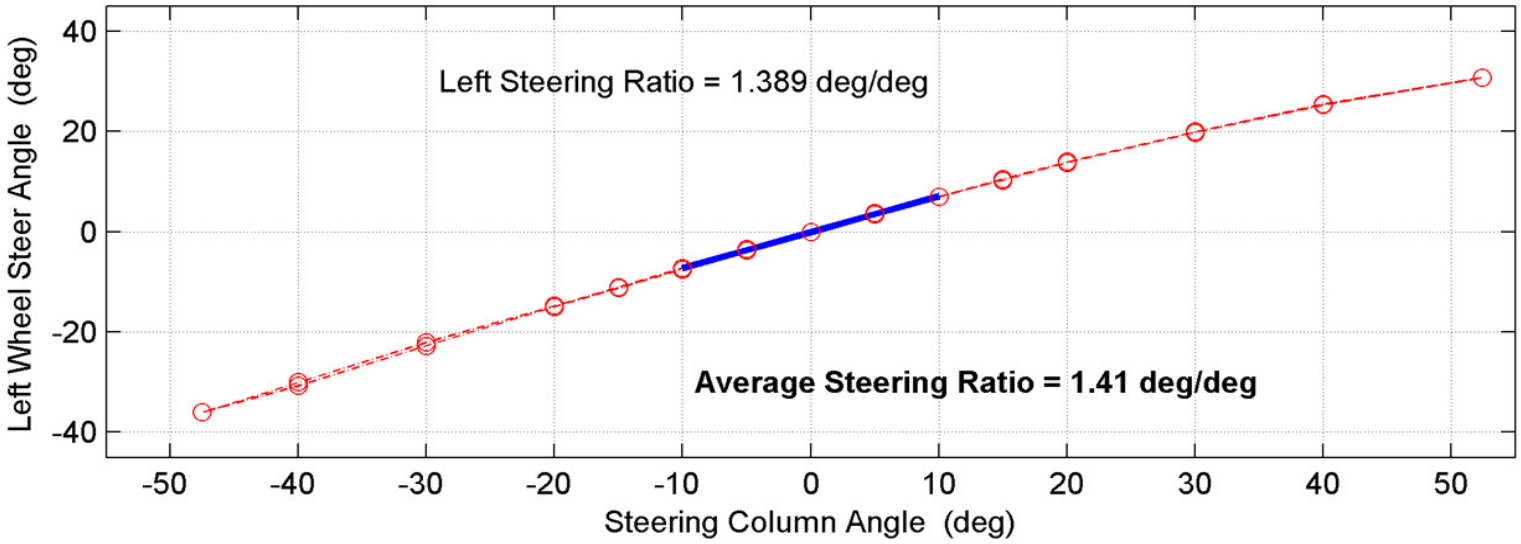

Vehicle N

	Curb	Driver	Autonomous Ballast to Driver Loading	Gross Vehicle Weight (GVW)
VIMF Test Number	7821	7822	7919	7823
Total Vehicle Weight (lb)	951.0	1164.9	1164.2	1463.5
Left Front Weight (lb)	240.3	274.2	273.0	309.1
Right Front Weight (lb)	235.8	271.8	266.9	300.9
Left Rear Weight (lb)	228.4	300.7	299.0	420.2
Right Rear Weight (lb)	246.5	318.2	325.3	433.3
Front Track Width (in)	39.80	39.90	39.90	40.10
Rear Track Width (in)	38.20	38.28	38.28	38.28
Average Track Width (in)	39.00	39.09	39.09	39.19
Wheelbase (in)	50.80	51.10	51.00	51.35
CG Longitudinal (in)	25.37	27.15	27.35	29.95
CG Lateral (in)	0.27	0.25	0.33	0.06
CG Height (in)	20.32	23.12	22.55	25.10
Roll Inertia - I_{XX} (ft-lb-s^2)	41	76	75	100
Pitch Inertia - I_{YY} (ft-lb-s^2)	118	144	181	232
Yaw Inertia - I_{ZZ} (ft-lb-s^2)	123	130	171	206
Roll/Yaw - I_{XZ} (ft-lb-s^2)	2	9	9	21
SSF	0.960	0.845	0.867	0.781
KST	0.960	0.846	0.868	0.784
Steering Ratio (deg/deg)			1.50	

Vehicle N

		Curb	Driver	Autonomous Ballast to Driver Loading	Gross Vehicle Weight (GVW)
Lateral Right Tilt	**Right Tilt First Wheel Lift**	Rear	Rear	Rear	Rear
	Right Tilt Angle (TTA) (deg)	38.6	31.7	33.7	26.5
	Right Tilt Ratio (TTR)	0.797	0.618	0.667	0.498
Lateral Left Tilt	**Left Tilt First Wheel Lift**	Rear	Rear	Rear	Rear
	Left Tilt Angle (TTA) (deg)	39.2	32.9	35.2	27.6
	Left Tilt Ratio (TTR)	0.817	0.647	0.706	0.522
	Average Lateral TTA (deg)	**38.9**	**32.3**	**34.5**	**27.0**
	Average Lateral TTR	**0.807**	**0.632**	**0.687**	**0.510**
Longitudinal Front Tilt	**Front Tilt First Wheel Lift**	Left	Left	Right	Left
	Front Tilt TTA (FTTA) (deg)	52.0	48.1	50.6	45.6
	Front Tilt TTR (FTTR)	1.279	1.113	1.219	1.020
Longitudinal Rear Tilt	**Rear Tilt First Wheel Lift**	Right	Right	Equal	Right
	Rear Tilt TTA (RTTA) (deg)	52.6	44.4	43.3	35.8
	Rear Tilt TTR (RTTR)	1.306	0.979	0.944	0.722

Vehicle N

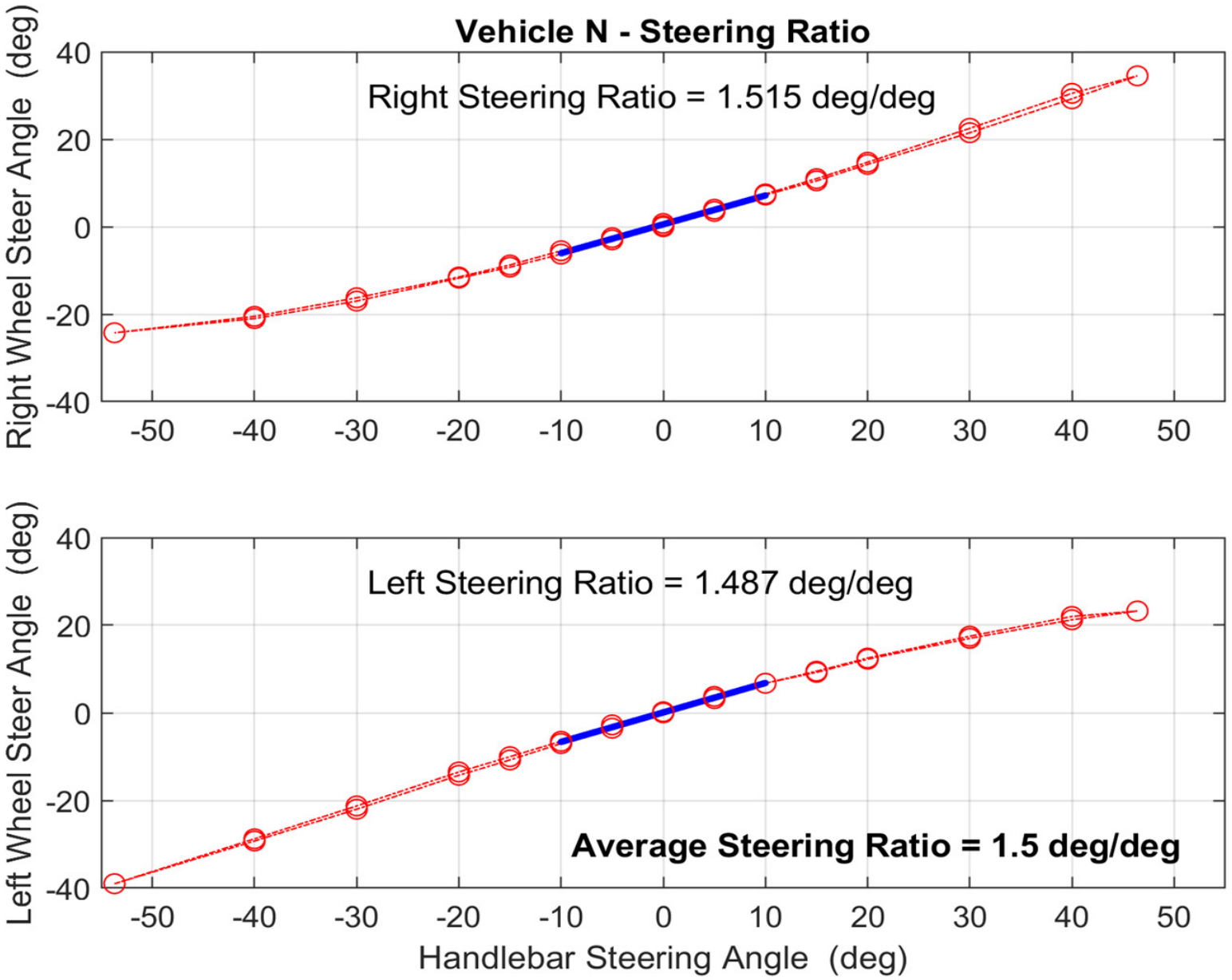

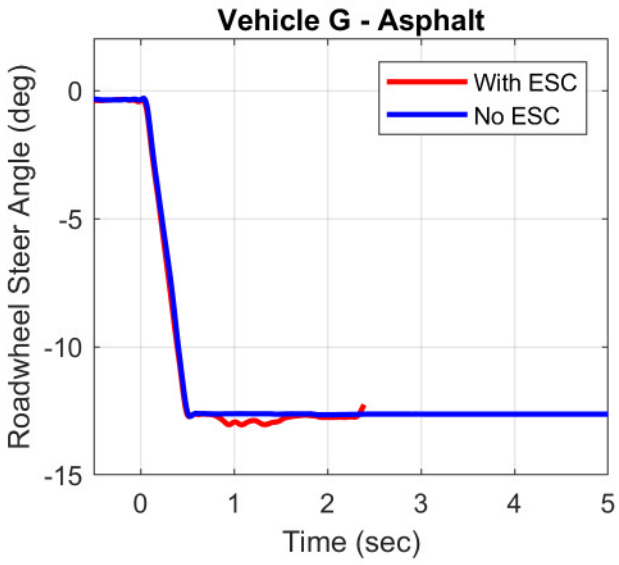

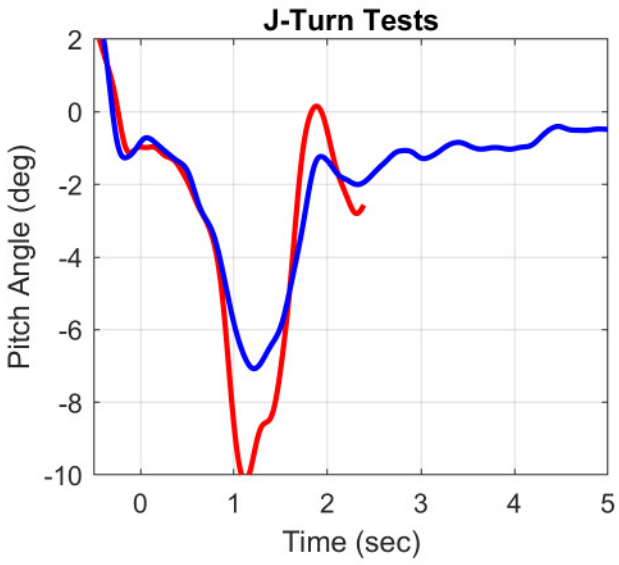

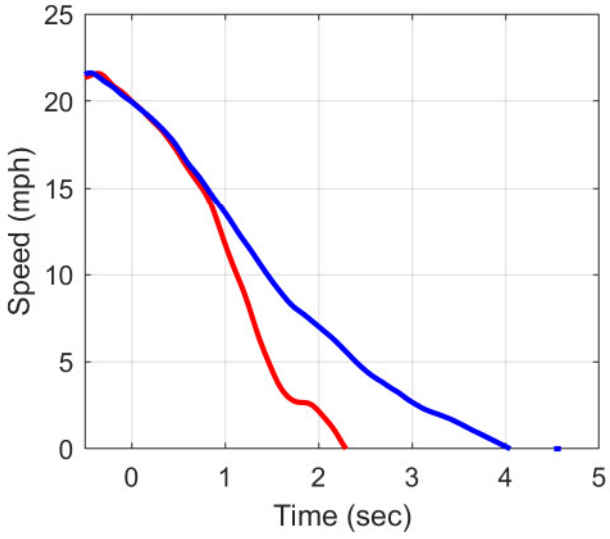

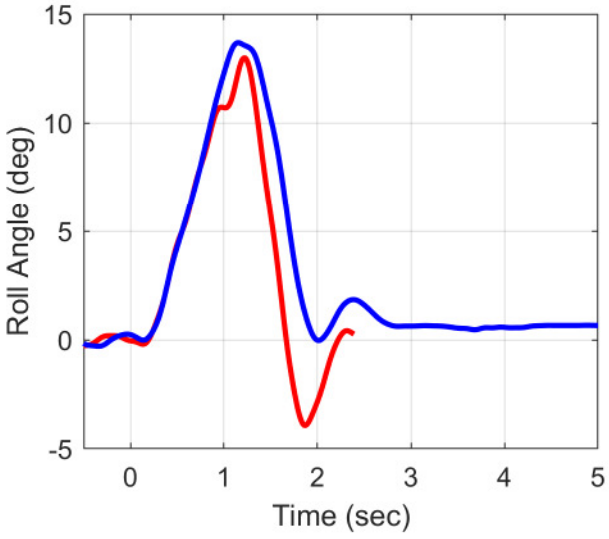

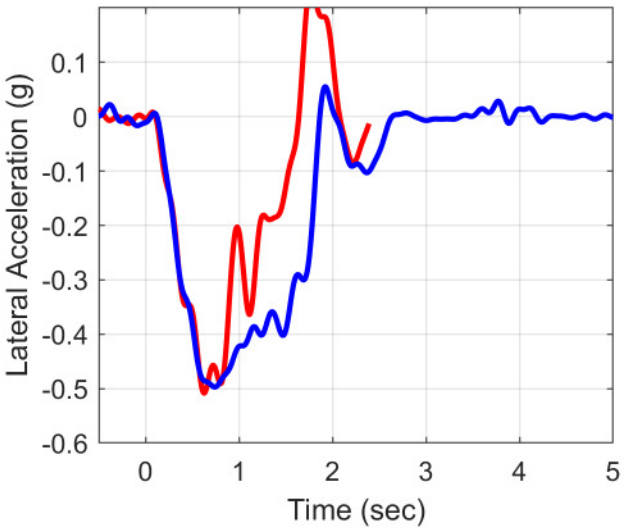

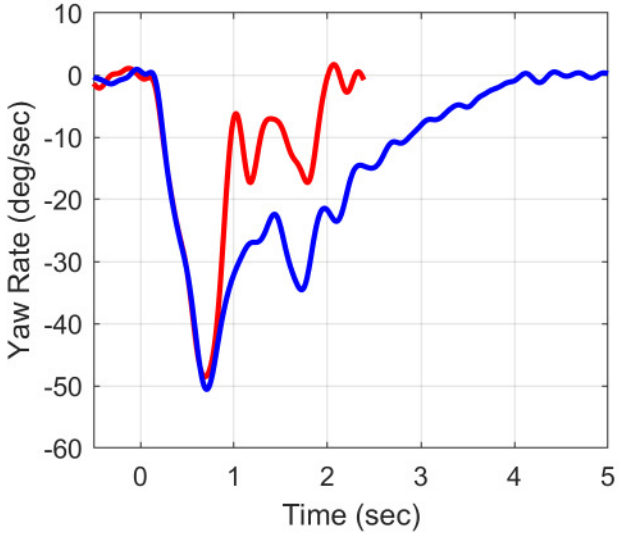

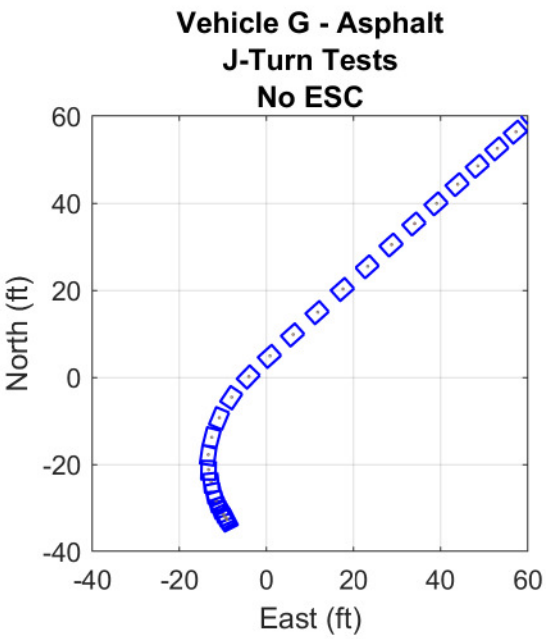

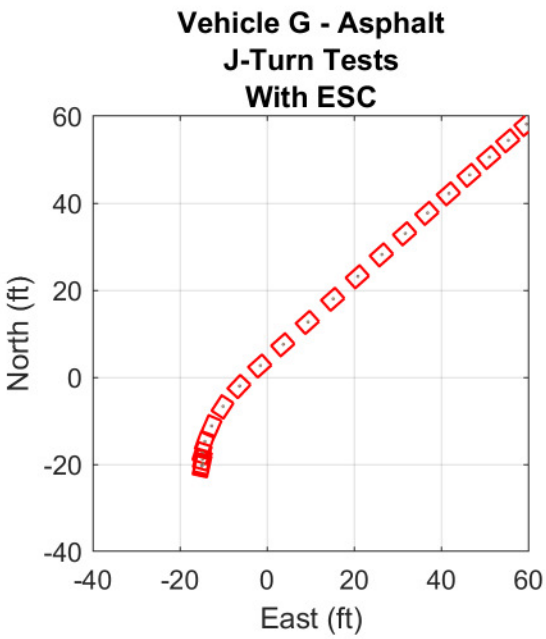

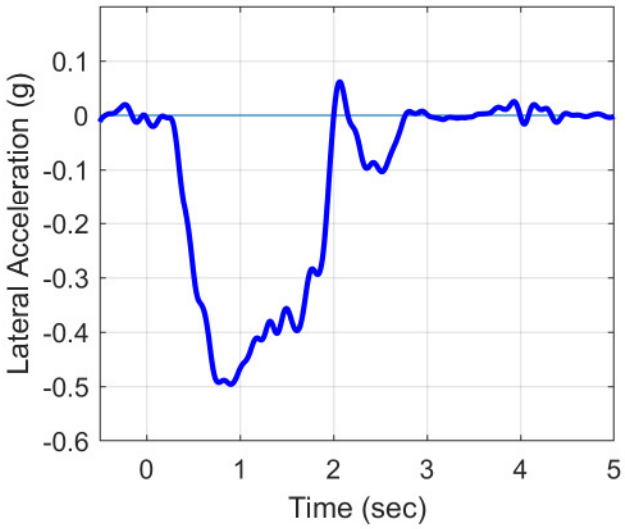

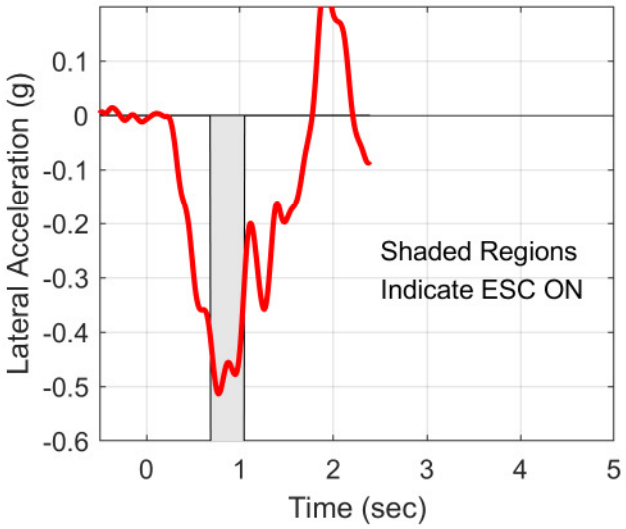

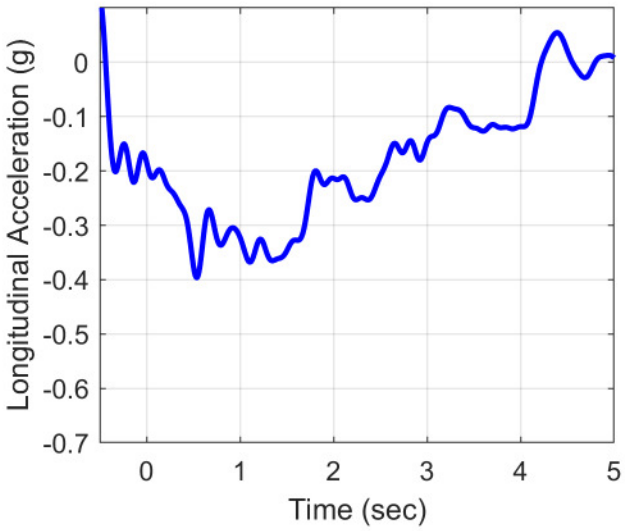

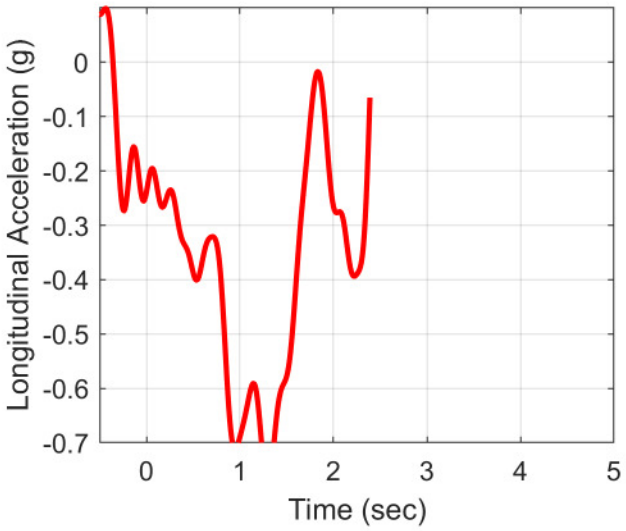

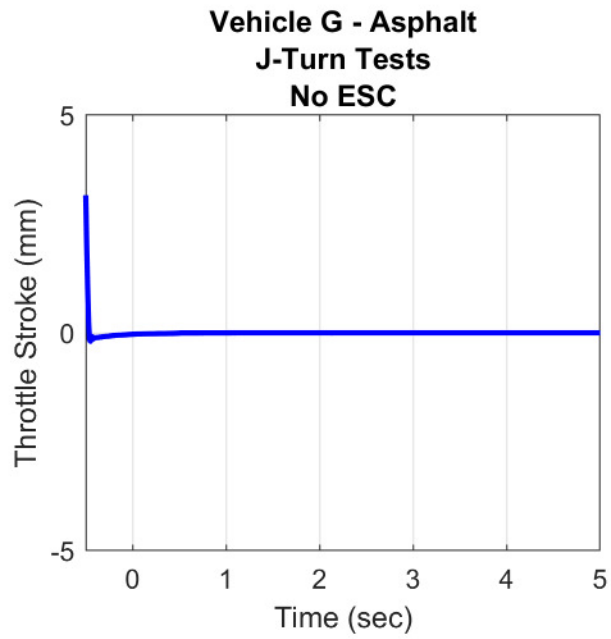

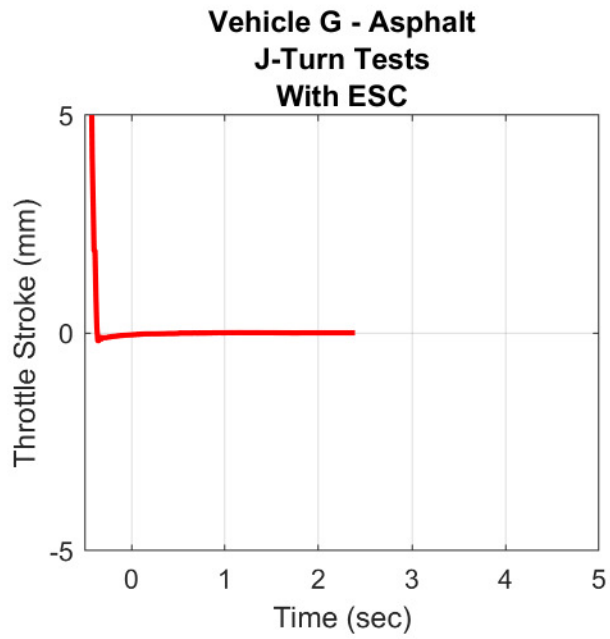

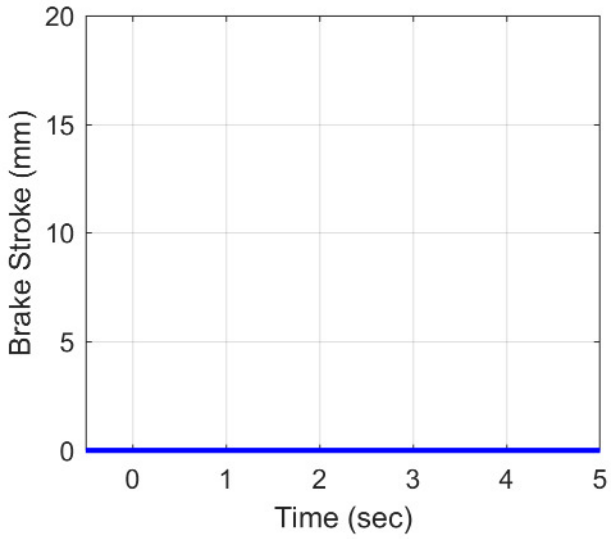

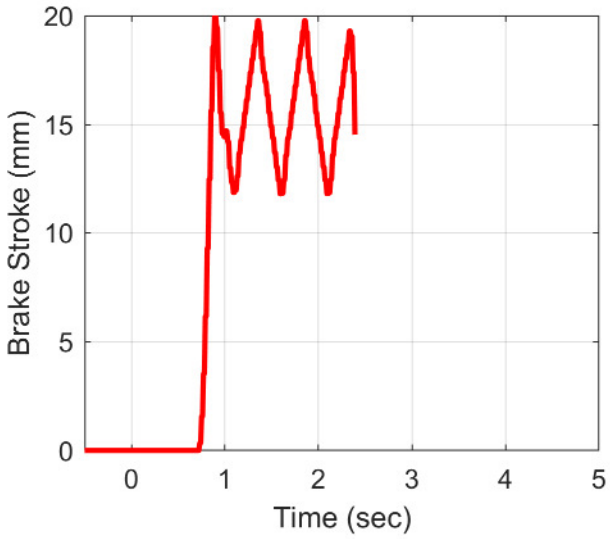

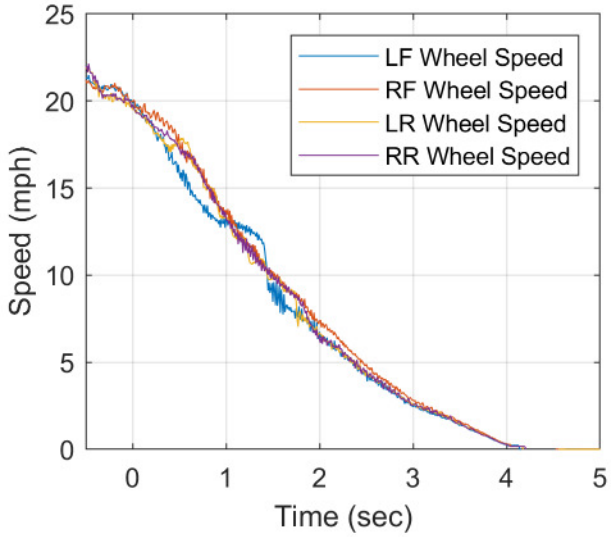

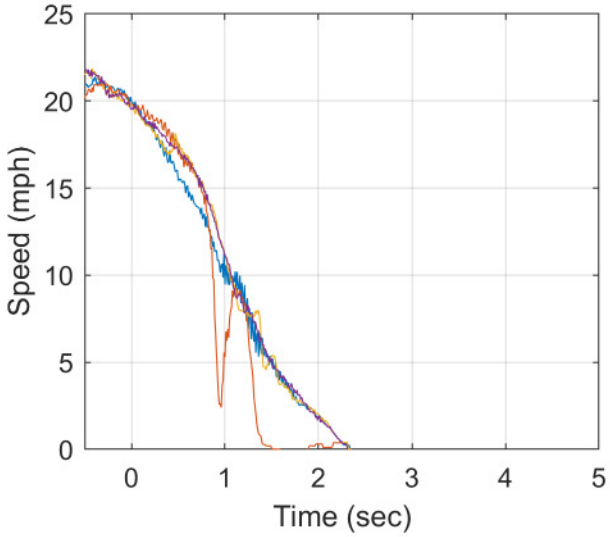

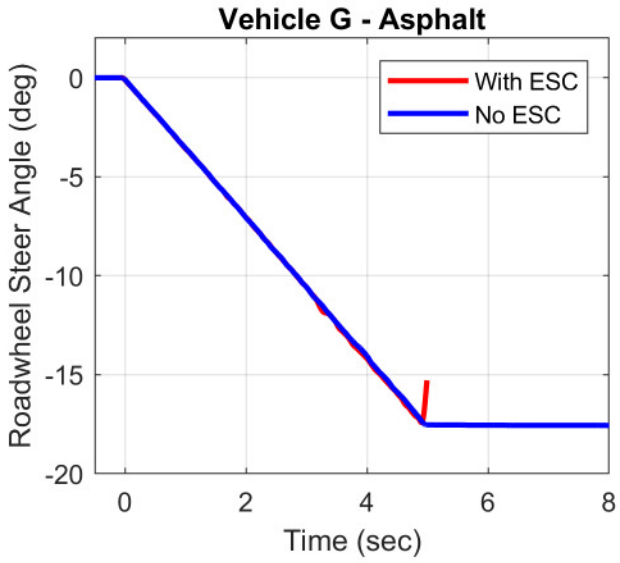

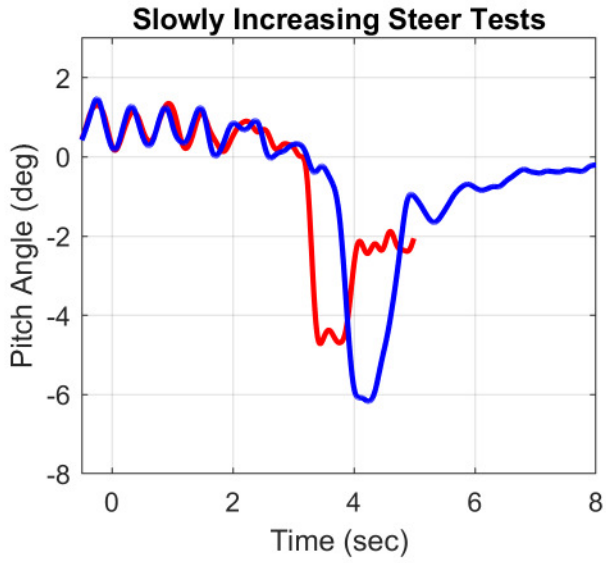

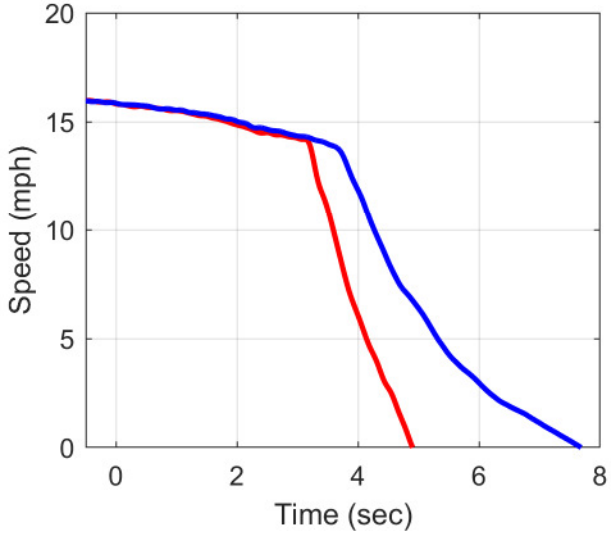

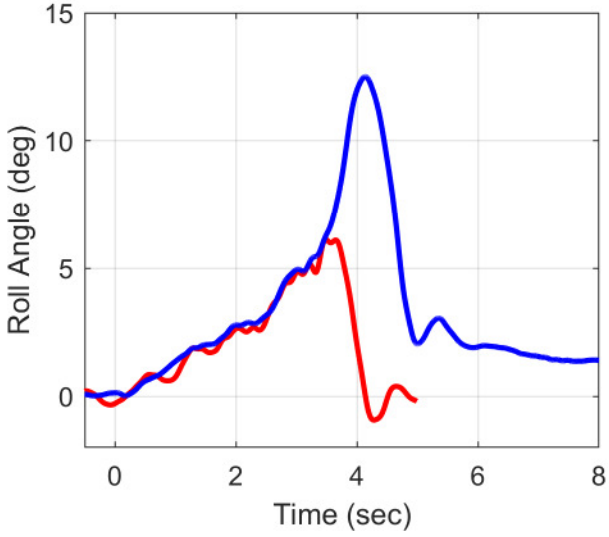

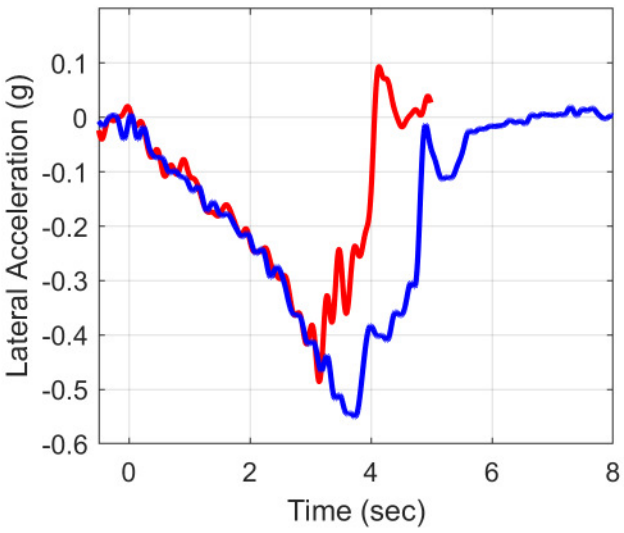

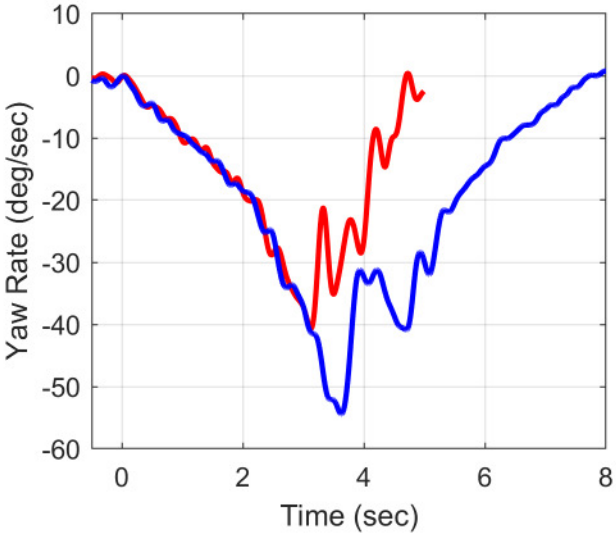

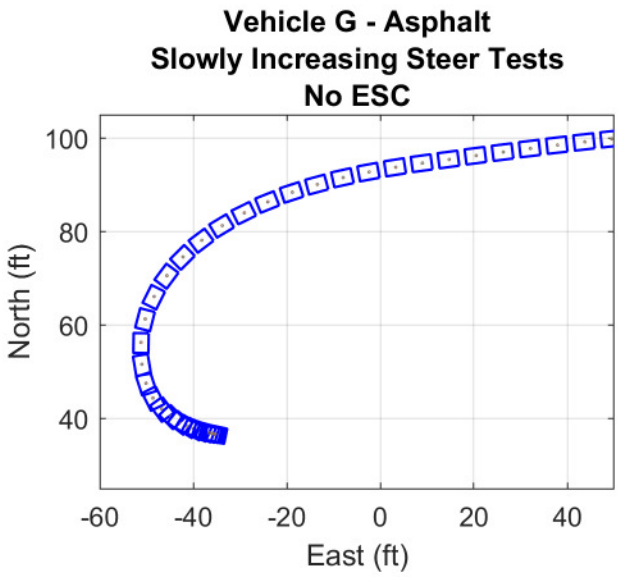

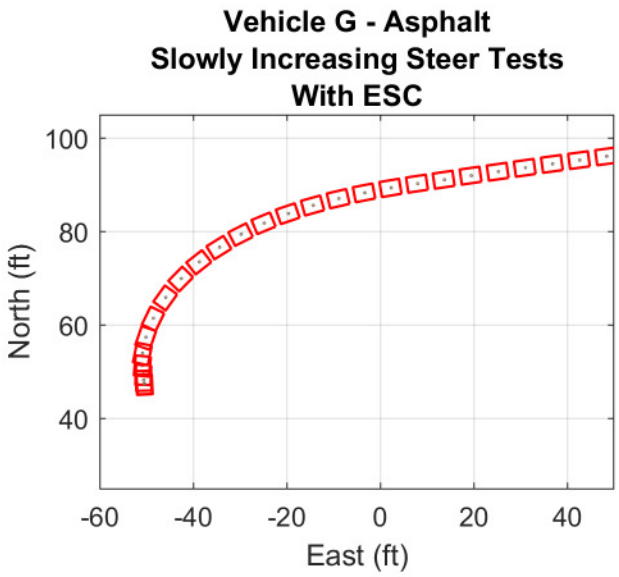

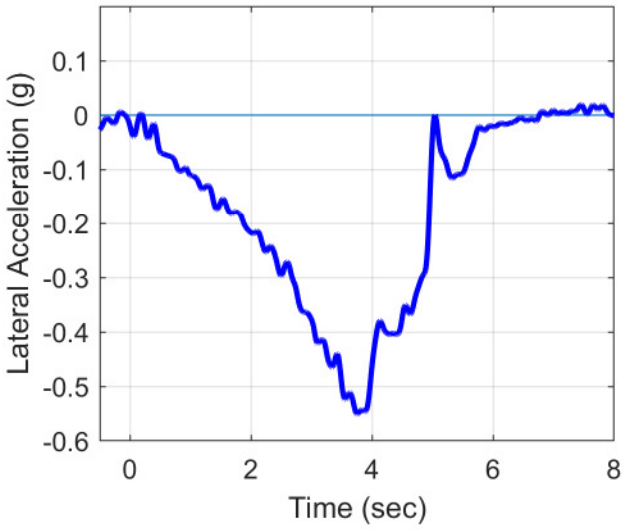

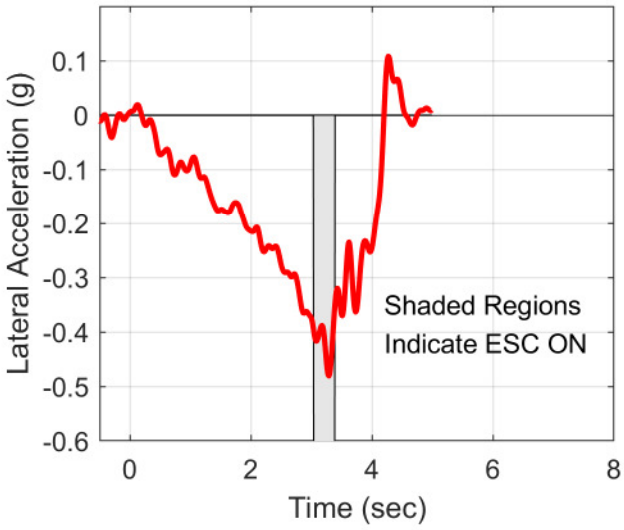

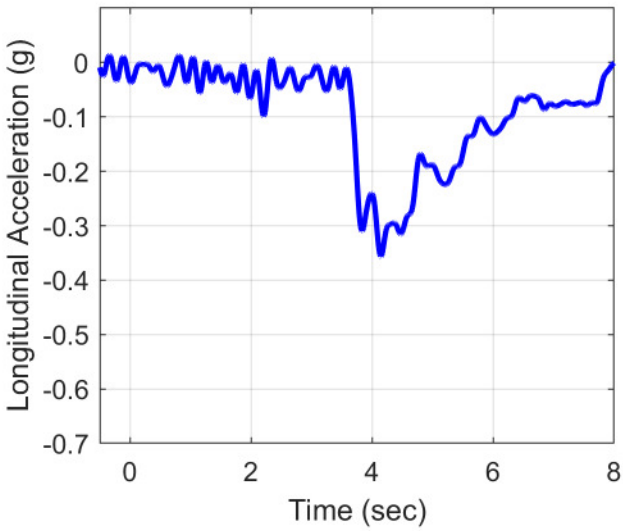

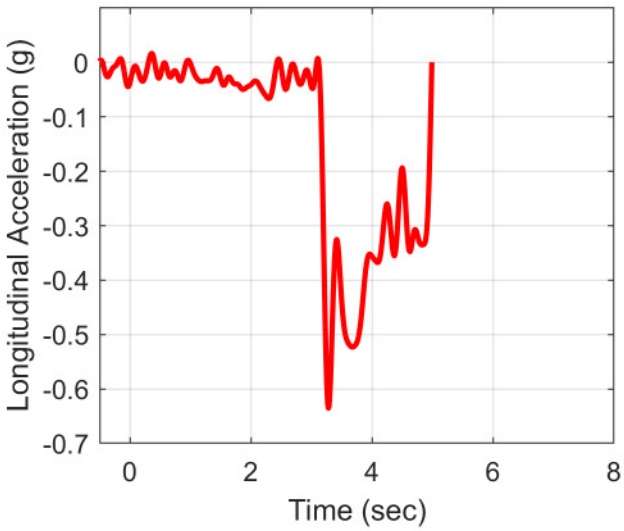

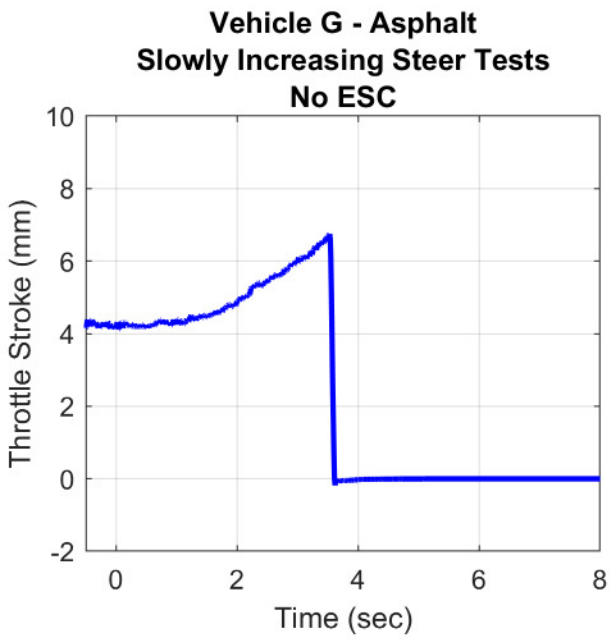

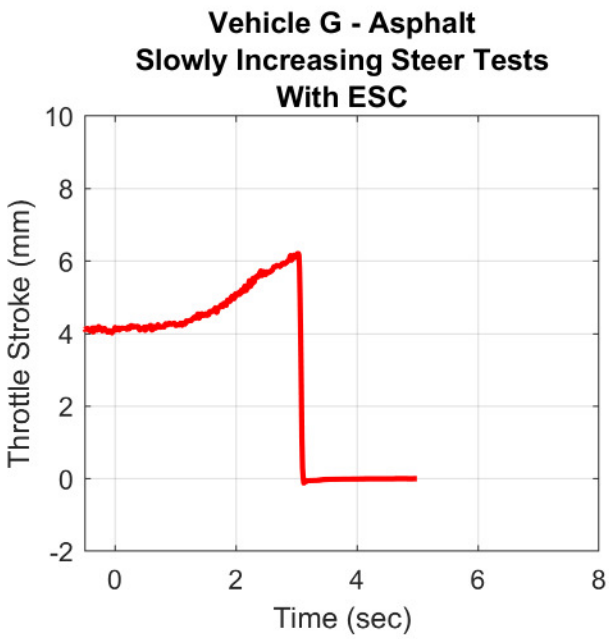

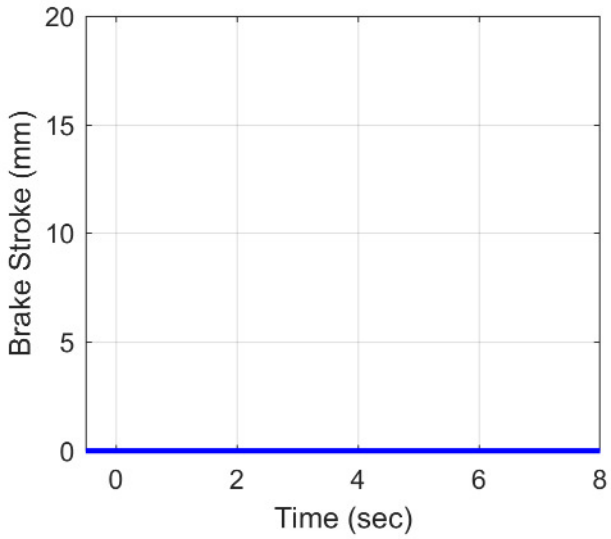

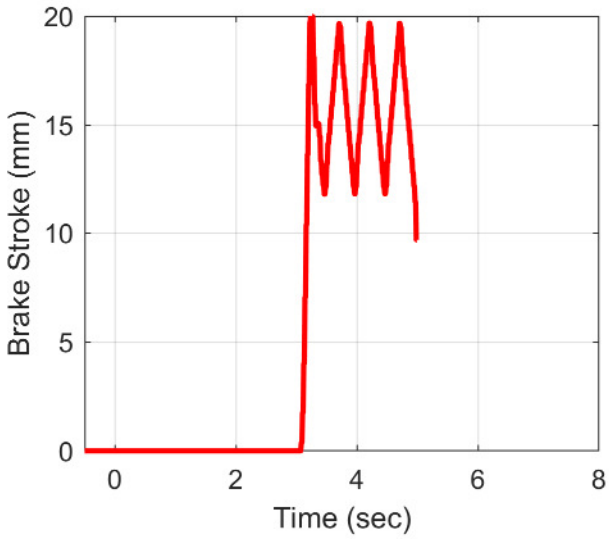

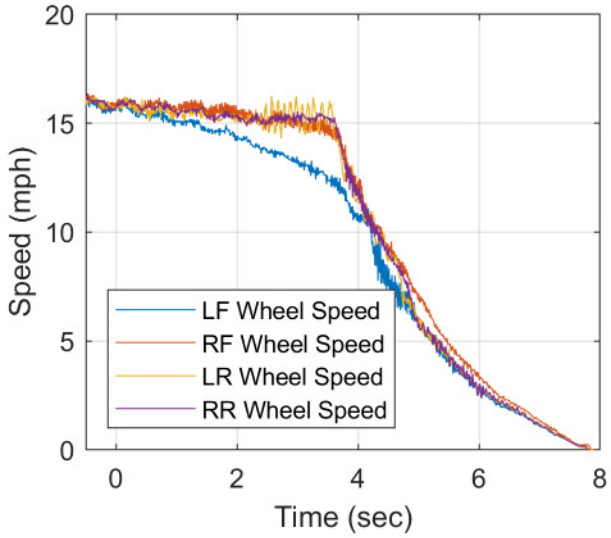

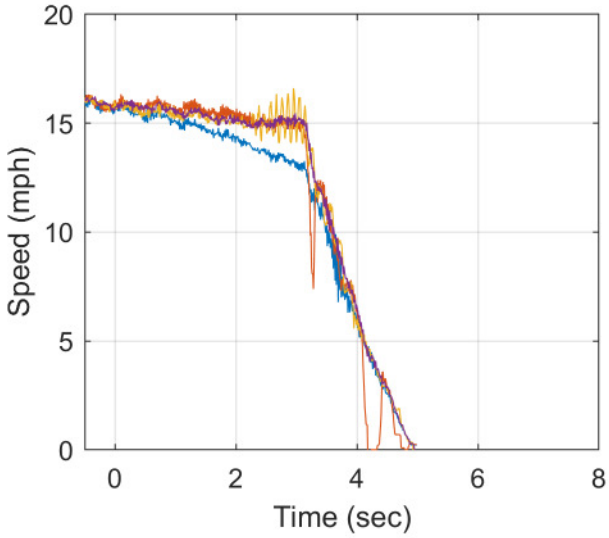

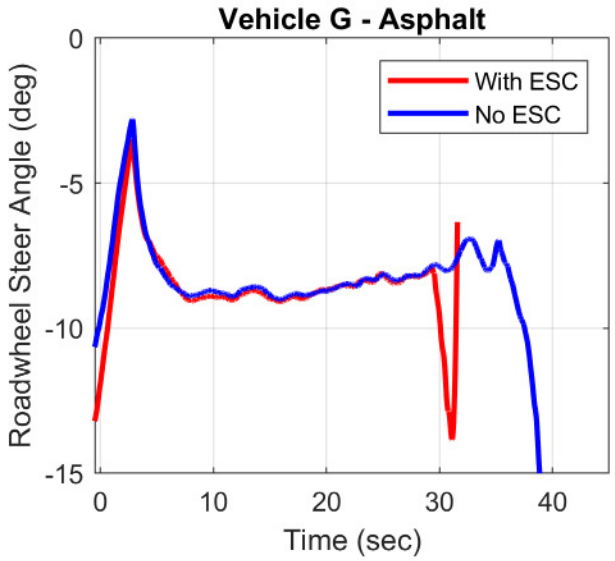

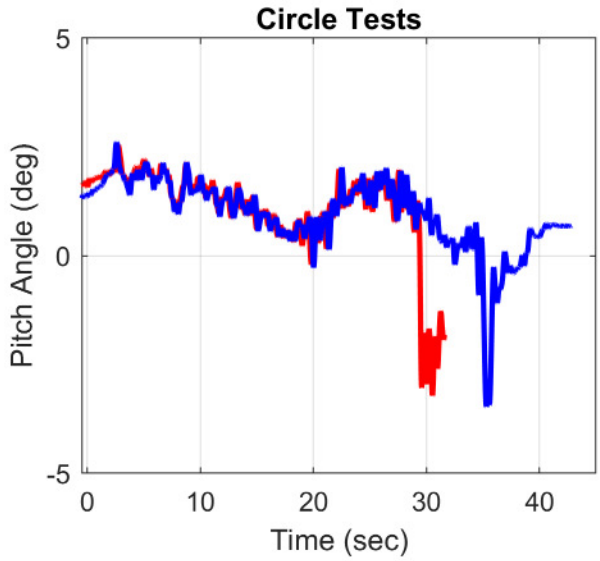

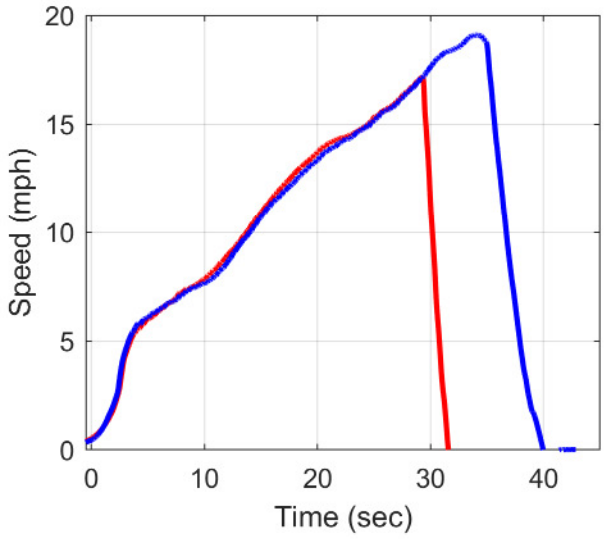

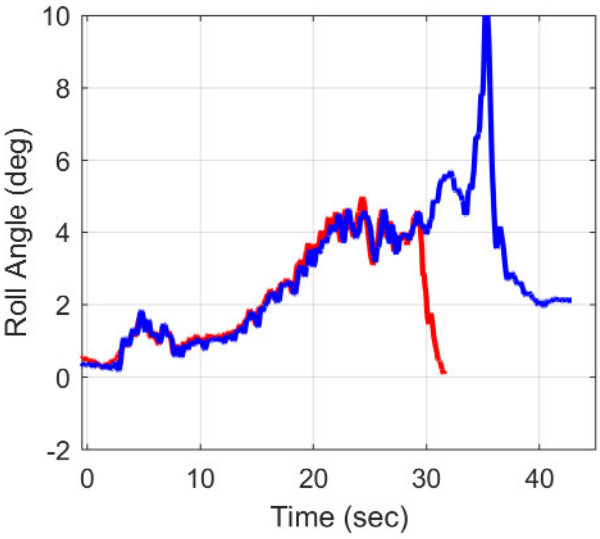

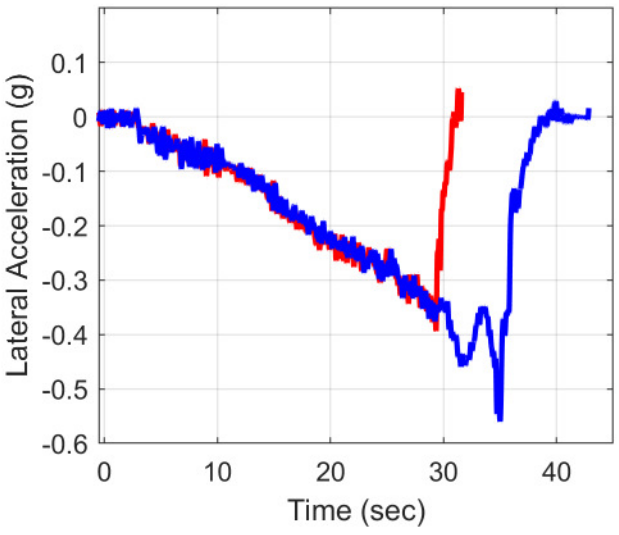

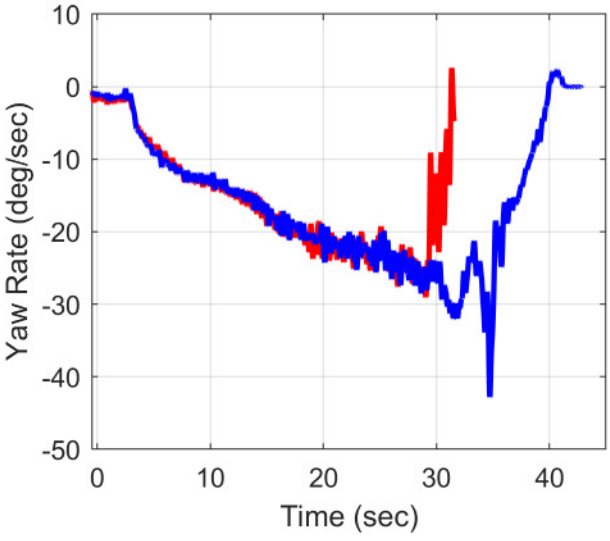

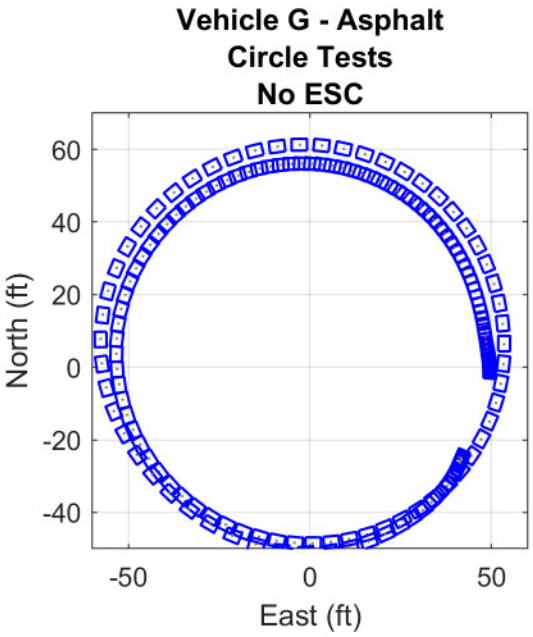

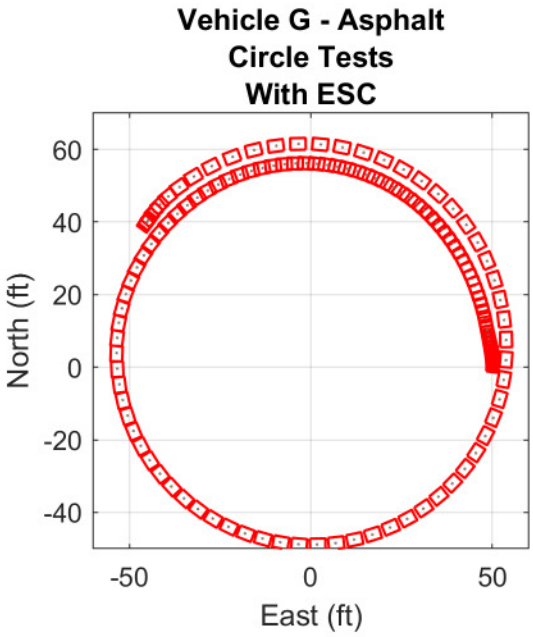

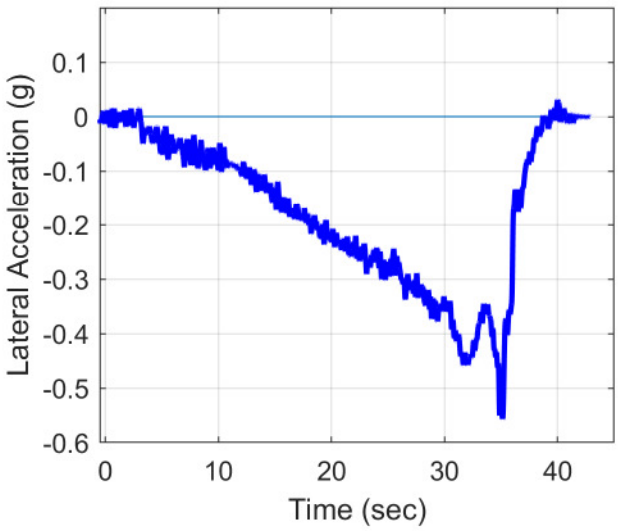

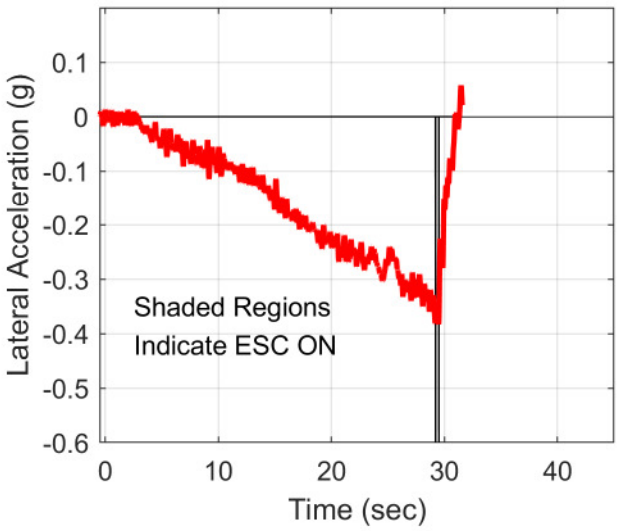

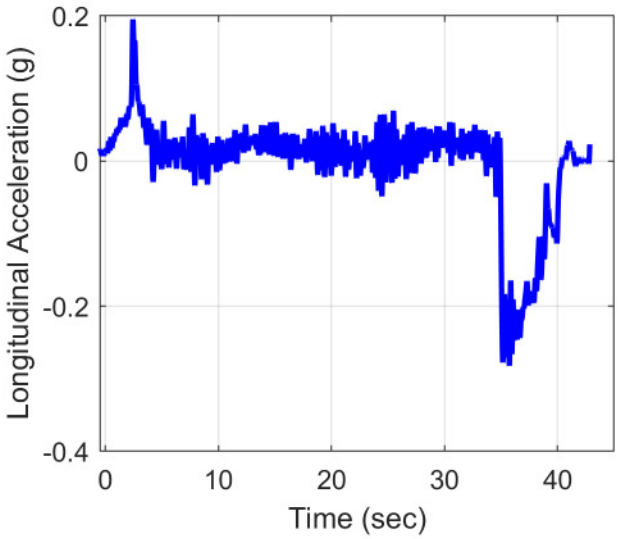

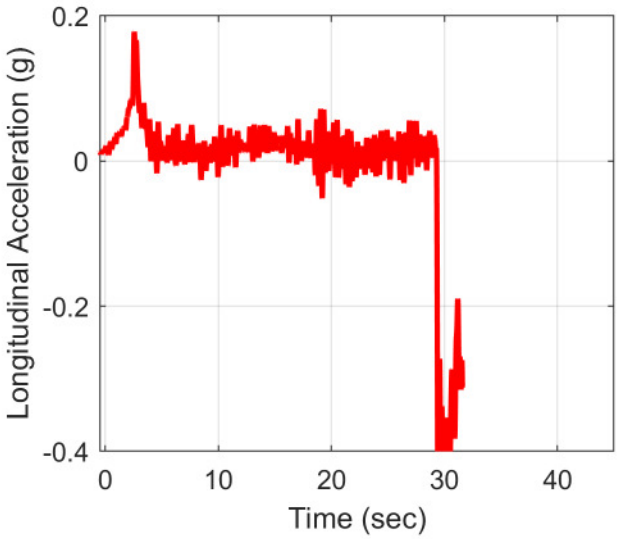

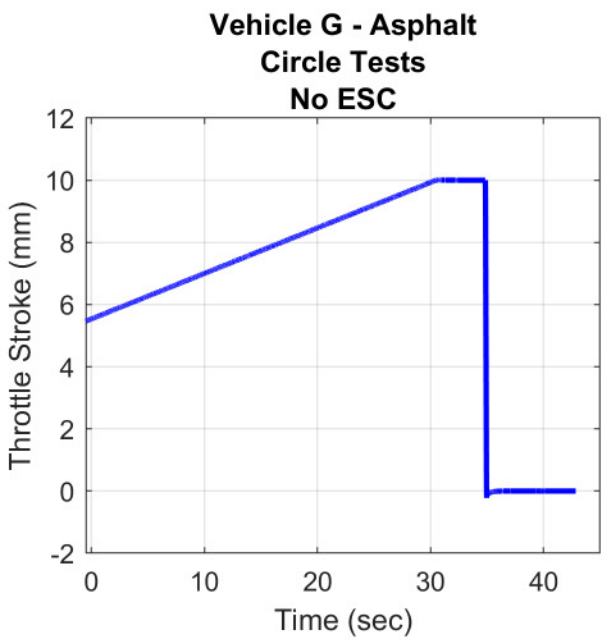

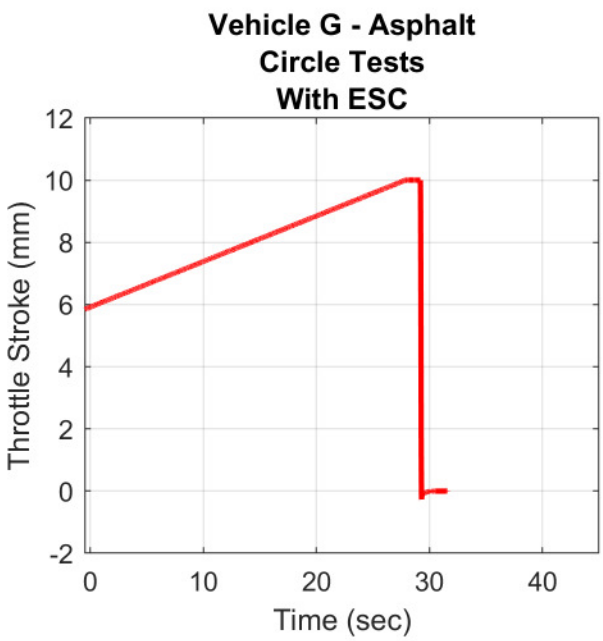

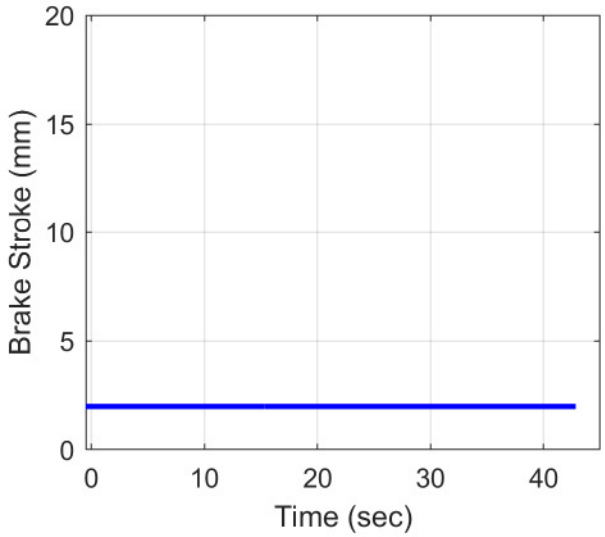

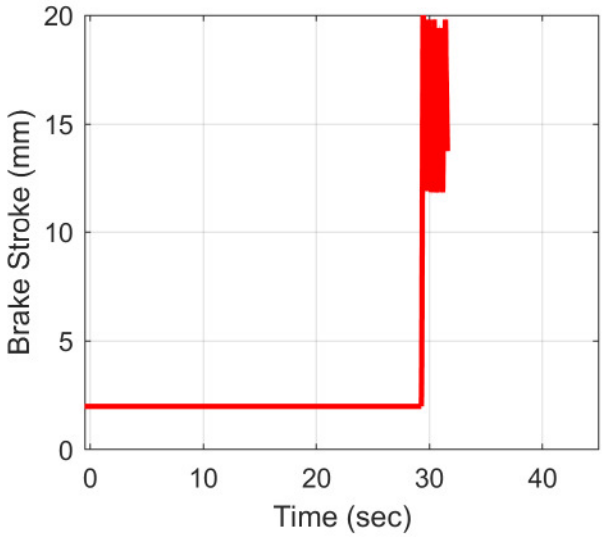

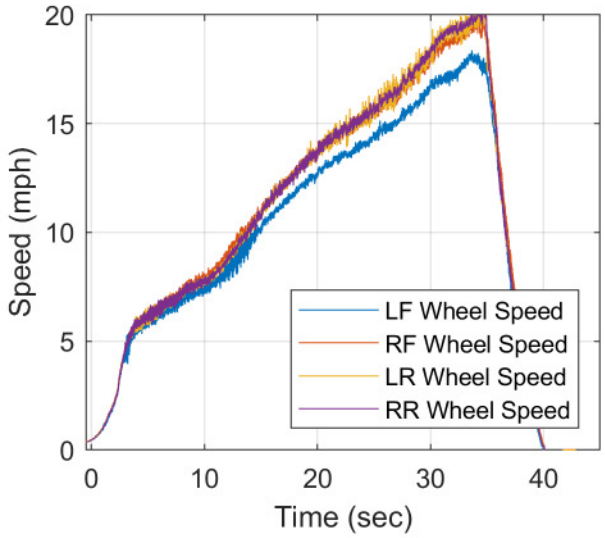

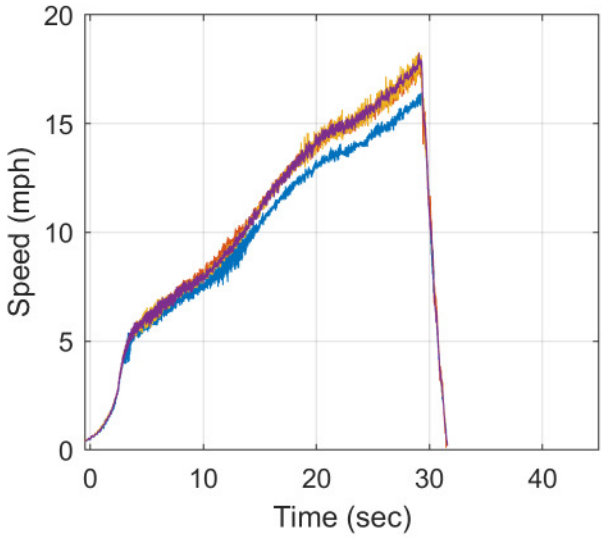

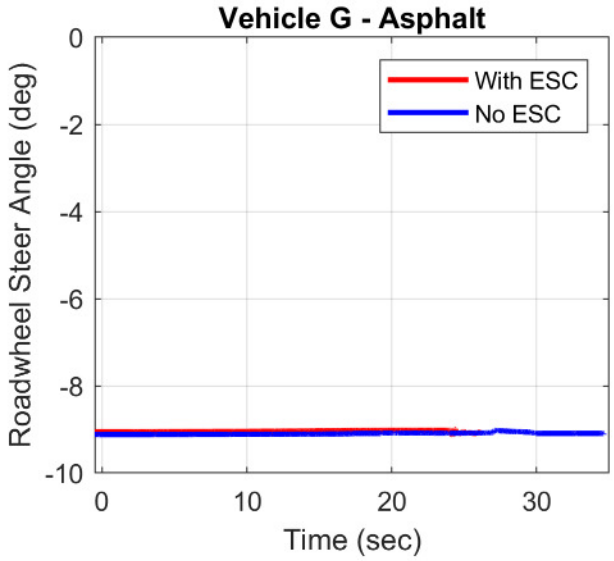

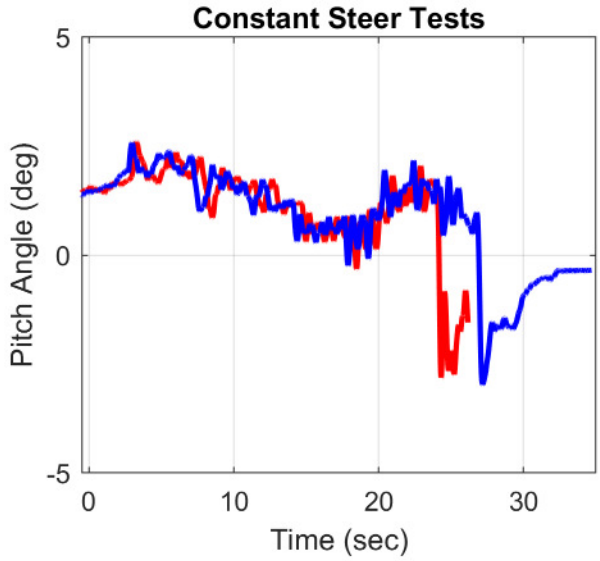

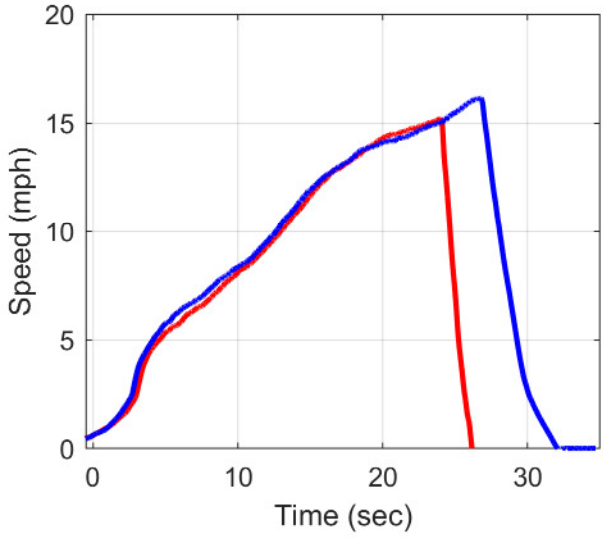

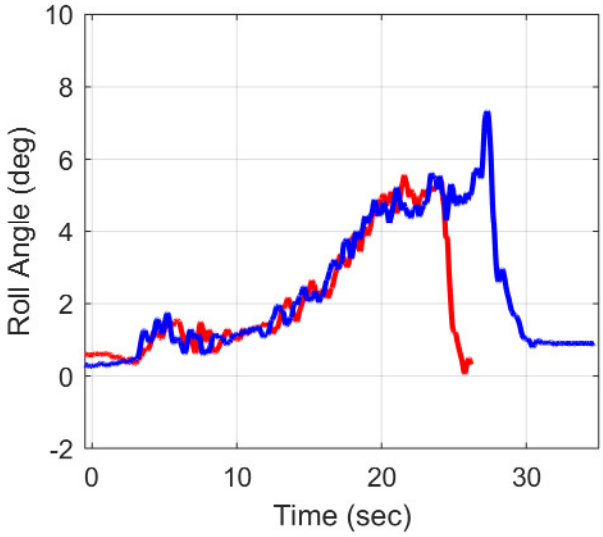

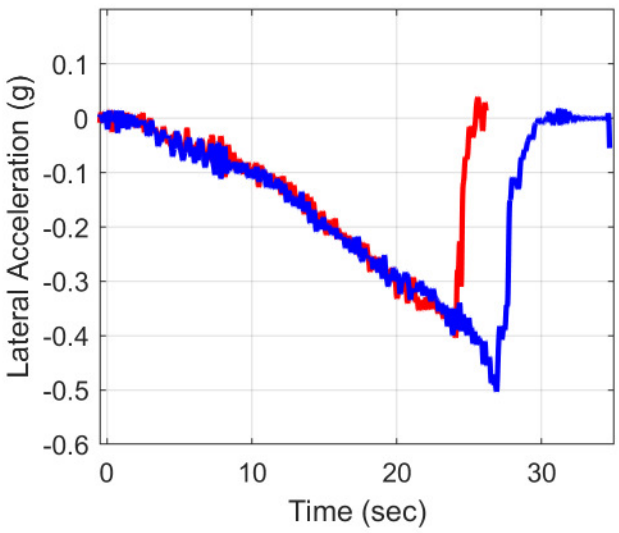

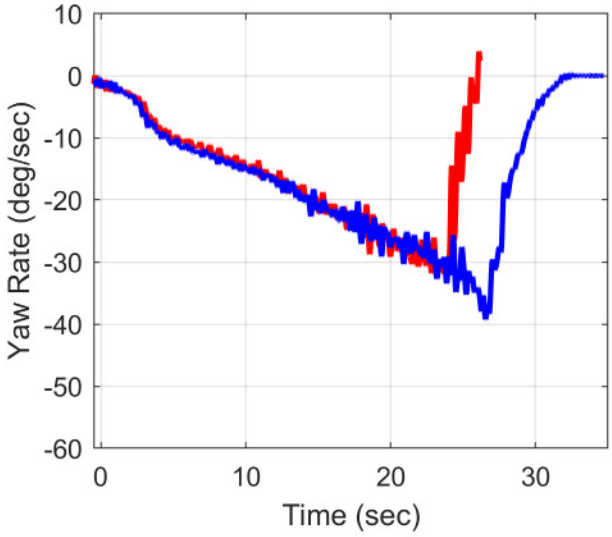

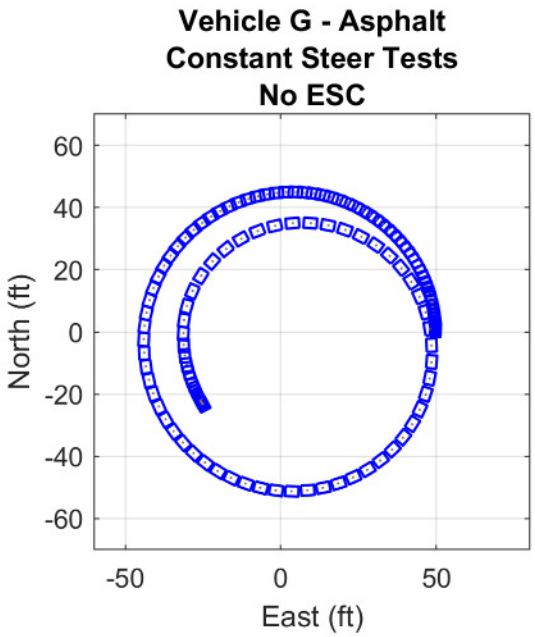

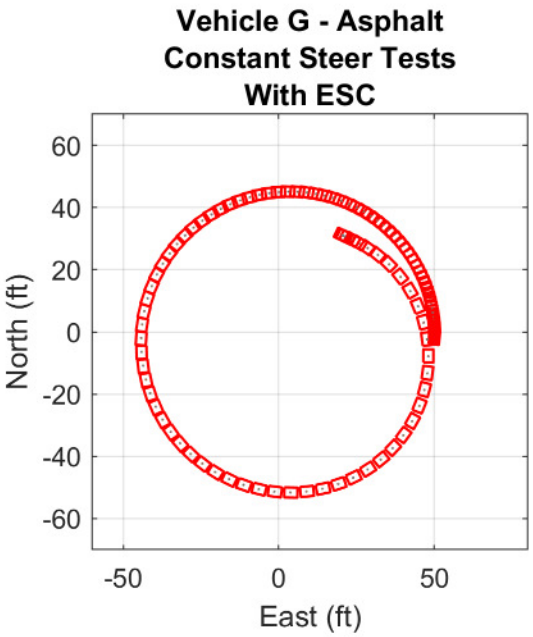

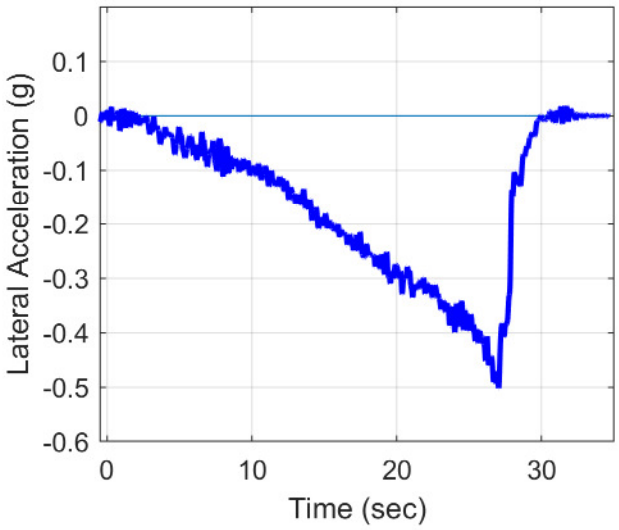

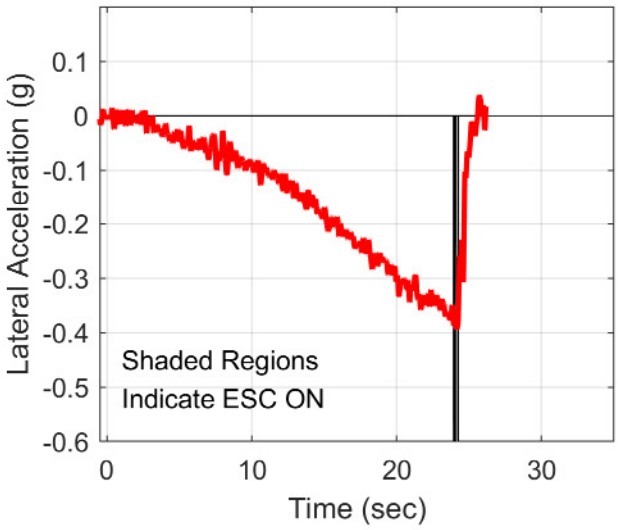

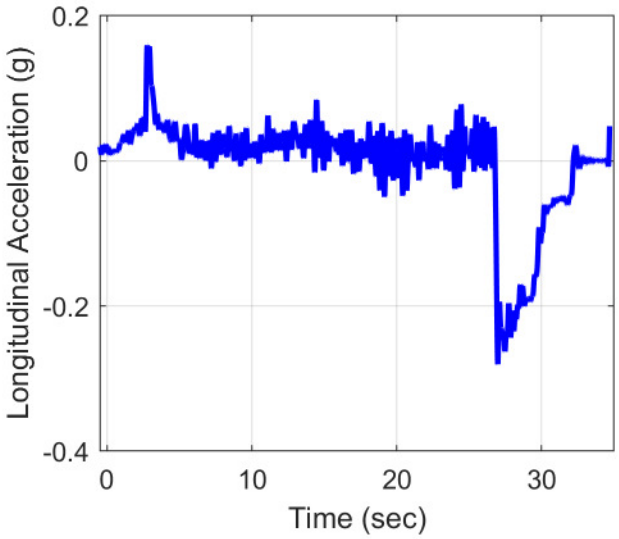

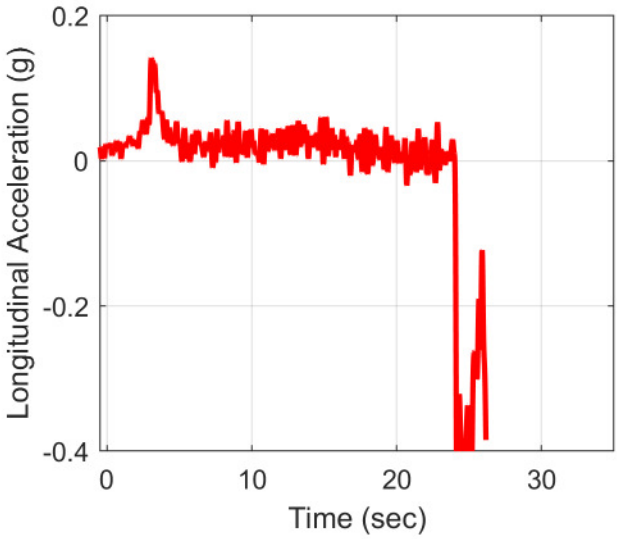

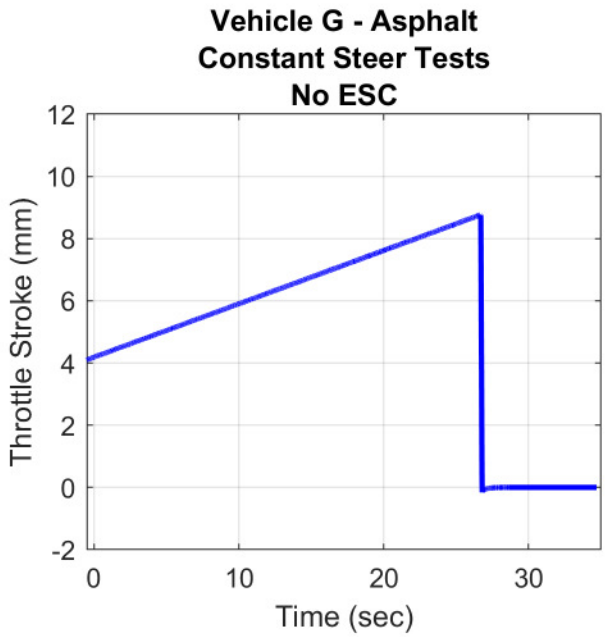

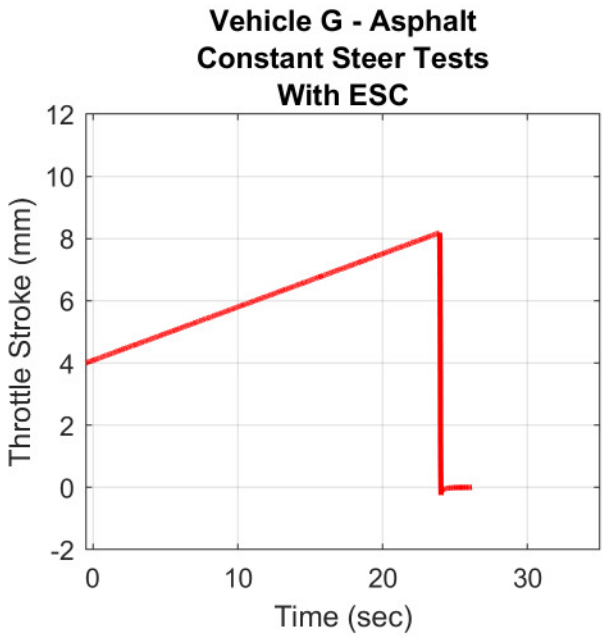

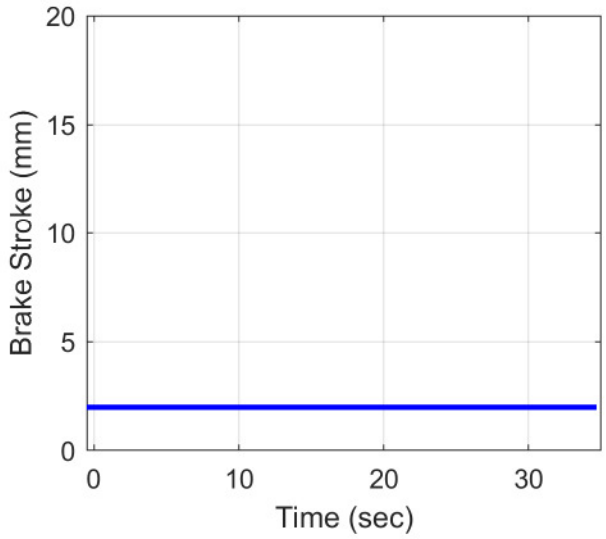

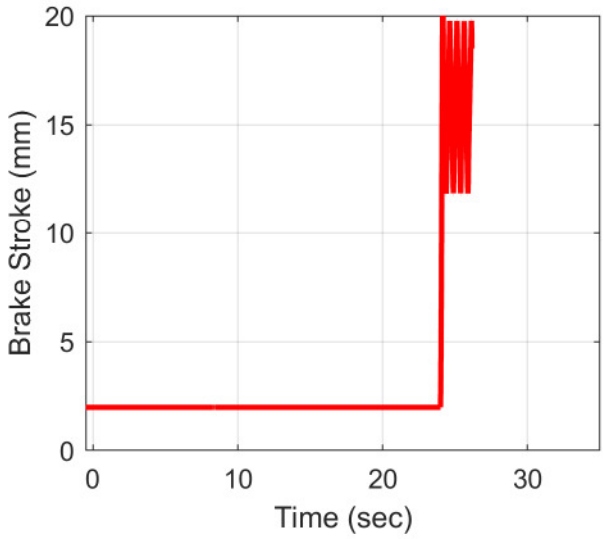

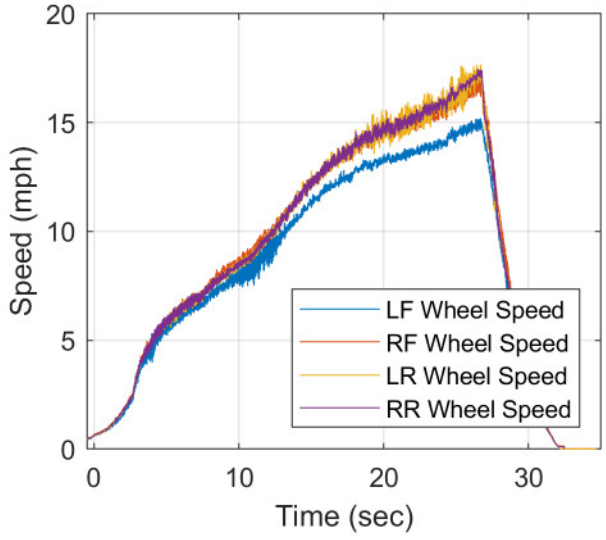

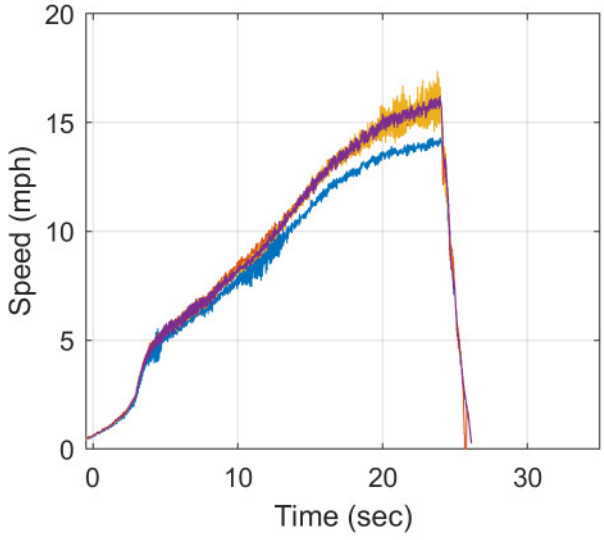

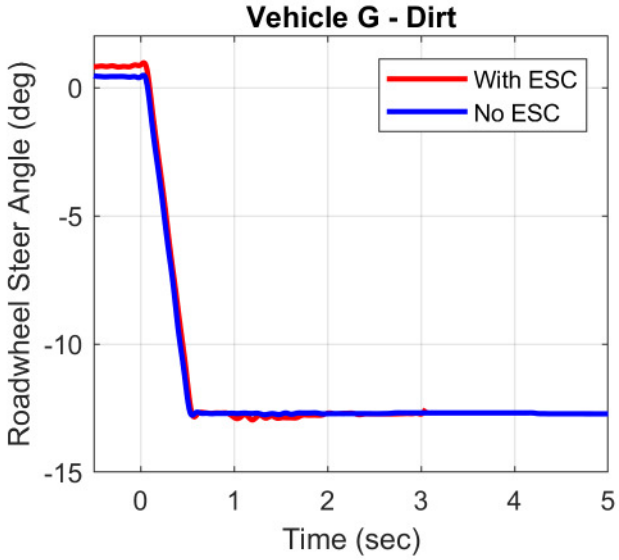

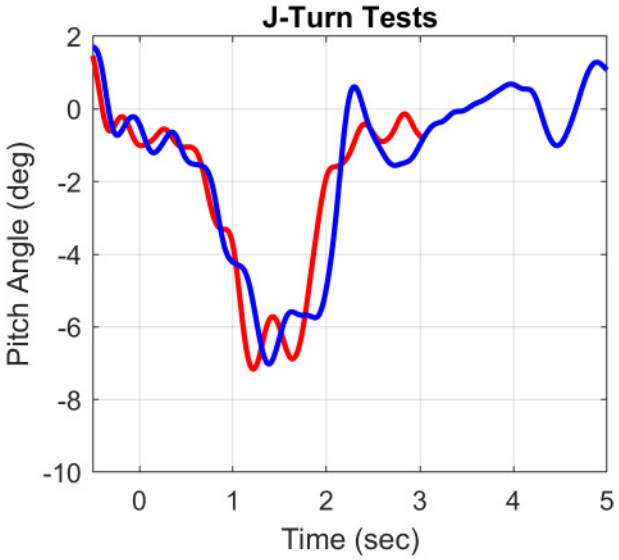

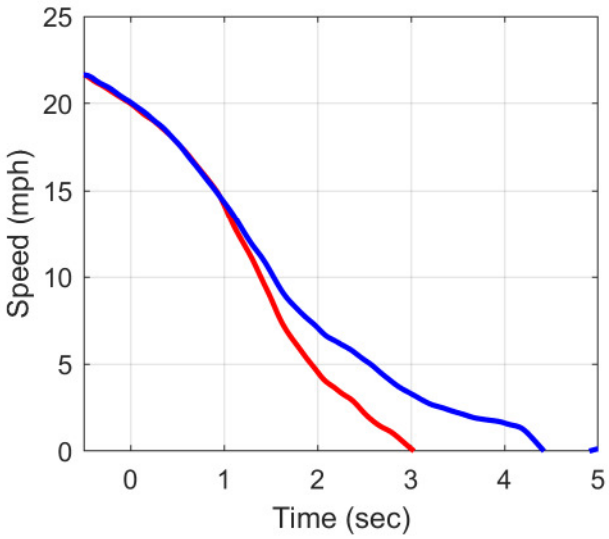

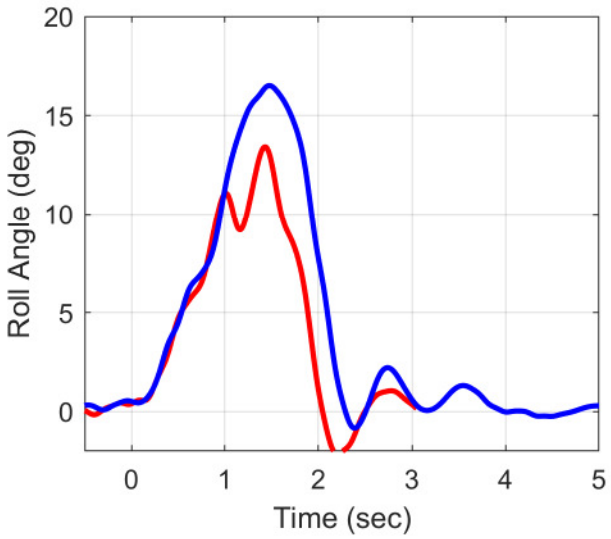

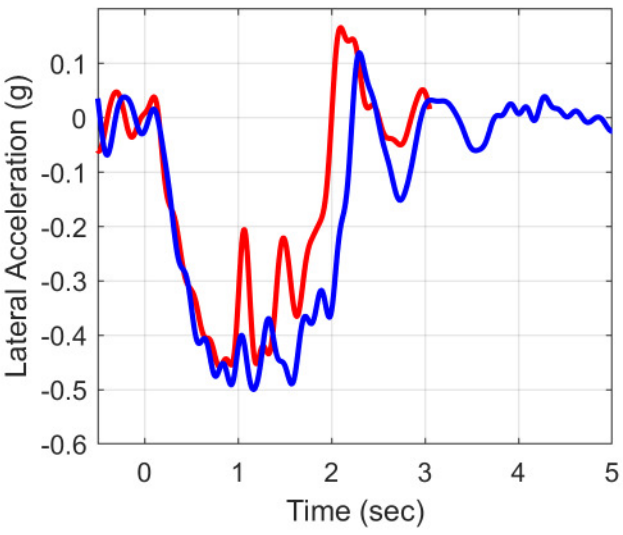

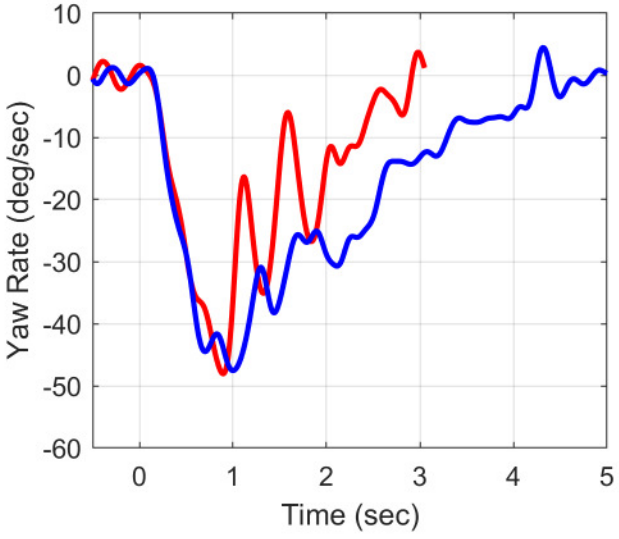

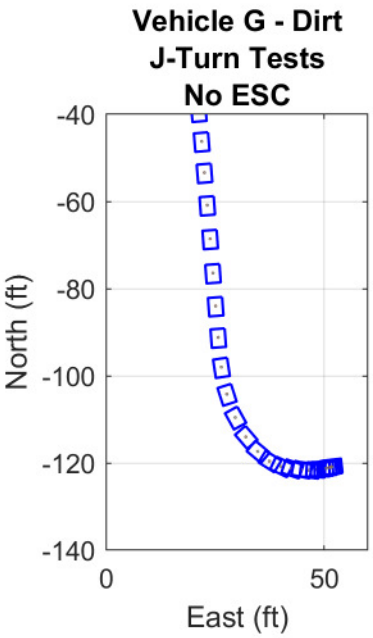

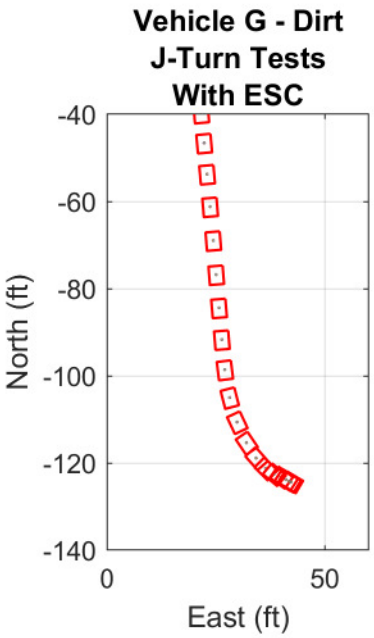

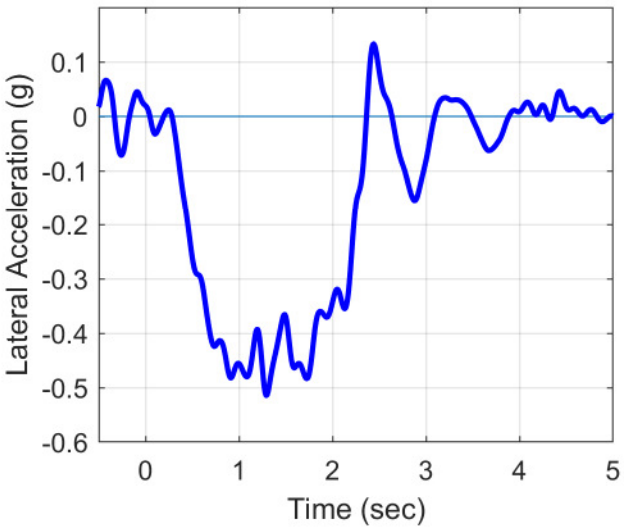

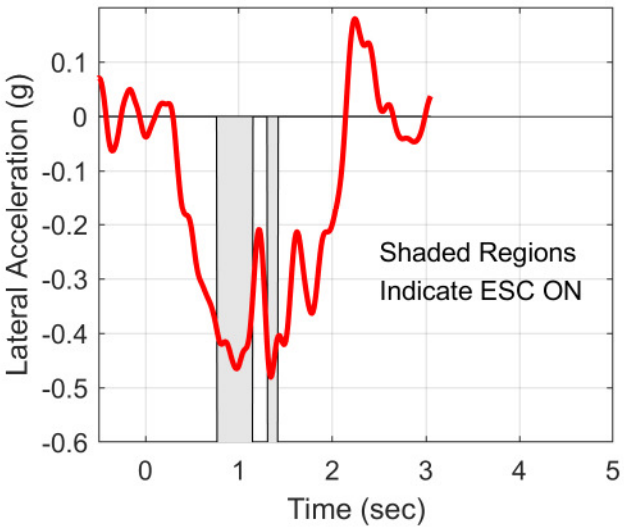

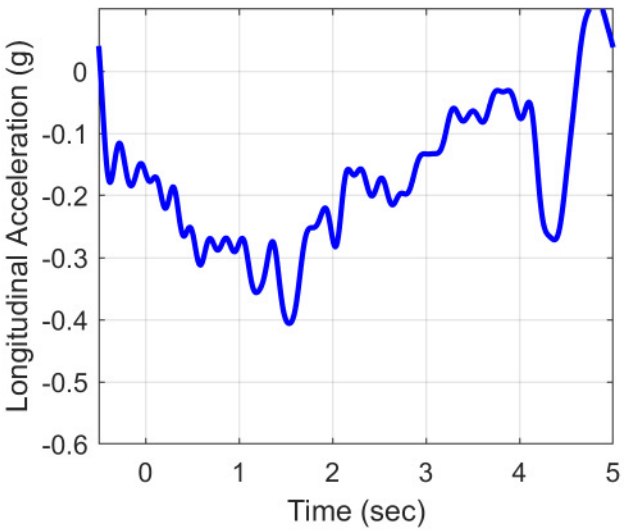

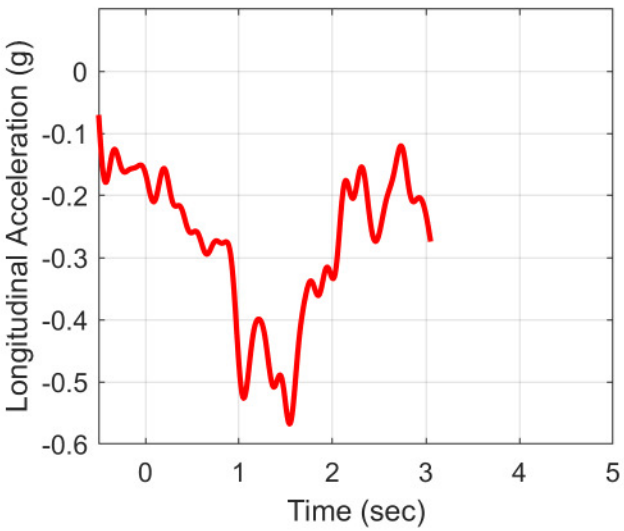

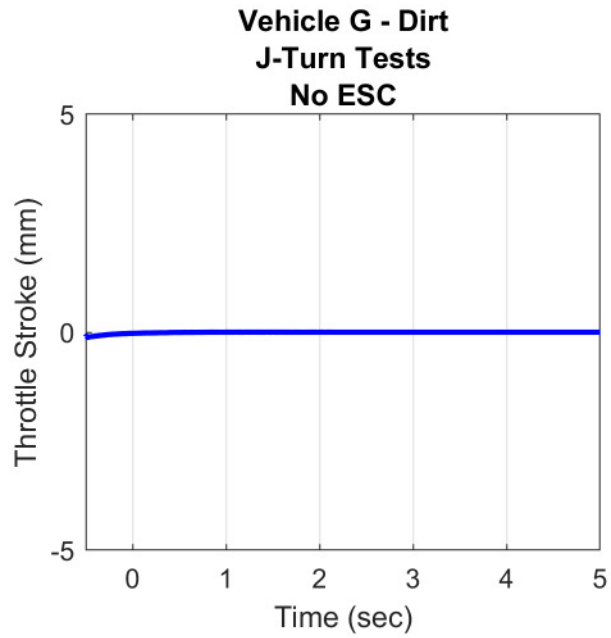

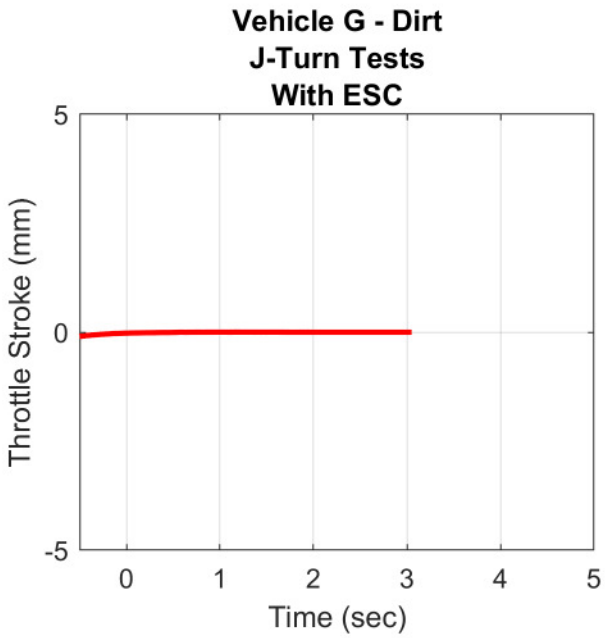

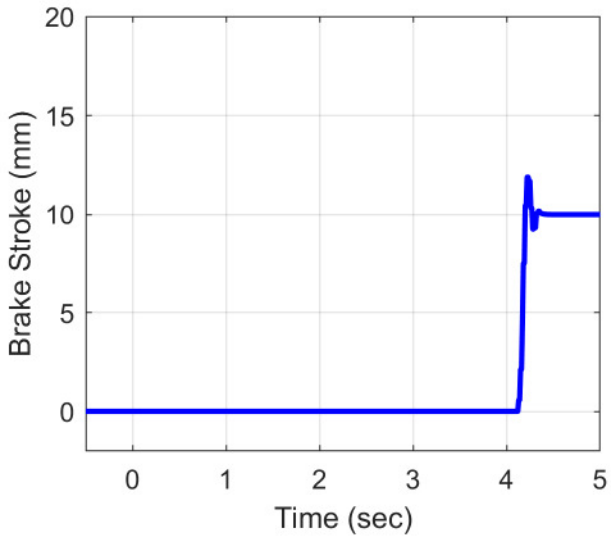

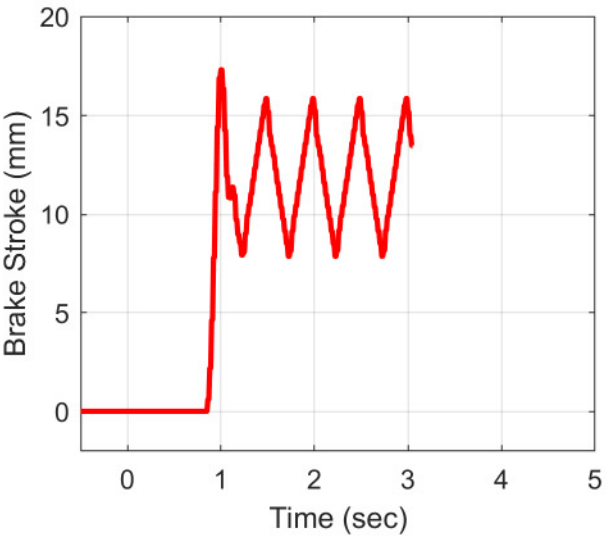

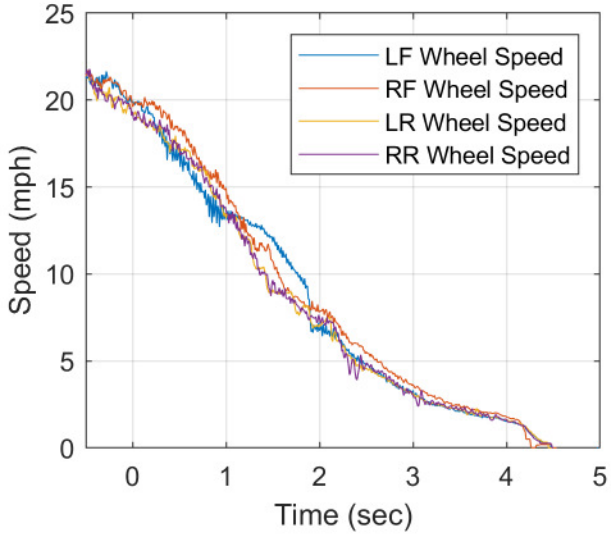

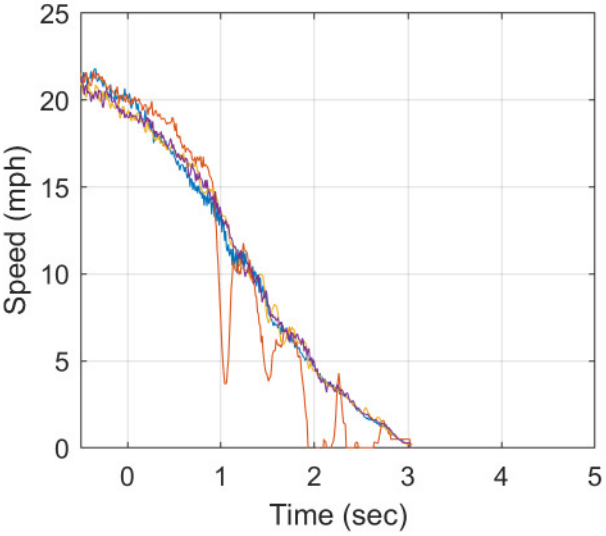

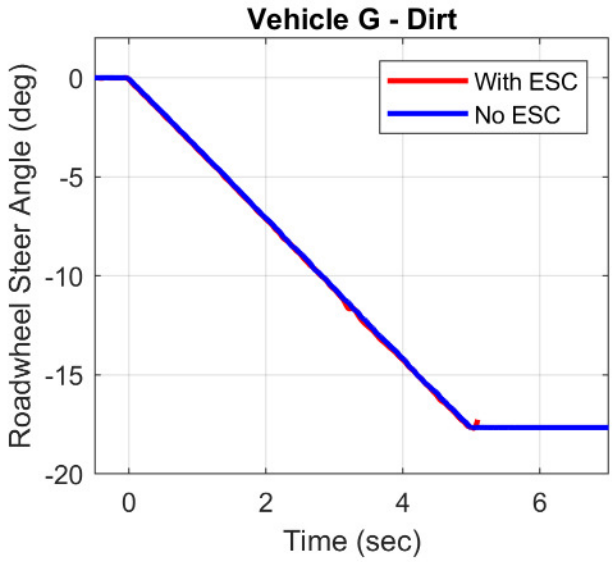

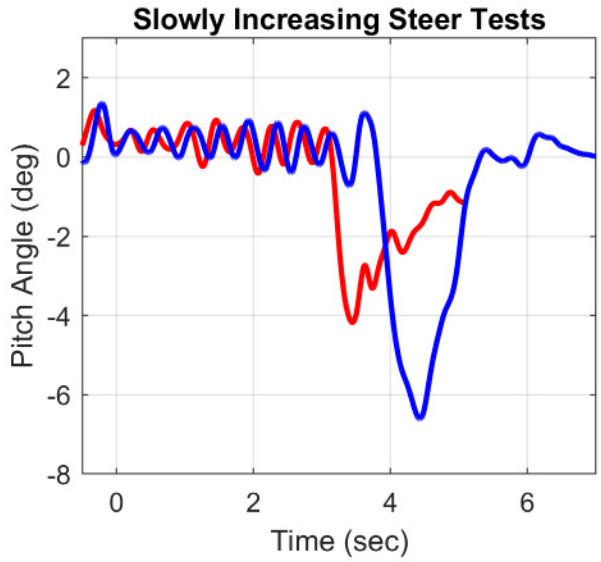

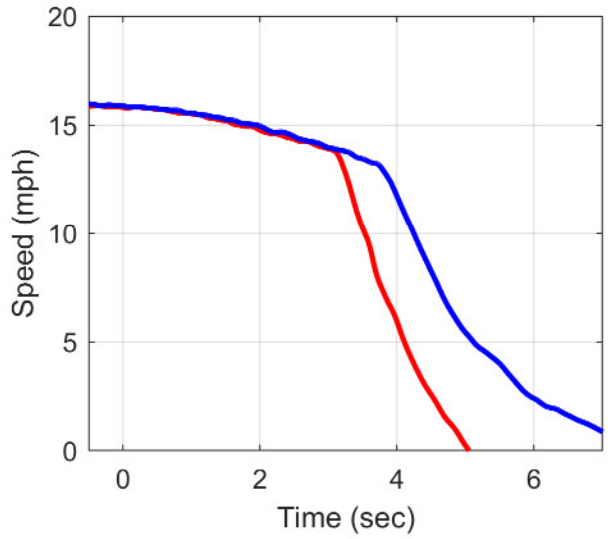

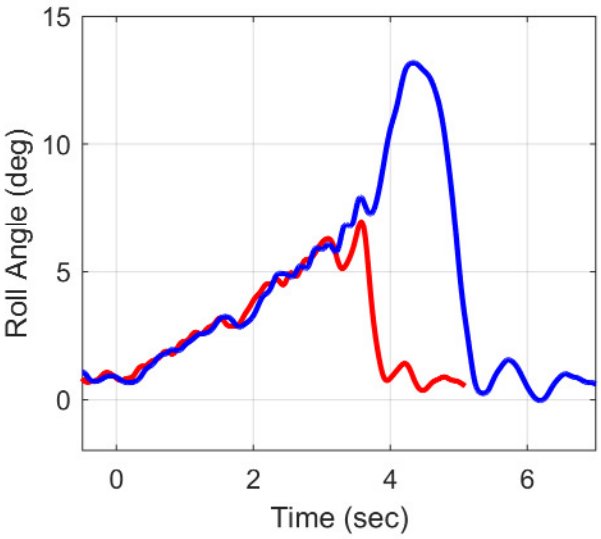

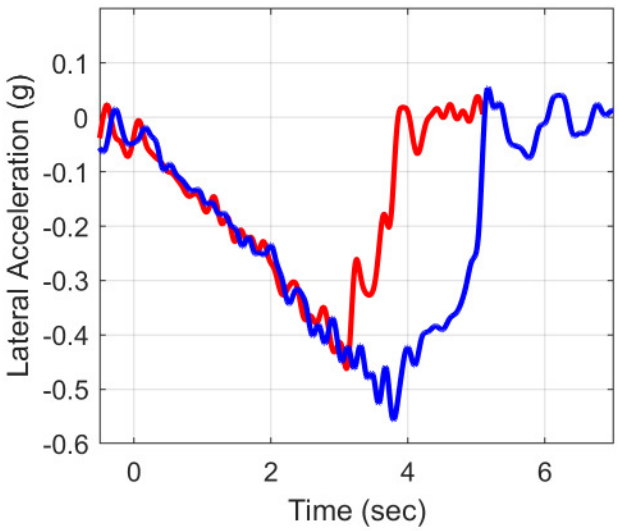

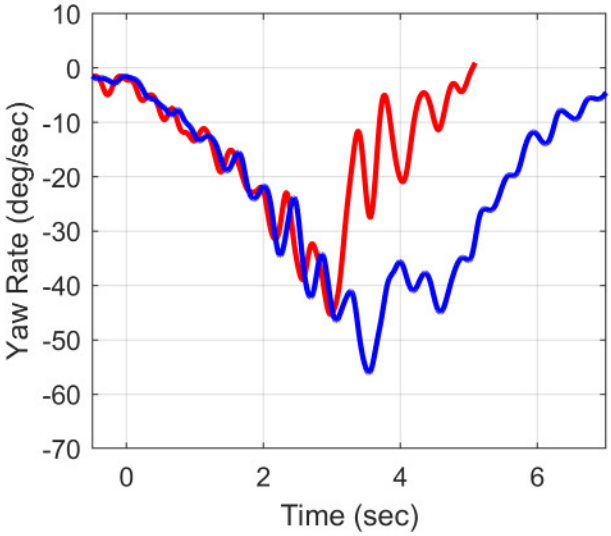

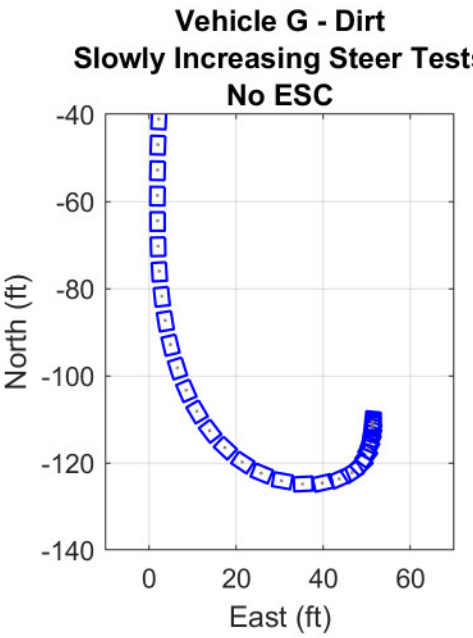

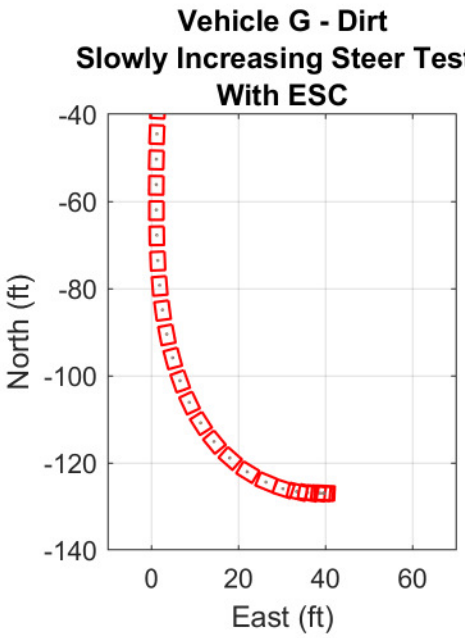

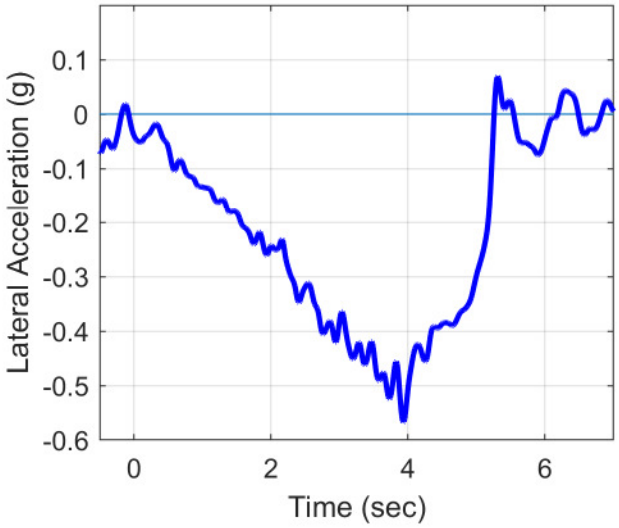

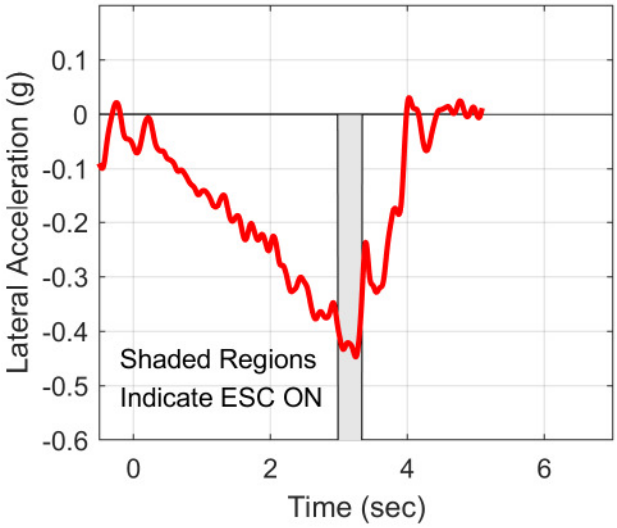

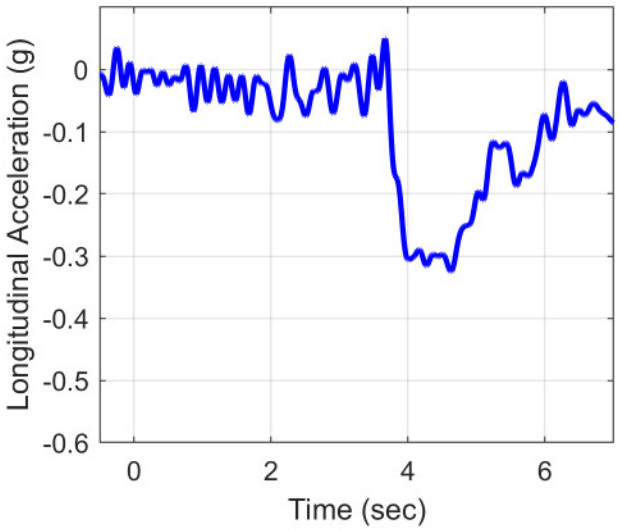

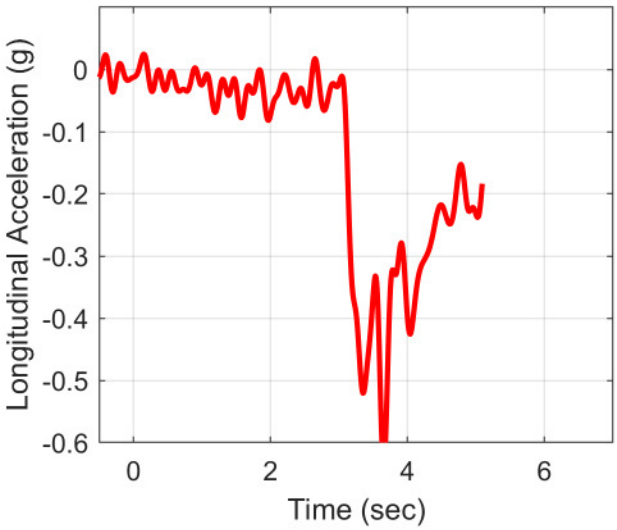

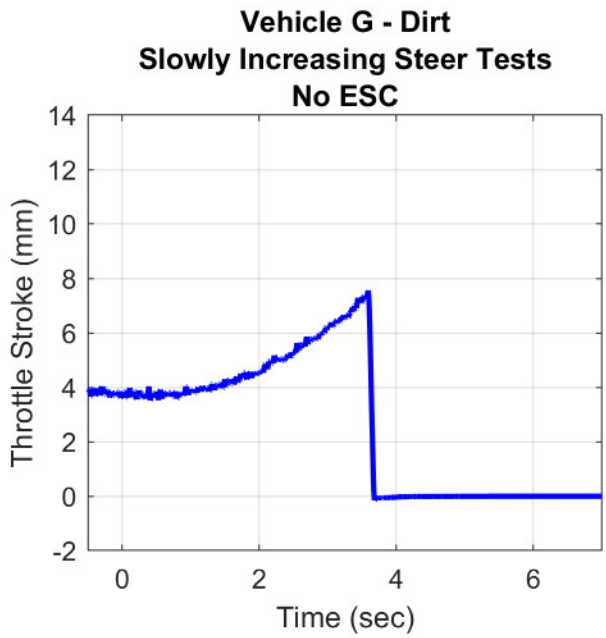

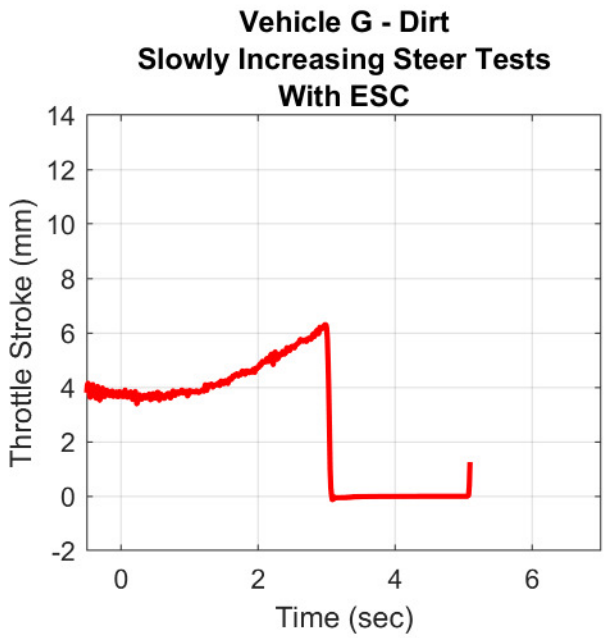

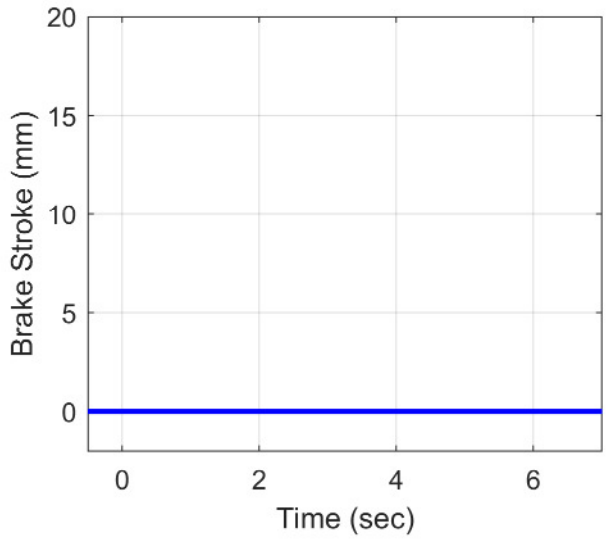

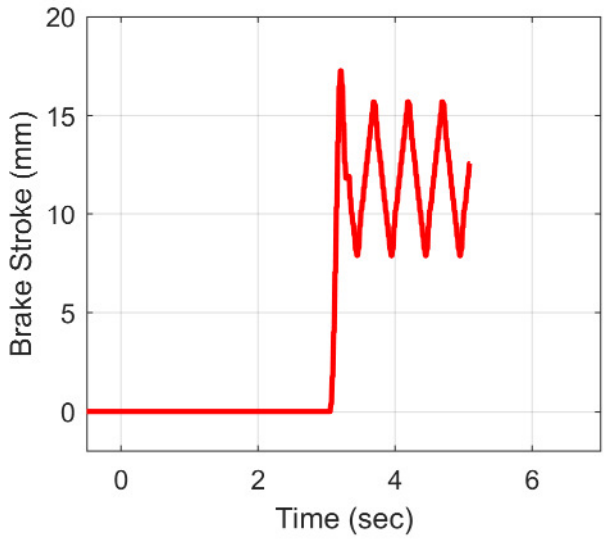

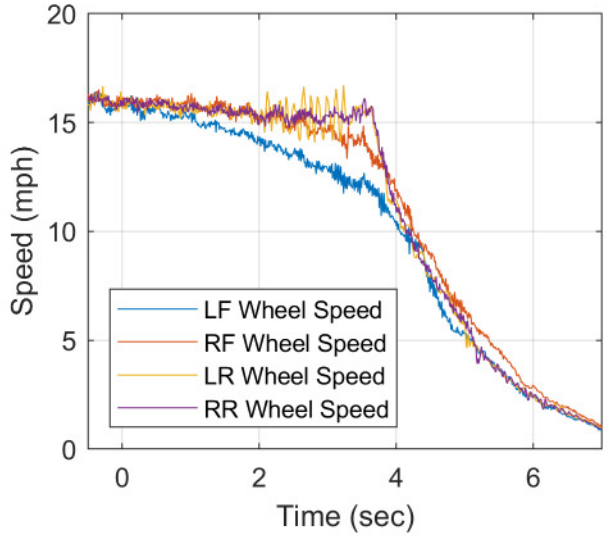

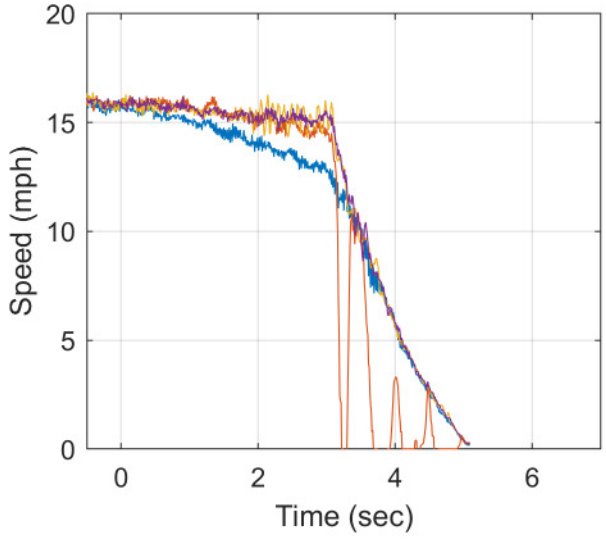

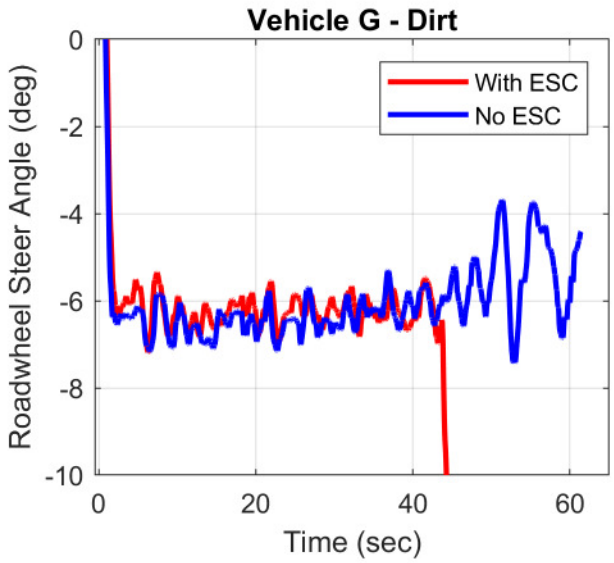

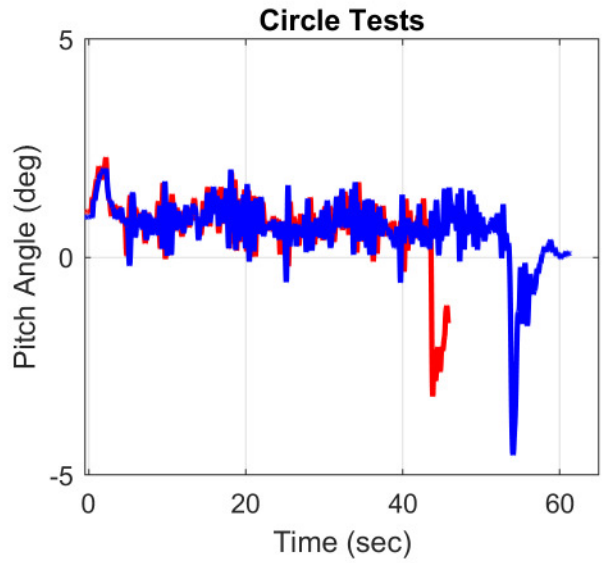

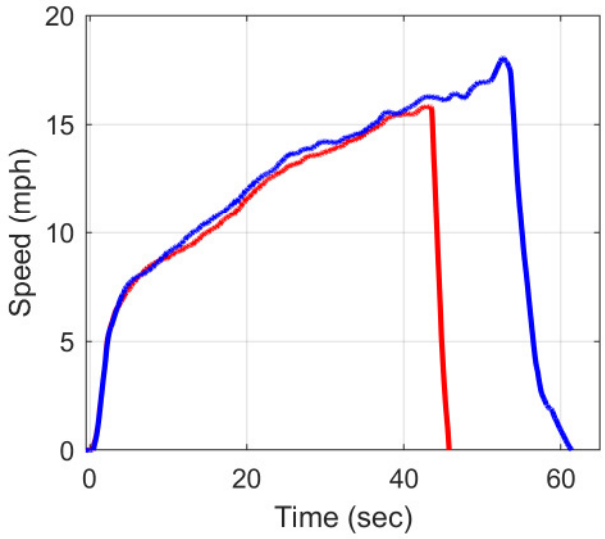

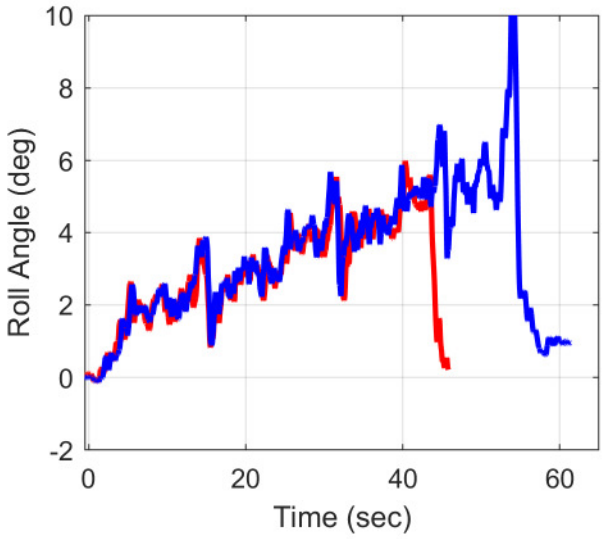

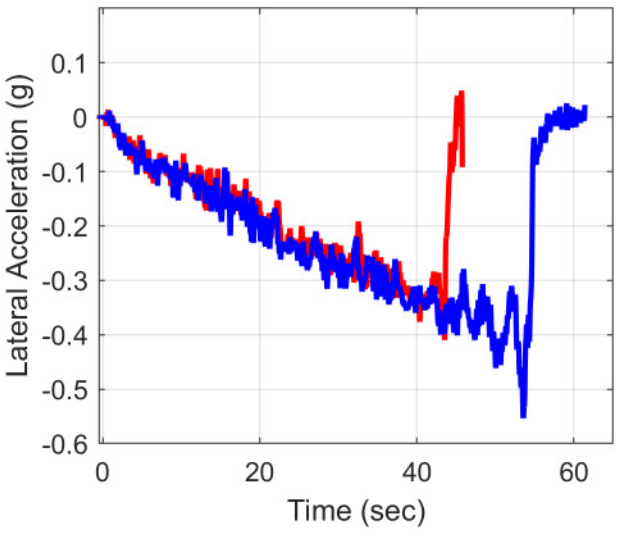

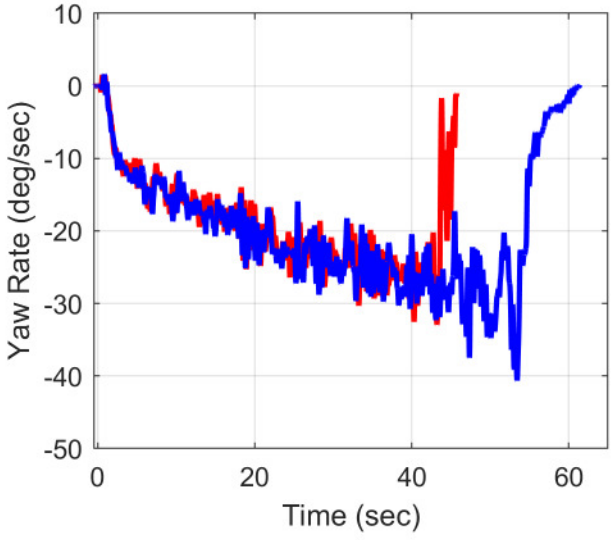

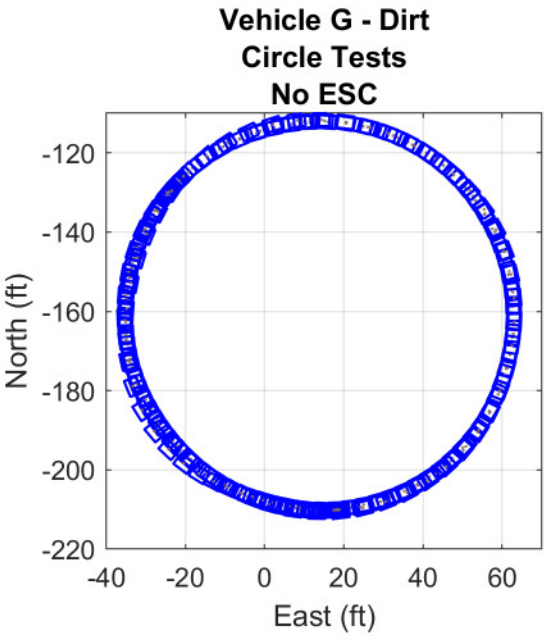

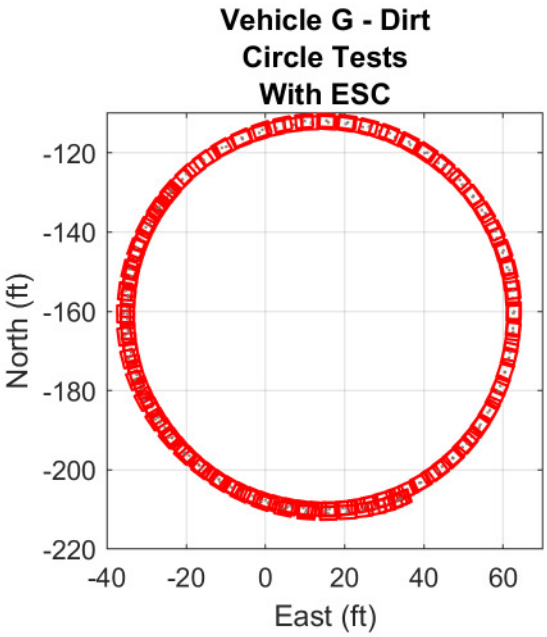

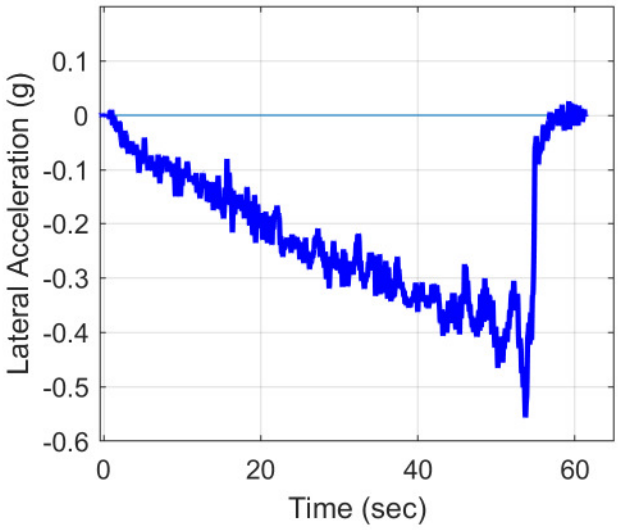

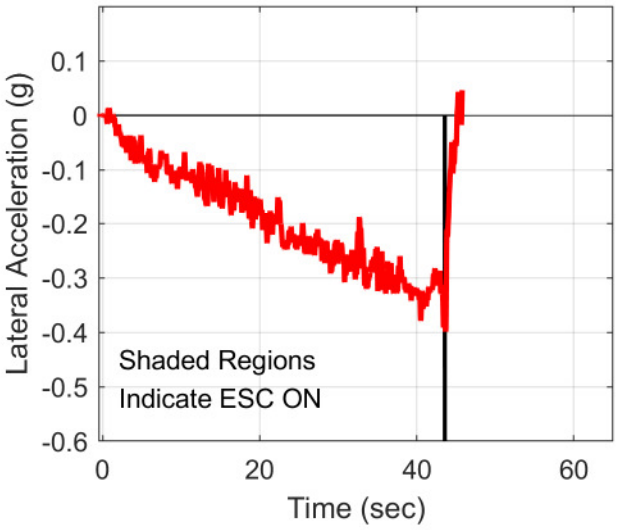

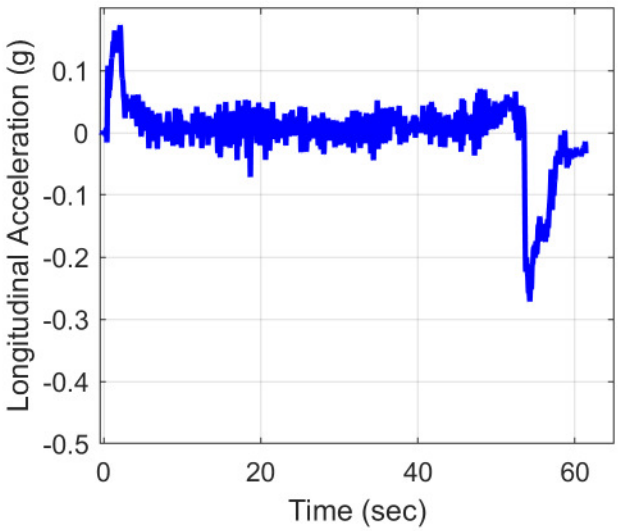

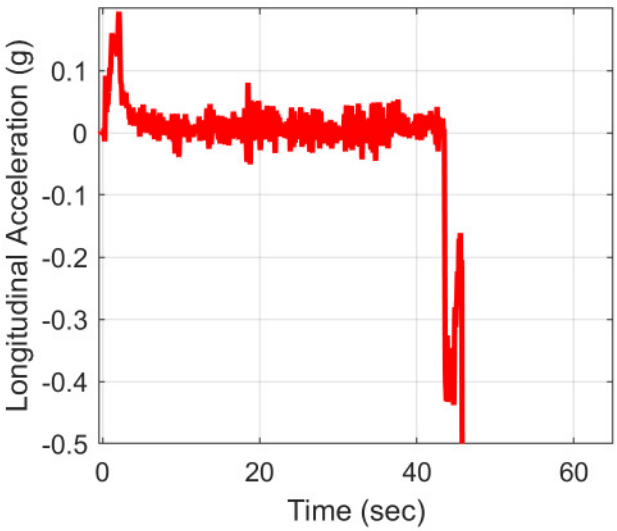

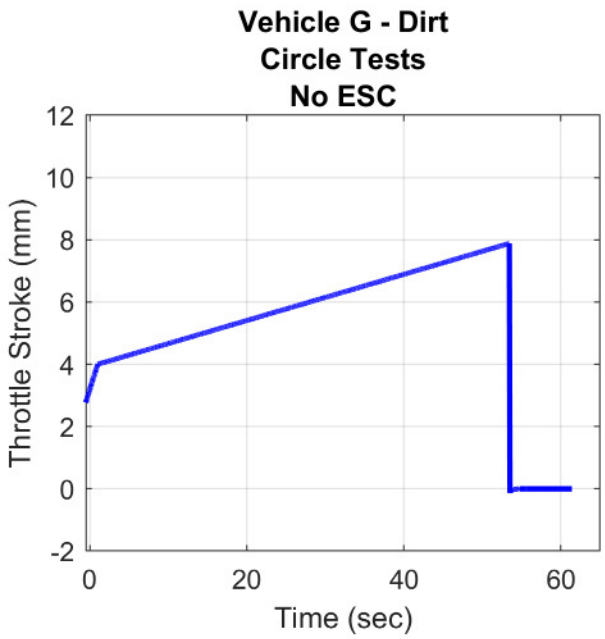

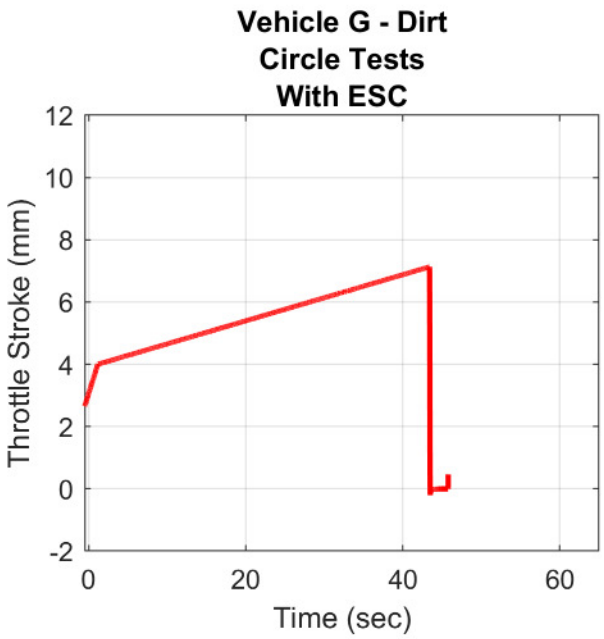

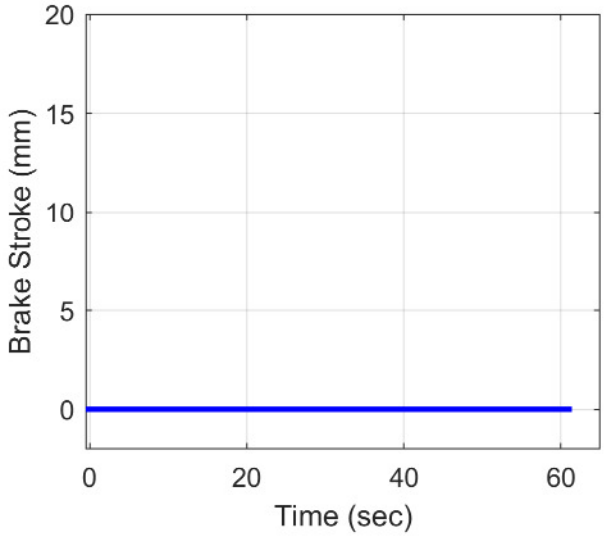

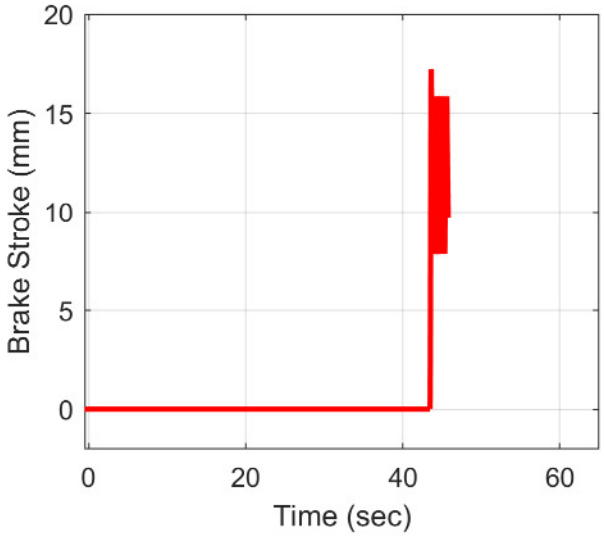

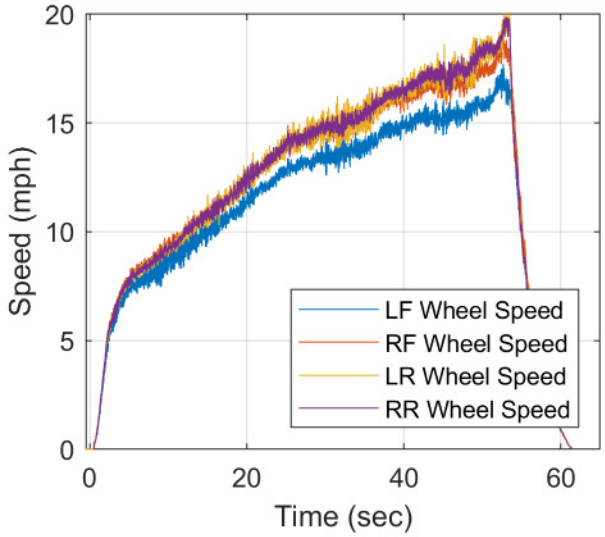

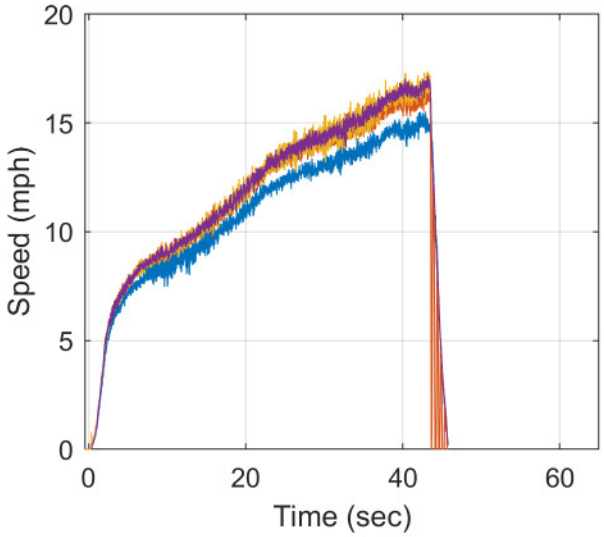

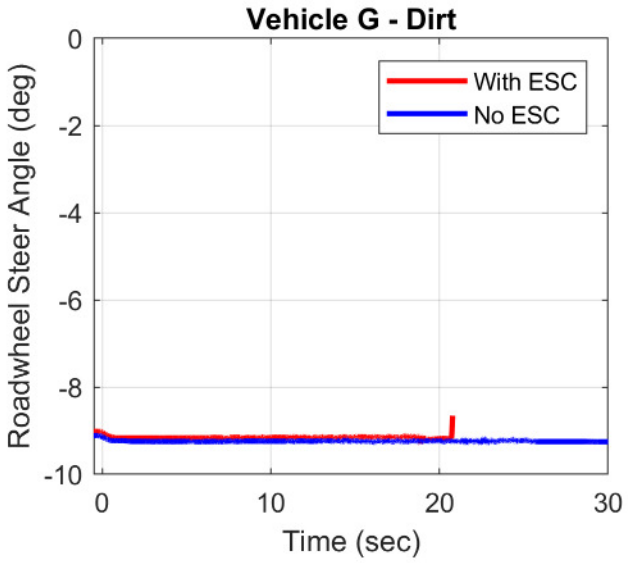

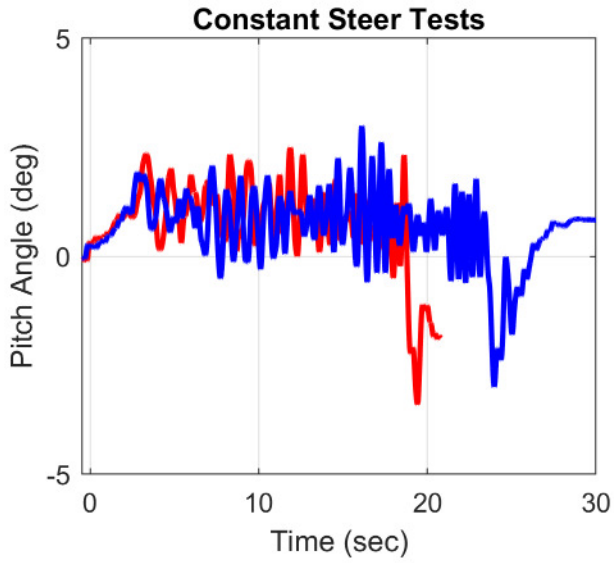

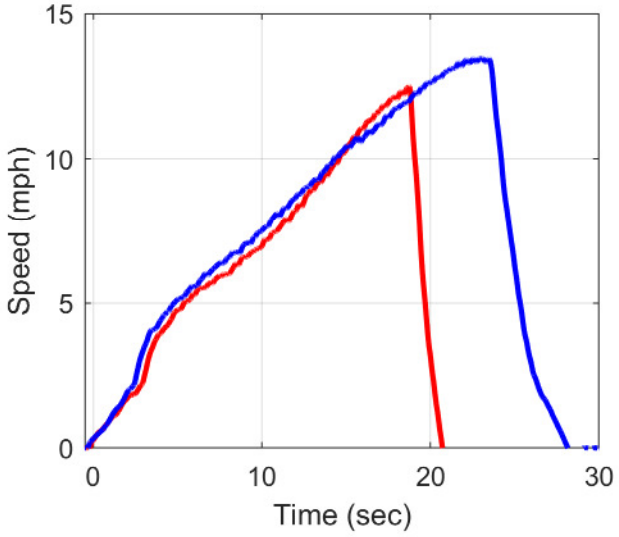

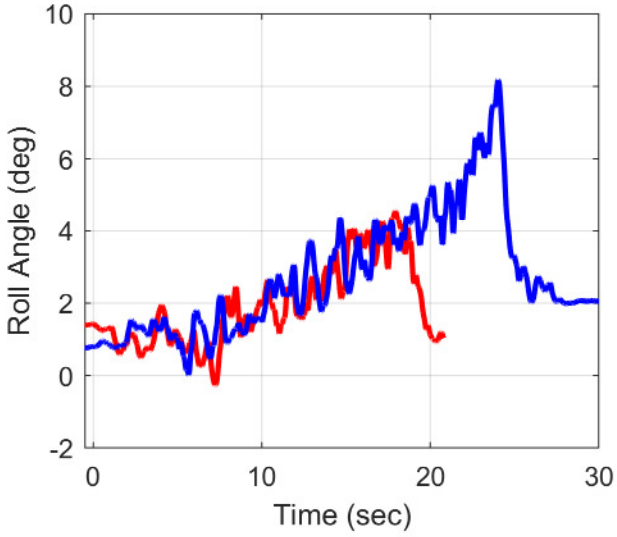

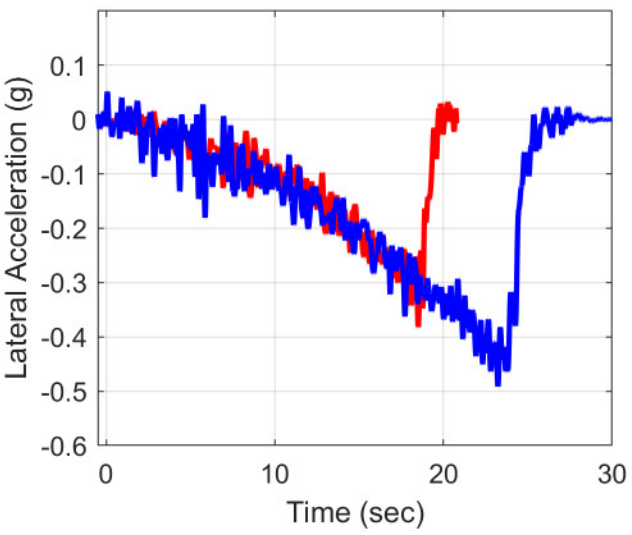

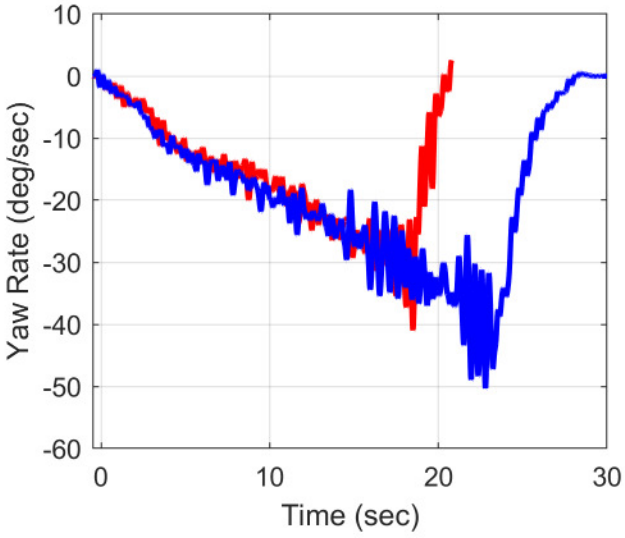

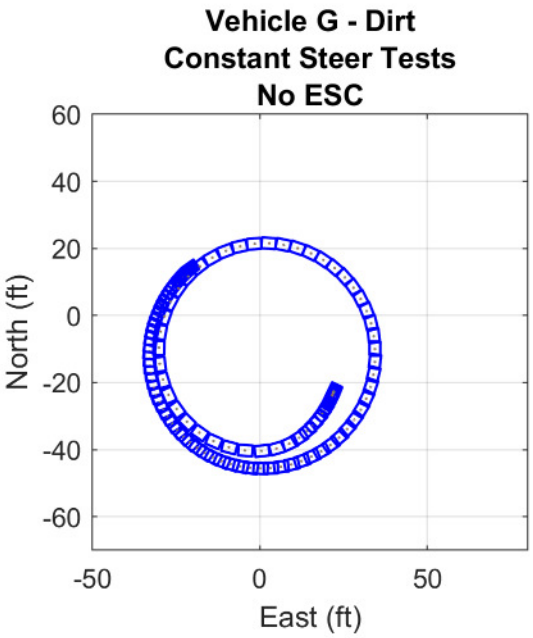

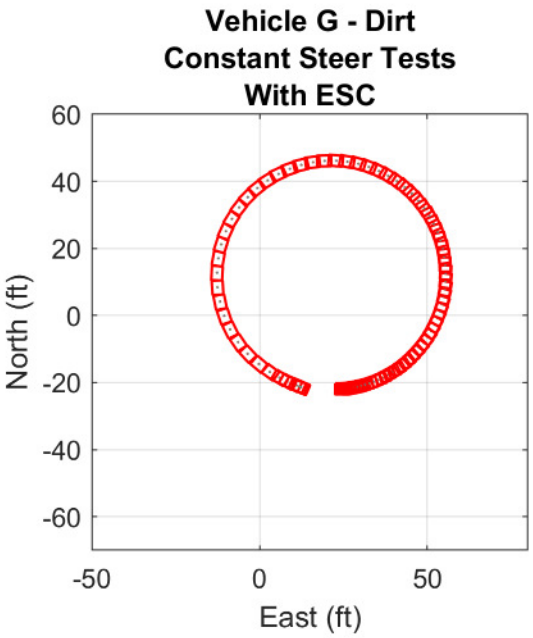

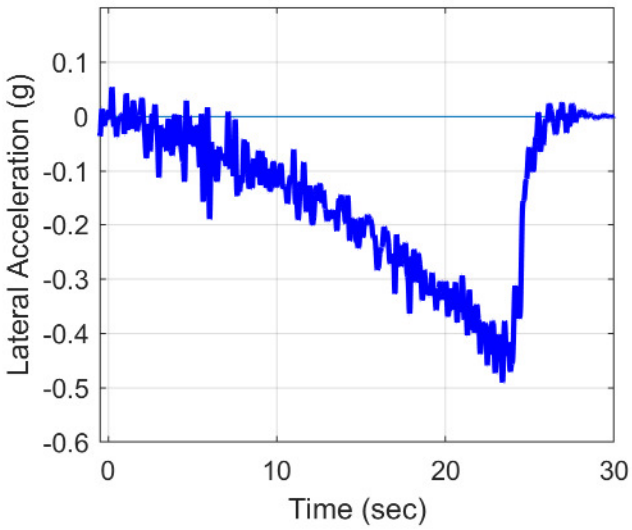

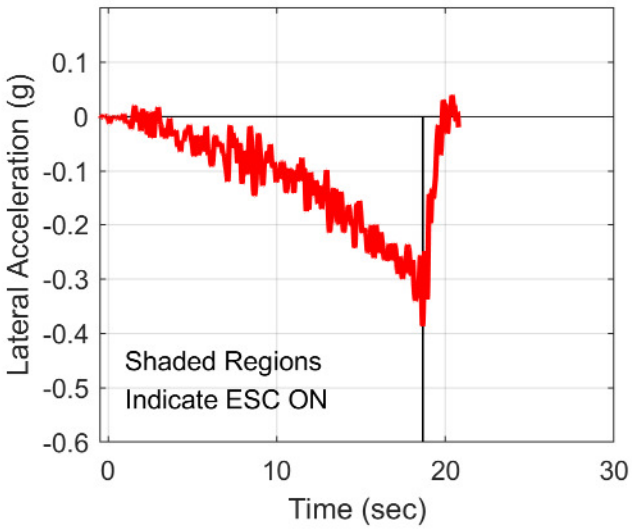

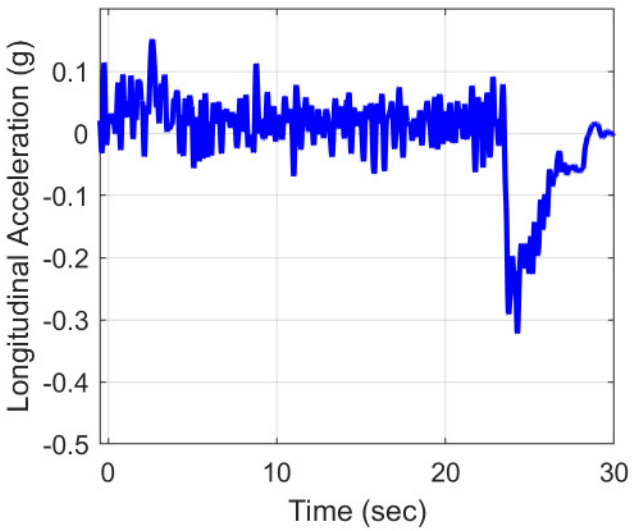

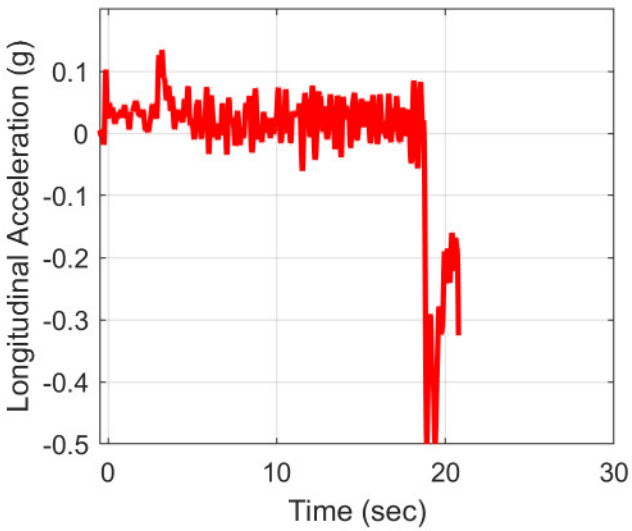

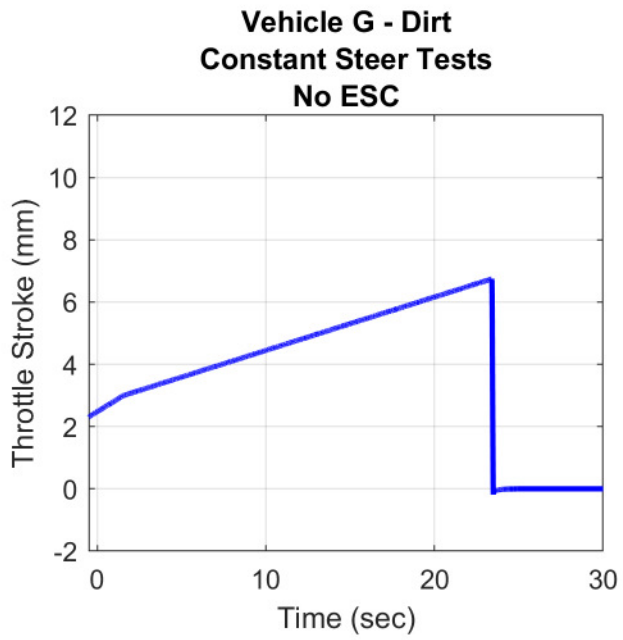

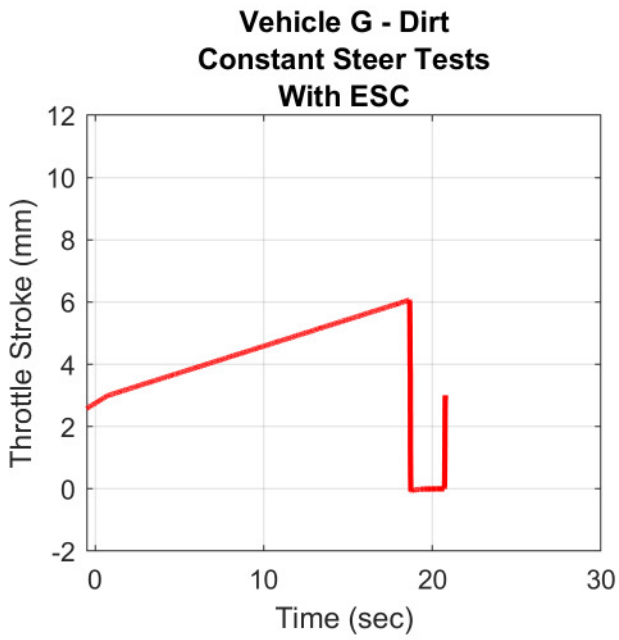

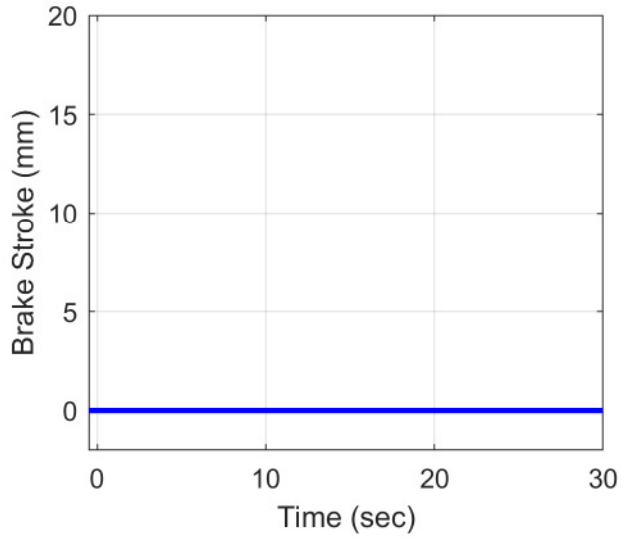

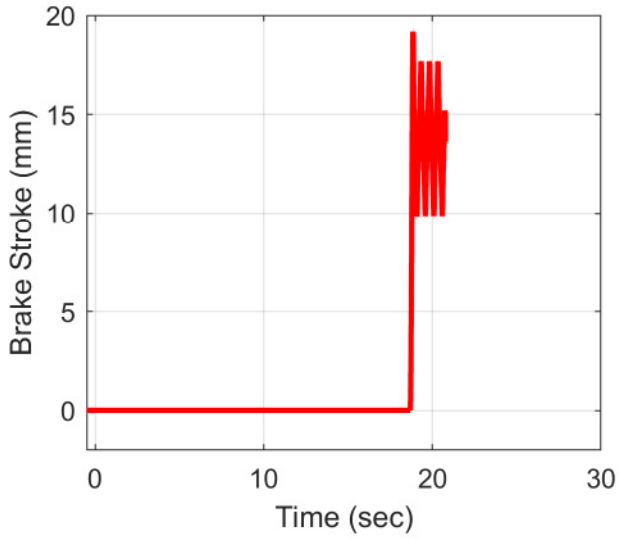

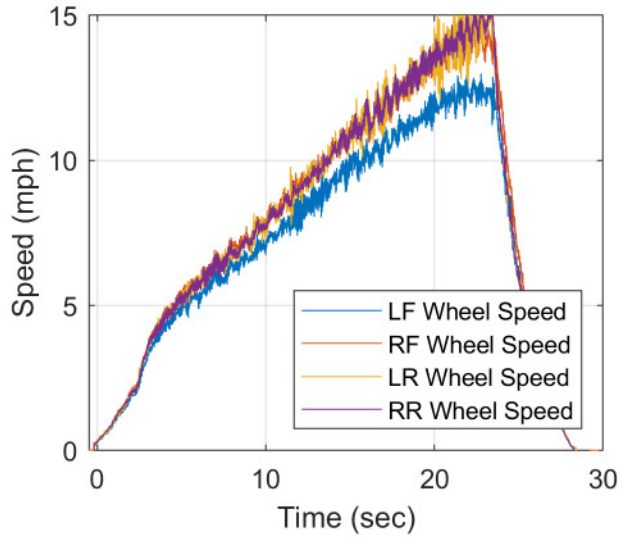

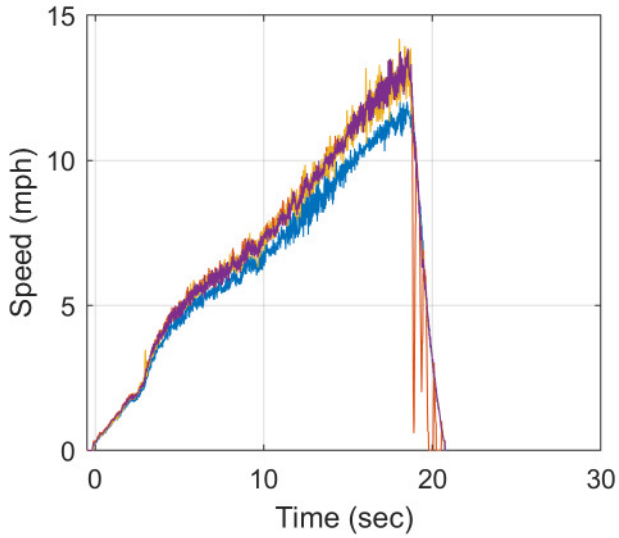

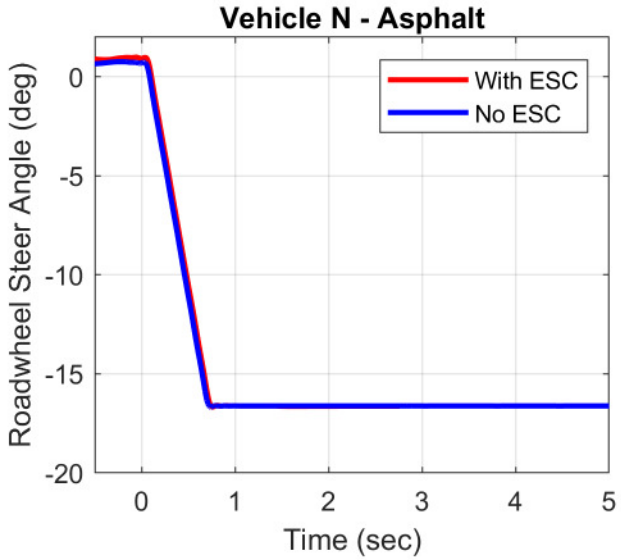

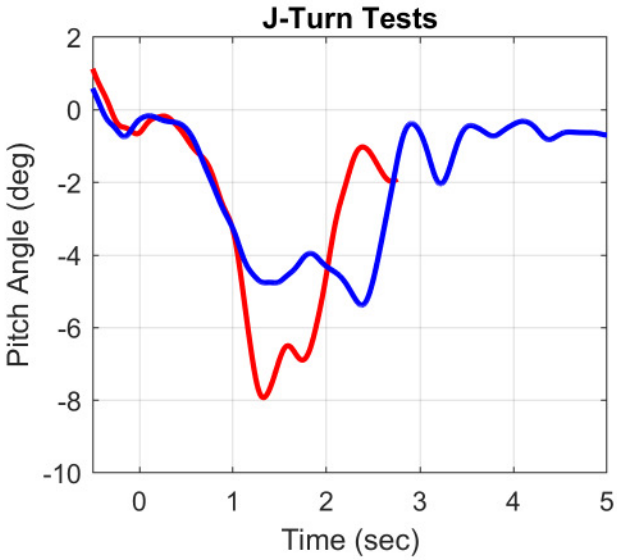

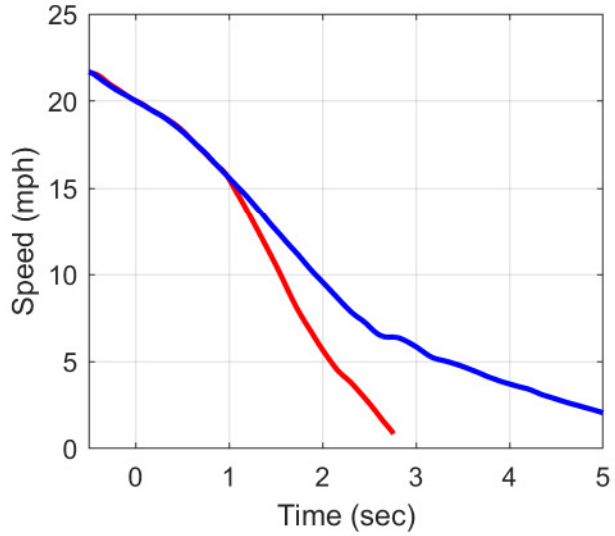

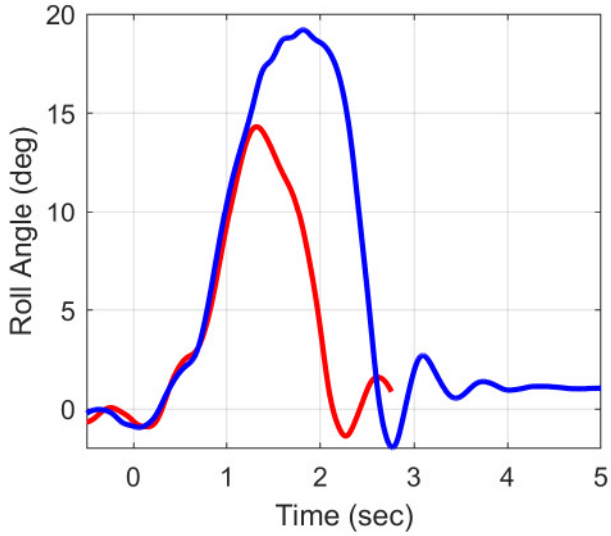

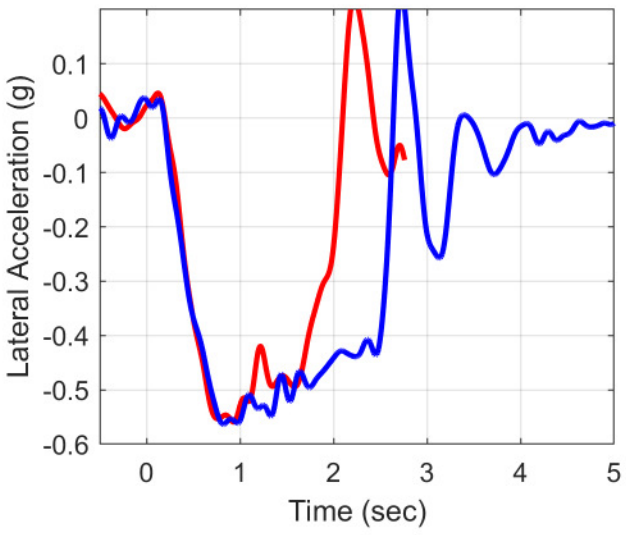

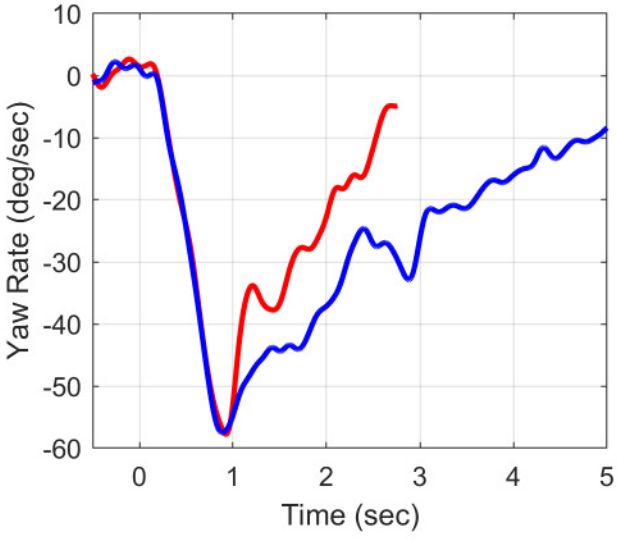

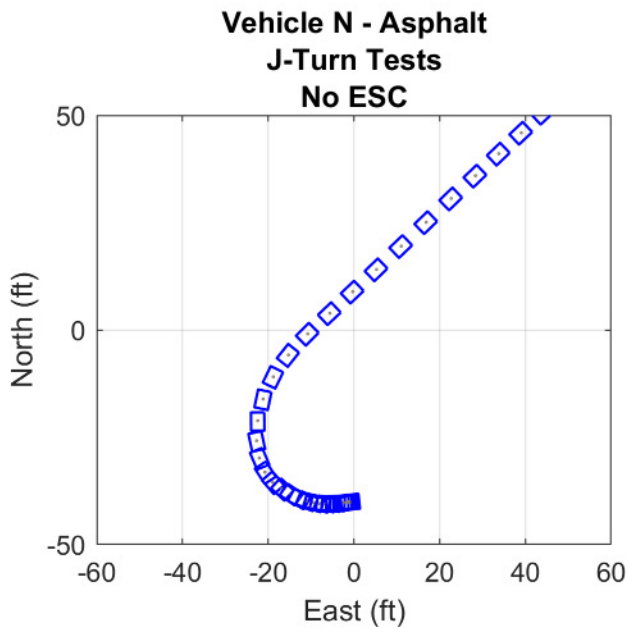

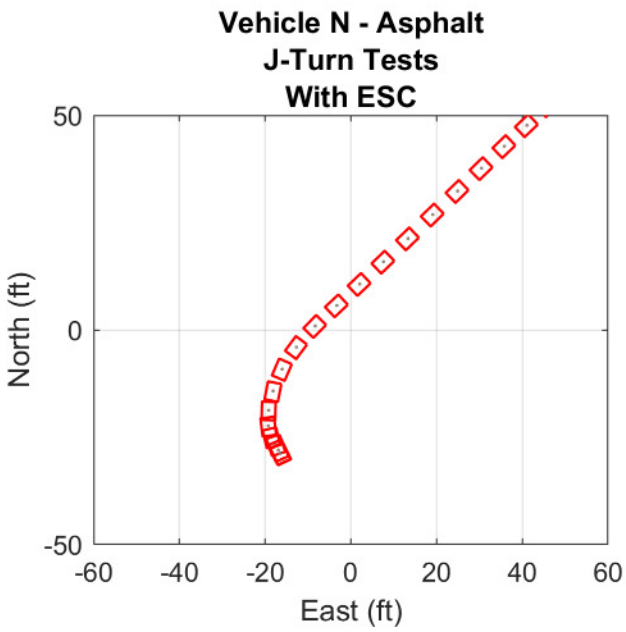

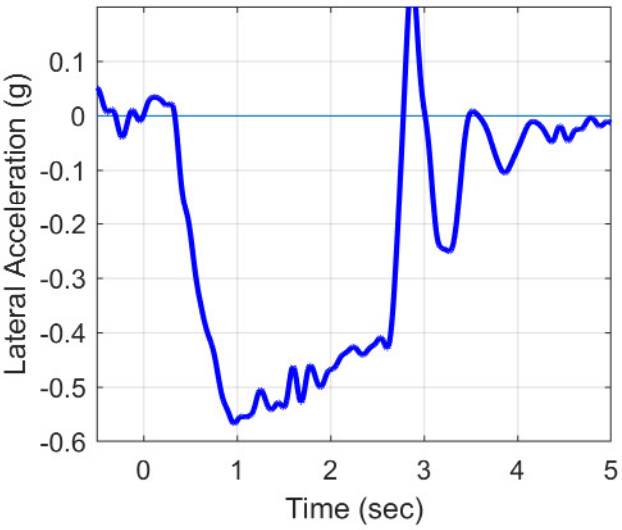

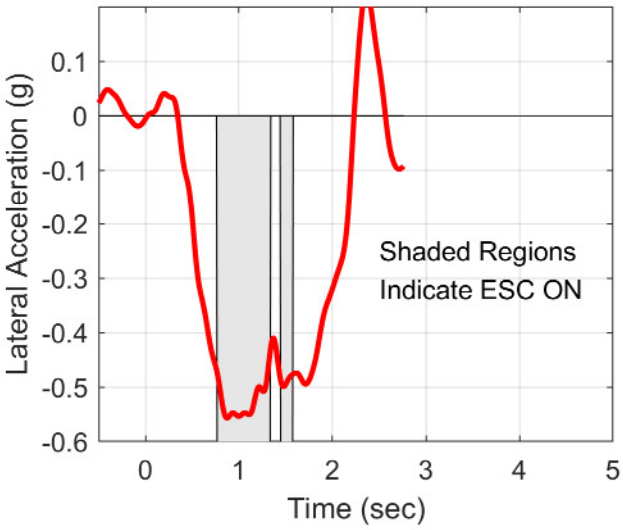

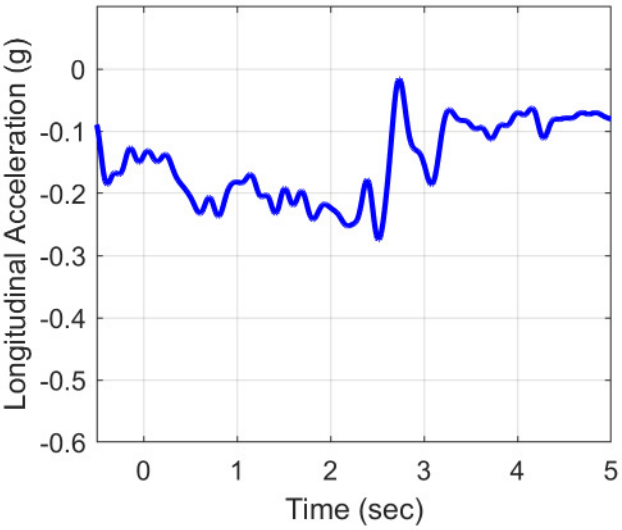

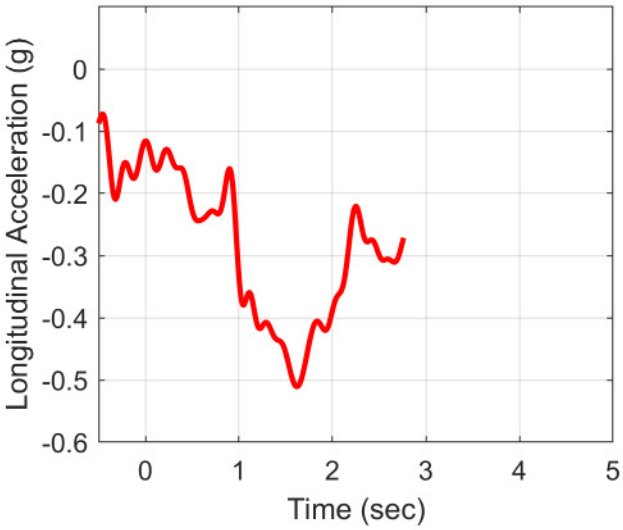

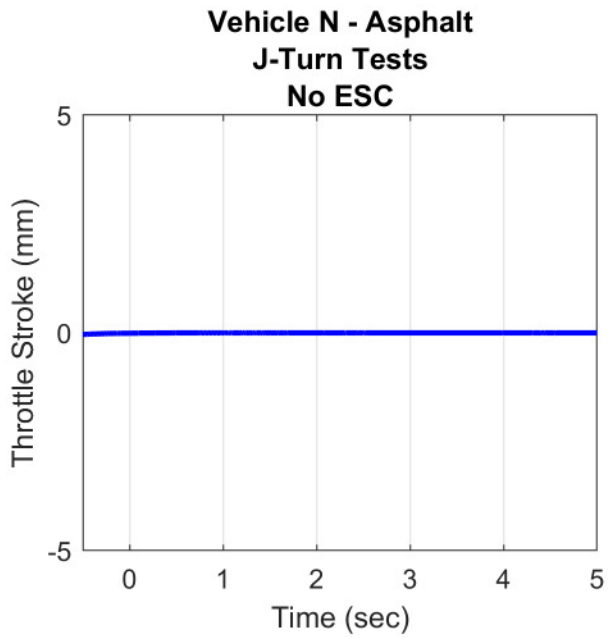

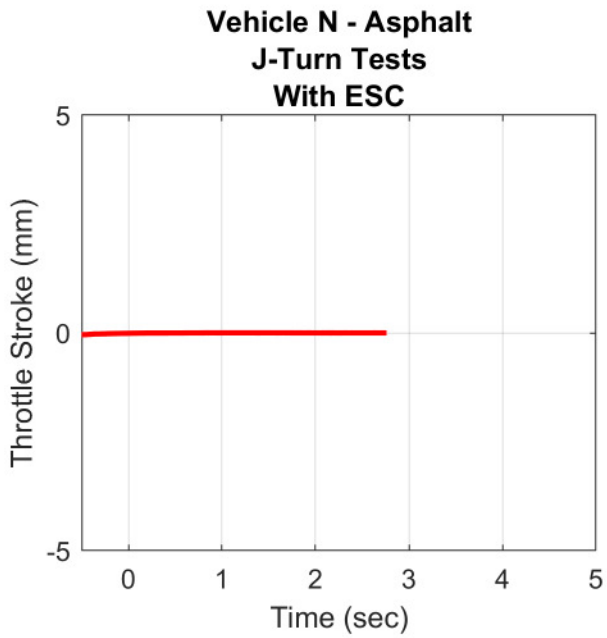

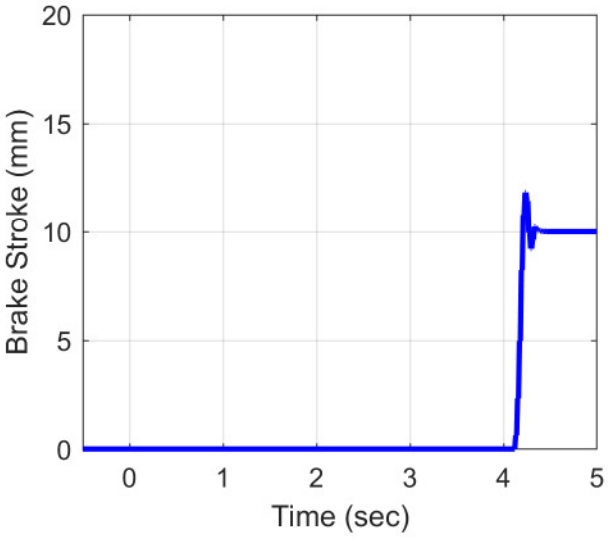

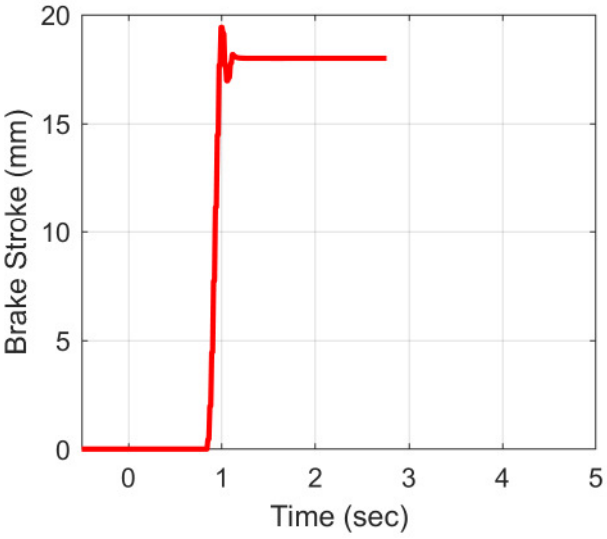

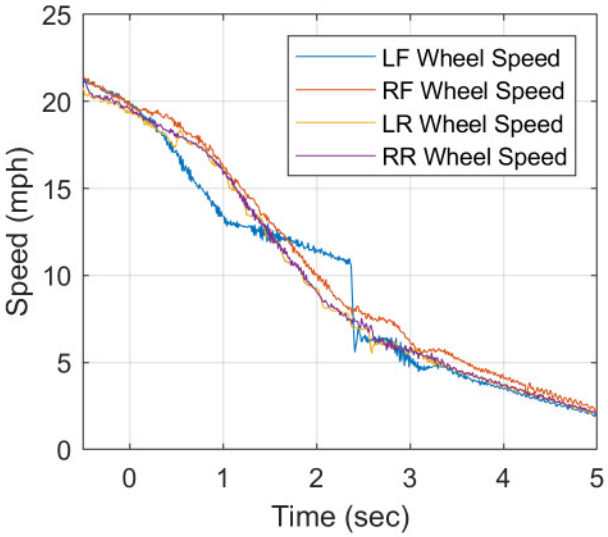

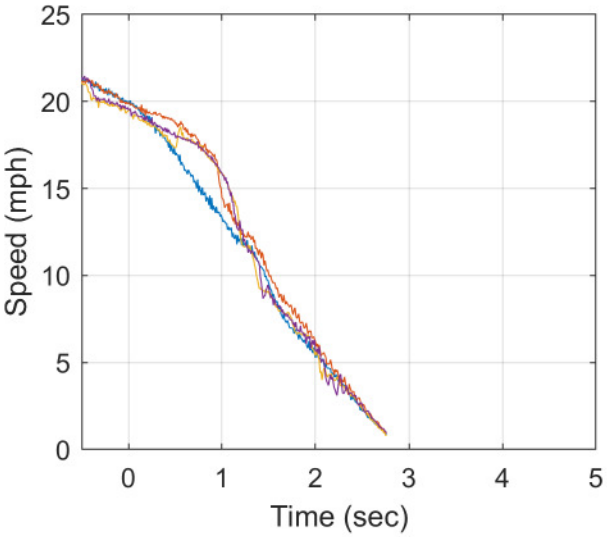

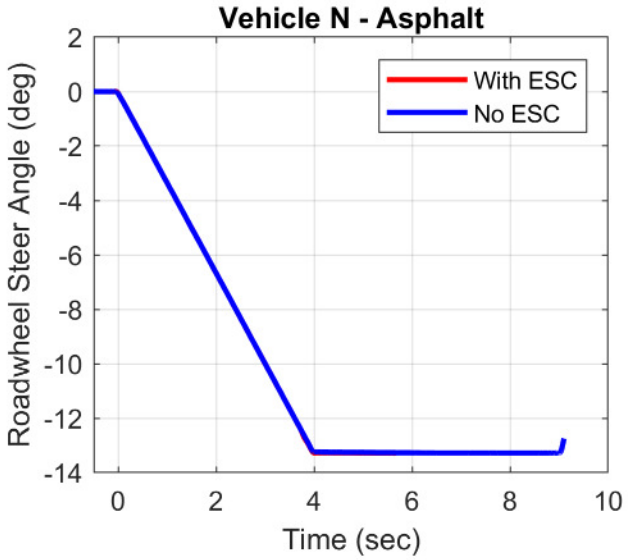

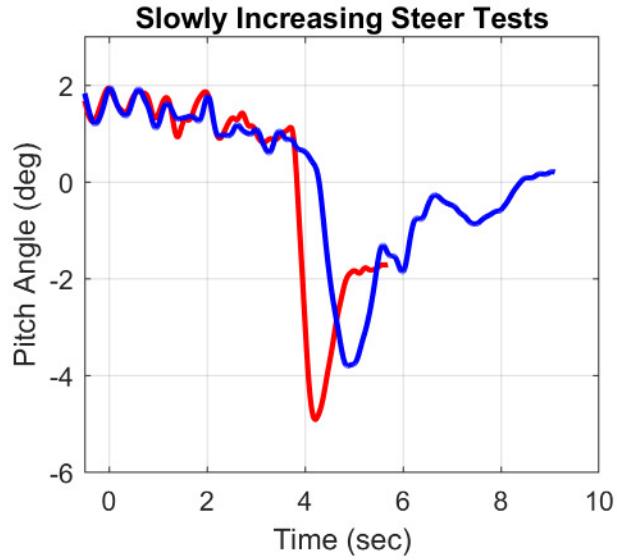

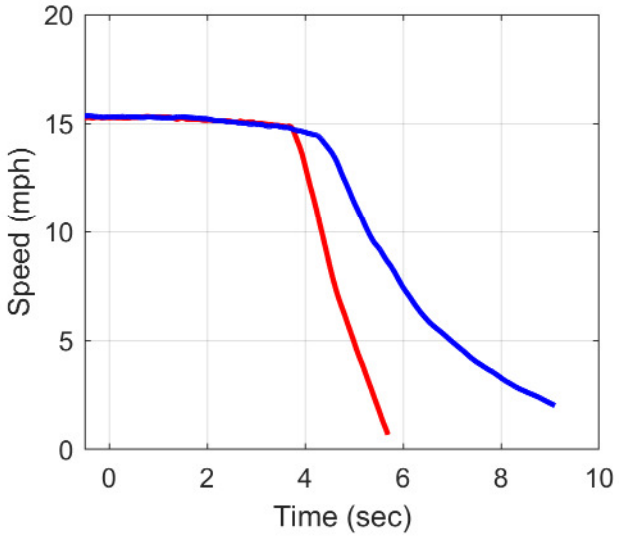

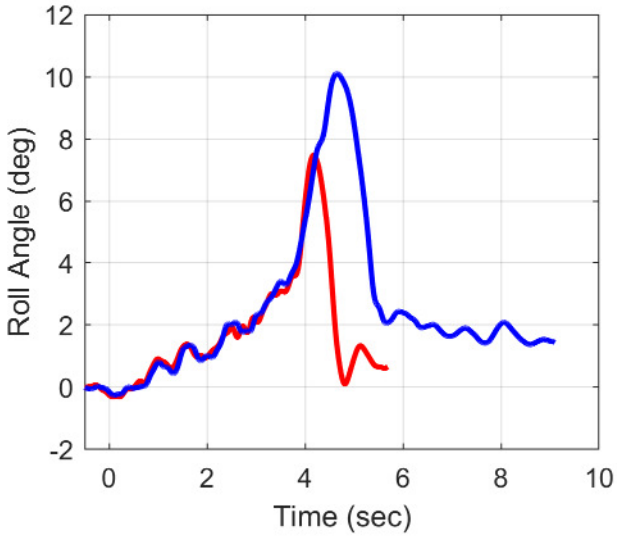

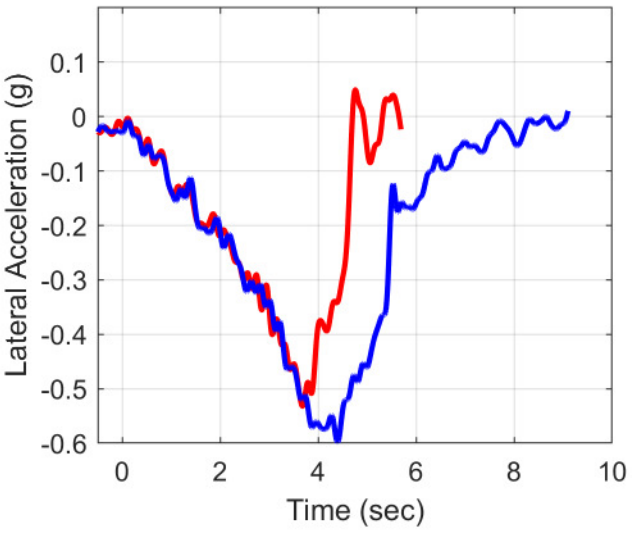

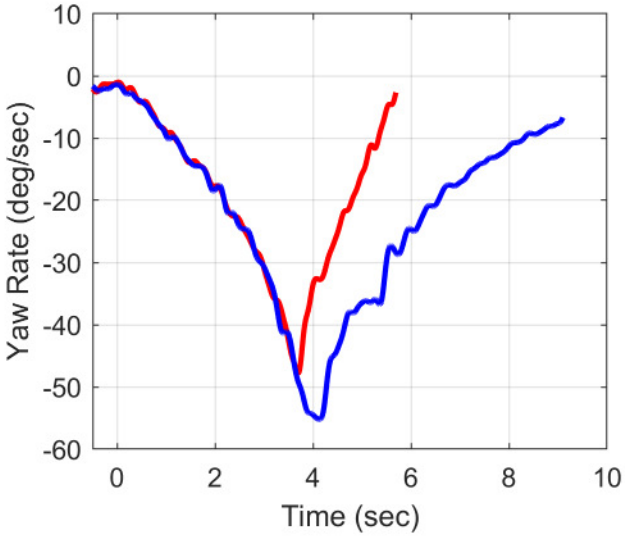

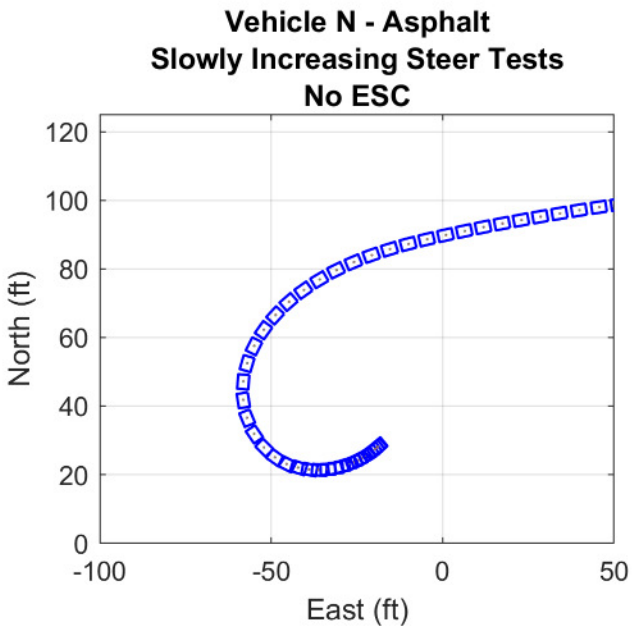

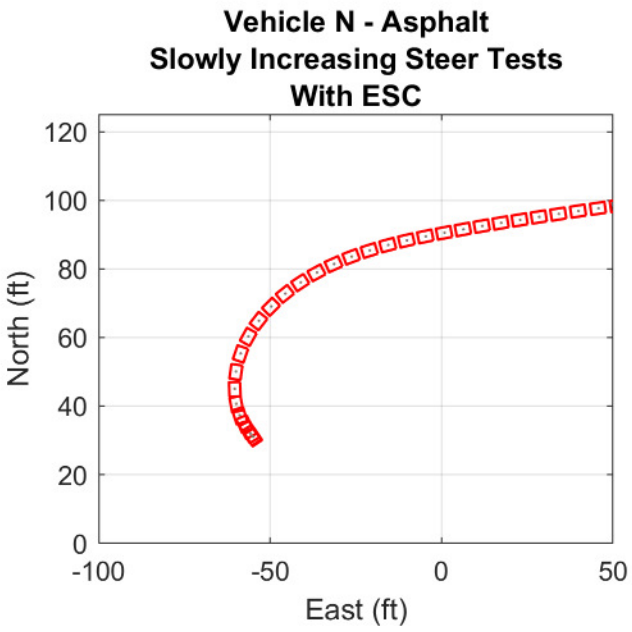

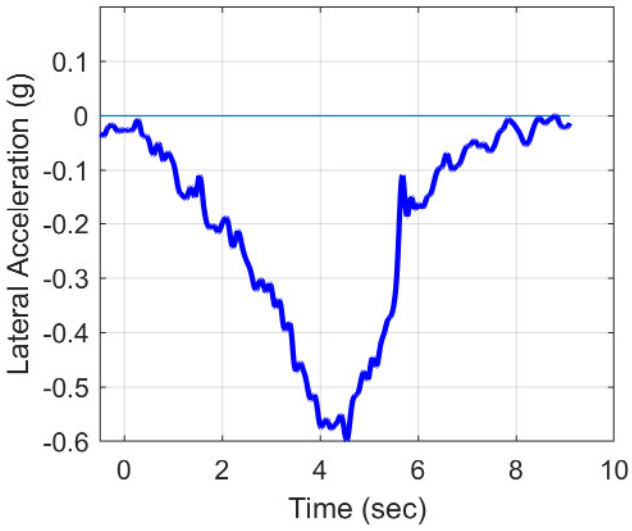

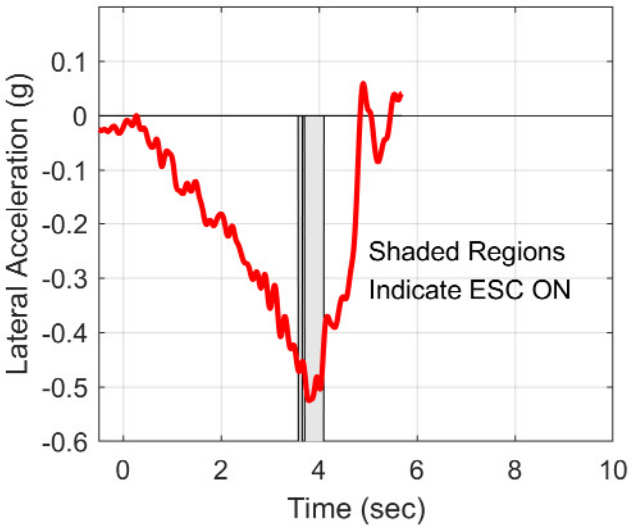

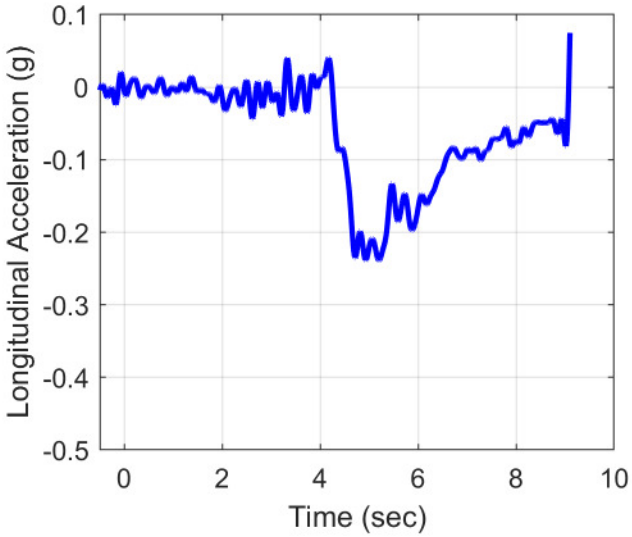

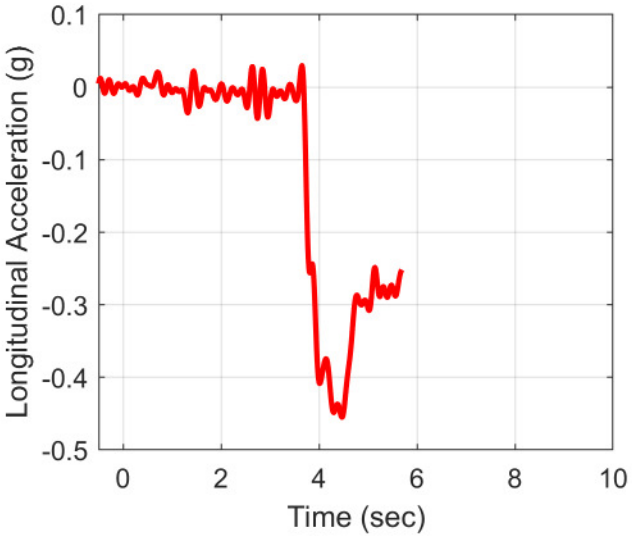

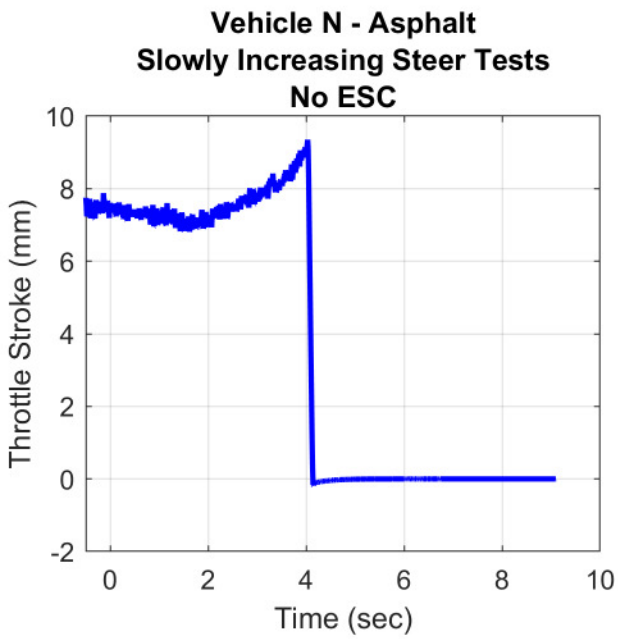

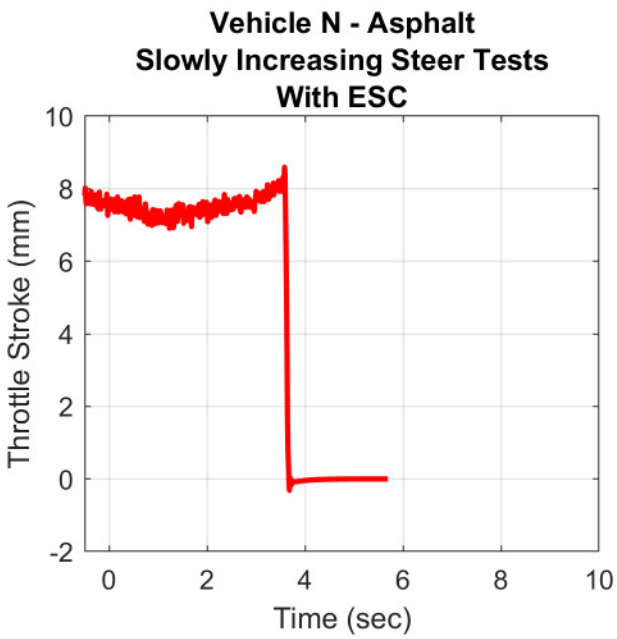

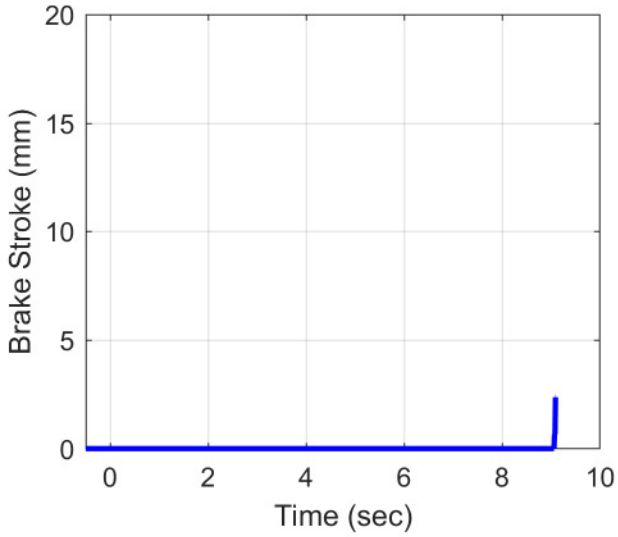

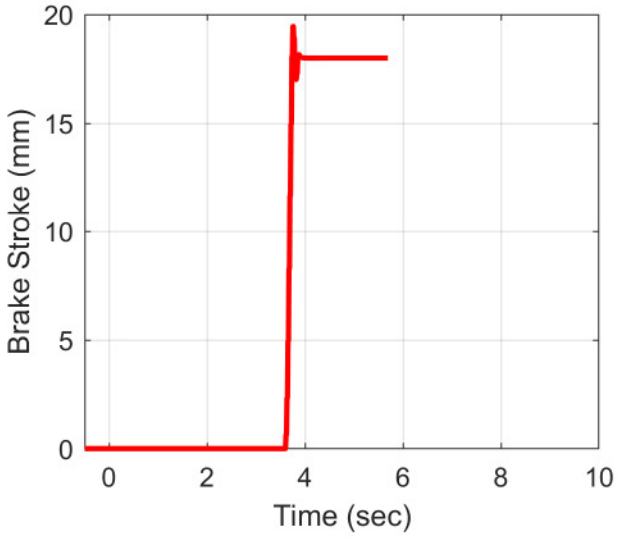

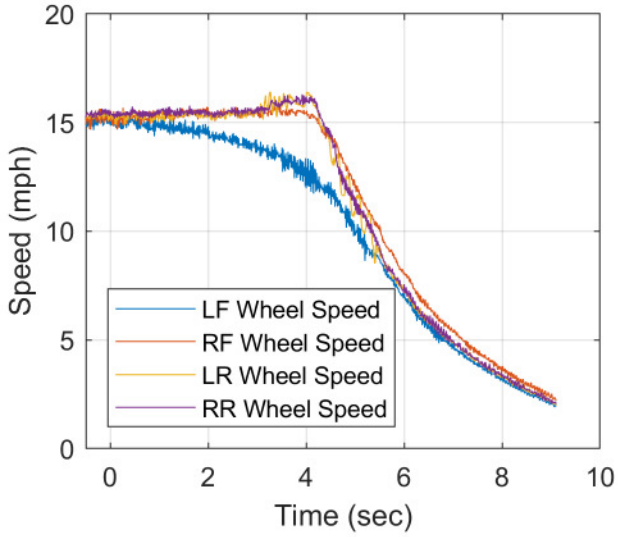

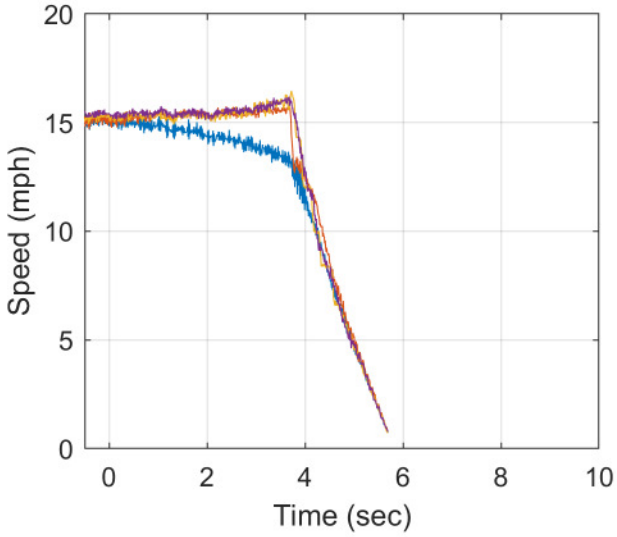

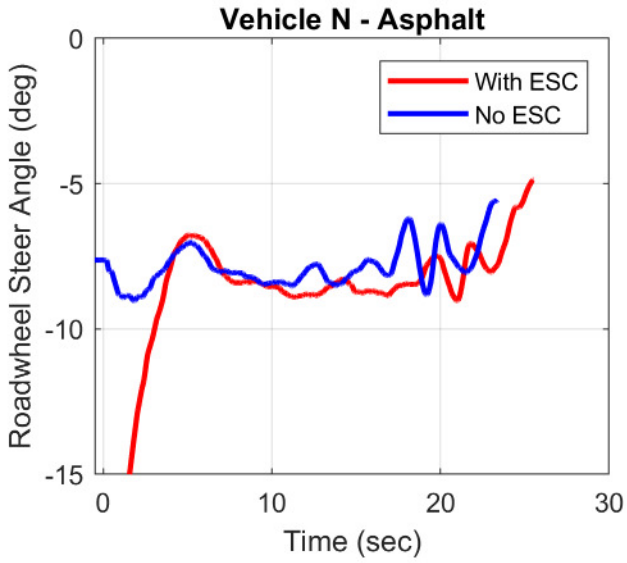

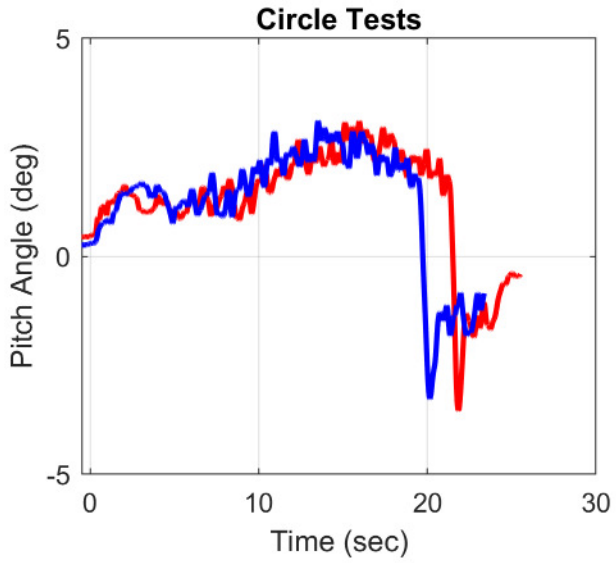

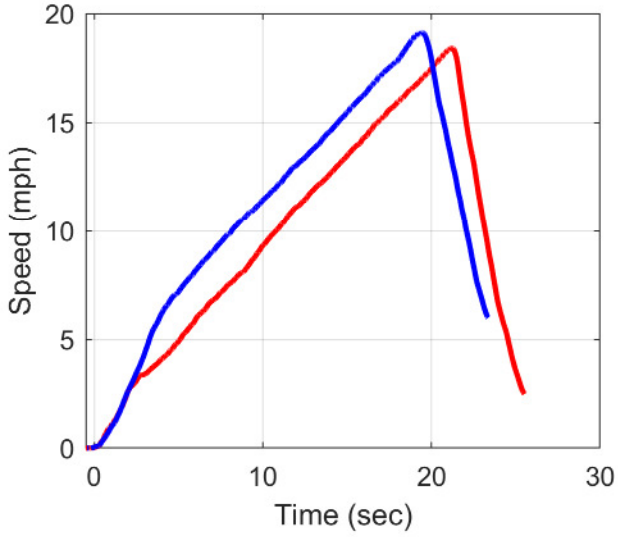

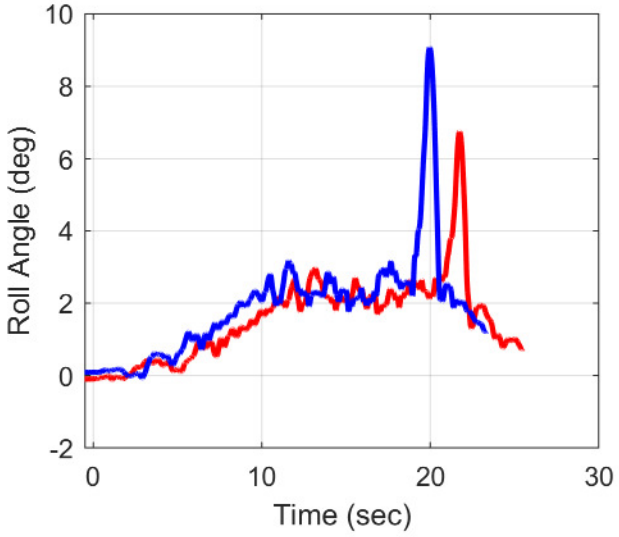

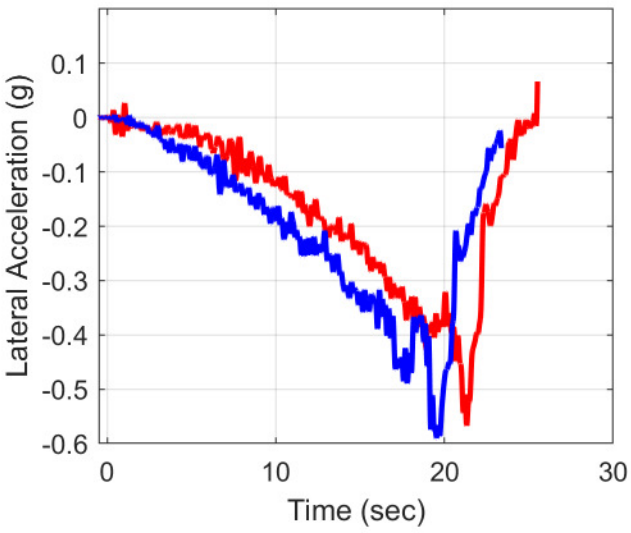

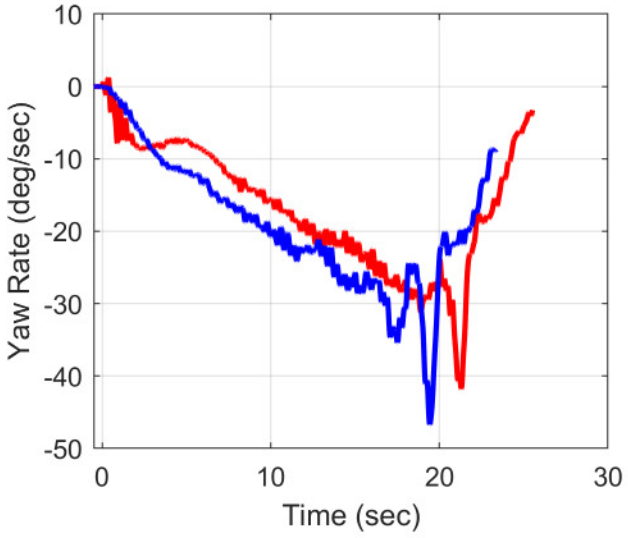

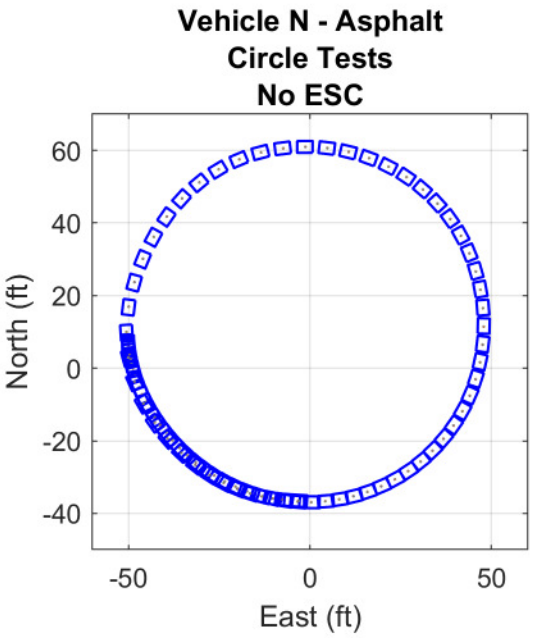

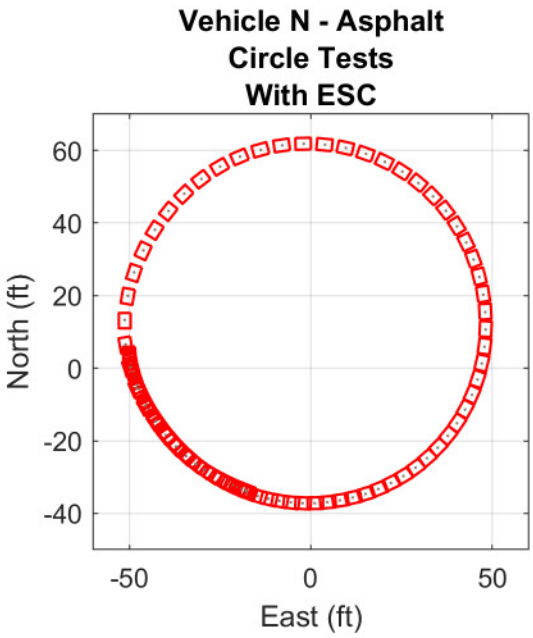

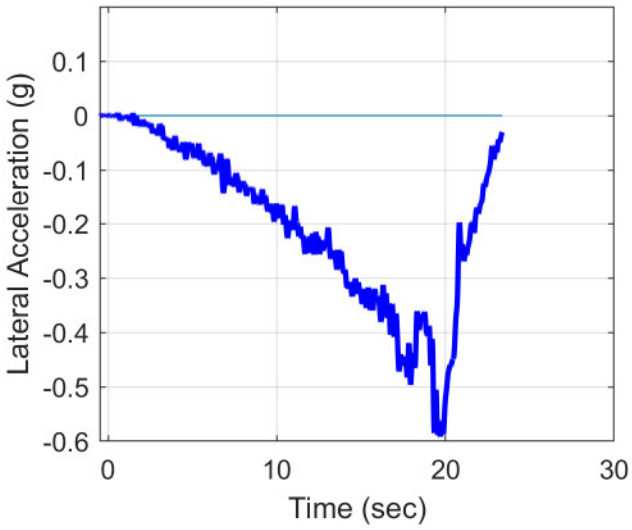

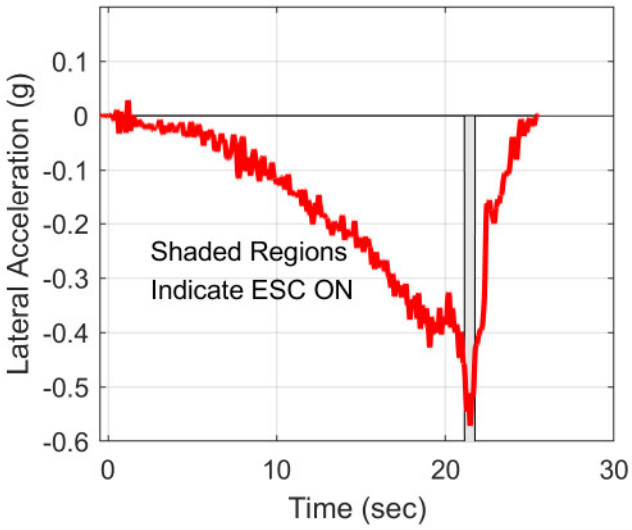

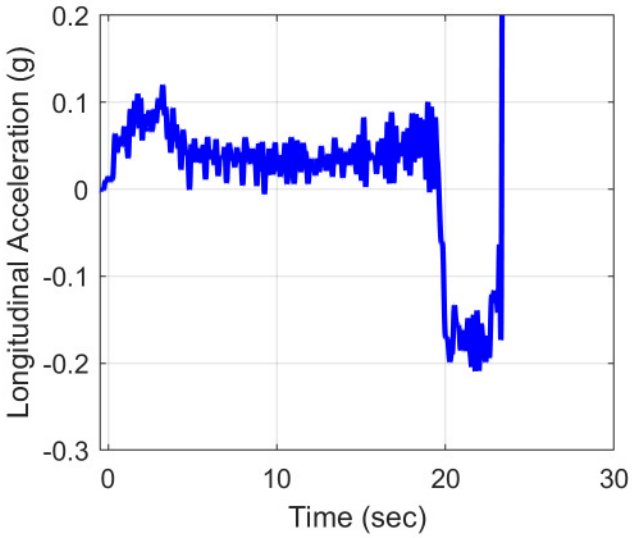

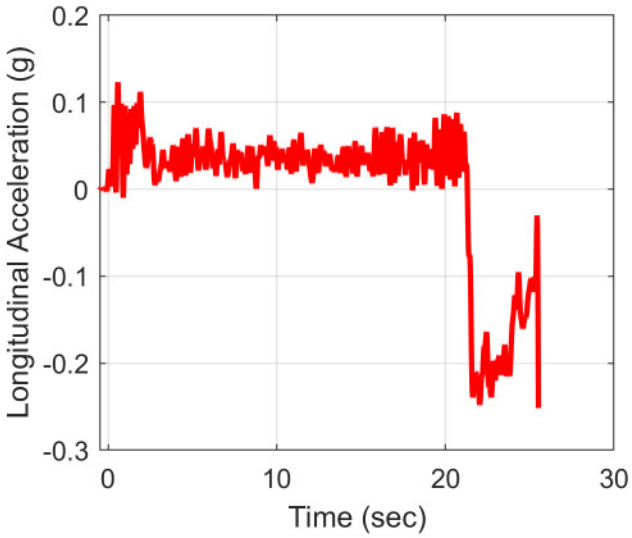

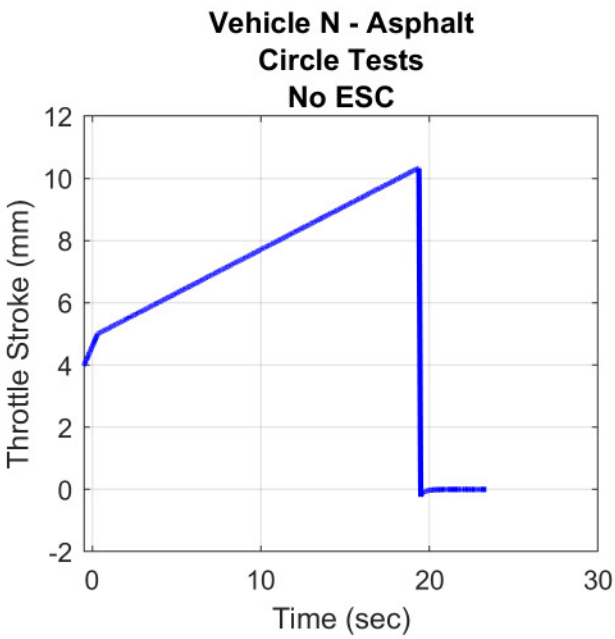

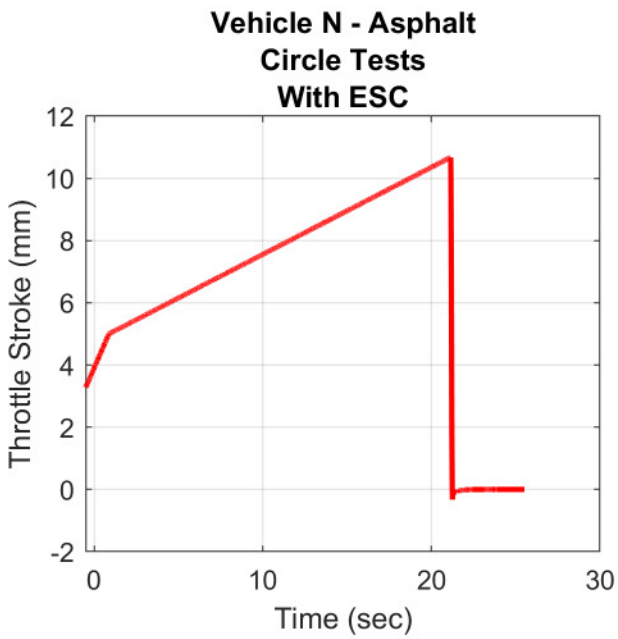

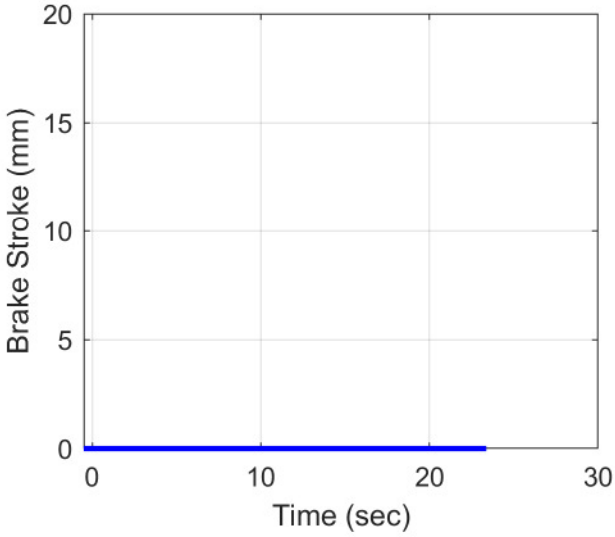

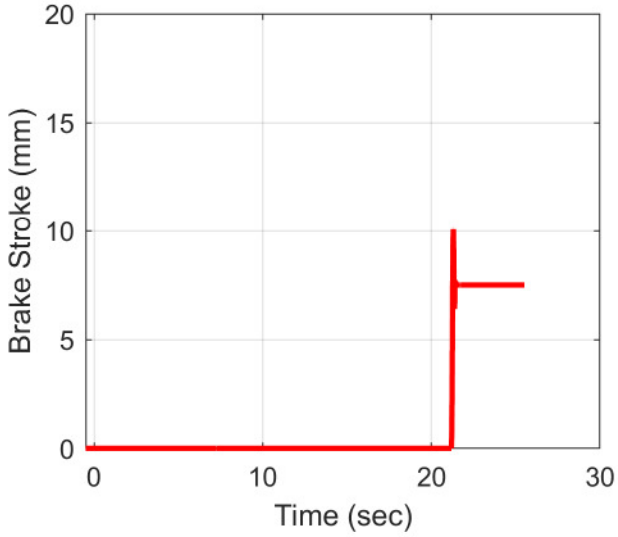

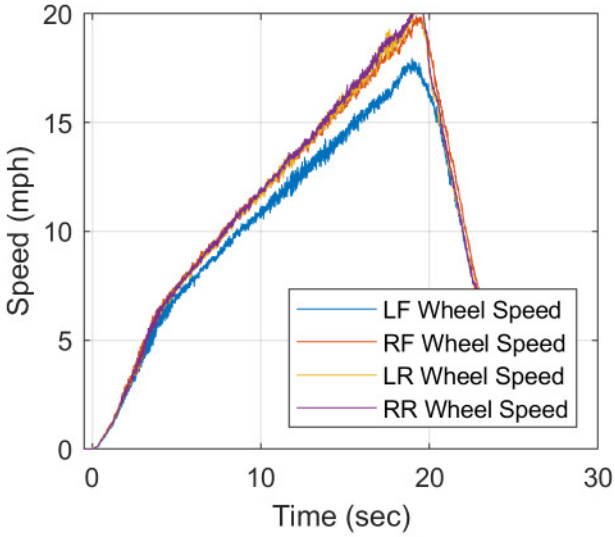

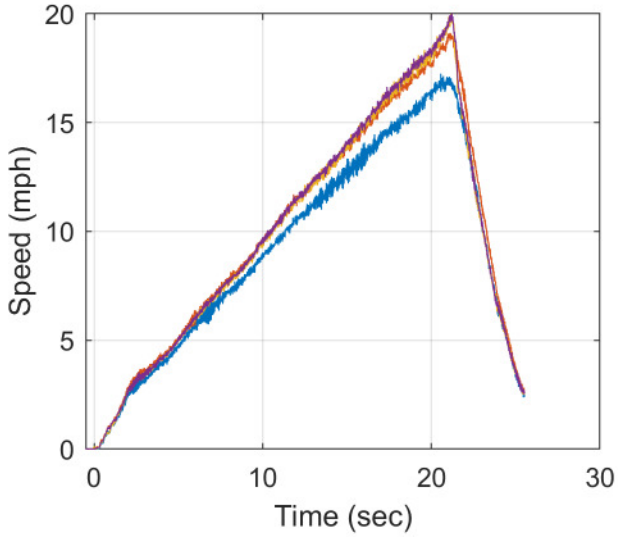

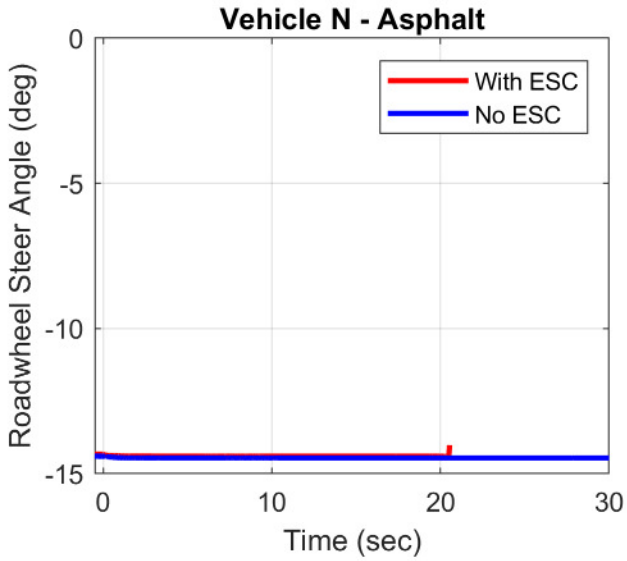

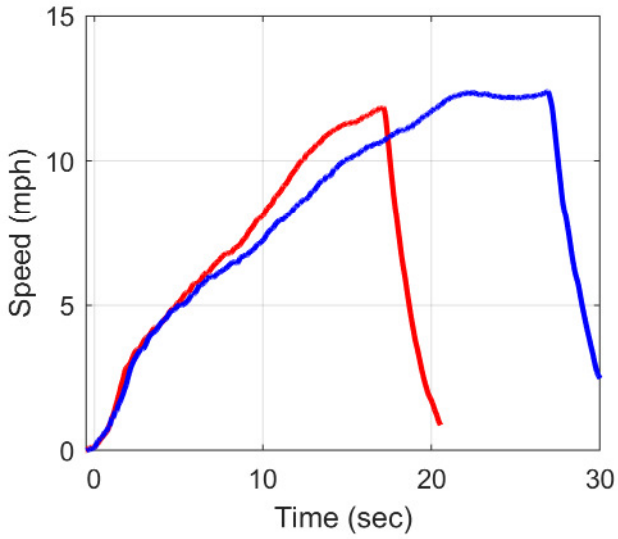

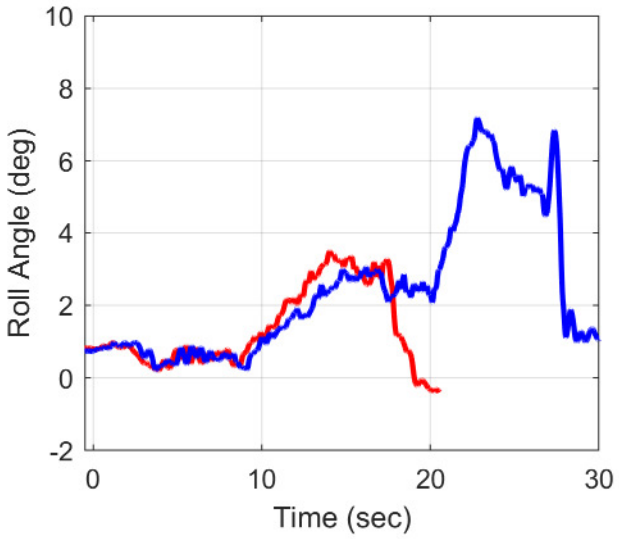

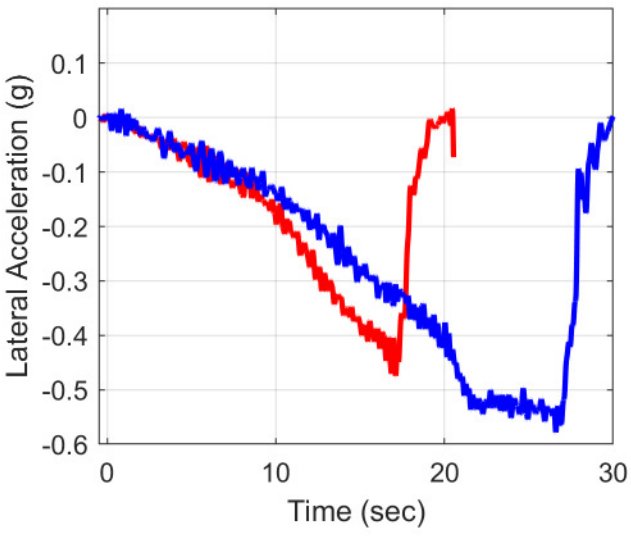

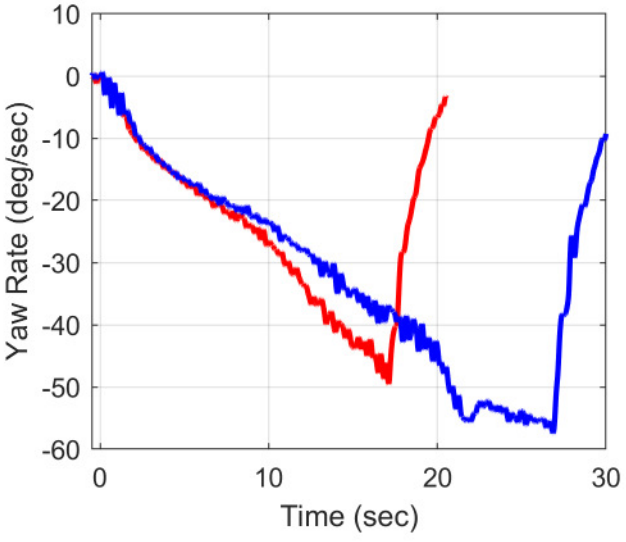

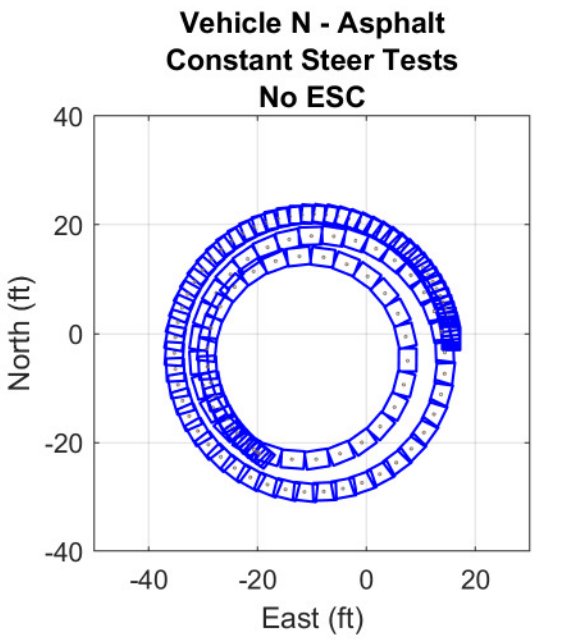

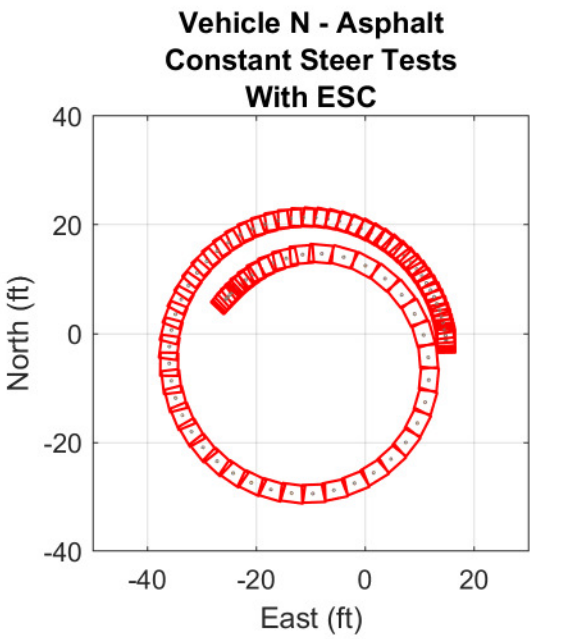

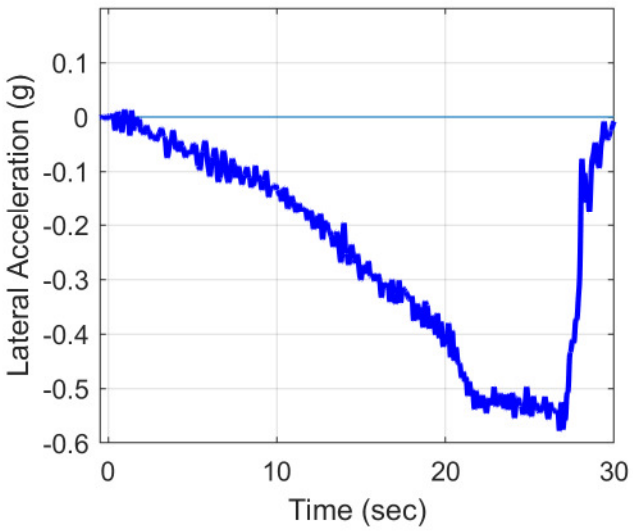

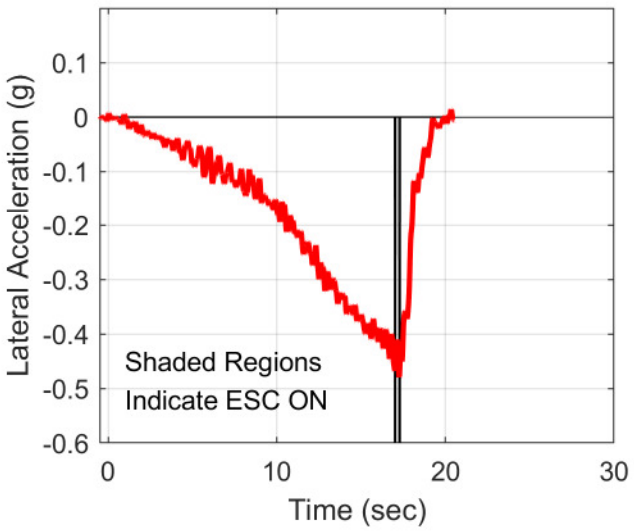

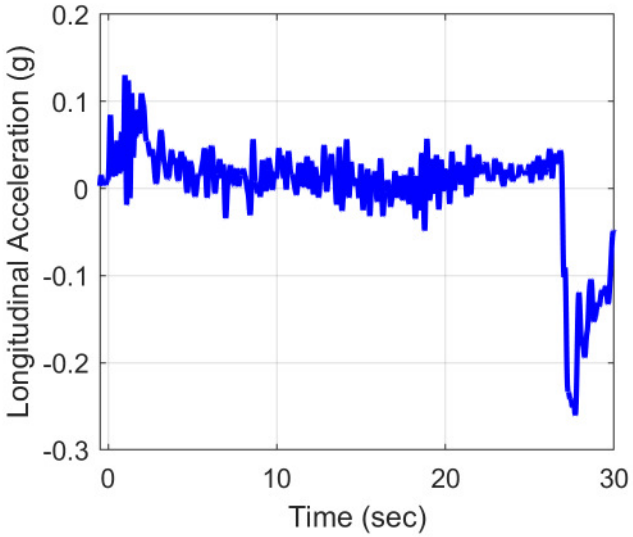

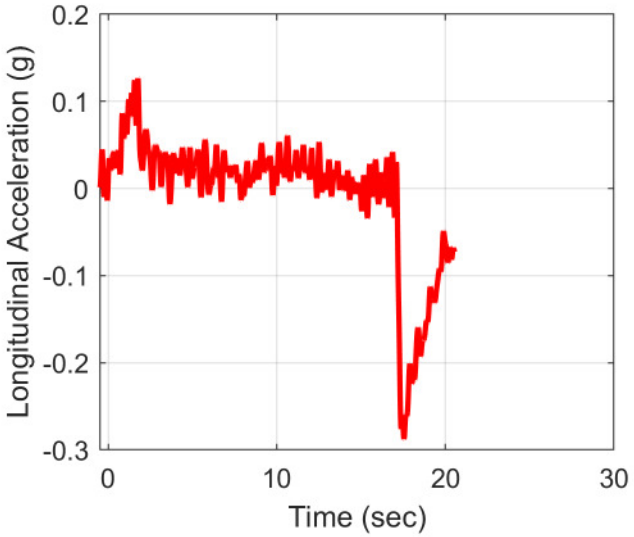

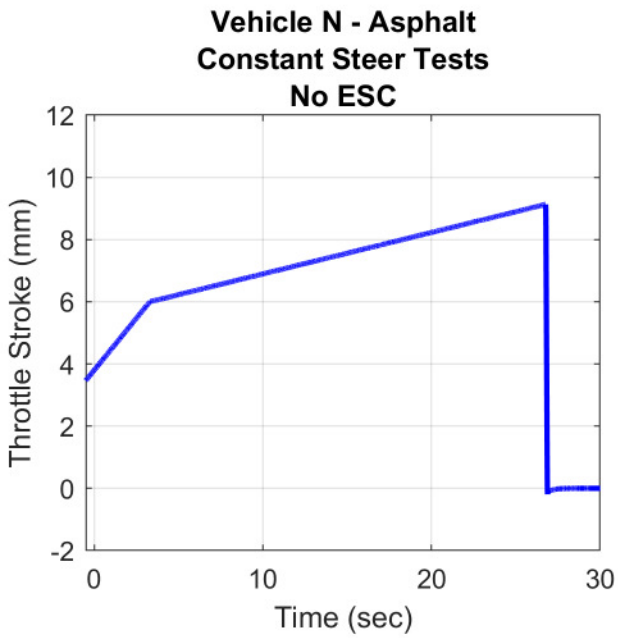

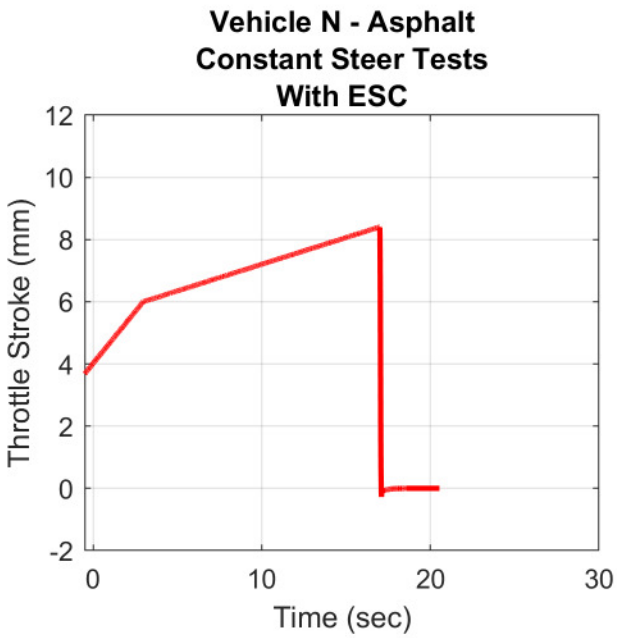

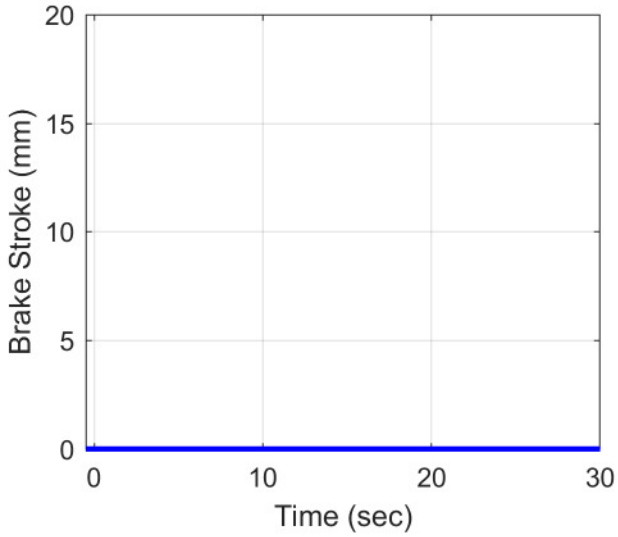

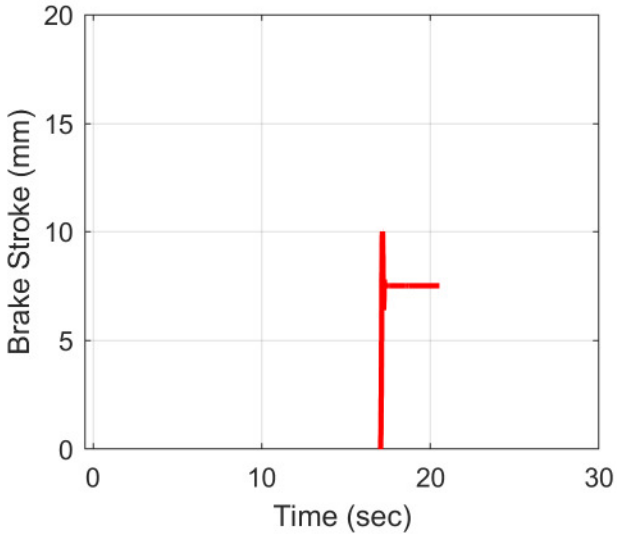

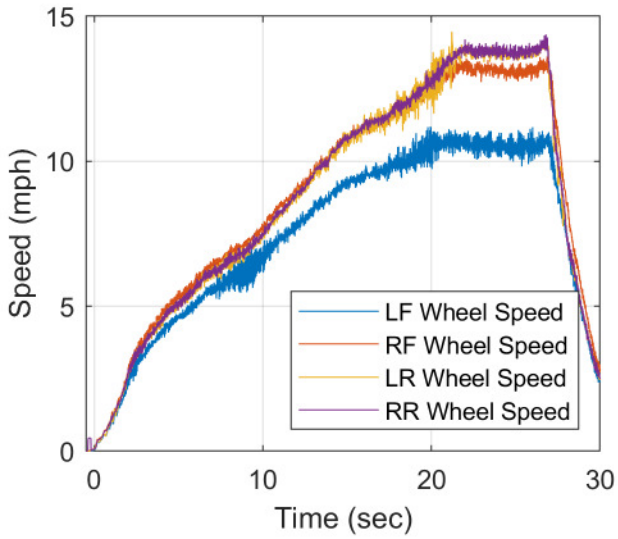

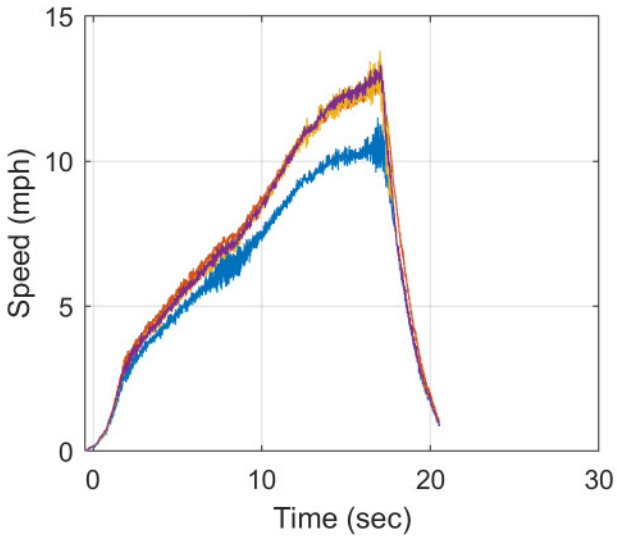

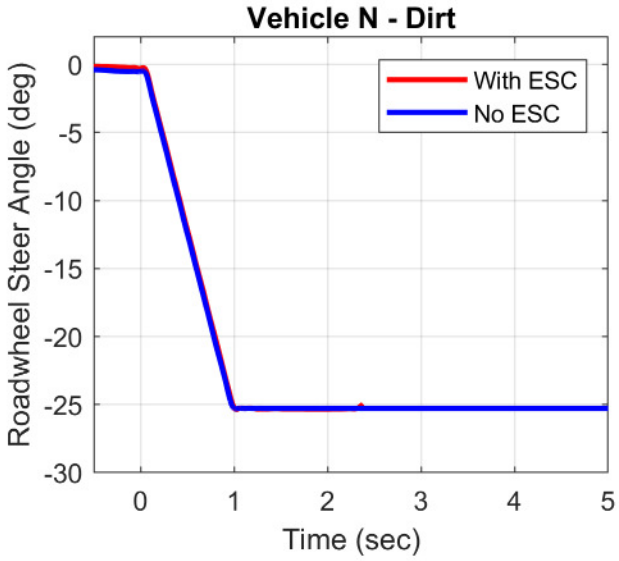

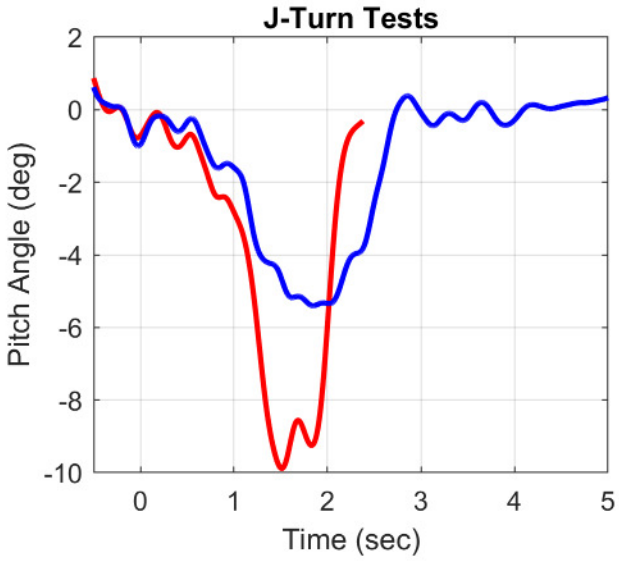

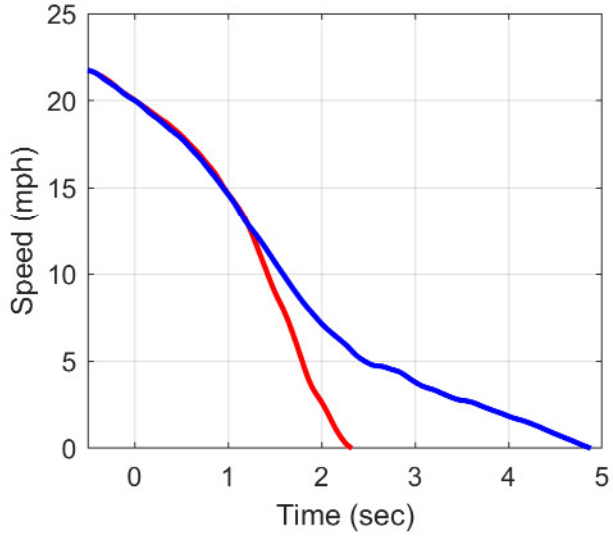

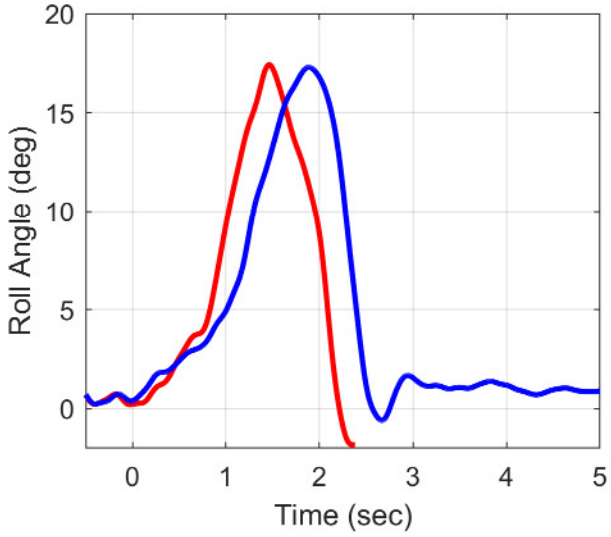

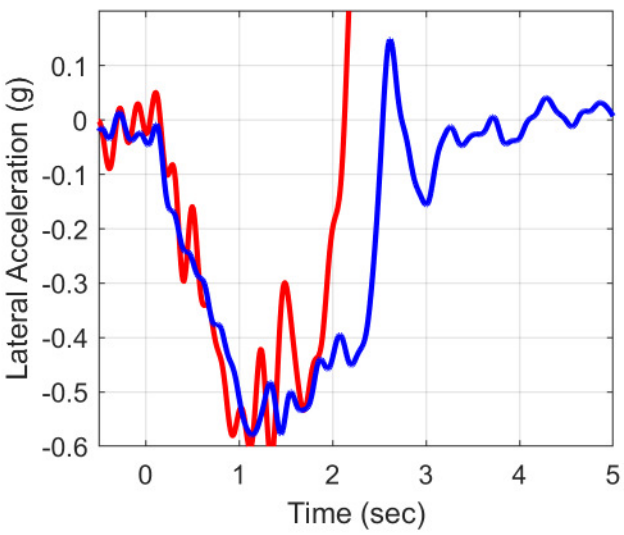

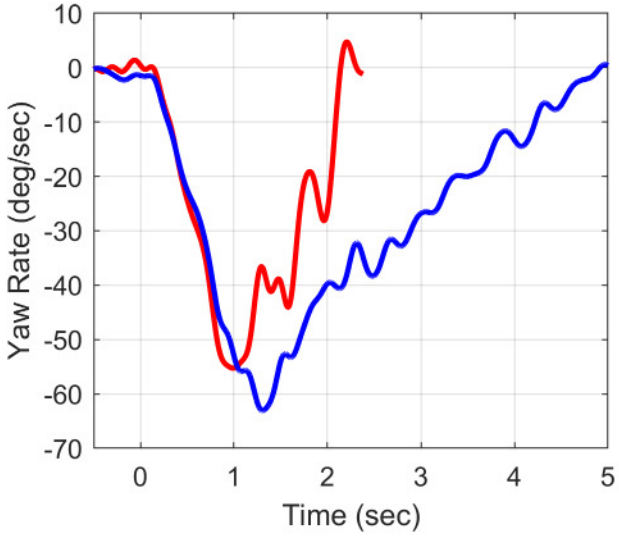

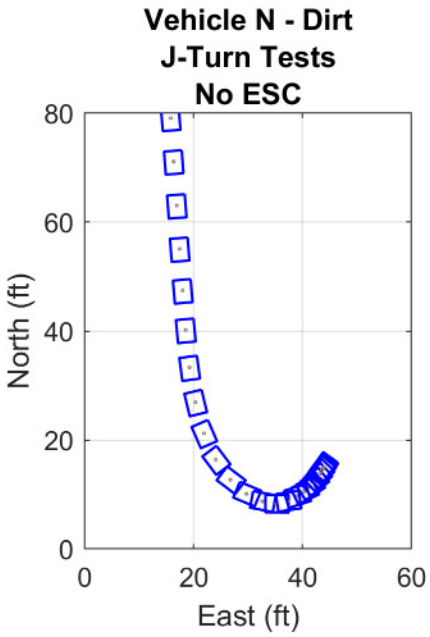

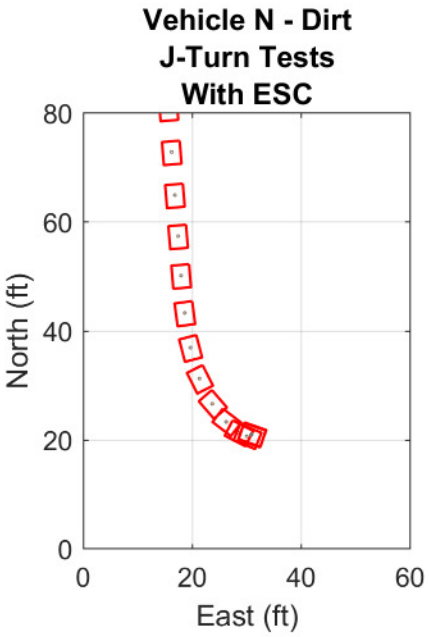

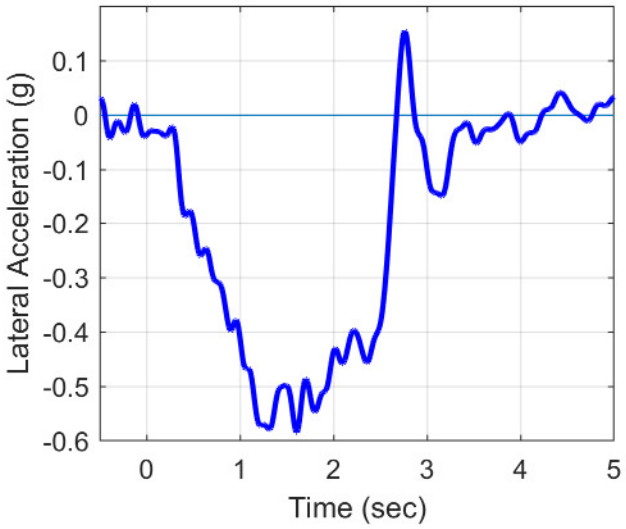

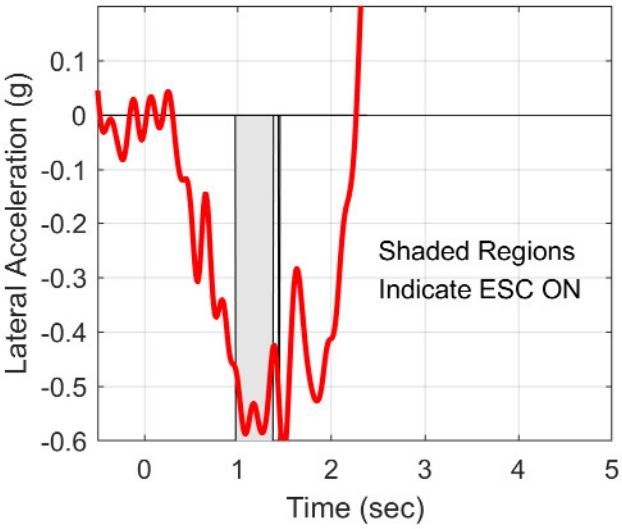

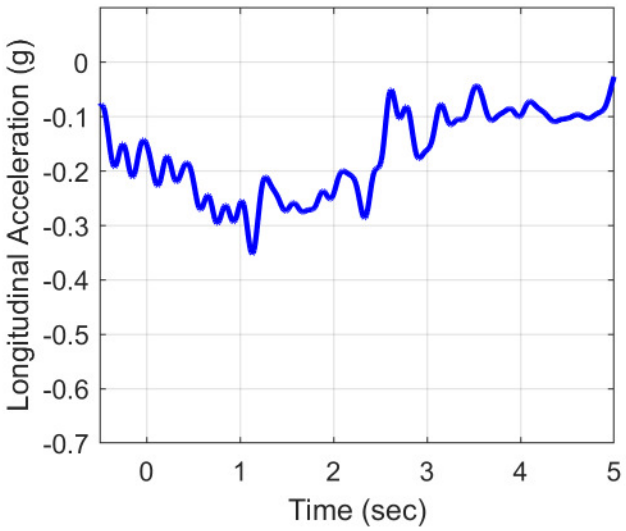

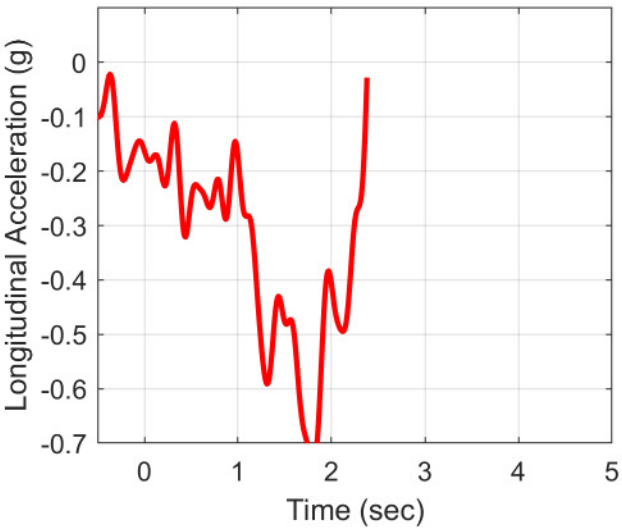

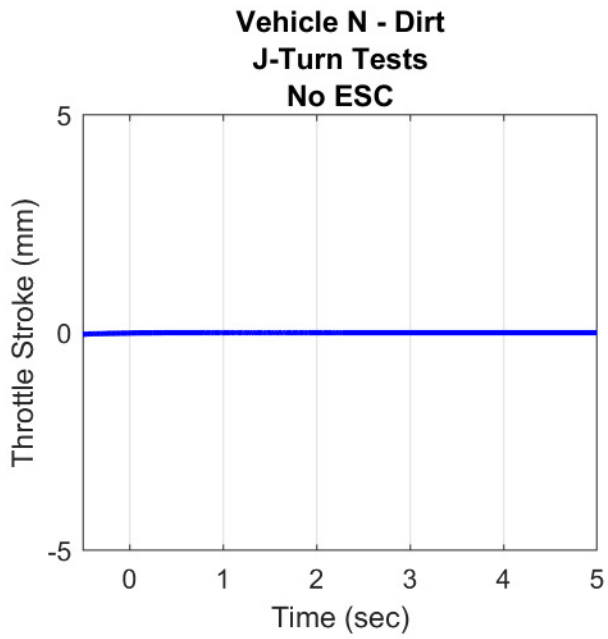

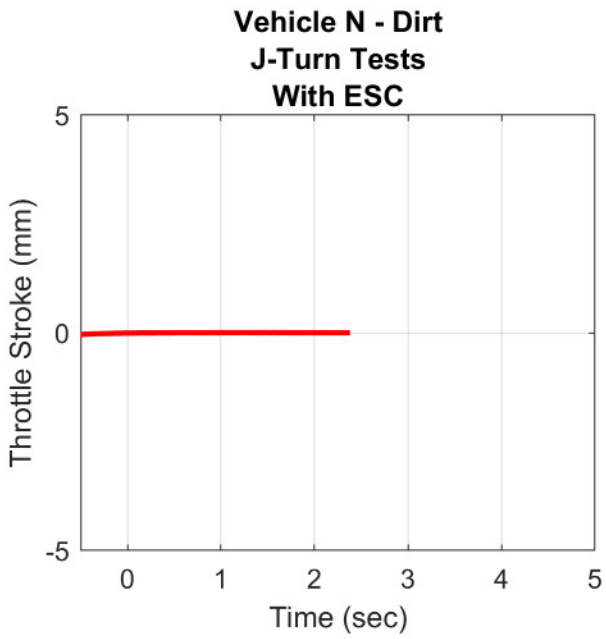

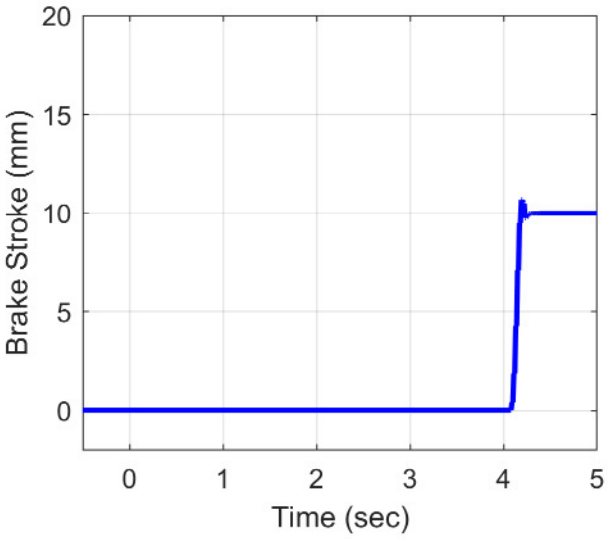

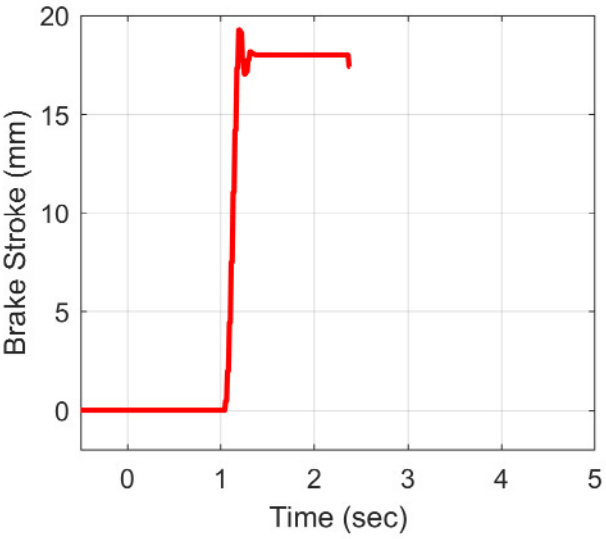

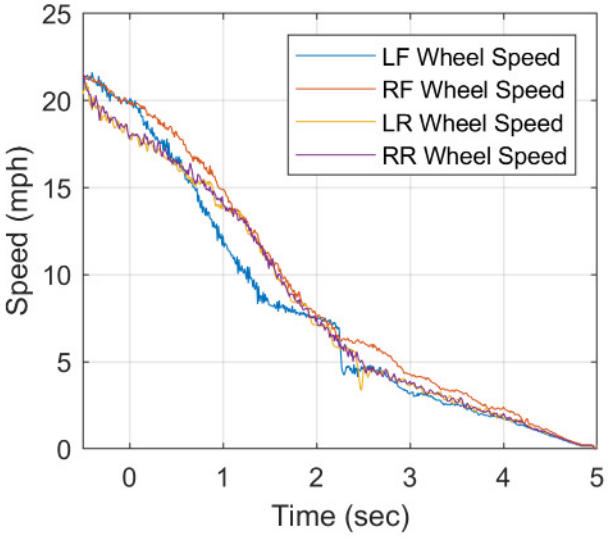

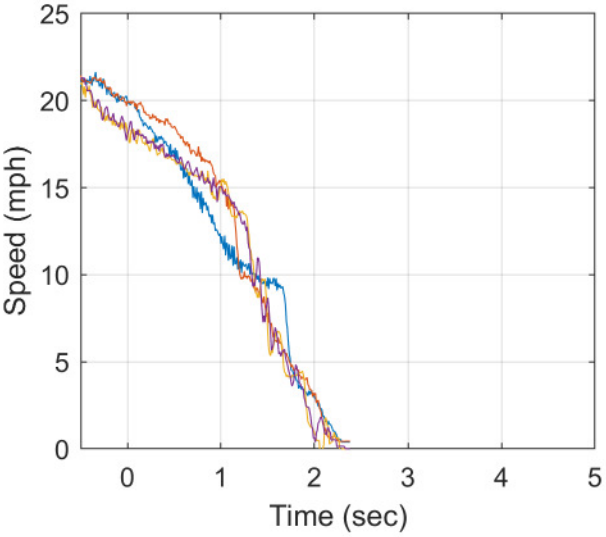

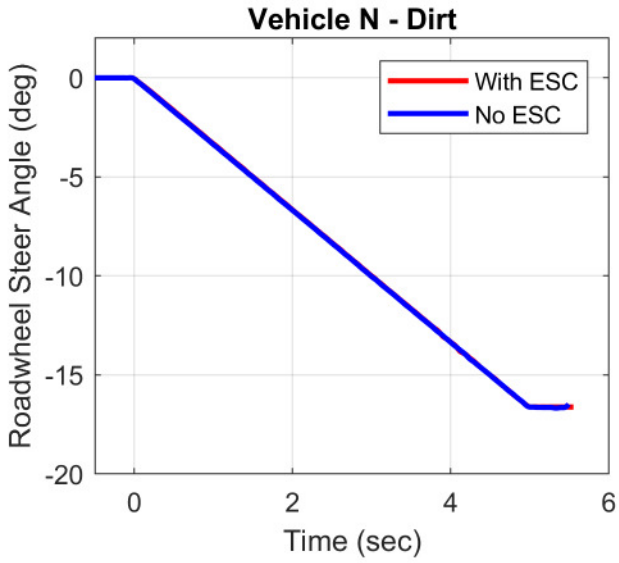

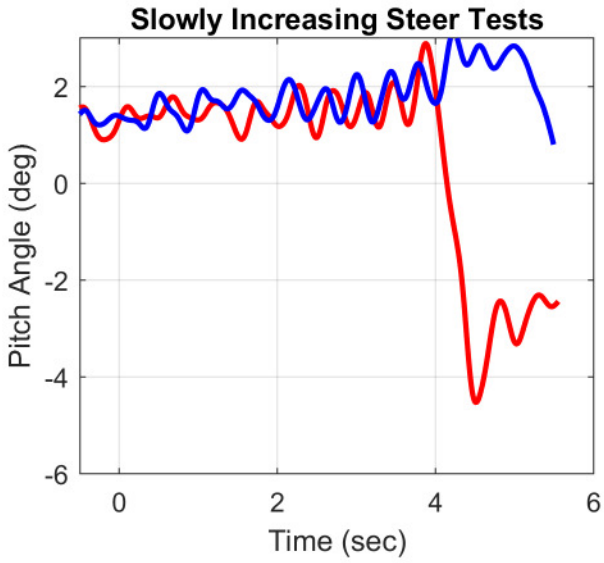

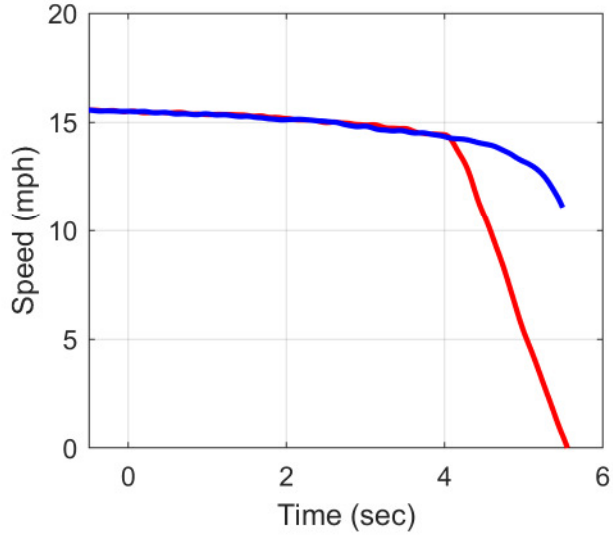

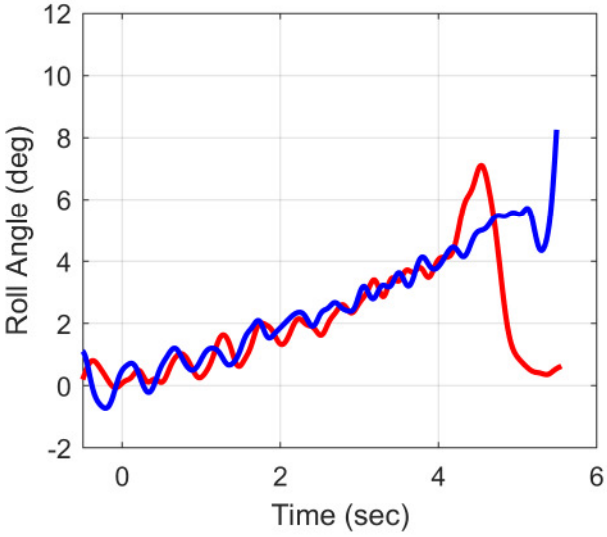

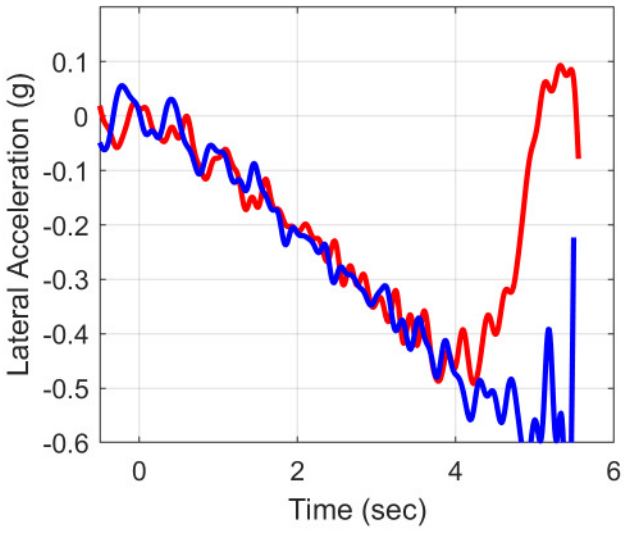

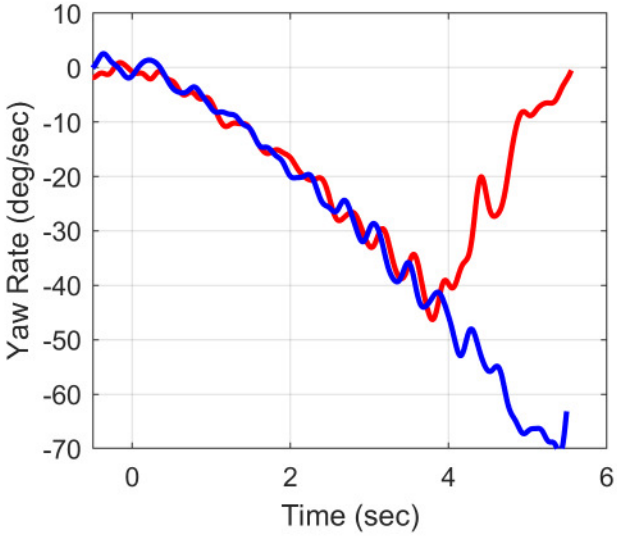

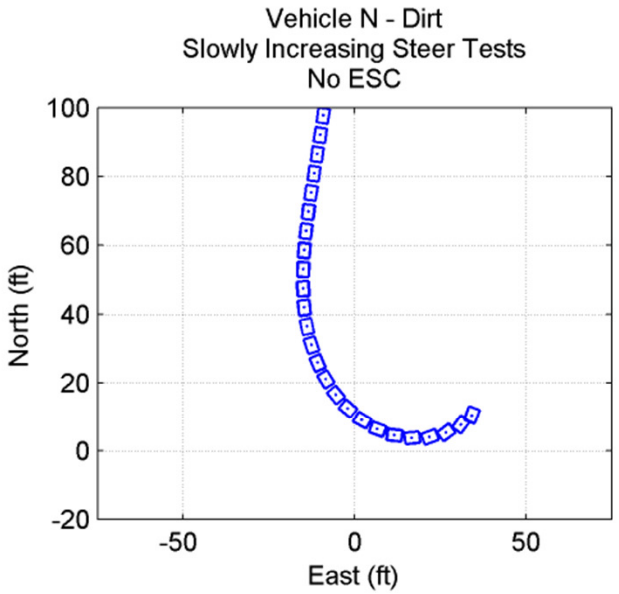

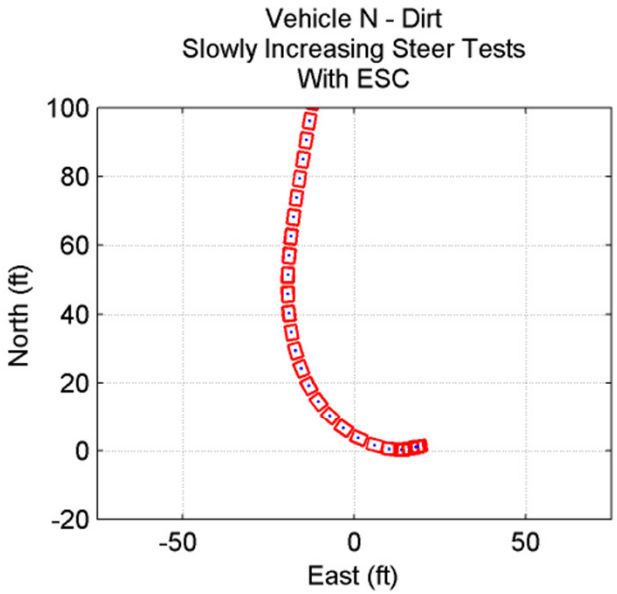

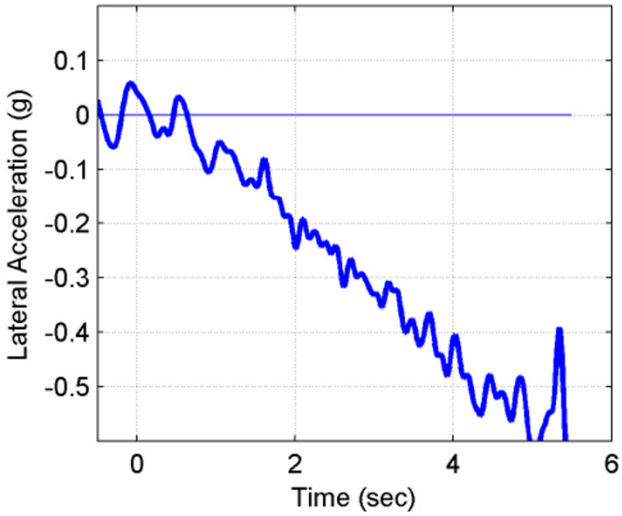

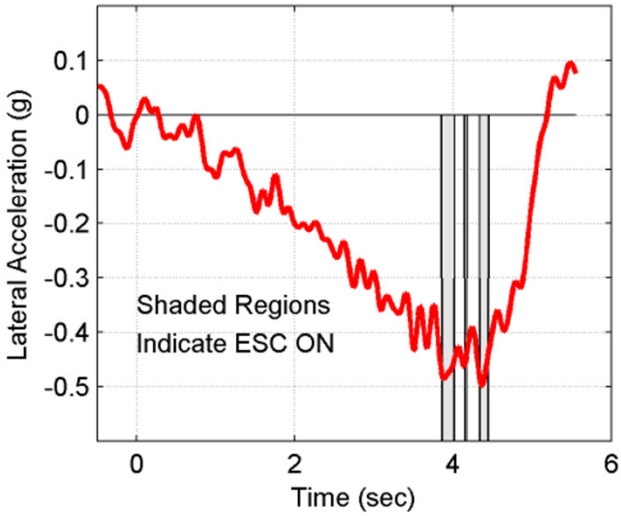

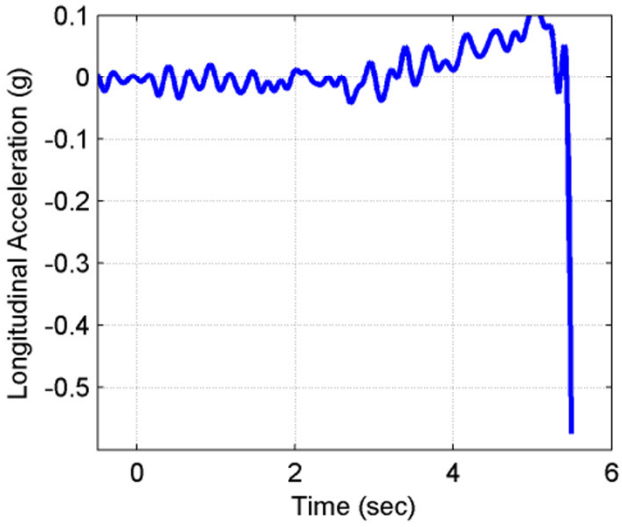

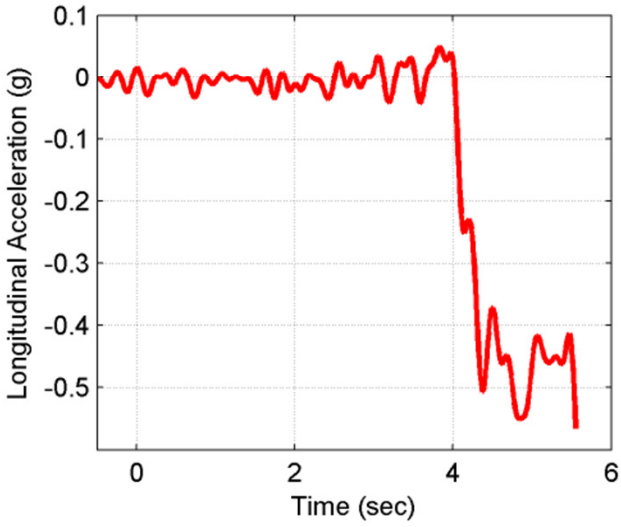

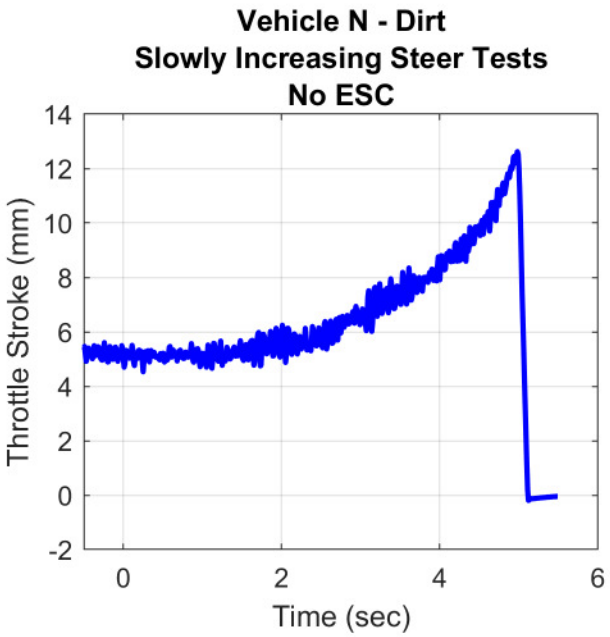

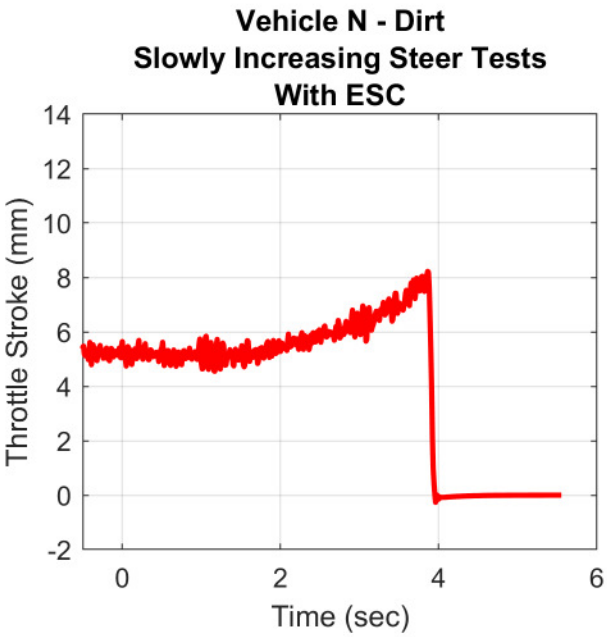

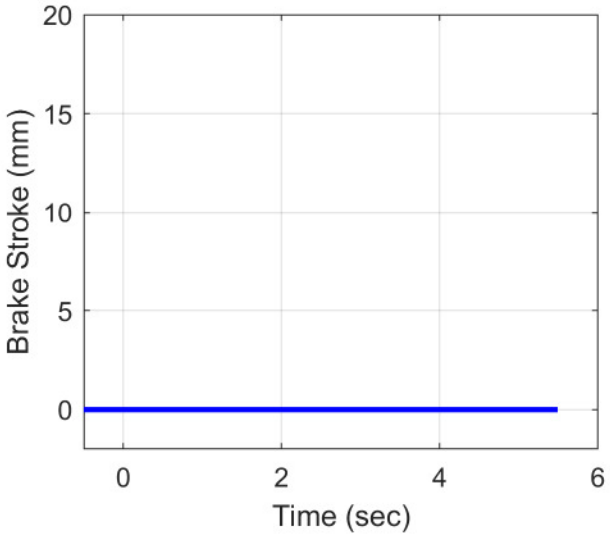

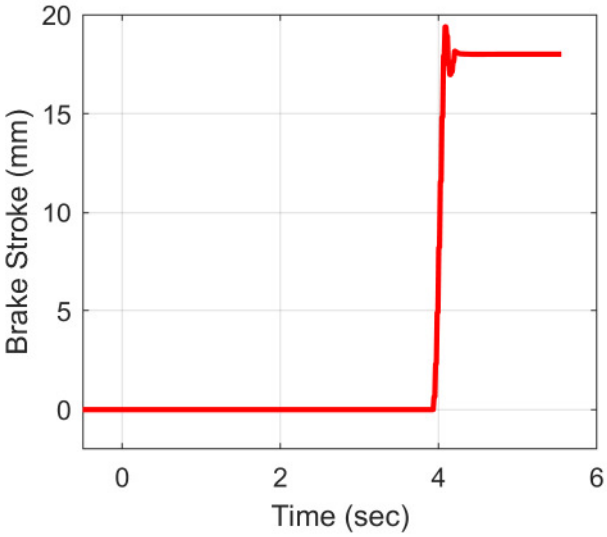

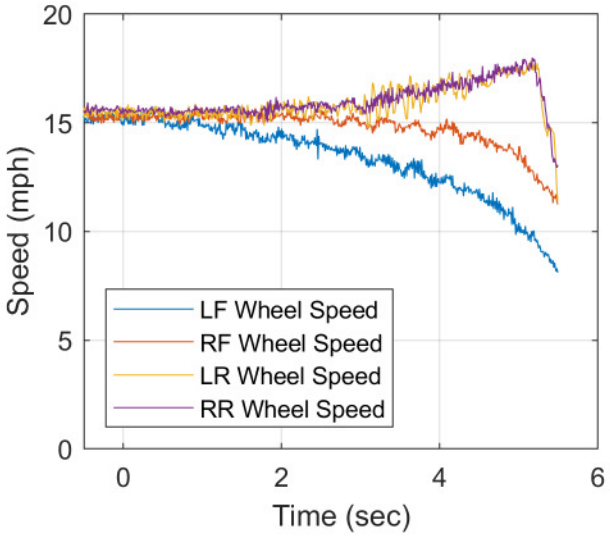

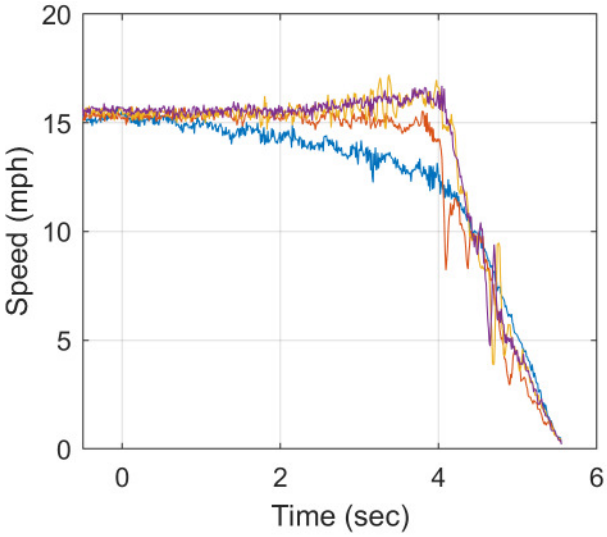

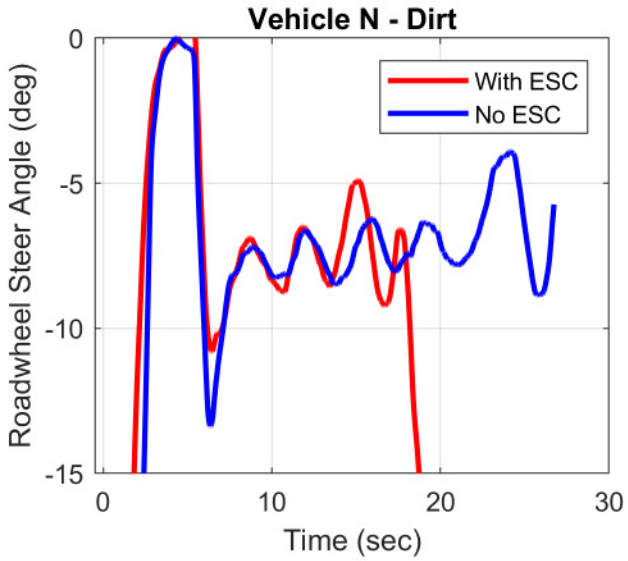

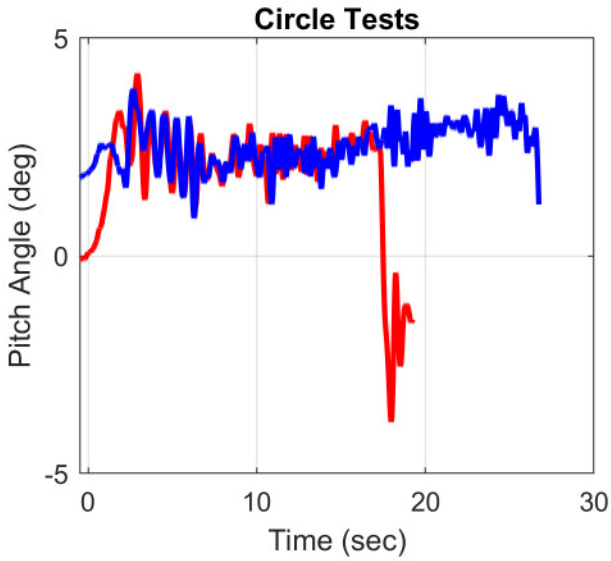

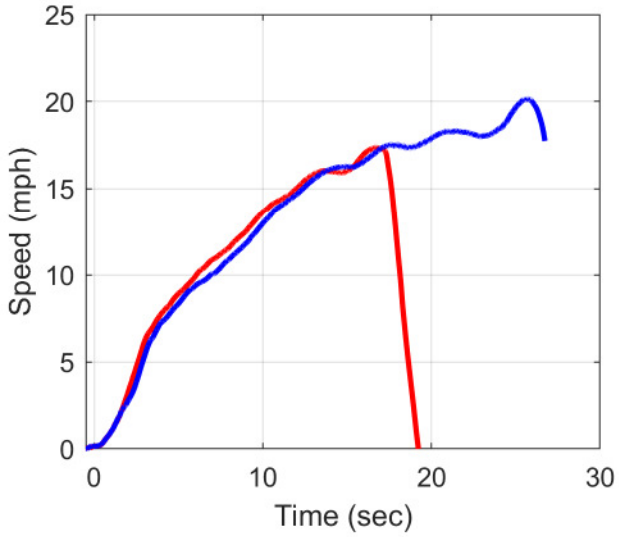

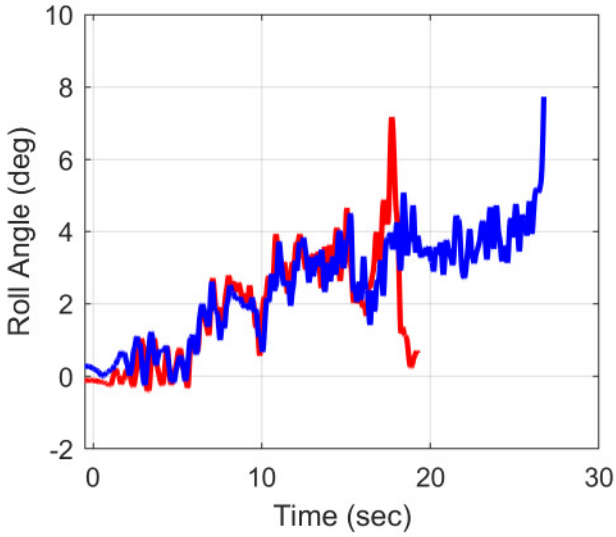

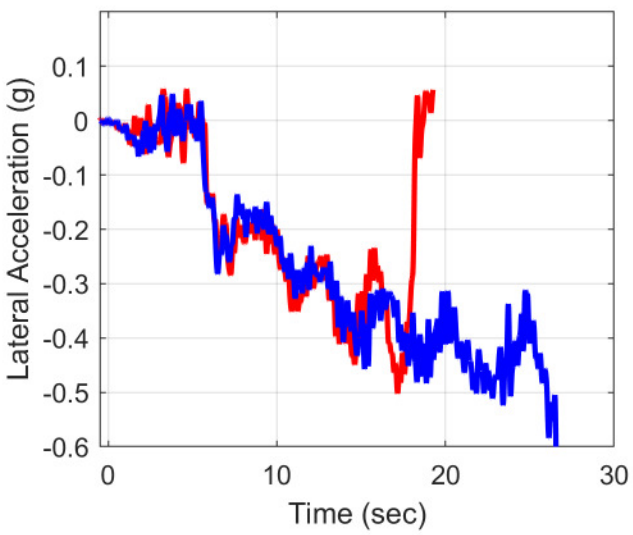

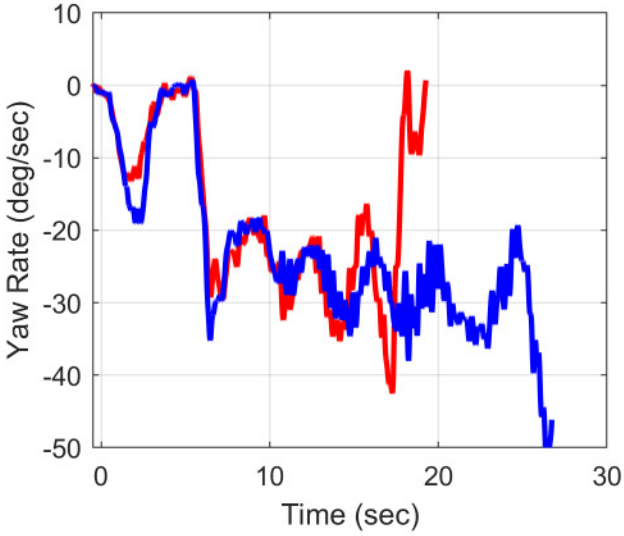

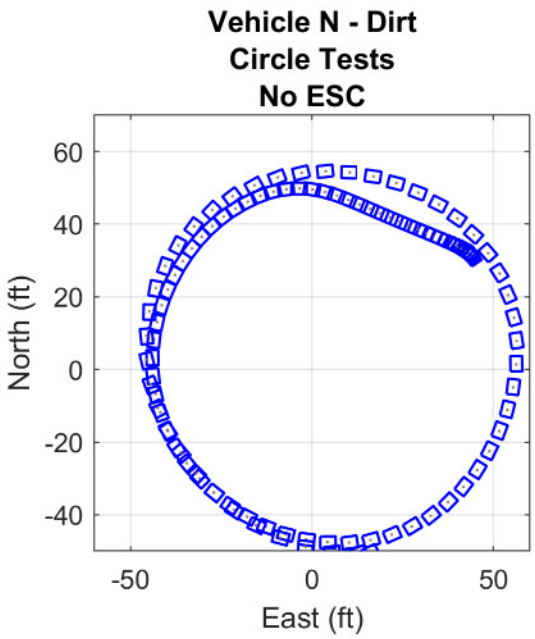

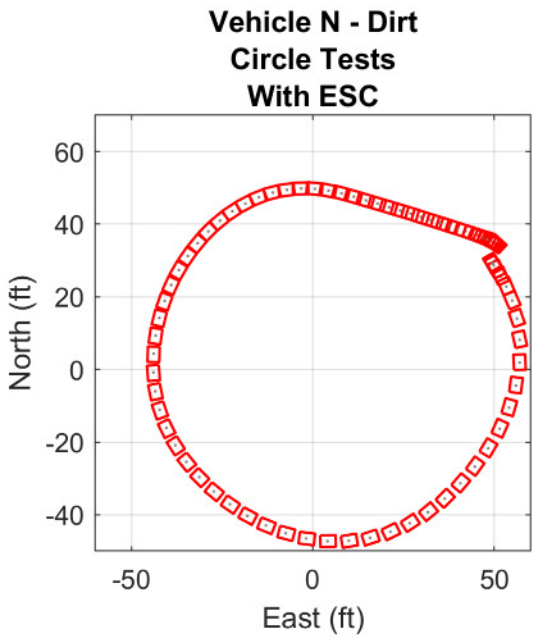

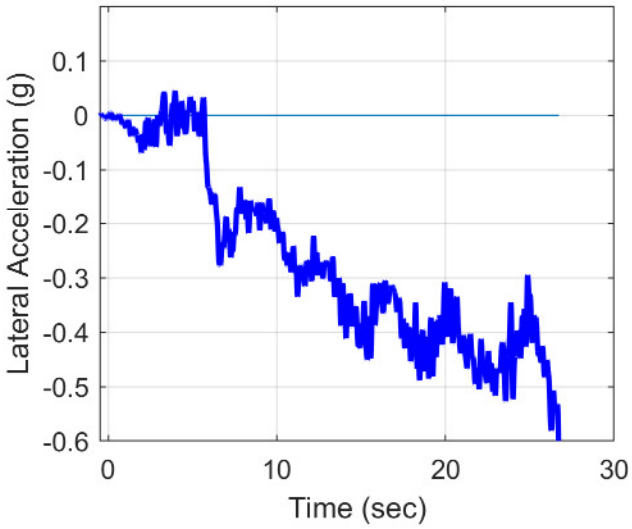

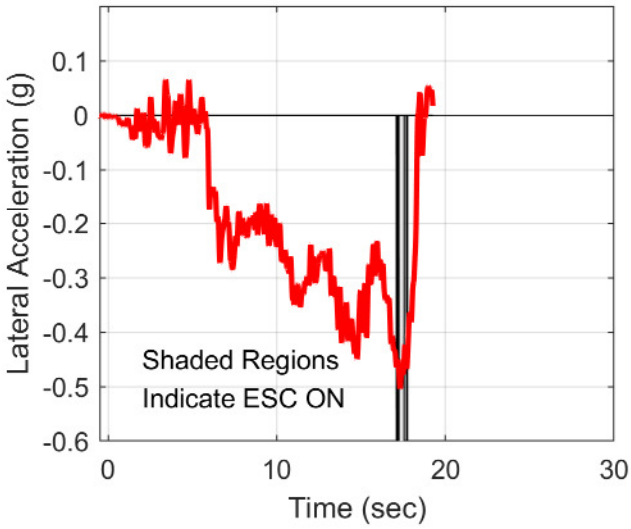

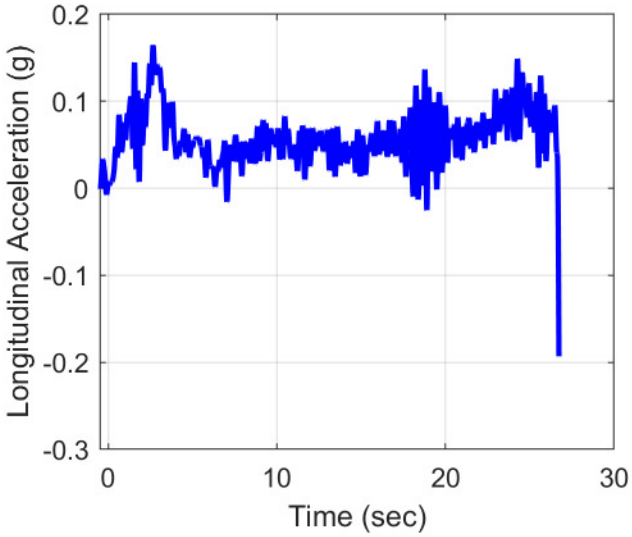

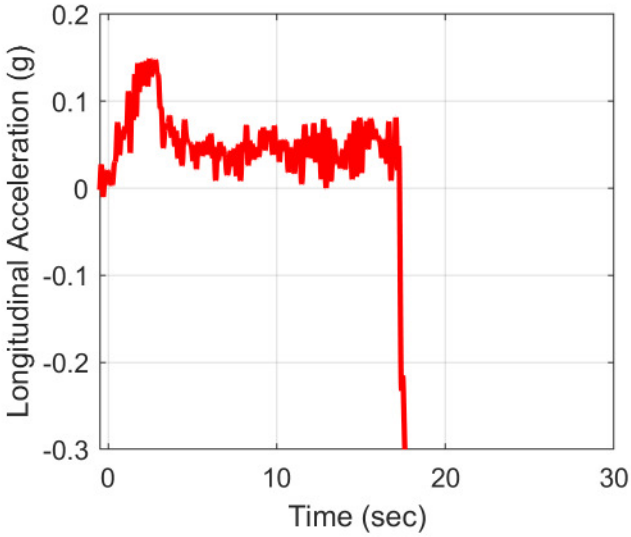

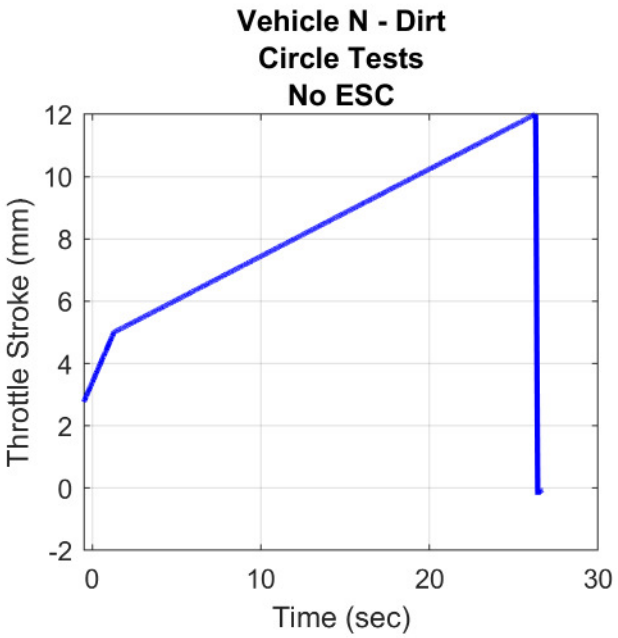

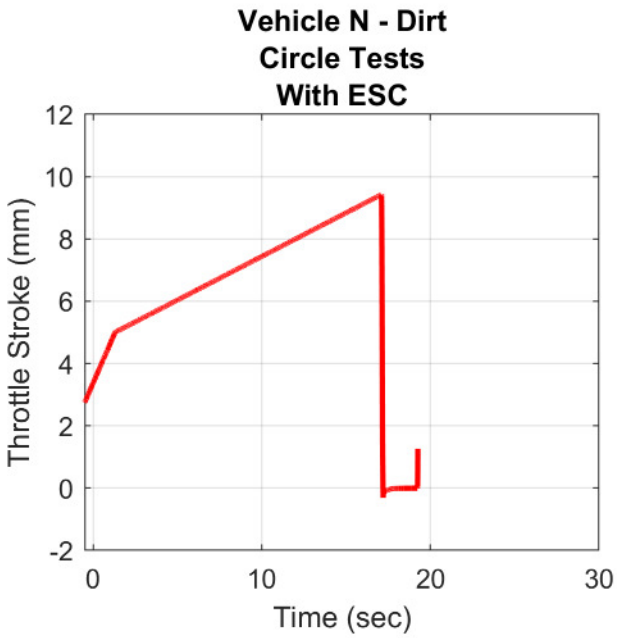

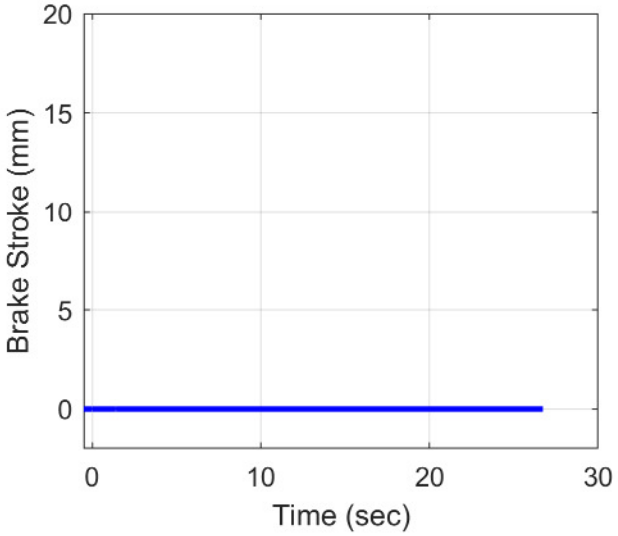

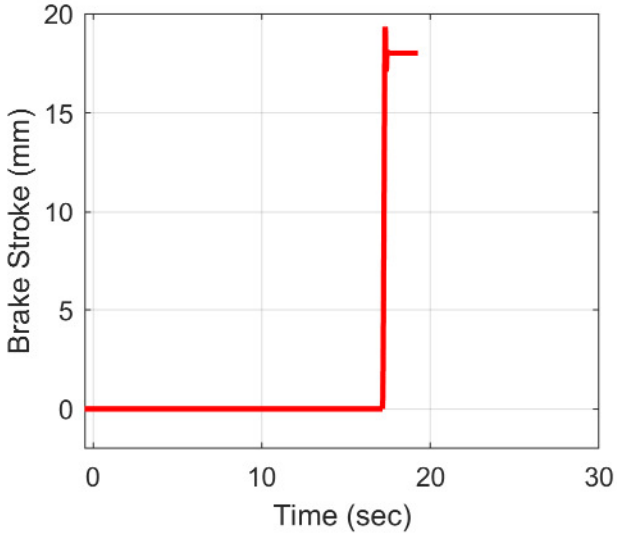

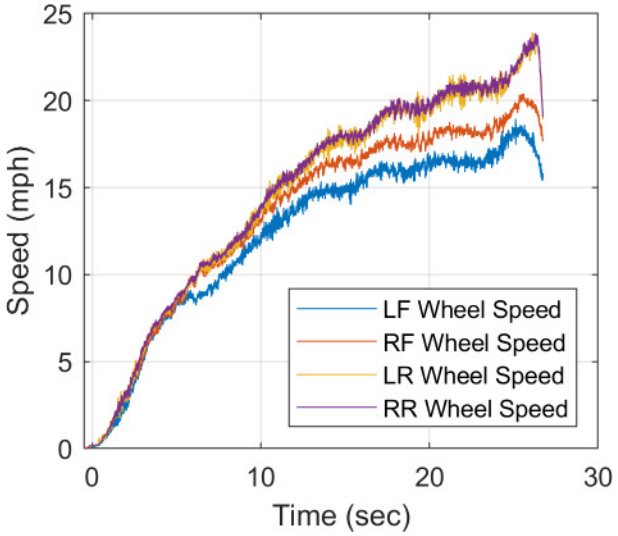

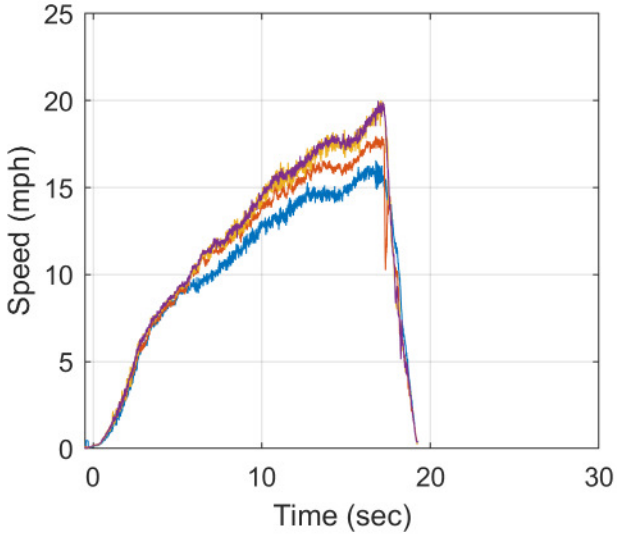

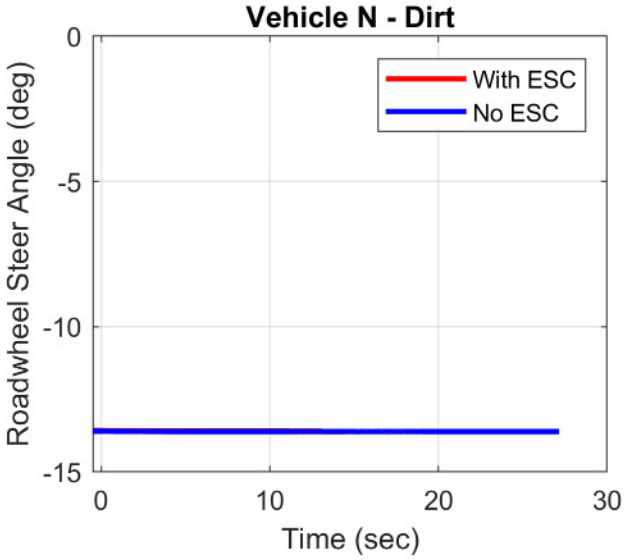

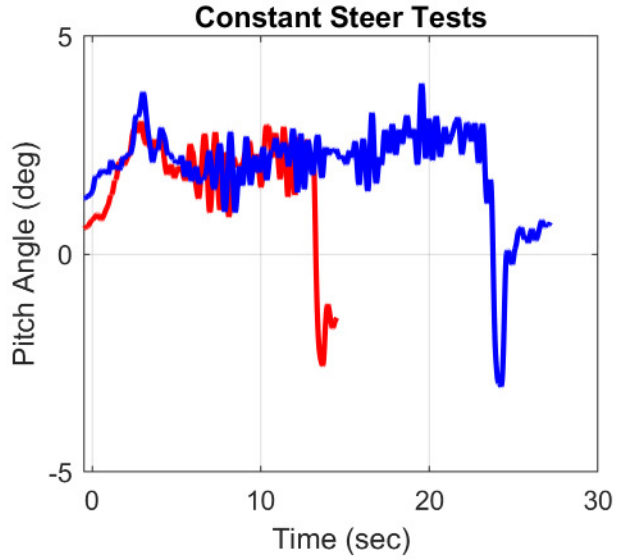

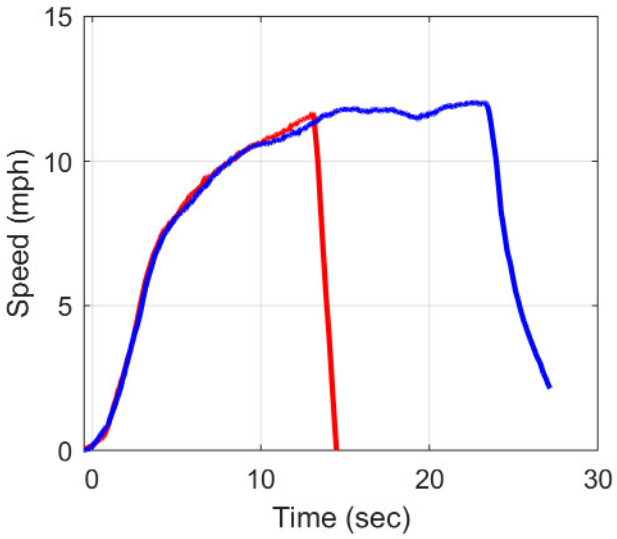

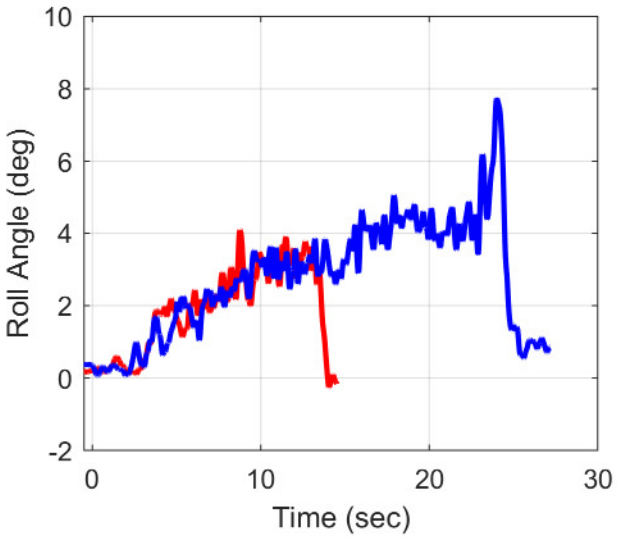

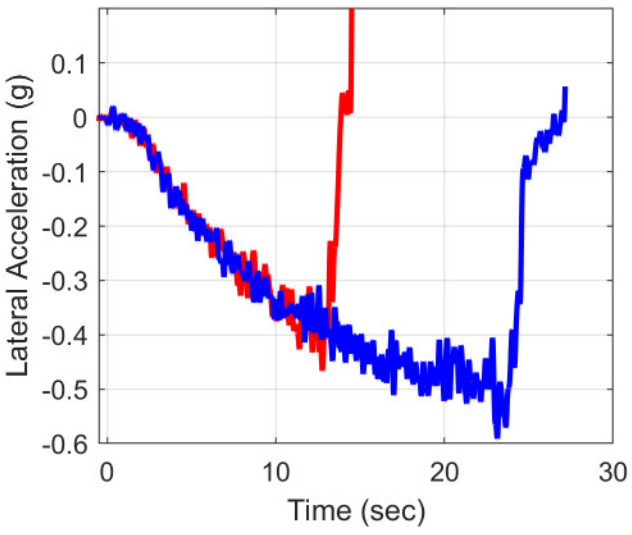

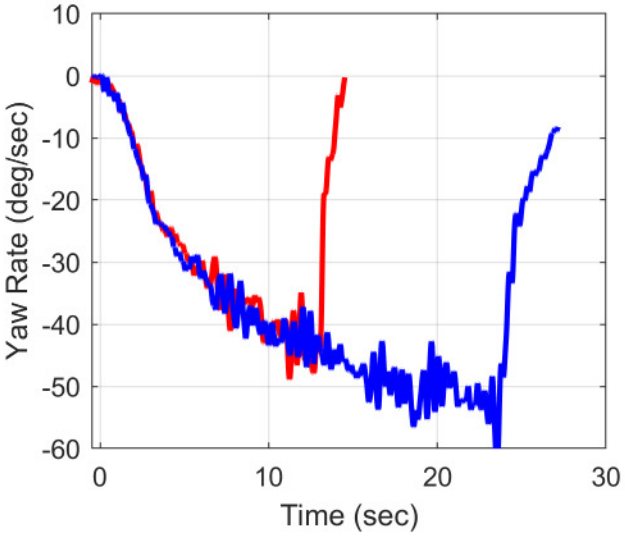

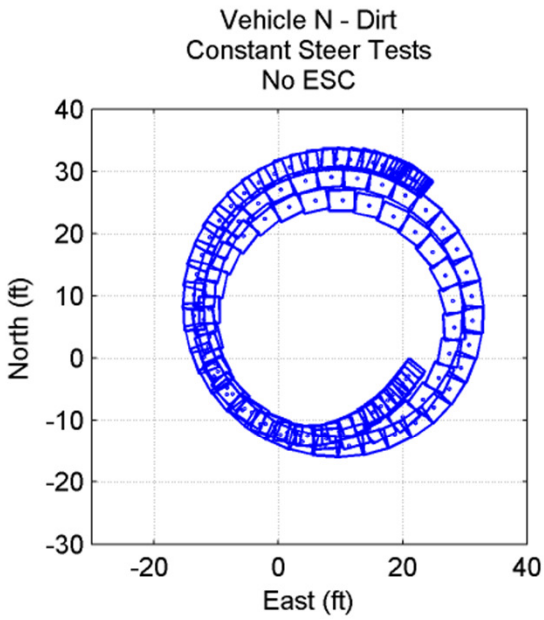

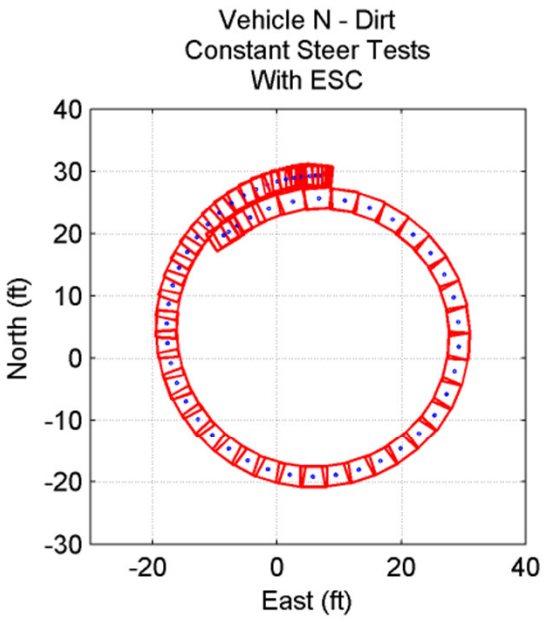

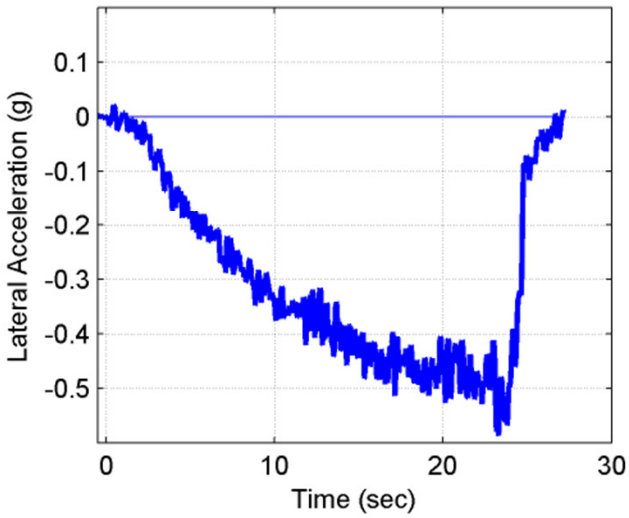

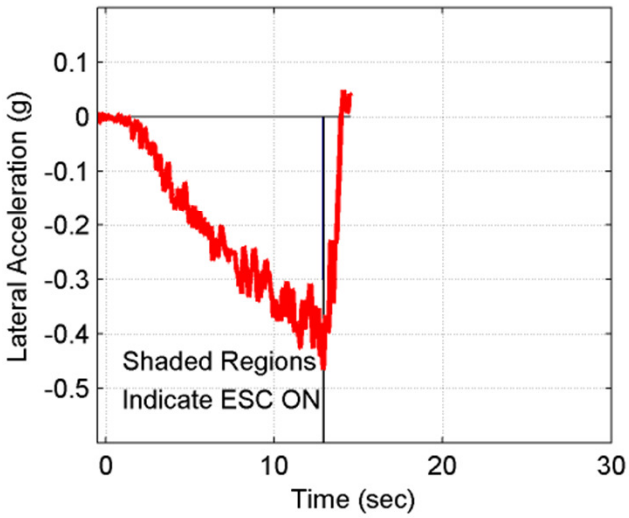

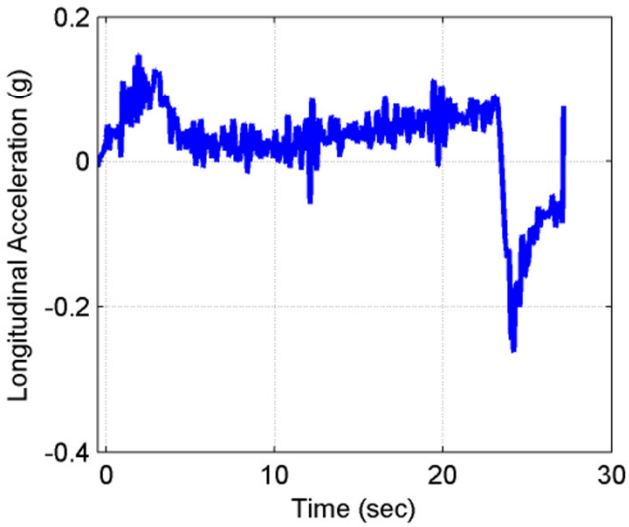

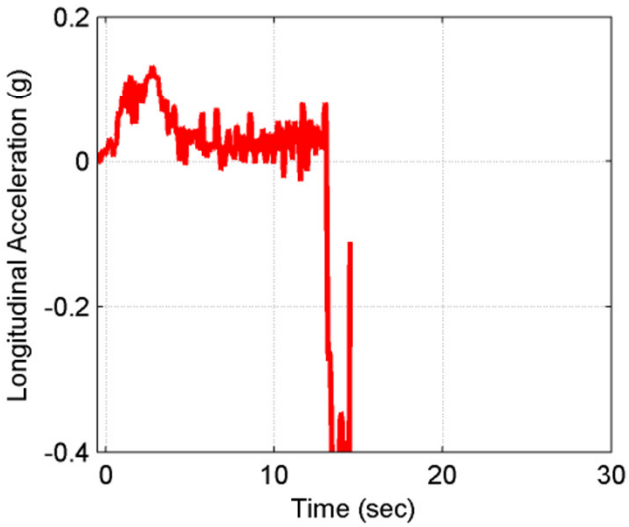

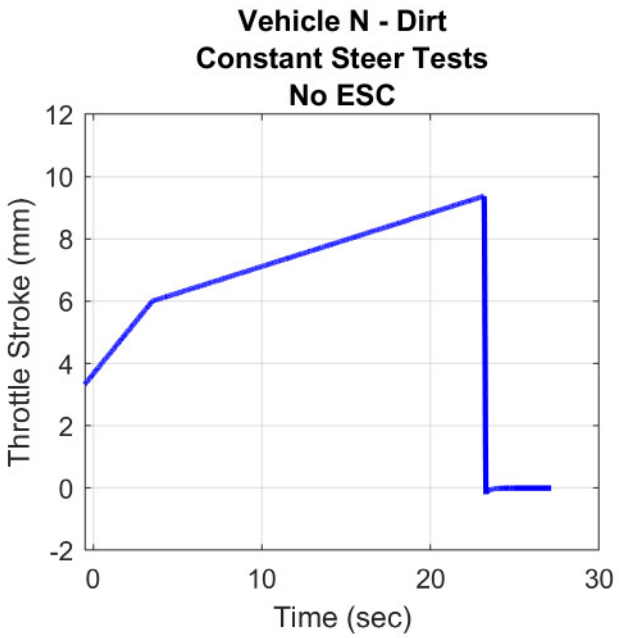

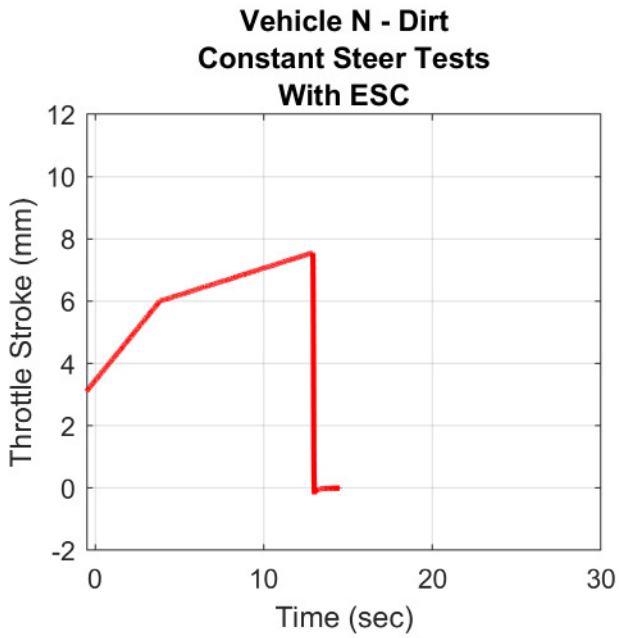

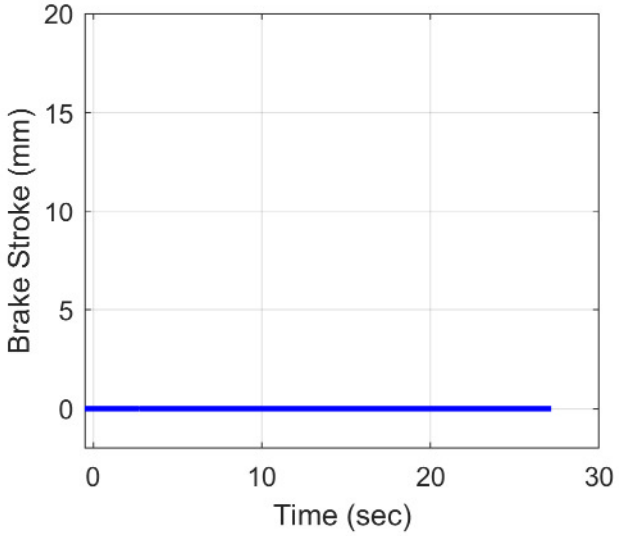

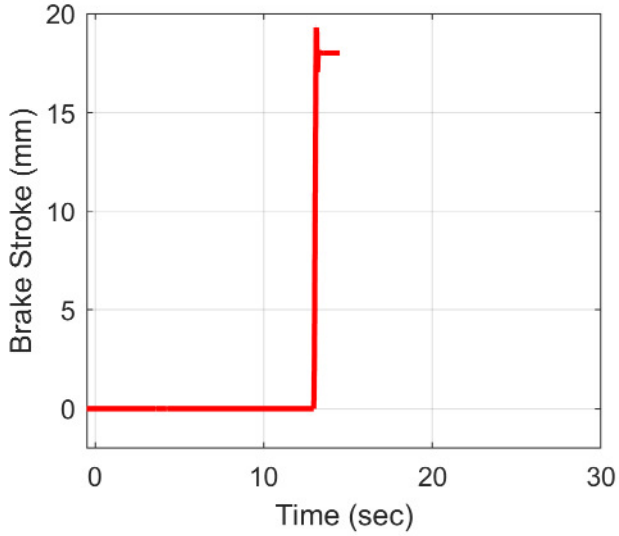

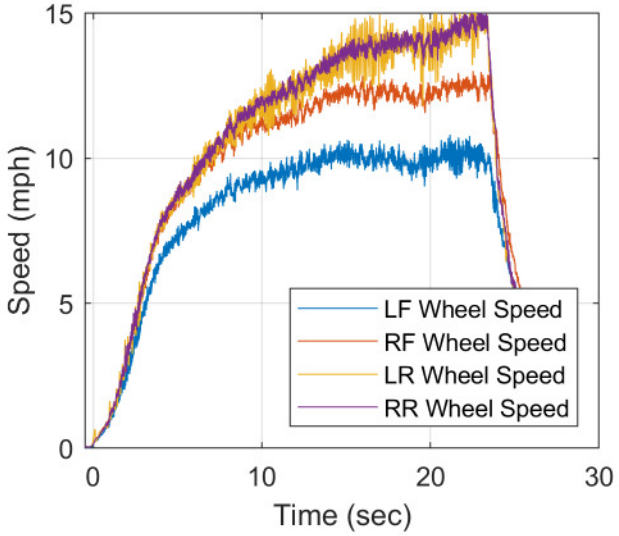

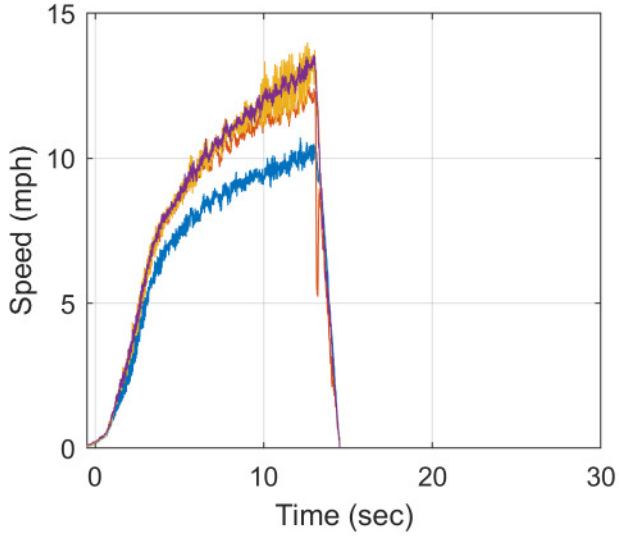

Side View of Vehicle G

Side View of Vehicle N

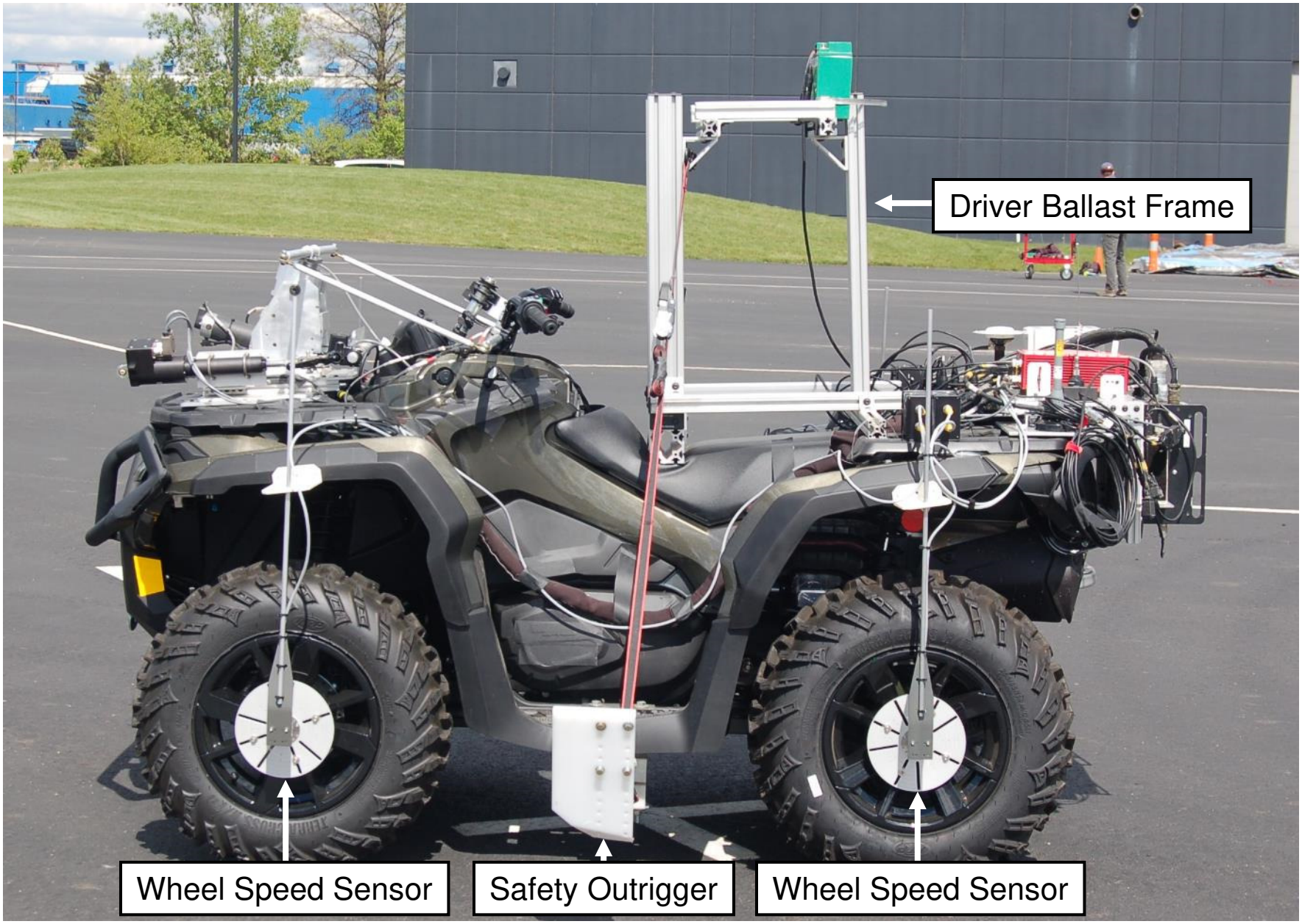

SEA ATV Robotic Test Driver (RTD) Components (Steer, Throttle, and Brake Actuators)

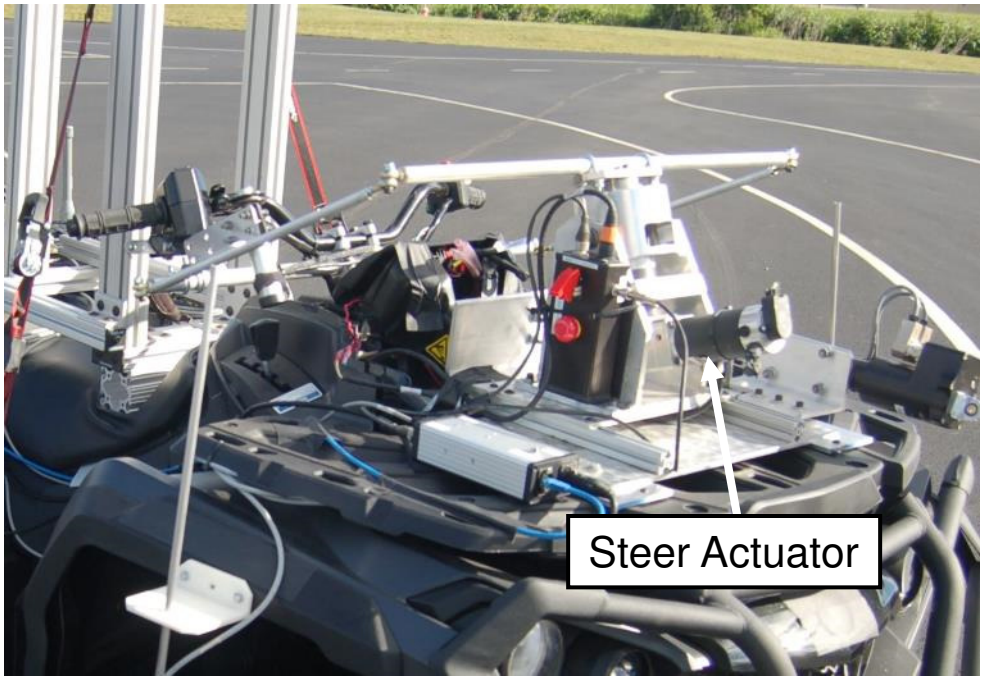

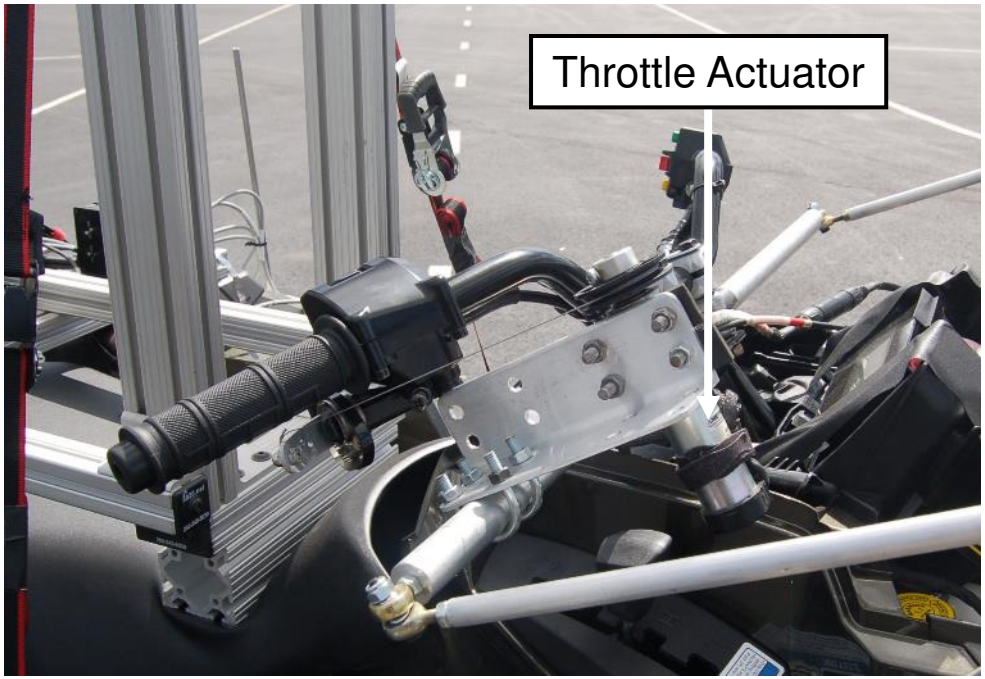

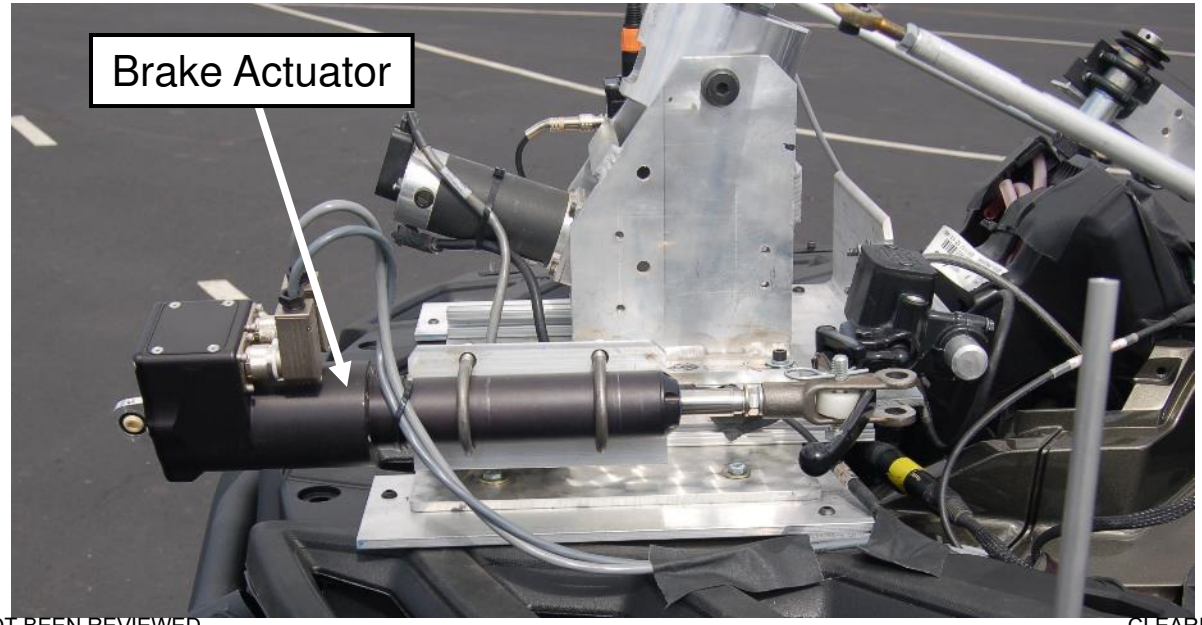

SEA ATV Robotic Test Driver (RTD) Components (GPS/IMU, Control Box, and Antennas)

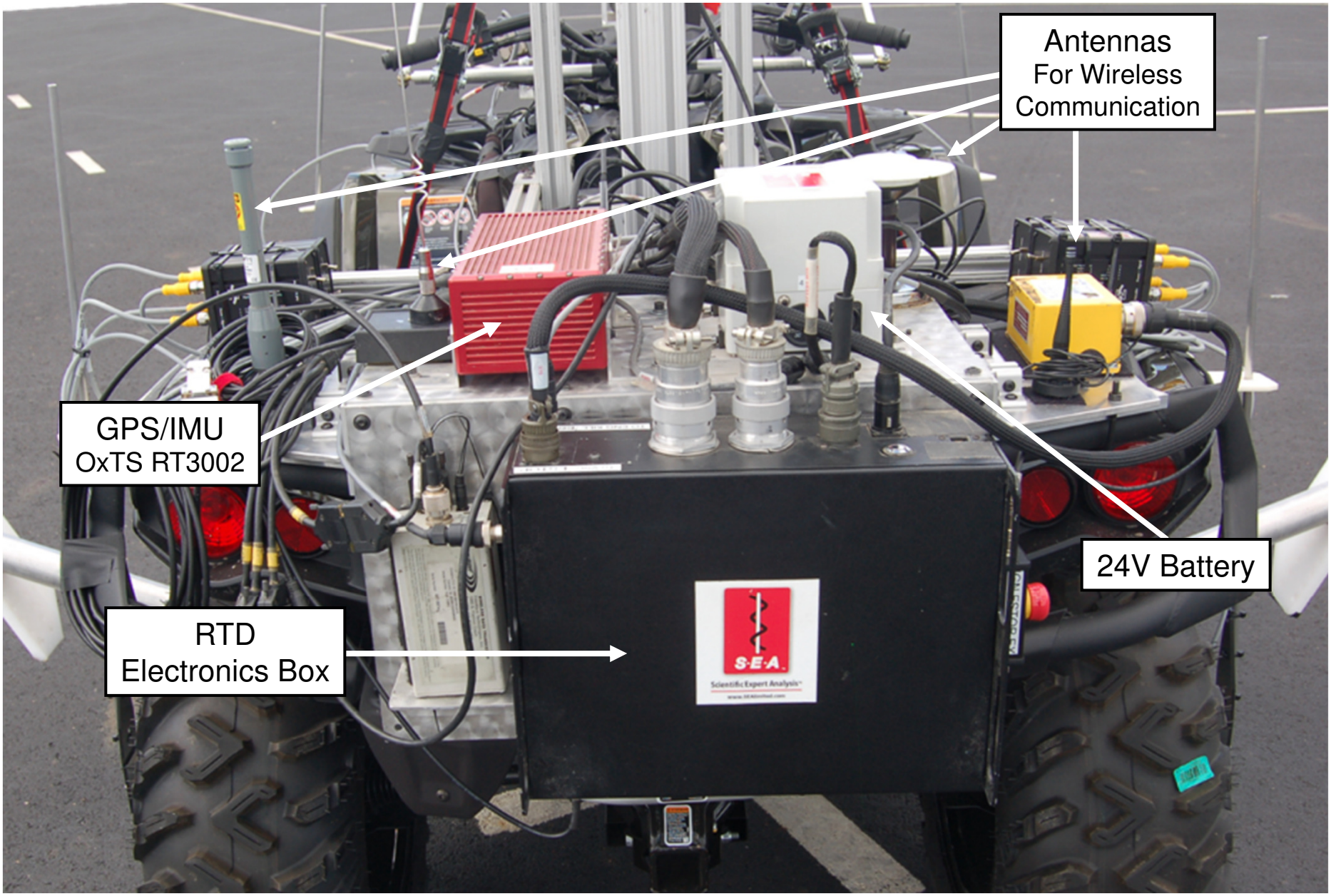

Photograph Showing Left Front Brake Caliper Removed from Brake Rotor and Cable-Tied to the Suspension Control Arm

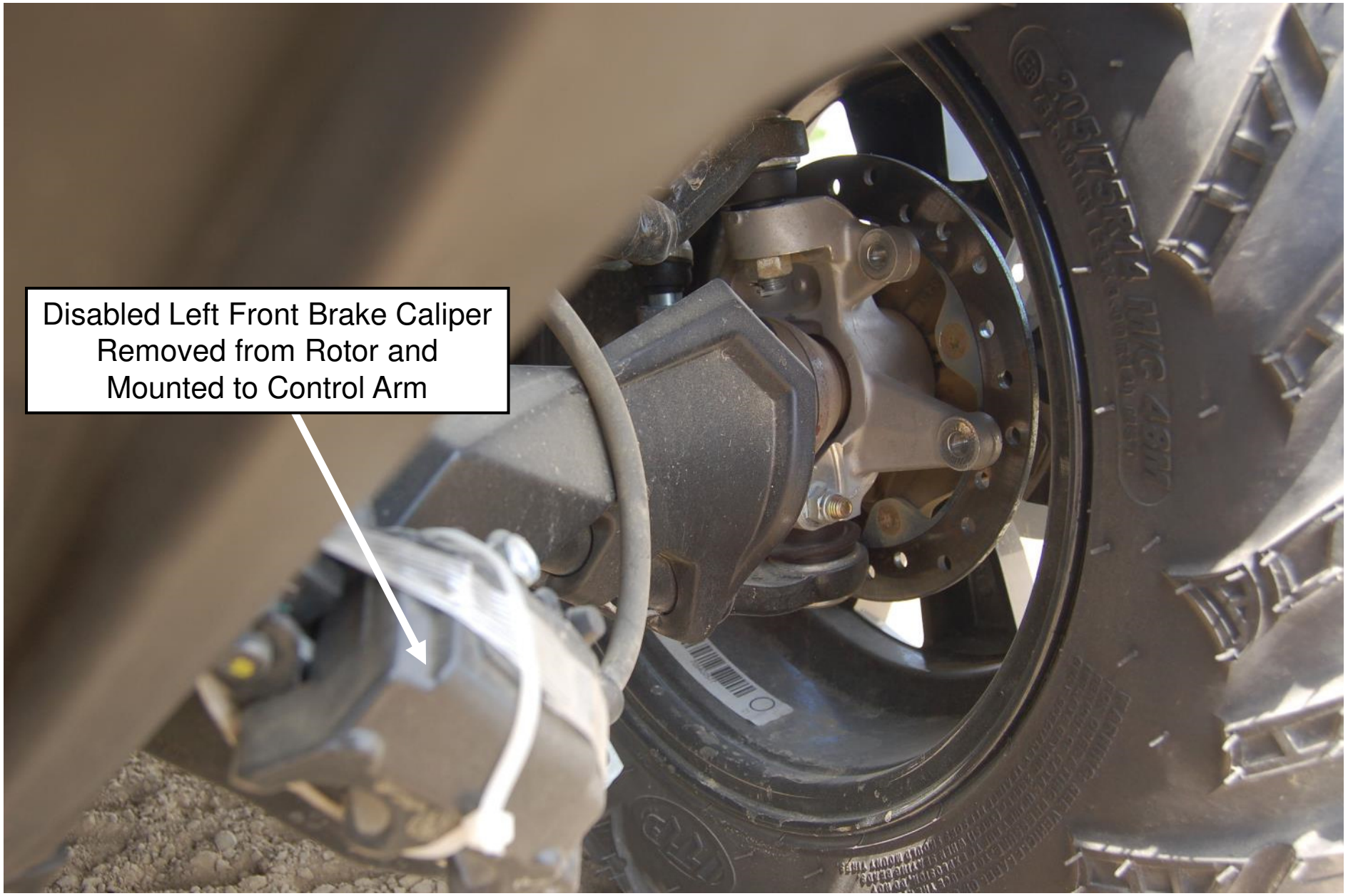

Lateral Acceleration Values Used for ESC Threshold Levels

Determined from Threshold Ay Values Measured During Two-Wheel Lift (2WL) Test Outcomes During 20 mph Dropped-Throttle J-Turn Tests

ESC Threshold Used = 85% Threshold Ay

	Threshold Ay Asphalt (g)	Threshold Ay Groomed Dirt (g)	Average Threshold Ay (g)	**ESC Threshold (g)**	**ESC Threshold (ft/s^2)**
Vehicle G	0.459	0.445	0.452	**0.384**	**12.4**
Vehicle N	0.540	0.556	0.548	**0.466**	**15.0**

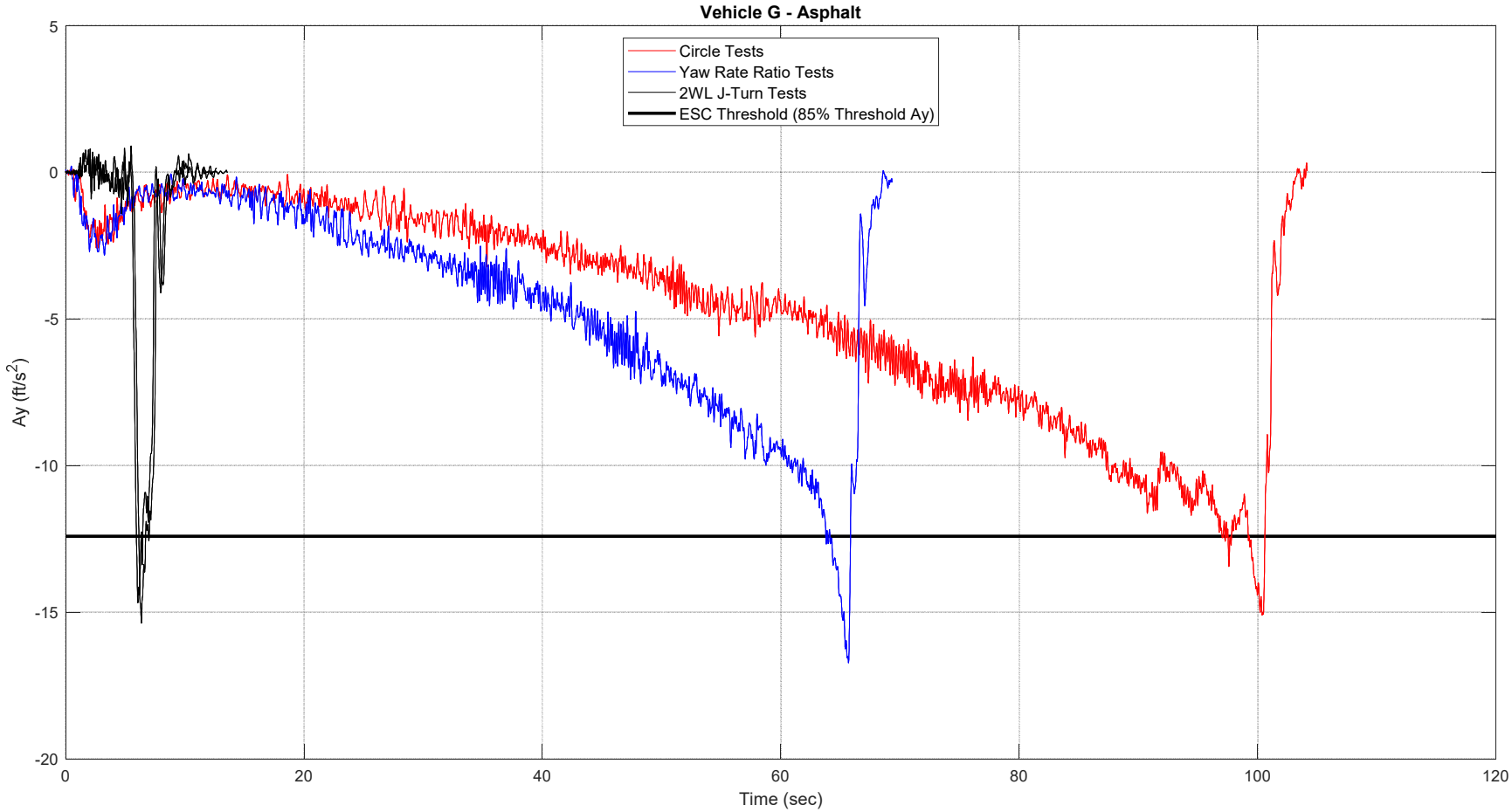

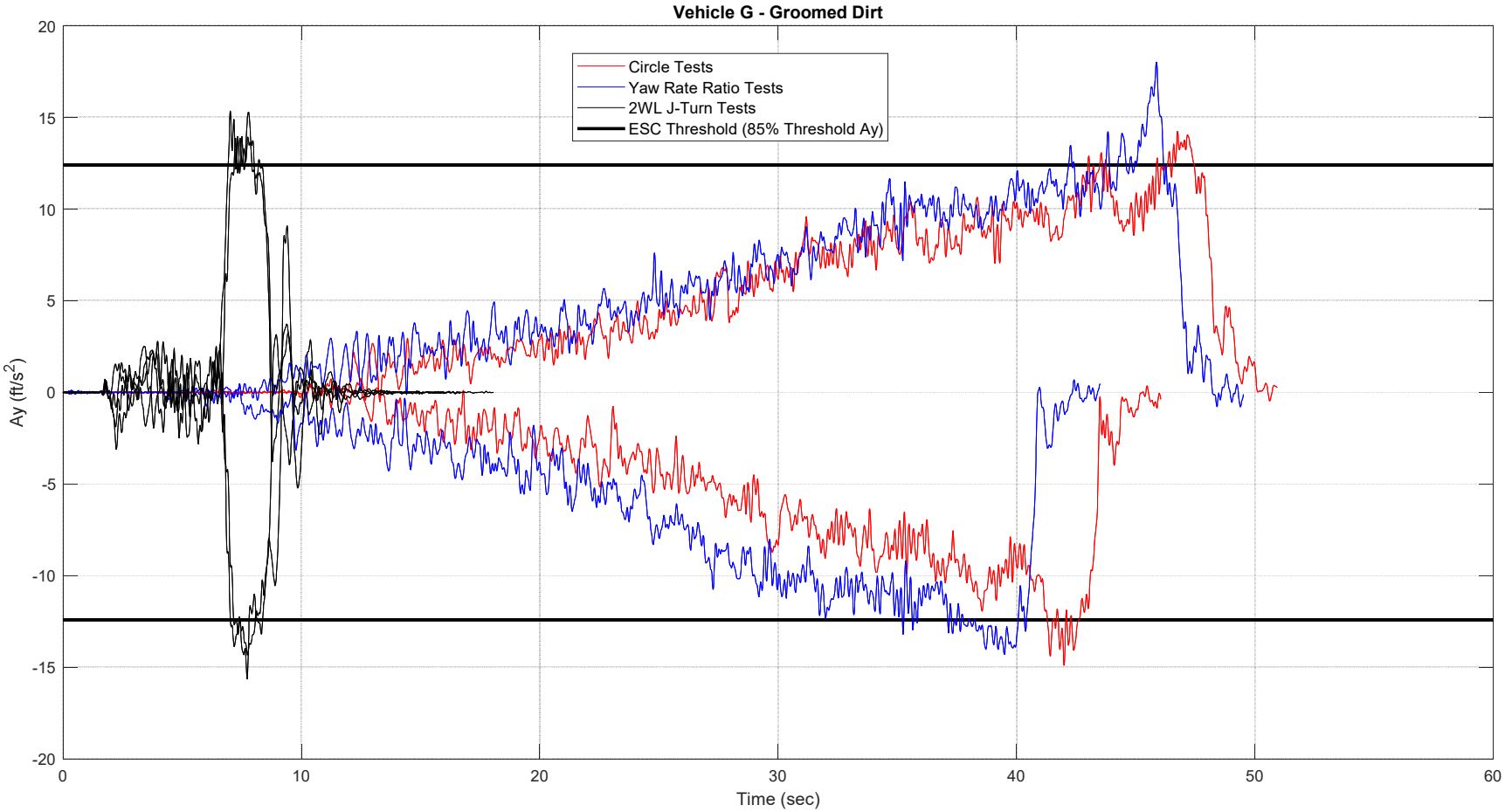

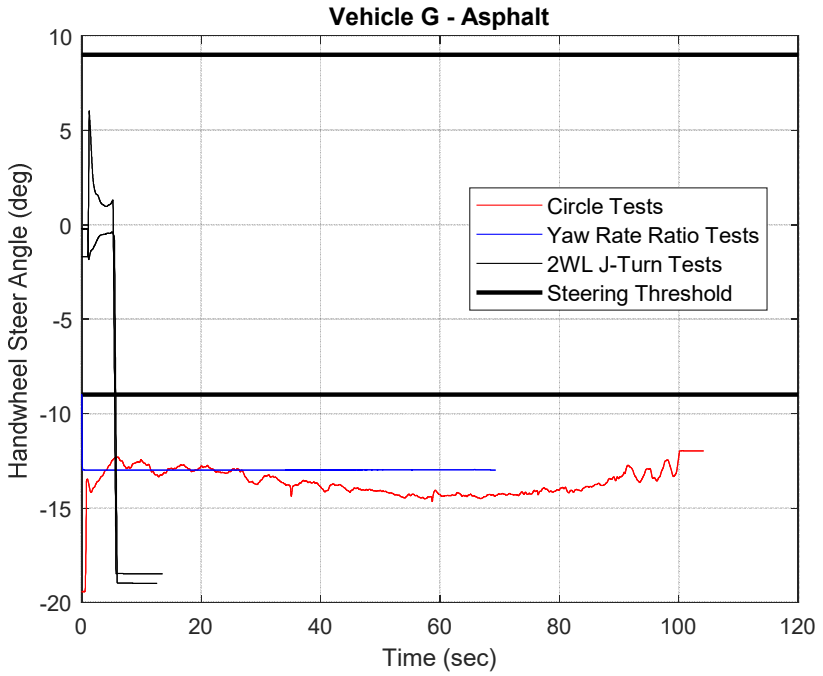

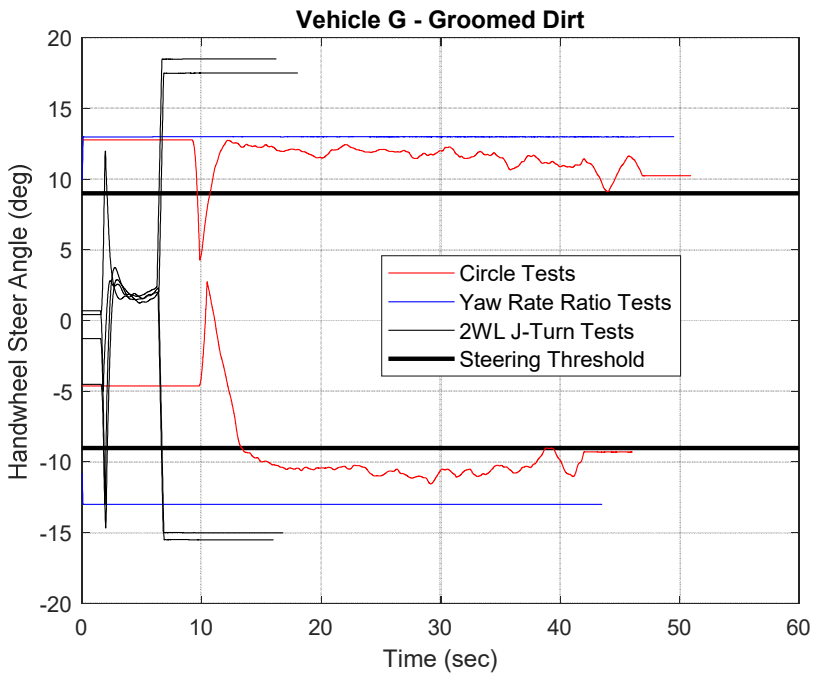

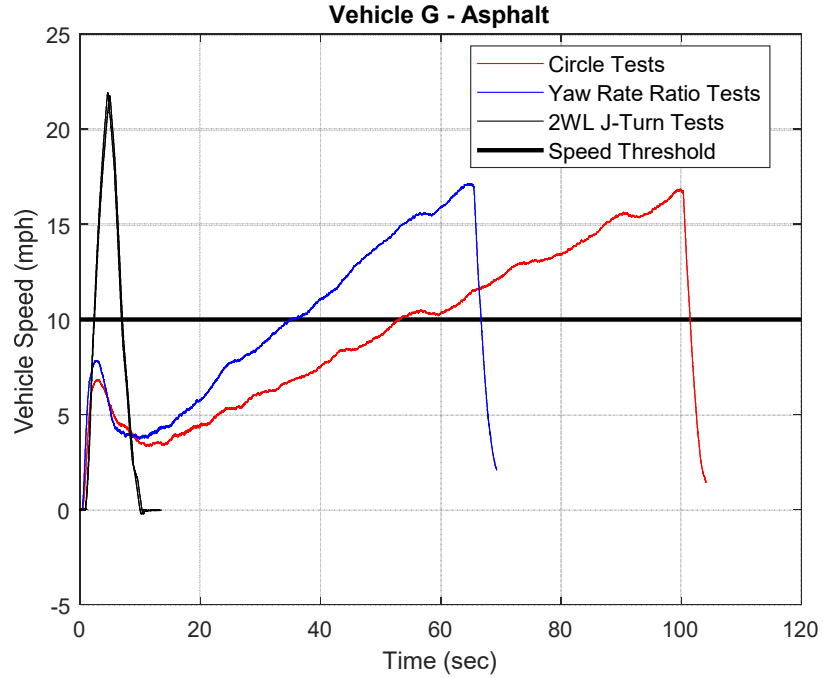

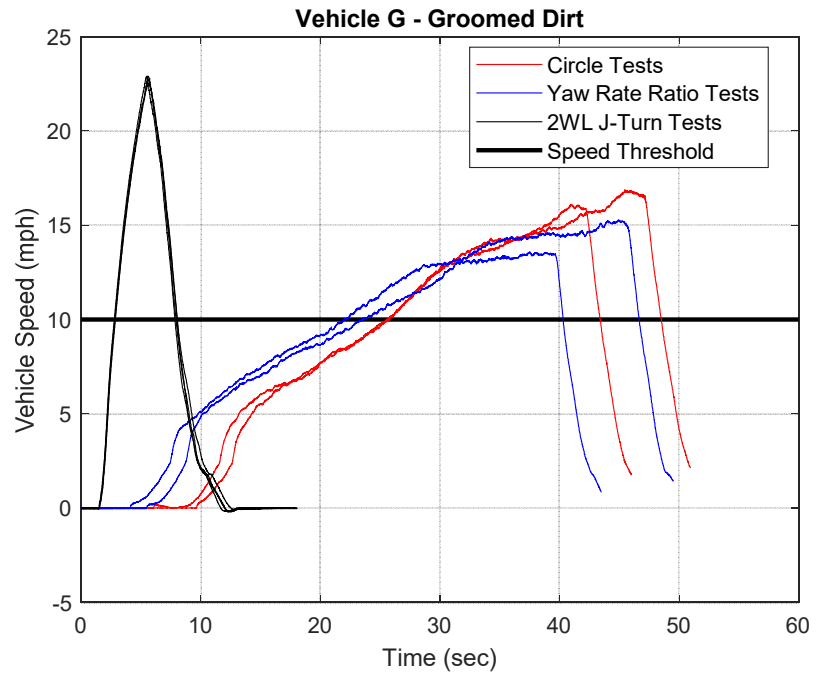

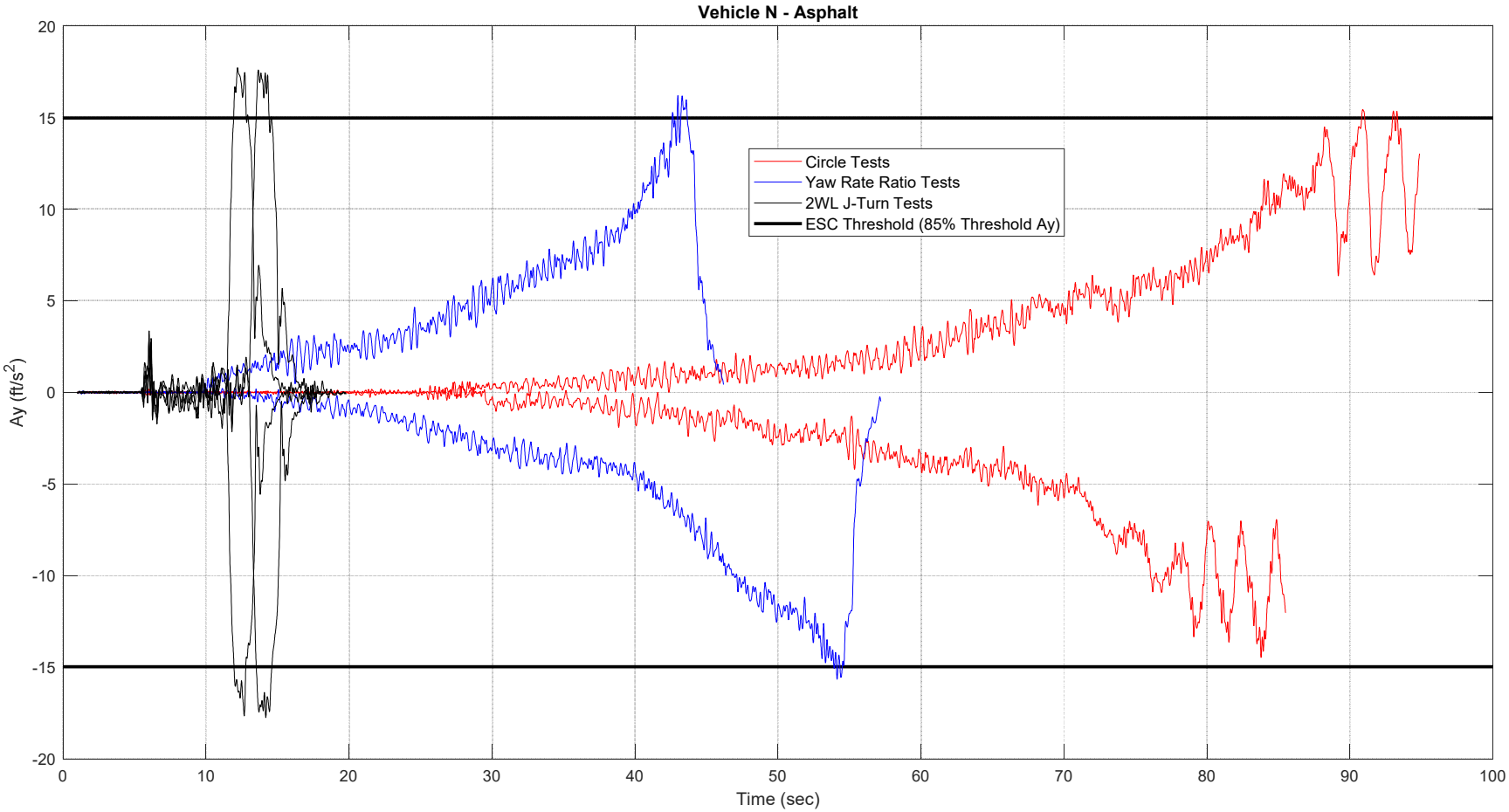

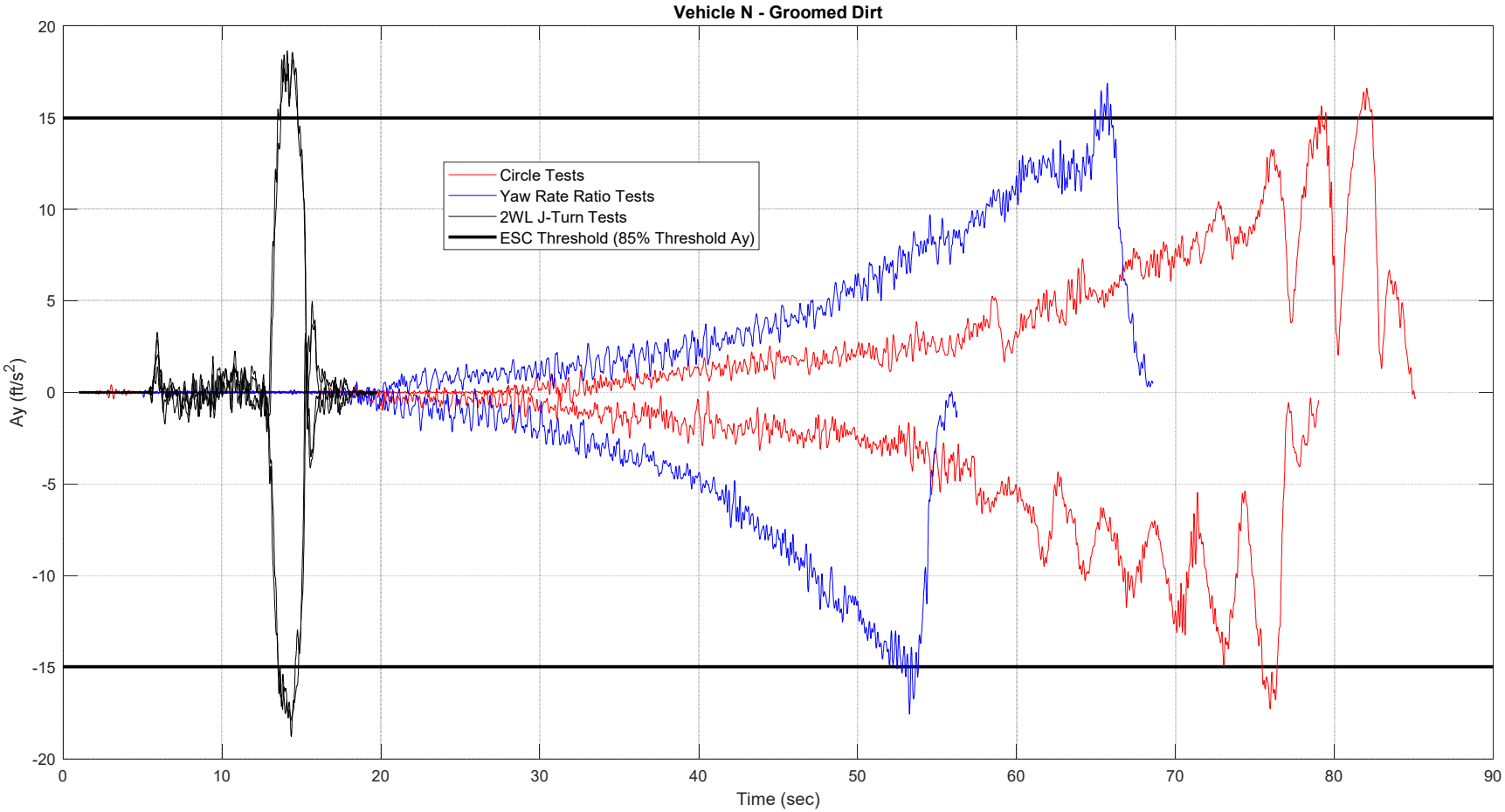

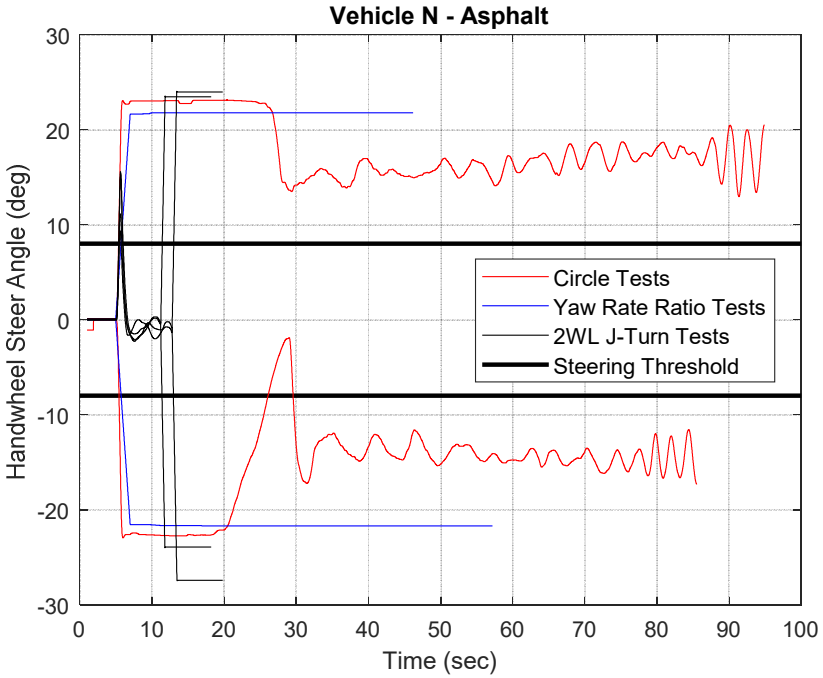

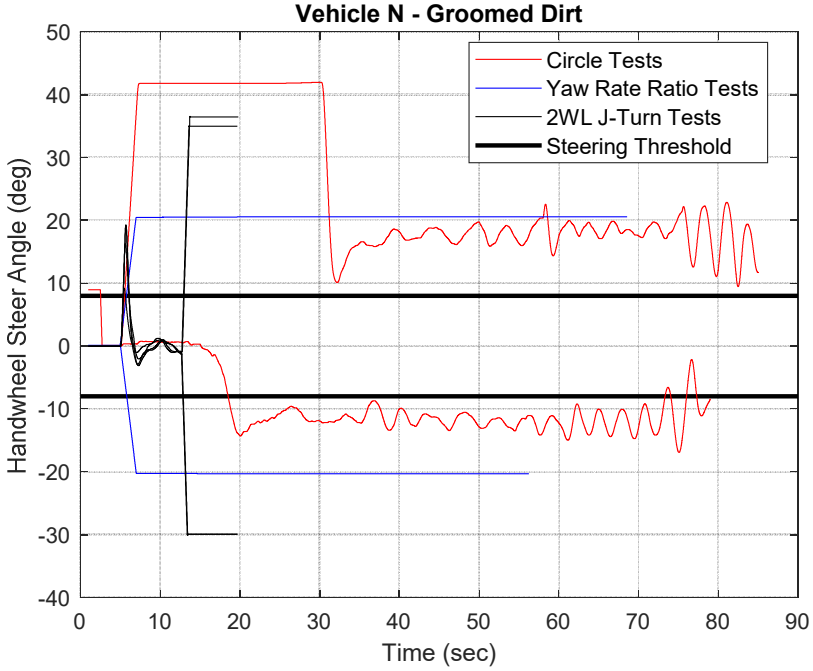

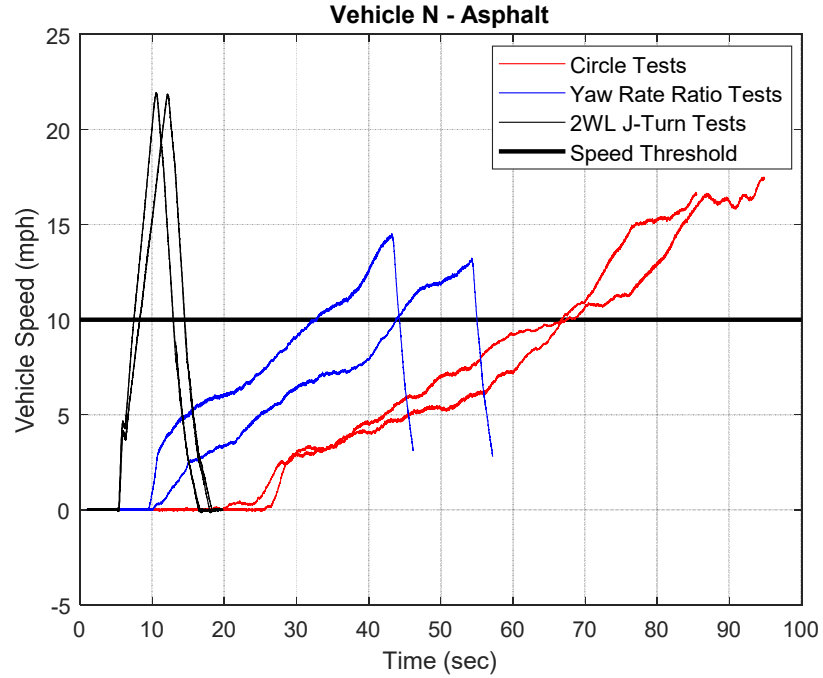

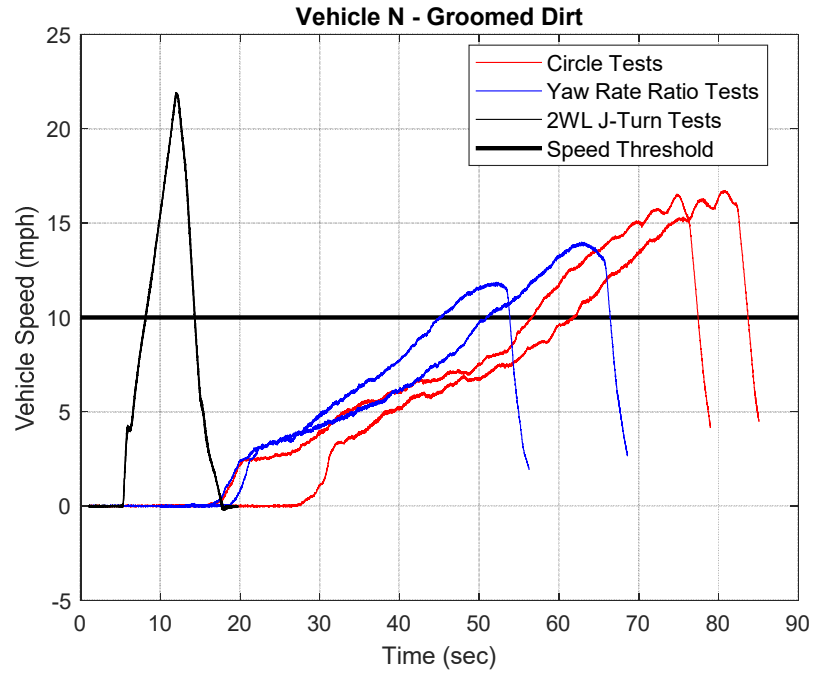

Results Showing Timing of ABS Cycling of Vehicle N

Results from Braking and Turning Maneuver Performed on Wet Grass

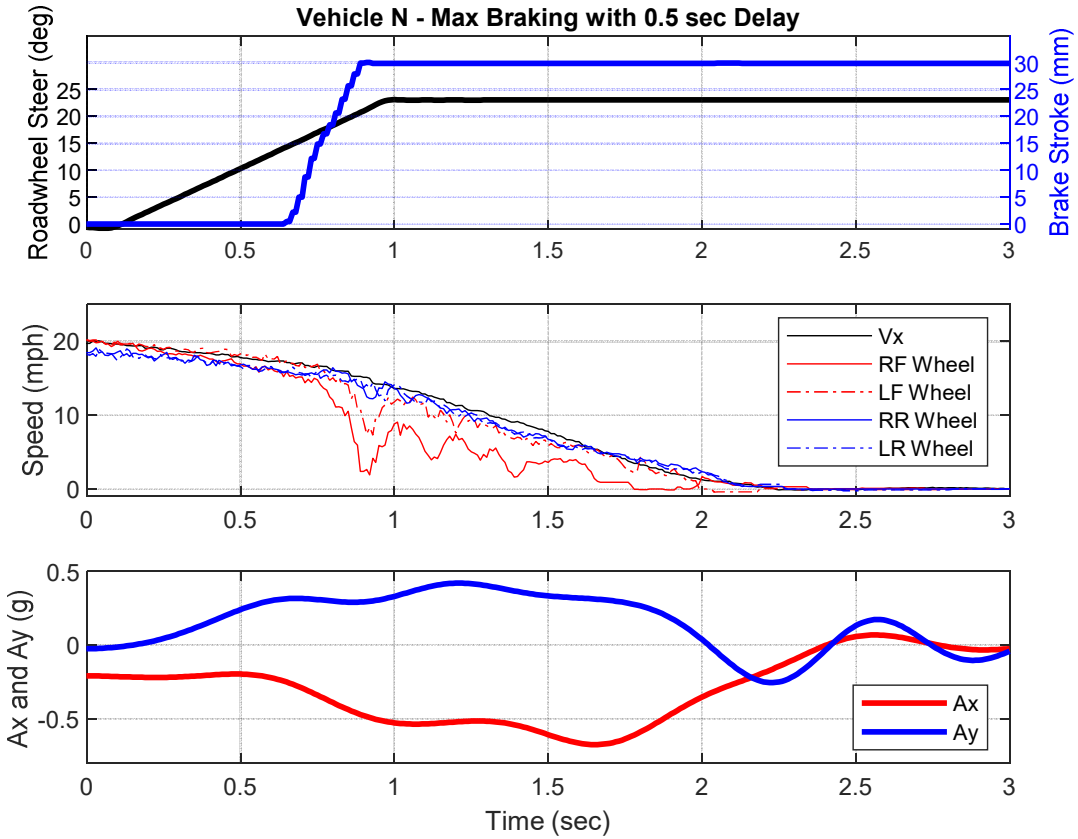

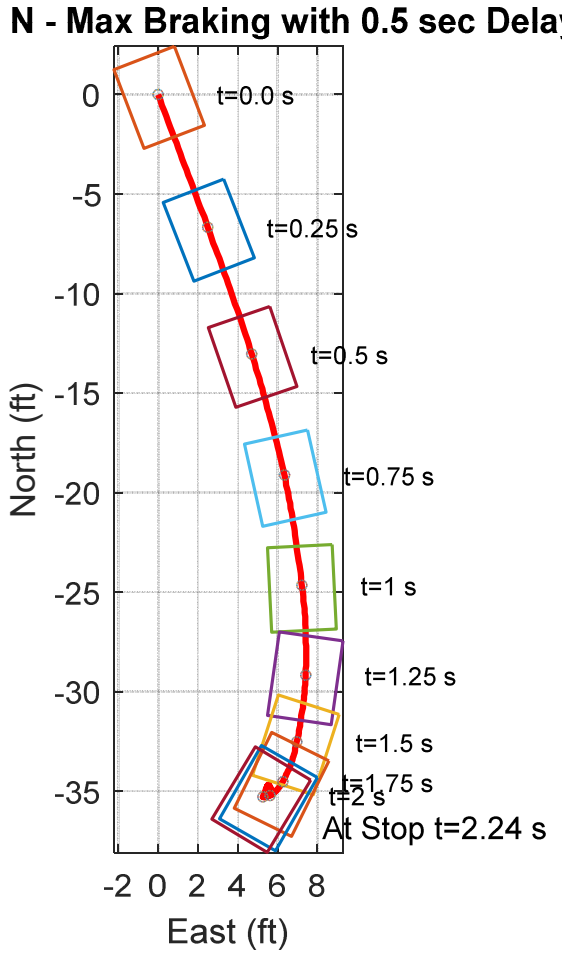

Demonstration of Capabilities of Electronic Motor Brake Actuator Used to Cycle Hand Brake to Emulate ABS on Vehicle G

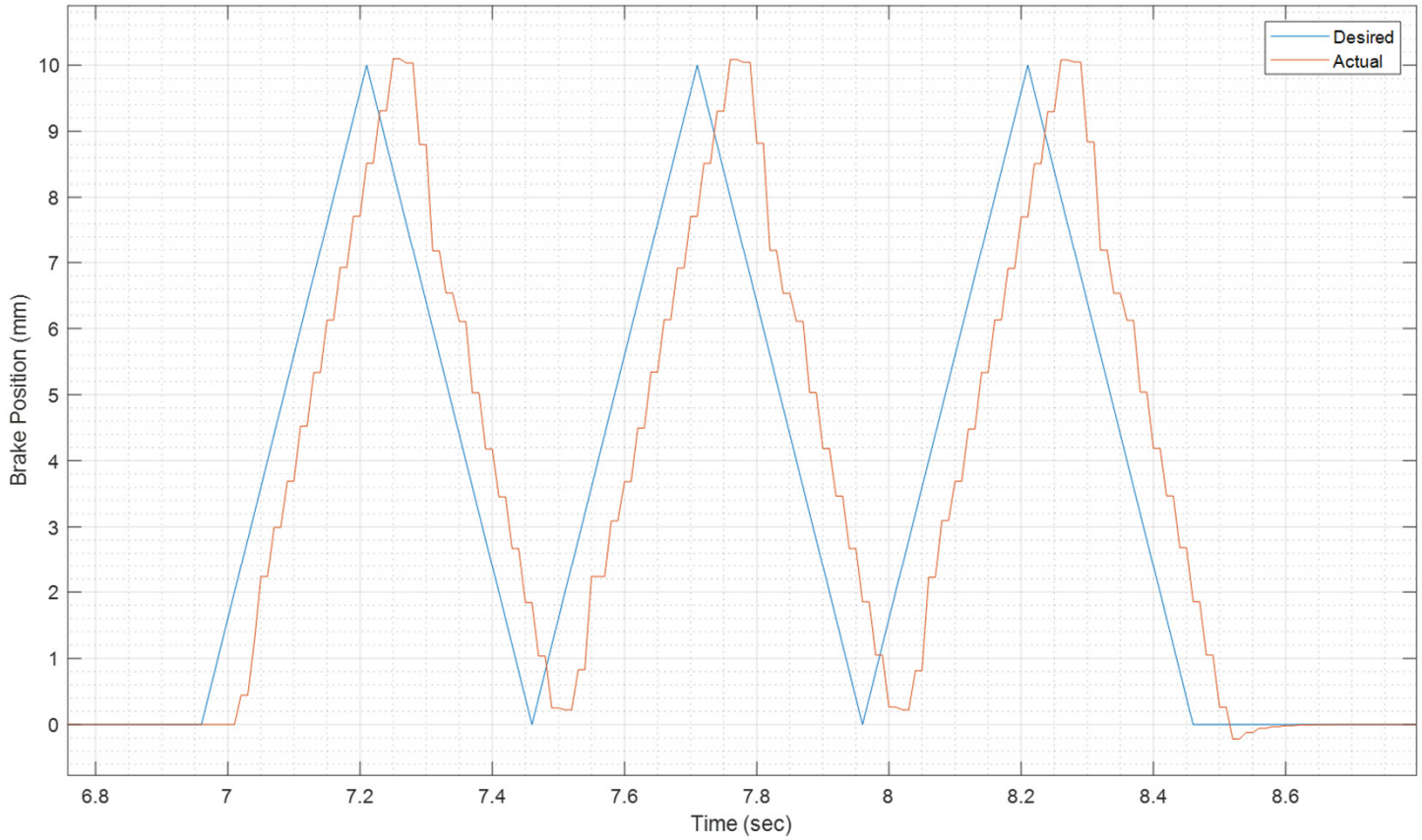

Brake Position 10 mm in 0.25 sec